

# University of Wollongong - Research Online

## Thesis Collection

Title: The effect of pulsed electromagnetic fields on protein unfolding

Author: Yoke Berry

Year: 2005

Repository DOI:

### Copyright Warning

You may print or download ONE copy of this document for the purpose of your own research or study. The University does not authorise you to copy, communicate or otherwise make available electronically to any other person any copyright material contained on this site.

You are reminded of the following: This work is copyright. Apart from any use permitted under the Copyright Act 1968, no part of this work may be reproduced by any process, nor may any other exclusive right be exercised, without the permission of the author. Copyright owners are entitled to take legal action against persons who infringe their copyright. A reproduction of material that is protected by copyright may be a copyright infringement. A court may impose penalties and award damages in relation to offences and infringements relating to copyright material.

Higher penalties may apply, and higher damages may be awarded, for offences and infringements involving the conversion of material into digital or electronic form.

**Unless otherwise indicated, the views expressed in this thesis are those of the author and do not necessarily represent the views of the University of Wollongong.**

Research Online is the open access repository for the University of Wollongong. For further information contact the UOW Library: [research-pubs@uow.edu.au](mailto:research-pubs@uow.edu.au)

*University of Wollongong Thesis Collections*

*University of Wollongong Thesis Collection*

---

*University of Wollongong*

*Year 2005*

---

The effect of pulsed electromagnetic  
fields on protein unfolding

Yoke Berry  
University of Wollongong

Berry, Yoke, The effect of pulsed electromagnetic fields on protein unfolding, PhD thesis, School of Chemistry, University of Wollongong, 2005. <http://ro.uow.edu.au/theses/485>

This paper is posted at Research Online.  
<http://ro.uow.edu.au/theses/485>

## **NOTE**

This online version of the thesis may have different page formatting and pagination from the paper copy held in the University of Wollongong Library.

## **UNIVERSITY OF WOLLONGONG**

### **COPYRIGHT WARNING**

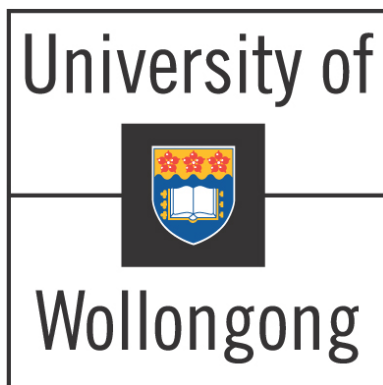
You may print or download ONE copy of this document for the purpose of your own research or study. The University does not authorise you to copy, communicate or otherwise make available electronically to any other person any copyright material contained on this site. You are reminded of the following:

Copyright owners are entitled to take legal action against persons who infringe their copyright. A reproduction of material that is protected by copyright may be a copyright infringement. A court may impose penalties and award damages in relation to offences and infringements relating to copyright material. Higher penalties may apply, and higher damages may be awarded, for offences and infringements involving the conversion of material into digital or electronic form.

# THE EFFECT OF PULSED ELECTROMAGNETIC FIELDS ON PROTEIN UNFOLDING

YOKE (*J.C.M.*) BERRY, *B. Sc. (HONS)*

Submitted in fulfilment of the requirements  
for the Degree of Doctor of Philosophy



DEPARTMENT OF CHEMISTRY  
WOLLONGONG  
AUSTRALIA

JUNE 2005

Printed on 80% Australian recycled paper

**DECLARATION OF AUTHENTICITY**

This thesis is submitted in accordance with the regulations of the University of Wollongong in fulfilment of the degree of Doctor of Philosophy. It does not include any material previously published by another person except where due reference is made in the text. The experimental work described in this thesis is original and has not been submitted for a degree to any other University.

Johanna Cornelia Maria (Yoke) Berry

**ACKNOWLEDGEMENTS**

There is no order of importance in the following acknowledgments. Each day, in the last four years, people have enriched my life with wisdom, knowledge, support and friendship. I have appreciated it all.

My supervisors, Professor John Carver, then a member of the Department of Chemistry and now Head of the School of Chemistry and Physics at the University of Adelaide and Professor David McKenzie, Head of the Department of Applied and Plasma Physics, University of Sydney, have stood by me well before the commencement of this project. With Dr. Peter French, John and David applied for several grants before the initial scholarship was funded by the University of Wollongong. Both John and David have instilled in me the highest degree of scientific approach and analysis and their enthusiasm and belief in the project have made the work very stimulating. I have the greatest respect for both my supervisors on both a professional and a personal level. Thank you for everything, John and David.

I am grateful to Dr. Peter French, formerly of the Centre for Immunology, St. Vincent's Hospital Darlinghurst. I first met Peter through a community project and was impressed by his scientific enquiry into possible effects of pulsed microwaves on proteins. Peter was generous in giving me the use of the TEM cell for some experiments.

I am indebted to the University of Wollongong and in particular Professor Chris Brink and Professor Margaret Sheil, past and present Pro-Vice Chancellor (Research) respectively, for giving me the chance to pursue a community interest and for providing me with a one year scholarship towards the PhD project.

A considerable scholarship, awarded through an ARC linkage grant between my supervisors, Professor John Carver and Professor David McKenzie together with Associate Professor Irene Yarovsky, School of Applied Physics, RMIT University and Dr. Herbert Treutlein of Cytopia,

permitted the project to continue. The new scholarship enabled me to travel to the annual Lorne protein conference where I presented posters with members of Irene's research group: Irene, Herbert, Dr. Sue Legge and Akin Budi. The RMIT group is dynamic and hard working. It was a pity that our work did not intertwine more. I thank you all for the friendship over the years.

It was a pleasure to have worked with members of the research group of Professor David McKenzie: Dr. Jocelyn Laurence, Bradley Steele and Doaa George. I would like to thank Mr. Phil Denniss who re-modelled the microwave oven and was always eager to help when the instrument needed adjustments.

The Carver Institute (TCI) was a great place to work and I thank my colleagues for their friendship and advice over the years: Dr. Robyn Lindner (now at Proteome Systems Ltd), Dr. Teresa Treweek, Dr. Andrew Aquilina, Dr. Agata Rekas, Dr. Sarah Meehan, Arezou Ghahghaei, Michael Friedrich, Amie Morris, David Thorn and Chris Brockwell.

I have not forgotten the support given to me prior to receiving a scholarship for this particular project. Thank you: Professor John Bremner, Professor Stephen Pyne and Associate Professor Roger Truscott.

The department of chemistry at the University of Wollongong must rate as one of the friendliest places to work. Thank you all: technical staff, administrative staff, academic staff and research students. Thank you for the smiles, kind words, support and assistance. A special "thank you" to Peter, Steve and Geoff of the workshop, who were always ready to help with equipment problems. A warm thank you also to Associate Professor Will Price, Head of the Department who took on the responsibility of academic supervisor after John moved to Adelaide.



Finally, but never lastly, I think of my husband Bill, children, family and friends who have believed in me all those years and who let me pursue my dream and have now welcomed me back in their lives. I dedicate this thesis to Louise and Lev, in the hope that they aspire to reach for the full potential within.

In the course of collating data and results, it became apparent that, although insight has been gained from this PhD study, I have to humbly admit that there is so much still to learn.

This is an opportune moment to reflect and to express my profound gratitude for being alive, for being conscious of the serene complexity of the natural world and for the soaring spirit of human kind. I have considered it a privilege to contribute to the pool of knowledge.

5 June 2005

---

**TABLE OF CONTENTS**

Declaration of authenticity	i
Acknowledgements	ii
List of figures	viii
List of tables	xix
List of abbreviations	xxi
List of appendices	xxiii
List of publications	xxv
Abstract	xxvii
 <b>CHAPTER 1    <i>INTRODUCTION</i></b>	 <b><i>1</i></b>
1.1.        Structure of proteins	1
1.2.        Protein turnover	3
1.3.        The role of molecular chaperones	5
1.4.        Protein aggregation and associated neurodegenerative diseases	6
1.5.        The electromagnetic spectrum	10
1.6.        Biological interactions with electromagnetic radiation	12
1.6.1.    Biological interactions with extremely low frequency fields	13
1.6.2.    Biological interactions with microwaves	13
1.7.        Safety standards of radio- and microwaves	14
1.7.1.    Extremely low frequency (50Hz)	14
1.7.2.    Radiowaves and microwaves	15
1.8.        Effects of low frequency and microwaves on proteins	16
1.9.        Possible mechanisms of interaction	18
1.9.1.    Moving charge interaction (MCI)	18
1.9.2.    Wring modes	18
1.10       Project aim and hypothesis	19
 <b>CHAPTER 2    <i>EXPERIMENTAL</i></b>	 <b><i>20</i></b>
2.1        Selection of Experiments	20
Flowchart of experimental design	20
2.2        Selection of Proteins and Buffers	22
2.2.1   Target proteins	22
2.2.1.1    Alcohol dehydrogenase from <i>Saccharomyces cerevisiae</i>	22
2.2.1.2    Bovine serum albumin from <i>Bos taurus</i>	23
2.2.1.3    Catalase from <i>Bos taurus</i>	23
2.2.1.4    Citrate synthase from <i>Susa scrofia</i>	24
2.2.1.5    Insulin from <i>Bos Taurus</i>	25
2.2.1.6 $\alpha$ -Lactalbumin from <i>Bos Taurus</i>	26
2.2.1.7    Lysozyme from <i>Gallus gallus</i>	27
2.2.1.8    Ovotransferrin from <i>Gallus gallus</i>	27
2.2.2    Materials	28

2.2.3	Buffers	28
2.2.4	Purification of citrate synthase	28
2.2.5	Purification of $\alpha$ -crystallin	29
2.2.6	Preparation of $\alpha$ -lactalbumin	30
2.2.7	Protein concentrations	30
2.3	Equipment and techniques	31
2.3.1	Microwave oven	31
2.3.2	Transverse electromagnetic mode (TEM) cell	32
2.3.3	Visible absorption spectroscopy	33
2.3.4	Fluorescence spectroscopy	33
2.3.5	Circular dichroism (CD) spectroscopy	34
2.3.5.1	CD temperature melts	34
2.3.6	Electrospray ionisation mass spectrometry	34
2.3.7	Fluoroptic probes	36
2.3.8	Conductivity meter	36
2.3.9	Dry block heater	36
2.4	Microwave exposure	36
2.4.1.1	Exposure system 1 <i>microwave oven</i>	38
	Exposure system 1 <i>TEM cell</i>	40
2.4.1.2	Exposure system 2	40
2.4.1.3	Exposure system 3	43
2.4.2	Electric field exposure	43
2.4.2.1	DC exposure	43
2.4.2.2	AC exposure	44
2.5	Temperature Measurements	45
2.5.1.1	Baseline temperature for <i>Exposure system 1</i>	46
2.5.1.2	Baseline temperature for <i>Exposure system 2 and 3</i>	46
2.5.2	SAR measurements	47
2.5.2.1	SAR measurements for <i>Exposure system 1</i>	47
2.5.2.2	SAR measurements for <i>Exposure systems 2 and 3</i>	48
2.5.3	Fall of temperature	50
2.5.3.1	Relaxation of temperature to baseline- <i>Exposure system 2</i>	50
2.5.3.2	Temperature average over six minutes- <i>Exposure system 2</i>	50
2.5.3.3	Relaxation of temperature to baseline- <i>Exposure system 3</i>	50
2.5.3.4	Temperature average- <i>Exposure system 3</i>	51
2.6	Light Scattering Experiments	52
2.6.1	Statistical analysis of data	52
2.6.2	Diffusion of proteins	53
2.7	Protein conformation studies	53
2.7.1	Enzyme activity assays	53
2.8	Additional protein studies	55
2.8.1	Effect of CO <sub>2</sub> on protein aggregation	55
2.8.2	Effect of molecular crowding on protein aggregation	55

<b>CHAPTER 3</b>	<b>TEMPERATURE ASSESSMENT</b>	<b>59</b>
3.1	Baseline temperature of incubators	59
3.1.1	Baseline <i>Exposure system 1</i>	59
3.1.2	Baseline <i>Exposure system 2</i>	59
3.1.3	Baseline <i>Exposure system 3</i>	62
3.2	SAR measurements	64
3.2.1	Relationship between conductivity and SAR	65
3.2.2	Relationship between sample height and SAR	67
3.3	Relaxation of temperature to baseline	70
3.3.1	Exposure system 2-Experimentally derived temperatures	70
3.3.2	Exposure system 2-Computationally derived temperatures	72
3.3.3	Exposure system 2-Average temperature over six minutes	72
<b>CHAPTER 4</b>	<b>PREPARATIVE EXPERIMENTS</b>	<b>77</b>
4.1	Alcohol dehydrogenase (ADH)	77
4.2	Bovine serum albumin (BSA)	78
4.3	Insulin	79
4.4	Purification of $\alpha$ -crystallin	79
4.4.1	Stability of $\alpha$ -crystallin	81
4.5	Light scattering profiles	81
<b>CHAPTER 5</b>	<b>LIGHT SCATTERING EXPERIMENTS MICROWAVE EXPOSURE IN EXPOSURE SYSTEM 1</b>	<b>85</b>
5.1	Apo alcohol dehydrogenase (ADH)	85
5.2	Catalase	87
5.3	Citrate synthase (CS)	89
5.4	Reduced apo $\alpha$ -lactalbumin	91
5.5	Summary of results	93
<b>CHAPTER 6</b>	<b>LIGHT SCATTERING EXPERIMENTS MICROWAVE EXPOSURE IN THE TEM CELL</b>	<b>95</b>
6.1	Apo alcohol dehydrogenase (ADH)	95
6.2	Summary of results	100
<b>CHAPTER 7</b>	<b>LIGHT SCATTERING EXPERIMENTS MICROWAVE EXPOSURE IN EXPOSURE SYSTEM 2</b>	<b>101</b>
7.1	Apo alcohol dehydrogenase (ADH)	101
7.1.1	Apo ADH at 37°C	101
7.1.2	Effect of number of pulse periods on precipitation	103
7.1.3	Holo ADH at 45°C and 60°C	104
7.2	Bovine serum albumin (BSA)	106
7.2.1	Reduced BSA at 45°C	106
7.2.2	Reduced BSA at high concentration, 37°C	108
7.2.3	Oxidised BSA at high concentrations, 50°C and 60°C	109
7.3	Catalase	111

7.3.1	Catalase at 42°C	111
7.4	Citrate synthase (CS)	113
7.4.1	CS at 37°C	113
7.4.2	CS at 42°C	115
7.5	Insulin	117
7.5.1	Reduced insulin	117
7.6	$\alpha$ -Lactalbumin	121
7.6.1	Reduced apo $\alpha$ -lactalbumin	121
7.6.2	Reduced holo $\alpha$ -lactalbumin	123
7.7	Lysozyme	123
7.7.1	Reduced lysozyme	123
7.8	Ovotransferrin	125
7.8.1	Reduced ovotransferrin	125
7.8.2	Oxidised ovotransferrin	128
7.9	Summary and interpretation of results	129
7.9.1	The effect of pulsed microwaves on temperature	131
7.10	Statistical analysis of results and testing of hypotheses	133
7.10.1	Analysis of reduced BSA (1.5 mg/ml)	136
7.10.2	Analysis of CS at 37°C compared to 42°C	138
7.10.3	Analysis of Insulin (reduced)	139
7.11	Controlling for small differences in average temperature between exposed and control samples	140
7.12	Diffusion of protein molecules during experiments	141
7.12.1	Calculation of translational movement	141
<b>CHAPTER 8</b>	<b><i>LIGHT SCATTERING EXPERIMENTS MICROWAVE EXPOSURE IN EXPOSURE SYSTEM 3</i></b>	<b>145</b>
8.1	Constant temperature vs. temperature excursions	145
8.1.1	Reduced apo alcohol dehydrogenase (ADH)	145
8.1.2	Citrate synthase (CS)	147
8.1.3	Summary of results	149
<b>CHAPTER 9</b>	<b><i>PROTEIN CONFORMATIONAL STUDIES MICROWAVE EXPOSURE IN EXPOSURE SYSTEM 2 AND 3</i></b>	<b>151</b>
9.1	Circular dichroism studies	151
9.1.1	Catalase	152
9.1.2	Citrate synthase (CS) at 42°C	154
9.1.3	$\alpha$ -Lactalbumin	157
9.1.3.1	Reduced apo $\alpha$ -lactalbumin	158
9.1.3.2	Reduced holo $\alpha$ -lactalbumin	162
9.2	Fluorescence studies	165
9.2.1	Intrinsic fluorescence citrate synthase at 37°C	166
9.2.2	Extrinsic fluorescence citrate synthase at 37.5°C	168
9.3	Electrospray mass spectrometry	169
9.3.1	Apo $\alpha$ -lactalbumin	171

9.4	Interpretation of results on protein conformational studies	174
-----	---	-----

---

<b>CHAPTER 10</b>	<b><i>ADDITIONAL STUDIES</i></b>	<b>177</b>
-------------------	----------------------------------	------------

---

10.1	Effect of CO <sub>2</sub> on unfolding	177
10.1.1	Alcohol dehydrogenase	177
10.1.2	Ovotransferrin	179
10.2	Effect of molecular crowding on ovotransferrin precipitation	182

---

<b>CHAPTER 11</b>	<b><i>ELECTRIC FIELD EXPOSURE</i></b>	<b>185</b>
-------------------	---------------------------------------	------------

---

11.1	Application of DC electric field	185
11.1.1	Citrate synthase	185
11.1.2	Alcohol dehydrogenase (ADH)	190
11.2	Application of a DC field followed by microwave exposure	191
11.2.1	Citrate synthase (CS)	191
11.3	Application of an AC field	192
11.3.1	Citrate synthase (CS)	192
11.4	Summary of results	194

---

<b>CHAPTER 12</b>	<b><i>CONCLUSIONS AND FUTURE DIRECTIONS</i></b>	<b>197</b>
-------------------	---	------------

---

<b><i>REFERENCES BY NUMBER</i></b>	<b>2134</b>
------------------------------------	-------------

<b><i>REFERENCES BY NAME</i></b>	<b>227</b>
----------------------------------	------------

<b><i>APPENDICES</i></b>
--------------------------

## LIST OF FIGURES

<b>CHAPTER 1</b>	<b>INTRODUCTION</b>	
Figure 1.1	Schematic overview of DNA encoding for the synthesis of a protein	2
Figure 1.2	Ubiquitin mediated proteolysis and its role in biological functions	4
Figure 1.3	Schematic diagram of interaction of sHsps with unfolding proteins	6
Figure 1.4	A schematic overview of the conformational states a protein can sustain	7
Figure 1.5	Fibril formation of A $\beta$ 40, the major component of Alzheimer's disease fibrils	9
Figure 1.6	A snapshot of one wave travelling at the speed of light	10
Figure 1.7	The electromagnetic spectrum	11
Figure 1.8	Hysteresis between the applied field and the induced electric field	14
 <b>CHAPTER 2</b>	 <b>EXPERIMENTAL</b>	
	Flowchart of experimental design	22
Figure 2.1	Ribbon structure of bacterial alcohol dehydrogenase	23
Figure 2.2	Ribbon structure of human serum albumin	24
Figure 2.3	Ribbon structure of bovine liver catalase	25
Figure 2.4	Ribbon structure of porcine citrate synthase	25
Figure 2.5	Ribbon structure of bovine insulin	26
Figure 2.6	Structure of apo bovine $\alpha$ -lactalbumin	27
Figure 2.7	Ribbon structure of hen egg-white lysozyme	28
Figure 2.8	Ribbon structure of hen egg-white ovotransferrin	29
Figure 2.9	View of the remodelled oven during a pulse period	33
Figure 2.10	TEM cell inside the incubator with equipment to generate 900 MHz	33
Figure 2.11	Schematic view of the cooling conditions for hydrogen exchange experiments	36
Figure 2.12	Schematic overview of the three exposure systems employed during the project	38
Figure 2.13	View of cavity of the microwave oven, <i>Exposure system 1</i>	39
Figure 2.14	View of microwave oven placed inside the incubator, <i>Exposure system II</i>	40
Figure 2.15	Diagram of the experimental procedure <i>Exposure system 2</i>	42
Figure 2.16	Exposure set up <i>Exposure system 2</i>	43
Figure 2.17	View of the microwave oven in <i>Exposure system 2</i>	43
Figure 2.18	View of microwave oven in close proximity of dry block heater	44
Figure 2.19	View of block heater and DC power equipment	45
Figure 2.20	View of the instruments used for the AC field experiment	46
Figure 2.21	Diagram of the expected temperature profile over a six minute period of a sample exposed to pulsed microwaves	47
Figure 2.22	View of the Cary spectrophotometer and the multicell holder	48
Figure 2.23	View of method of SAR calibration	50
Figure 2.24	The distribution of a normal population	54
Figure 2.25	Schematic overview of enzymatic role of citrate synthase in the TCA cycle	55

<b>CHAPTER 3</b>	<b>TEMPERATURE ASSESSMENT</b>	
Figure 3.1	Temperature of buffer in a quartz cuvette placed in different positions in the multi-cell holder of the spectrophotometer	61
Figure 3.2	Profile of baseline temperature for cells 5 and 6 in the multi-cell holder when the software temperature was set to 43°C	62
Figure 3.3	Profile of temperature of buffer in cells 1 and 4 of heating block when dial was set to “50°C	63
Figure 3.4	Temperature of a buffer solution exposed to pulsed microwaves during a 50 minute period	64
Figure 3.5	Relationship between conductivity and SAR	66
Figure 3.6	Relationship between conductivity and SAR, polynomial curve	66
Figure 3.7	The specific absorbance rate (SAR) of the various buffer systems as a function of sample height	67
Figure 3.8	SAR at the position of the light beam (13-19 mm from base of cuvette) Buffer and exposure conditions I and II	68
Figure 3.9	SAR at the position of the light beam (13-19 mm from base of cuvette) Buffer and exposure conditions III and IV	69
Figure 3.10	Temperature profile of an exposed and control sample that was returned to the incubator after one exposure of microwave pulses	70
Figure 3.11	Temperature profiles of two 1.0 ml 80mM phosphate buffer solutions during a six minute exposure period	74
Figure 3.12	Six minute temperature profile of buffer/exposure condition I	74
Figure 3.13	Six minute temperature profile of buffer/exposure condition II and III-37°C	75
Figure 3.14	Six minute temperature profile buffer/exposure condition III-45°C and IV	76
<b>CHAPTER 4</b>	<b>PREPARATIVE EXPERIMENTS</b>	
Figure 4.1	Effect of storage on ADH unfolding	77
Figure 4.2	Effect of storage on BSA unfolding	78
Figure 4.3	Effect of storage on insulin unfolding	79
Figure 4.4	Typical separation of crystallin proteins by size exclusion	80
Figure 4.5	Separation of $\alpha$ -crystallin on a size exclusion column	80
Figure 4.6	Suppression of 1.5 mg/ml BSA, 20 mM DTT in 0.1 M phosphate buffer, 0.1 M NaCl incubated at 45°C by $\alpha$ -crystallin at the molar ratio of 1:0.1	81
Figure 4.7	Examples of precipitation profiles of three different proteins	82
Figure 4.8	Free energy change $\Delta G$ for the initial stages of protein aggregation	83



<b>CHAPTER 5</b>	<b>LIGHSCATTERING EXPERIMENTS</b>	
	<b>MICROWAVE EXPOSURE IN <i>EXPOSURE SYSTEM 1</i></b>	
Figure 5.1	Exposure of 0.5 mg/ml ADH at 37°C to 3.2 seconds of pulsed 2.450 GHz every 6 minutes, for 20 hours at 37°C	86
Figure 5.2	Sham exposure experiment on 2 x 1.0 ml of 0.5 mg/ml ADH pH 7 at 37°C	86
Figure 5.3	Exposure of 0.4 mg/ml catalase to 3.2 seconds of pulsed 2.450 GHz every 6 minutes, for 30 hours	87
Figure 5.4	Exposure of 0.8 mg/ml catalase to 3.2 seconds of pulsed 2.450 GHz every 6 minutes, for 30 hours	88
Figure 5.5	Sham exposure experiment on CS at 37°C	89
Figure 5.6	Exposure of CS to pulsed microwaves of 3.2 seconds duration every six minutes for 43 and 92 hours	90
Figure 5.7	The enzymatic activity of 0.4 mg/ml CS samples at 37°C	91
Figure 5.8	$\alpha$ -Lactalbumin, pH 7, exposed to pulsed 2.450 GHz at 37°C	92
Figure 5.9	$\alpha$ -Lactalbumin, pH 2, exposed to pulsed 2.450 GHz	92
<b>CHAPTER 6</b>	<b>LIGHSCATTERING EXPERIMENTS</b>	
	<b>MICROWAVE EXPOSURE IN THE TEMCELL</b>	
Figure 6.1	Exposure of large volume of ADH to pulsed microwaves	96
Figure 6.2	Exposure of ADH in TEM cell	97
Figure 6.3	Exposure of ADH in TEM cell with the supply of CO <sub>2</sub> disconnected	97
Figure 6.4	Profile of temperature loss in incubator	98
Figure 6.5	Sham experiment in TEM cell	99
<b>CHAPTER 7</b>	<b>LIGHSCATTERING EXPERIMENTS</b>	
	<b>MICROWAVE EXPOSURE IN <i>EXPOSURE SYSTEM 2</i></b>	
Figure 7.1	Incubation of four samples of 0.5 mg/ml ADH at 37°C	102
Figure 7.2	ADH incubated at 37°C and exposed to 2.450 GHz in the presence of $\alpha$ -crystallin	103
Figure 7.3	Exposure of ADH to 2, 8 or 15 pulse periods of 2.450 GHz at 37°C	104
Figure 7.4	Exposure of ADH to 7 pulse periods of 2.450 GHz at 45°C	105
Figure 7.5	Exposure of ADH to 4 pulse periods of 2.450 GHz at 60°C	106
Figure 7.6	Incubation of four samples of 1.5 mg/ml BSA at 45°C	107
Figure 7.7	BSA (reduced) incubated at 45°C and exposed to pulsed 2.450 GHz in the presence of $\alpha$ -crystallin	108
Figure 7.8	Exposure of 50 mg/ml BSA (reduced) to pulsed 2.450 GHz at 37°C	109
Figure 7.9	Exposure of 45 mg/ml BSA (oxidised) to pulsed 2.450 GHz at 60°C	110
Figure 7.10	Exposure of 45 mg/ml BSA (oxidised) to pulsed 2.450 GHz at 50°C	110
Figure 7.11	Incubation of four samples of 0.2 mg/ml catalase at 42°C	112
Figure 7.12	Catalase incubated at 42°C and exposed to pulsed 2.450 GHz in the presence of $\alpha$ -crystallin	113
Figure 7.13	CS exposed to 15 pulse periods of 2.450 GHz at 37°C	114

Figure 7.14	CS exposed to 8 pulse periods of 2.450 GHz in the presence of $\alpha$ -crystallin at 37°C	114
Figure 7.15	Effect of small temperature differences on CS aggregation	115
Figure 7.16	CS incubated at 42°C and exposed to pulsed 2.450 GHz in the presence of $\alpha$ -crystallin	116
Figure 7.17	Incubation of four samples of 0.25mg/ml insulin at 19 and 25°C	118
Figure 7.18	Insulin incubated at 25°C and exposed to pulsed 2.450 GHz in the presence of $\alpha$ -crystallin	119
Figure 7.19	Insulin exposed to 2 and 10 pulse periods of 2.450 GHz at 19°C	120
Figure 7.20	Apo $\alpha$ -Lactalbumin exposed to 5 pulse periods of 2.450 GHz at 36°C	121
Figure 7.21	Apo $\alpha$ -Lactalbumin exposed to pulsed 2.450 GHz at room temperature	122
Figure 7.22	Holo $\alpha$ -lactalbumin exposed at 32°C to 5 pulse periods of 2.450 GHz	123
Figure 7.23	Lysozyme exposed to 15 pulse periods of 2.450 GHz at 30°C in the presence of $\alpha$ -crystallin	124
Figure 7.24	The light scattering measurements for samples in Figure 7.23 continued	124
Figure 7.25	Incubation of four samples of ovotransferrin at 45°C	125
Figure 7.26	The initial rate of precipitation of four samples of ovotransferrin	126
Figure 7.27	Ovotransferrin exposed to pulsed 2.450 GHz at 45°C, 50°C and 60°C	127
Figure 7.28	Ovotransferrin exposed to pulsed 2.450 GHz in the presence of $\alpha$ -crystallin	128
Figure 7.29	Ovotransferrin exposed to 8 pulse periods of 2.450 GHz at 65°C	129
Figure 7.30	Thermal unfolding of oxidised and reduced BSA as determined by ellipticity at 224 nm	137
Figure 7.31	Thermal unfolding of CS as determined by ellipticity at 222 nm	139
Figure 7.32	The initial rate of precipitation of CS vs. temperature	140
<b>CHAPTER 8</b>	<b>LIGHSCATTERING EXPERIMENTS</b>	
	<b>MICROWAVE EXPOSURE IN EXPOSURE SYSTEM 3</b>	
Figure 8.1	The effect of constant temperature compared to a transient microwave induced temperature increase on the aggregation and precipitation of ADH at 45°C	146
Figure 8.2	The effect of temperature on the initial rate of precipitation for four samples of ADH incubated in either the spectrophotometer or the heating block	146
Figure 8.3	The effect of constant temperature compared to transient microwave induced temperature increase on the aggregation and precipitation of CS at 42°C	148
Figure 8.4	The effect of temperature on the initial rate of precipitation for the four samples of CS in Figure 8.3	148
<b>CHAPTER 9</b>	<b>PROTEIN CONFORMATION STUDIES</b>	
	<b>MICROWAVE EXPOSURE IN EXPOSURE SYSTEM 2 AND 3</b>	
Figure 9.1	Far UV CD spectrum of 0.2 mg/ml catalase at 22°C of	153
Figure 9.2	Far UV CD spectrum of CS at 22°C	155
Figure 9.3	Far UV CD spectrum at 22°C of 0.2 mg/ml CS incubated at 42°C and exposed to 10 pulse periods of 2.450 GHz	159

Figure 9.4	Near UV CD spectra of apo- $\alpha$ -lactalbumin exposed to pulsed 2.450 GHz	161
Figure 9.5	Far UV CD spectra of holo- $\alpha$ -lactalbumin exposed to pulsed 2.450 GHz	163
Figure 9.6	Near UV CD spectra of holo- $\alpha$ -lactalbumin exposed to pulsed 2.450 Gz	165
Figure 9.7	Tryptophan fluorescence of CS exposed to pulsed 2.450 GHz	166
Figure 9.8	Tryptophan fluorescence of CS exposed to pulsed 2.450 GHz at high power	167
Figure 9.9	ANS binding of CS exposed to pulsed 2.450 GHz.	169
Figure 9.10	Hydrogen exchange of apo $\alpha$ -lactalbumin after initial incubation in D <sub>2</sub> O	171
Figure 9.11	Plot of kinetics from data in Figure 9.10	172
Figure 9.12	Hydrogen exchange of apo- $\alpha$ -lactalbumin after dilution into D <sub>2</sub> O	173
Figure 9.13	Hydrogen exchange of apo- $\alpha$ -lactalbumin after exposure to pulsed 2.450 GHz	173
<b>CHAPTER 10</b>	<b>ADDITIONAL STUDIES</b>	
Figure 10.1	Exposure of ADH with CO <sub>2</sub> bubbled through the solution, to pulsed 2.450 GHz at 37°C	178
Figure 10.2	Exposure of ovotransferrin, with CO <sub>2</sub> bubbled through solution, to pulsed 2.450 GHz at room temperature	180
Figure 10.3	Exposure of ovotransferrin in the presence of 20% dextran to pulsed 2.450 GHz at 45°C	182
<b>CHAPTER 11</b>	<b>ELECTRIC FIELD EXPOSURE</b>	
Figure 11.1	Exposure of CS to 10 minutes of 5kV/cm DC at an average temperature of 32.9°C	186
Figure 11.2	Exposure of CS to 10 minutes of 5 and 10 kV/cm DC at 42°C	187
Figure 11.3	Exposure of CS to 10 minutes of 5 and 10 kV/cm DC at room-temperature	188
Figure 11.4	Binding of ANS by CS after exposure to 10 kV/cm DC	189
Figure 11.5	Exposure of CS to 10 minutes of 5kV/cm DC at ~35°C	190
Figure 11.6	Binding of ANS by ADH after exposure to 10 kV/cm DC	191
Figure 11.7	Comparison of CS after electric field and pulsed 2.450 GHz exposure	192
Figure 11.8	Exposure of CS to 10 and 20 minutes of 4kV/cm AC field	193

## LIST OF TABLES

<b>CHAPTER 1</b>	<b>INTRODUCTION</b>	
Table 1.1	Neurodegenerative diseases characterised by protein aggregation	9
Table 1.2	Frequency bands in the RF region	12
Table 1.3	Summary of exposure limits recommended for occupational and general public exposures to 50/60 Hz electric and magnetic fields	15
Table 1.4	Safety guidelines for time varying electric and magnetic fields, set by ICNIRP	16
<b>CHAPTER 3</b>	<b>TEMPERATURE ASSESSMENT</b>	
Table 3.1	Overview of buffer and exposure conditions that were used in experiments	60
Table 3.2	Data for the temperature rise and fall of the 8 pulse periods in Figure 3.4	65
Table 3.3	Experimental temperatures at specific time points of a 1.0 ml solution of 80mM phosphate buffer	71
Table 3.4	Experimental and mathematically derived temperatures over a six minute period	73
<b>CHAPTER 7</b>	<b>LIGHT SCATTERING EXPERIMENTS</b>	
	<b>MICROWAVE EXPOSURE IN EXPOSURE SYSTEM 2</b>	
Table 7.1	Temperature and initial rate of precipitation of four samples ADH	102
Table 7.2	Temperature and initial rate of precipitation of four samples of BSA	107
Table 7.3	Temperature and initial rate of precipitation of four samples of catalase	112
Table 7.4	Temperature and initial rate of precipitation of four samples of CS	116
Table 7.5	Temperature and initial rate of precipitation of four samples of insulin	118
Table 7.6	Temperature and initial rate of precipitation of four samples of ovotransferrin	127
Table 7.7	Initial rate of precipitation and average temperatures of Figure 7.30	127
Table 7.8	Summary of light scattering experiments in Chapter 7	130
Table 7.9	One-tailed $t$ test for the hypothesis $H_0: \mu \leq 1$ and $H_A: \mu > 1$ for light scattering experiments in which one protein sample was exposed to pulsed microwaves and another sample was kept as a control; ADH, BSA, insulin, lysozyme and ovotransferrin	134
Table 7.10	One-tailed $t$ test for the hypothesis $H_0: \mu \leq 1$ and $H_A: \mu > 1$ for light scattering experiments in which one protein sample was exposed to pulsed microwaves and another sample was kept as a control; catalase, CS at 37°C and CS at 42°C	135
Table 7.11	Summary of statistically analysed experiments in Chapter 7	136
Table 7.12	Slope of BSA temperatures between 40 and 70 °C	138
Table 7.13	Calculated hydrodynamic radius of proteins	
<b>CHAPTER 9</b>	<b>PROTEIN CONFORMATION STUDIES</b>	
	<b>MICROWAVE EXPOSURE IN TANDEM WITH CIRCULAR DICHROISM</b>	
Table 9.1	Summary of exposure experiments of $\alpha$ -lactalbumin, monitored by CD	157

<b>CHAPTER 10</b>	<b>ADDITIONAL STUDIES</b>	
Table 10.1	Experimental data for experiment in Figure 10.1	179

**LIST OF ABBREVIATIONS USED**

A	absorbance
AC	alternating current
ADH	alcohol dehydrogenase
ANS	8-anilino-1-naphthalene sulfonate
ARPANSA	Australian Radiation Protection and Nuclear Safety Agency
ATP	adenosine triphosphate
BSA	bovine serum albumin
CD	circular dichroism
CO <sub>2</sub>	carbon dioxide
CS	citrate synthase
CW	continuous wave
Da	dalton
DC	direct current
D,L	dextrorotatory, levorotatory
DNA	deoxyribonucleic acid
D <sub>2</sub> O	deuterated water
DTT	dithiothreitol
EDTA	ethylenediaminetetraacetic acid
EHF	extremely high frequency
ELF	extremely low frequency
EM	electromagnetic
ESI-MS	electrospray mass spectrometry
G	gauss
GHz	giga hertz
HMW	high molecular weight
Hsp	heat shock protein
ICNIRP	International Commission on Non-Ionizing Radiation Protection
Hz	hertz
kHz	kilo hertz
kg	kilogram
km	kilometre
kV	kilo volts
LCZ	electrospray ionization single quadrupole platform
$\alpha$ -La	alpha lactalbumin
$\mu$ l	micro litre
M	molar

mHz	mega hertz
min	minute
ml	millilitre
mm	millimetre
mM	millimolar
ms	millisecond
mRNA	messenger ribonucleic acid
$\mu$ M	micro molar
NaCl	sodium chloride
NaN <sub>3</sub>	sodium azide
NHMRC	National Health and Medical Research Council (Australia)
nm	nanometre
NSW	New South Wales
P	probability
PDB	Protein Data Bank
RF	radio frequency
RNA	ribonucleic acid
S	second
SAR	specific absorption rate
SDS	sodium dodecyl sulphate
SHF	super high frequency
sHsp	small heat shock protein
$\mu$ s	micro second
$\mu$ S	micro Siemens
TEM	transverse electromagnetic mode
TRIS	trisaminomethane
tRNA	transport ribonucleic acid
UHF	ultra high frequency
UV	ultraviolet
V	volts
W	watts
Zn	zinc

**LIST OF APPENDICES**

<b>APPENDIX 1</b>	Buffers	203
<b>APPENDIX 2</b>	Description of electronics microwave oven	204
<b>APPENDIX 3</b>	Conversion factors for the Luxtron Fiber Optic Probes	206
<b>APPENDIX 4</b>	Buffer and exposure conditions I and II	207
<b>APPENDIX 5</b>	Buffer and exposure conditions III and IV	208
<b>APPENDIX 6</b>	Diffusion constant from hydrodynamic data	209
<b>APPENDIX 7</b>	Temperature determinations in multi-cell block	211
<b>APPENDIX 8</b>	Units of circular dichroism	212



## LIST OF PUBLICATIONS

### JOURNALS

- Lindsay, E. A., Berry, Y., Jamie, J. F. and Bremner, J. B. (2000). Antibacterial compounds from *Carissa lanceolata* R.Br. *Phytochemistry* 55, 403-406.
- Berry, Y. and Truscott, R. J. W. (2001). The presence of a human UV filter within the lens represents an oxidative stress. *Experimental Eye Research* 72, 411-421.
- Müller, J. F., Harden, F., Moore, M. R., Berry, Y. and Malisch, R. (2002). 3rd WHO-coordinated exposure study. PCDDS, PCDFS and dioxin-like PCBs in human milk samples from Australia. *Organohalogen Compounds* 56, 321-324.
- Meehan, S., Berry, Y., Luisi, B., Dobson, C. M., Carver, J. A. and MacPhee, C. E. (2004). Amyloid fibril formation by lens crystallin proteins and its implications for cataract formation. *Journal of Biological Chemistry* 279, 3413-9.
- Berry, Y., Bremner, J. B., Davis, A. and Samosorn, S. (2005). Isolation and NMR spectroscopic clarification of the alkaloid 1,3,7-trimethylguanine from the ascidian *Eudistoma maculosum*. *Natural Product Research* (in print).
- Berry, Y. C., McKenzie, D. R., French, P. W. and Carver, J. A. (manuscript in preparation). The enhancement of protein aggregation by pulsed microwave exposure and its suppression by the chaperone action of  $\alpha$ -crystallin.

### CONFERENCE POSTERS AND ABSTRACTS

- Berry, Y. C., Carver, J. A., McKenzie, D. R. and French, P. W. (2002). (2002). *Pulsed microwave radiation facilitates protein aggregation and precipitation*. 27th Annual Lorne Conference on Protein Structure and Function, Lorne.
- Berry, Y., Budi, A., Carver, J., Treutlin, H. and Yarovsky, I. (2002). (2002). *Response of proteins to external non-ionising radiation: An experimental and computer modelling investigation*. 26th Annual Conference Australian Society for Biophysics, Melbourne.
- Berry, Y., Carver, J., George, D., Bilek, M. M. M., McKenzie, D. R. and Dos Remedios, C. (2002). *Experimental studies of temperature and microwave exposure on protein unfolding*. 26th Annual Conference Australian Society for Biophysics, Melbourne.
- Berry, Y. C., Carver, J. A., McKenzie, D. R. and French, P. W. (2003). *Microwave-exposed proteins exhibit enhanced aggregation which is suppressed by the molecular chaperone  $\alpha$ -crystallin*. 28th Annual Lorne Conference on Protein Structure and Function, Lorne.
- Berry, Y. C., Carver, J. A. and McKenzie, D. R. (2004). *Applied electric field increases rate of protein precipitation*. 29th Annual Lorne Conference on Protein Structure and Function, Lorne.

## ABSTRACT

This thesis describes a spectroscopic investigation of the effects of pulsed electromagnetic radiation on the conformation, unfolding, aggregation and precipitation of a variety of proteins. Initial experiments required the calibration of a microwave exposure system thus the temperature of different buffer solutions was studied in detail. The exposure system comprised of an incubator and a rebuilt domestic microwave oven that delivered pulses every six minutes to give a plot of the temperature before, during and after a pulse period of microwaves. All solutions returned to their baseline temperature prior to the next pulse period.

The effect of exposure to microwave pulses of several seconds duration on the aggregation rate of six stressed target proteins (alcohol dehydrogenase, bovine serum albumin, catalase, citrate synthase, insulin and ovotransferrin) was examined in solution. The hypothesis tested was that the initial rate of precipitation of samples exposed to microwave pulses once every six minutes was significantly higher than that of a control held at the same average temperature. The results show statistical significance to confirm the hypothesis in all cases except for insulin, bovine serum albumin and citrate synthase when the latter two proteins were maintained at an average temperature of 45°C and 37°C respectively. In these exceptional cases, the microwave induced temperature excursion was not expected to induce a change in the precipitation rate on the basis of previous knowledge of the unfolding behaviour of the proteins. The second hypothesis tested was that the molecular chaperone,  $\alpha$ -crystallin prevents the aggregation and precipitation of target proteins under the above regimes. It was found that  $\alpha$ -crystallin suppressed precipitation but it was not as effective when proteins were also exposed to pulsed microwaves.

The effect of exposure to 50 Hz DC and AC electric field was examined on stressed alcohol dehydrogenase and citrate synthase. The hypothesis tested was that the initial rate of precipitation of samples exposed to microwave pulses once every six minutes was significantly higher than that of a control held at the same average temperature. This was not detected. When a difference could be detected, it was only observed in a increase or decrease in precipitation, well after exposure.

The results of this thesis are relevant to the setting of standards for microwave exposure as they show that a six-minute averaging period of temperature is not appropriate in the prediction of protein unfolding.

---

## CHAPTER 1

---

### INTRODUCTION

The objective of this PhD project is to establish if pulsed microwaves are capable of inducing a higher rate or a greater extent of conformational change (unfolding) in a target protein compared to a control protein kept at the same average temperature. As an extension to the microwave investigation, the effect of applied low frequency electric fields on protein conformation is examined. There are no previous systematic reports in the scientific literature on conformational studies of proteins *in vitro*, exposed to either a pulsed radio frequency field or an applied low frequency field.

To appreciate the significance of this study it is fundamental to understand how a change in protein conformation *in vitro*, as is the basis of the investigation, is related to processes in a living cell or in the extra cellular compartments. In this chapter are discussed the synthesis of proteins in the cells of higher organisms, protein aggregation and degradation and associated diseases as well as the role of heat shock proteins in preventing protein aggregation.

The nature of electromagnetic radiation and the use of microwaves in the form of pulses are briefly discussed. Demand for escalating rates of information transfer has driven the expansion of the bandwidth available in the GHz range. This has lead to a shift towards the use of these higher frequencies for communications and a rapid increase in exposure of the population. The lack of reliable experimental information on the biological effects of non-ionising radiation at the molecular level and the need to identify plausible mechanisms for effects, have motivated this study.

The aims and hypothesis of this PhD project are presented in section 1.10.

#### 1.1 STRUCTURE OF PROTEINS

Proteins are the central biological molecules in plants, animals and humans. They are formed in

a linear chain of combinations of amino acids of which there are twenty naturally occurring. It is the unique three-dimensional fold which determines the function of a protein in or outside cells. Proteins are structural (hair, tendons, part of cell membranes) or functional in that they perform a host of biochemical processes such as catalysis and regulation (enzymes), transport of other proteins, electrons and molecules, information between cells (hormones), conversion of energy (in muscles), defence (antibodies) etc. <sup>1</sup>. The blueprint for a protein is encoded in the cell's DNA, inside the nucleus. When a particular protein is required, a signal is sent out into the nucleus and a related gene is turned on in the DNA. The enzyme RNA polymerase unwinds the designated region of the DNA and a single stranded copy of this region is formed into a template, called mRNA. (Figure 1.1). This process is called *transcription*.

**Figure 1.1: Schematic overview of DNA encoding for the synthesis of a protein. In the cell's nucleus, the blueprint for a protein is enzymatically copied (RNA polymerase) from a segment of the unwound DNA into mRNA (transcription). With the help of tRNA, each base pair on mRNA is translated, on the ribosome in the cytoplasm, into one of 20 amino acids. The amino acids are then linked together into a polypeptide. The figure was reproduced from The National Health Museum <sup>2</sup>.**

mRNA diffuses out of the nucleus to the ribosome in the cytoplasm where groups of three nucleotides (codon) on the mRNA are translated to a complementary amino acid (Figure 1.1). Amino acids have the common structure  $\text{-NH-CHR-CO-}$ . The amino acids are linked by their amide (NH) and carbonyl (CO) groups into a polypeptide.

The *R* group attached to the central carbon atom is the defining feature of an amino acid. Sequences of amino acids, with the help of molecular chaperones are formed into one of three secondary structures:  $\alpha$ -helices, beta sheets or turns. Amino acids (residues) also form loops between helices and beta sheets. The  $\alpha$ -helix structure has 3.6 amino acid residues per turn and the *R* groups are arranged such that they extend outwards from the backbone of the helix <sup>1</sup>. The tertiary structure of a protein is the result of folding and entwining of the turns, beta sheets and helices and is stabilized by disulphide bonds, hydrophobic and electrostatic interactions such as hydrogen bonding and van der Waals forces. A typical protein requires a few seconds to fold <sup>3</sup>; the rate of folding is known to be greater than the rate of synthesis <sup>3</sup>. The three dimensional folding, and therefore the conformation of the protein, is dependent on the composition of the solvent as the polarity generally compels the hydrophobic amino acid to be buried together into an inner core while most of the hydrophilic amino acids establish hydrogen bonds with surrounding water molecules and thus constitute the exterior of the protein. Changing physical conditions such as temperature and pH does not result in a gradual change in conformation until a threshold is reached and the protein denatures and loses biological function <sup>1</sup>.

## 1.2 PROTEIN TURNOVER

Cells have a high turnover of proteins and there is a continual balance between synthesis and breakdown, which is regulated at all stages. The protein half-life, depending on the function of the protein is in the order of hours, days, months or even years <sup>4</sup> (e.g. crystallin proteins have a half life of a few years <sup>5</sup>). In humans, the daily break down of proteins and re-synthesis in the body is ~ 400 grams; this estimate takes into account consumption of ~ 100 grams through food and elimination of ~100 grams in catabolism and excretion <sup>4</sup>. Proteins that exist outside the cell are degraded by proteases inside lysosomes. Intracellular proteins are degraded (proteolysed) via the three-enzyme ubiquitin-proteasome pathway. Proteins from food in-take (“foreign” proteins) are broken down to amino acids in the lumen of the gastrointestinal tract and are absorbed and utilised by the cells for protein synthesis <sup>5</sup>.

The reason for some proteins being eliminated when their structure is stable and the protein still functional could arise from the efficient management of amino acids in the cell. One of the mechanisms of eliminating unwanted proteins is through the ubiquitin-proteasome pathway which is involved in the break down of a myriad of functional proteins (Figure 1.2). When a protein is no longer required, it is targeted for degradation by one of the enzymes in the pathway (E3). This may require modification of the target protein or of the E3 enzyme itself <sup>5</sup>. The protein is then tagged by the attachment of at least four ubiquitin proteins <sup>6</sup> that are covalently bonded to the protein by enzymes, in several steps. The ubiquitin tag is recognized by the proteasome, the degradation complex, which removes the ubiquitin proteins for recycling and degrades the target protein to short peptides of 7 to 9 amino acids <sup>7</sup>. The ubiquitin system recognizes mutated, misfolded and denatured proteins, which it selectively degrades. It appears that about 30% of protein synthesis is erroneous in amino acid composition so that folding cannot proceed <sup>5</sup>.

**Figure 1.2: Ubiquitin mediated proteolysis and its role in many biological functions as described in text. Reproduced from Kungl Vetenskapakademien, The Royal Swedish Academy of Sciences <sup>7</sup>.**

Ubiquitin proteins are heat-inducible; it has been found that the intracellular concentration of ubiquitin is increased during cell stress <sup>8</sup>. The ubiquitin pathway is known to also have

important post-translational functions such as cell-cycle progression, differentiation, apoptosis, transcriptional regulation, DNA repair etc <sup>6</sup>. *In vitro*, the proteasome or subunits of the complex have been found to act like a molecular chaperone by binding to unfolded proteins, assisting in the refolding and subsequent release in their native form <sup>5;9</sup>.

### 1.3 THE ROLE OF MOLECULAR CHAPERONES

The initial discovery that certain proteins are activated in organisms in response to elevated temperatures led to the term heat-shock proteins (Hsps). Since then, research has shown that the heat-shock response is highly conserved throughout evolution as a mechanism to protect cells from harmful conditions <sup>8</sup>. In addition to thermal stress, Hsps are expressed as a result of cellular stress caused by a range of conditions such as oxidation, heavy metals, fever, inflammation and alcohol <sup>10</sup>, osmotic variations or hormonal stimuli <sup>11</sup>.

The Hsps are classified into two protein families: proteases that assist in degradation of misfolded proteins and molecular chaperones that assist during synthesis, folding, transport <sup>12</sup> and refolding <sup>6 10</sup>. Both families have in common that, *in vivo*, they recognize and stabilize partially folded proteins intermediates <sup>13</sup>. They are mostly named after the mass of their monomeric subunits: Hsp70, Hsp60, Hsp90, Hsp100 and small heat shock proteins (sHsps) <sup>11</sup>. The sHsps, up to 40 kDa in size, contain the core conserved  $\alpha$ -crystallin domain, of 80-100 amino acids that is located in the C-terminal region <sup>14 15</sup>.  $\alpha$ -Crystallin, the major eye lens protein that is composed of two related subunits  $\alpha A$  and  $\alpha B$ , is a sHsp<sup>16</sup>. sHsps interact with target proteins which are on their off folding pathway as compared to other Hsps, e.g. Hsp 70 and GroEl that interact on the on-off folding pathway (Figure 1.3).

The cell is crowded with many organelles, proteins and numerous ribosomes from which nascent proteins emerge. In this environment, hydrophobic amino acid residues of a growing polypeptide chain are in close contact with hydrophobic residues of other emerging chains so that the hydrophobic attraction between chains is potentially high. The result of such interactions can lead to protein mis-folding and aggregation. Molecular chaperones, often in cooperation with other chaperones <sup>17</sup>, weakly bind to one or more hydrophobic regions of a



peptide chain (see the emerging chain in Figure 1.1) and thereby assist proteins in folding correctly<sup>18</sup>. Besides recognizing hydrophobic interactions between residues of different proteins, molecular chaperones in general intercept hydrophobic attractions and unstructured regions within single proteins.<sup>17</sup> Some chaperones form a cage, e.g. the GroEL-GroES system in *E.coli*, in which the nascent protein folds in an enclosed environment created by the cage, rather than in the cytoplasm<sup>19</sup>. Figure 1.3 illustrates the role of sHsps in the prevention of protein aggregation.

**Figure 1.3: Schematic diagram of interaction of sHsps with unfolding proteins. The folding, unfolding and off-folding pathways of proteins occurs via intermediately folded molten globule states, e.g.  $I_1$  and  $I_2$  (discussed in section 1.4). The intermediates exhibit significant secondary but little tertiary structure and are reversible states between the native and unfolded protein. Under stress conditions, the more unfolded  $I_2$  intermediate has the potential to aggregate, which may be prevented by the presence of sHsps. Reproduced from Treweek, Morris and Carver<sup>11</sup>.**

#### 1.4 PROTEIN AGGREGATION AND ASSOCIATED NEURODEGENERATIVE DISEASES

*In vitro* experiments that studied the folding and unfolding of proteins have led to the understanding that under normal physiological conditions, the structure of globular proteins represents a mixture of conformations ranging from folded to multiple unfolded conformations due to structural fluctuations (the so called conformational breathing), with a prevalence for the folded state<sup>20</sup>. The folding/unfolding pathway of proteins (Figures 1.3 and 1.4) occurs via short-lived intermediate species that are often described as molten globule states. Of these, the molten

globule  $I_2$  state is less structured and stable than  $I_1$  and has the propensity to aggregate (Figure 1.3) <sup>21</sup>. The molten globule states exhibit secondary structure content similar to the native protein but lack defined tertiary structure. They are about 10-30% expanded and their hydrophobic core has increased solvent accessibility <sup>22; 23</sup>. Molecular chaperones are attracted to the unfolded and exposed hydrophobic regions of these intermediate species and thereby prevent their aggregation. For some chaperones, this interaction enables the protein to fold correctly with the input of energy (coupled with the hydrolysis of ATP). However if the conditions are such that chaperones are in short supply or the degradation complex becomes deficient, the equilibrium will be shifted towards aggregation. There is evidence that, if the ubiquitin-proteasome system (see section 1.2) is impaired the degradation process collapses. This impairment could occur for example by mutation in a proteasome subunit <sup>24; 25</sup>, in ubiquitin ligases <sup>6</sup>, by over expression of aggregation prone proteins <sup>26</sup> or when molecular chaperones are engaged elsewhere <sup>27</sup>.

The unfolding proteins either become disordered aggregates or they form fibrils (Figure 1.4).

**Figure 1.4: A schematic overview of the conformational states that a protein can sustain, starting from the emerging peptide chain on the ribosome. With the help of chaperones a chain proceeds from unfolded, U, to intermediate, I to the correctly folded native state, N. In the unfolded and partially folded states, the protein is prone to aggregate or can enter the pathway to form amyloid fibrils in Figure 1.3 where the I state is further divided between  $I_1$  and  $I_2$ . Reproduced from Dobson <sup>28</sup>. Note that fibre formation from the native state of a protein is the underlying process into formation of structural proteins such as keratins, collagen, silks and insect fibres.**

The distinction between these two pathways is thought to lie in the nature of the unfolded region<sup>29; 30</sup>. If a beta region is partially unfolded, it may form structured associations with  $\beta$ -strands thus inducing these intermediates towards amyloid formation<sup>28</sup>. Once the fibril formation has been initiated, the process occurs at a fast rate as has been confirmed by the seeding of protein solutions with existing amyloid fibrils<sup>28; 31</sup>. The term *amyloid* comes from the mistaken identity of the initial discovery of protein plaques in tissues, as starch (*amyl*) like (*oid*)<sup>32</sup>.

The ability to form amyloid fibrils is believed to be an inherent property of proteins<sup>28</sup> and occurs under appropriate partially denaturing conditions such as pH and temperature. Proteins such as  $\alpha$ -crystallin<sup>33</sup>, insulin<sup>34</sup>,  $\alpha$ -lactalbumin<sup>30</sup> and lysozyme<sup>35 34</sup> have been found to form insoluble fibrils *in vitro*. However, proteins that are found to be amyloidogenic *in vitro* are not as a rule found to form amyloid fibres *in vivo*. Amyloid fibrils are rich in crossed parallel and anti-parallel  $\beta$ - sheets held together by hydrogen bonds<sup>31; 36</sup>. sHsps are known to prevent aggregation and fibril formation<sup>6; 27; 37; 38</sup> and have been found in a cooperative action by Hsp 104, Hsp 70 and Hsp 40 to solubilize denatured and aggregated proteins<sup>39</sup>.

Protein aggregation is the underlying cause of age-related nuclear cataract in the eye<sup>40; 41</sup>. The crystallins exist in the mammalian lens as three types:  $\alpha$ ,  $\beta$  and  $\gamma$  and are found in high concentrations (33% in the human lens and 50% in bovine lenses)<sup>42</sup>. The transparency of the lens is maintained by way of the chaperone action of  $\alpha$ -crystallin to prevent aggregation of proteins. Proteins of healthy lenses are water soluble but with age the water soluble crystallin fraction is greatly reduced due to binding of crystallins to UV filters<sup>43</sup>, membrane proteins<sup>44; 45</sup> or to crystallin modifications such as oxidation or deamidation<sup>46-48</sup>.

*In vivo*, amyloid deposits are found intracellularly and in extra cellular space. Isolated amyloid fibrils, as well as fibrils formed *in vitro*, are generally identified by staining with the dye Congo Red, thioflavin T, X-ray diffraction and Electron Microscopy<sup>36</sup>. Fibril formation has been associated with many neurodegenerative diseases that can be characterised as a group of late-onset progressive diseases in which symptoms vary widely: for example, dementia in Alzheimer's disease (AD), uncontrolled movements in Huntington's disease (HD), the inability

**Figure 1.5: Electron microscope images of fibril formation of A $\beta$ 40 a 40-43 residue peptide that is the major component of Alzheimer's disease fibrils <sup>49</sup>, occurs via intermediate oligomeric forms (protofibrils and pores) that are less stable but more toxic than the fibril. Reproduced from Caughey and Lansbury <sup>50</sup>.**

**Table 1.1: Neurodegenerative diseases characterised by protein aggregation. Reproduced from Caughey and Lansbury <sup>50</sup>.**

to initiate movement in Parkinson's disease (PD), and severe insomnia in fatal familial insomnia<sup>50</sup>. The onset of these diseases is marked by a genetic or environmental trigger that causes expression of a precursor disease protein<sup>51</sup>, for example the peptide A $\beta$ 40 in Alzheimer's disease (Figure 1.5), that forms soluble toxic intermediate protofibrils and pores<sup>50; 52</sup>. These intermediates have the ability to exist in solution for long times and are dependent on equilibrium forces for formation of amyloid fibres (Figure 1.4)<sup>6; 28</sup>. The underlying fibril morphology of stacked  $\beta$ -sheets is almost identical between the diseases even though the precursor proteins lack primary or tertiary structural homology<sup>49</sup>. Table 1.1 was reproduced from Caughey and Lansbury<sup>50</sup> and shows the type of fibril formation (pathology) associated with various diseases.

## 1.5 THE ELECTROMAGNETIC SPECTRUM

Electromagnetic radiation is emitted from natural sources such as the sun, stars and planets and man-made sources such as radar, power lines, radio and television transmitters and microwave ovens. The energy is in the form of photons, which are quanta of energy ( $E = h.v$ )<sup>\*</sup> that travel at the speed of light and behave as particles in a wavelike manner (Figure 1.6). Photons have both an electric and a magnetic field that are perpendicular to each other.

**1.6: A snapshot of one wave travelling at the speed of light. The blue and red arrows represent the magnetic and electric fields respectively. The strength of the wave varies along the propagation which is indicated by the different lengths of the arrows. Reproduced from<sup>53</sup>.**

---

<sup>\*</sup> h is Planck's constant  $6.62618 \times 10^{-34}$  J·s  
 v is frequency in seconds;  $s^{-1} = 1$  Hertz (Hz)  
 c is the speed of light,  $2.9979250 \times 10^8$  ms<sup>-1</sup>

The amplitude of the waves varies along the propagation direction, as indicated by the different lengths of the arrows in Figure 1.6. The number of wavelengths of the same strength to pass a particular point in one second is called the frequency ( $\nu$ ) and the relationship between wavelength ( $\lambda$ ) and frequency is expressed as:  $c = \lambda \cdot \nu$ .

If the energy of the photon is sufficient to release electrons from bonded to non-bonded energy levels, the term *ionizing radiation* is used. If the energy is not high enough to break covalent bonds, the energy is termed *non-ionizing*. The threshold for the onset of the ionization process, for molecular systems in the cell, occurs in the visible region of the electromagnetic spectrum. In this project the radiation of interest, at the frequencies in the GHz range and below, is considered to be non-ionizing.

Figure 1.7 shows the electromagnetic spectrum that groups the wavelengths by energy and identifiable objects of similar size.

**Figure 1.7: The electromagnetic spectrum showing the grouping of the wavelengths by energy and their size relative to defined objects. Reproduced from NASA <sup>54</sup>.**

The annotation given to bands (e.g. the visible spectrum is the band of wavelengths between 700 to 400 nanometers) is a historical development. The spectrum from 3 kHz to 300 GHz is referred to as the radiofrequencies. The generic term “radiowaves” is given to frequencies from 3 kHz to 300 MHz and “microwaves” are given to the frequencies in UHF, SHF and EHF

bands; microwaves are typically in the range from 0.1 to 100 cm. Table 1.2 was adapted from<sup>55-57</sup> and provides an easy reference to the terminology of this field.

**Table 1.2 : Frequency bands in the RF region. Adapted from Young<sup>56</sup>.**

## **1.6 BIOLOGICAL INTERACTIONS WITH ELECTROMAGNETIC RADIATION**

The frequency of sunlight lies in the infrared region and has a wavelength of between 0.2 and 2.6  $\mu\text{m}$ . The energy of sunlight is perceived as warmth on the skin and is utilized by molecules in the skin of higher animals to synthesize vitamin D3 whilst plants use this particular energy for photosynthesis. The visible spectrum ranges from 700 to 400 nm and this energy interacts with the human retina to give sight. Photons with wavelengths smaller than 100 nm such as ultraviolet, X rays and gamma rays (ionizing radiation) are considered harmful to life forms and are mostly intercepted by the ozone layer around the earth. Humans, animals and plants have thus evolved in synergy with the cosmic and solar background electromagnetic radiation that reaches the biosphere. Man-made radiation is new in the physiological environment on the time scale of human evolution. The effect of non ionising radiation is an active area of research and has been the subject of many inquiries around the world to establish if man-made radiation causes health risks<sup>58-65</sup>. Microwaves have important applications in the medical field<sup>66; 67</sup>. For

example, hyperthermia, a treatment that applies heat directly to tumours using a microwave source, has proved to be successful in synergy with radiotherapy or chemotherapy<sup>55; 68</sup>.

### **1.6.1 BIOLOGICAL INTERACTIONS WITH EXTREMELY LOW FREQUENCY FIELDS**

A 50 Hz field, generated by electrical devices produces an electromagnetic wave with a wavelength of almost 6000 km (see Figure 1.6). The energy carried by these waves is quite small compared to the energy transferred by the electric currents that cause them. For example, the power radiated by transmission lines, although amounting to a considerable loss over many hundreds of kilometres, is very small compared to the power carried by the transmission lines. The electric and magnetic fields generated by low frequency power lines and similar currents are considerably separated and low in energy however they are locally intense. The radiowaves do not produce a heating effect but may induce, independently, weak electric currents in biological tissue<sup>69</sup>. It is these non-radiative local fields that are important in the interactions with biological systems at very low frequencies. The electric field is expressed in units of V/m and the magnetic field in Gauss (1 Tesla is 10,000 Gauss). An electric field can be shielded by conductive materials such as metal whereas the magnetic field passes through most materials. The typical magnetic field of an overhead transmission power line that carries 230 kV, measured directly under the line, is 57.5 mGauss<sup>233</sup>. The electric field at the same position is typically 2 kV/m<sup>70</sup>. Some epidemiological studies suggest a link between childhood leukaemia and electrification of human dwellings<sup>60; 71; 72</sup>.

### **1.6.2 BIOLOGICAL INTERACTIONS WITH MICROWAVES**

Microwaves produce molecular rotation and torsion<sup>73</sup>; the energy delivered to a solution or biological tissue is dependent on the exact frequency, the dielectric property of the molecules in the solution or tissue and the “hysteresis between the applied field and the induced electric field”<sup>55</sup>, also called the dielectric loss factor. For example, water is a polar dielectric solvent with a high dipole moment. In the presence of a microwave field, the dipoles of the water molecules tend to align themselves to the oscillating electric field (see Figure 1.6) and may



move with the field (red wave in Figure 1.8), remain unaffected or lag behind (blue dotted wave in Figure 1.8). When the dipoles lag behind, a term called *hysteresis*, energy in the form of heat is dissipated ( $\delta$  in Figure 1.8) <sup>55</sup>.

**Figure 1.8: Hysteresis between the applied field and the induced electric field. P is the polarization (coulombs) and E the amplitude of the potential. The polarization lags behind the field by the phase ( $\delta$ , radius). Reproduced from <sup>74</sup>**

Since early research into the biological effects of microwaves, controversy has existed about the nature of the radiation. Already in 1932, Audiat <sup>55</sup> proposed that the effects of microwaves were either thermal (microwaves caused an observed heating) or athermal (no change in temperature was detected). There are thousands of scientific papers reporting either an effect or no effect of microwaves on cells, tissues, lenses and whole animals, from insects to mammals. Many are listed in reviews <sup>55; 75-80</sup>. There is no widely accepted mechanism for explaining the effects of electromagnetic fields on the structure or function of cells or molecular systems.

## **1.7 SAFETY STANDARDS FOR ELECTROMAGNETIC EXPOSURES**

### **1.7.1 EXTREMELY LOW FREQUENCY (50 Hz)**

In Australia there is currently no protection standard for exposure to 50 Hz fields. In 1989 the National Health and Medical Research Council (NHMRC) published interim guidelines on the limits of exposure to 50/60 Hz electric and magnetic fields <sup>69</sup>. This document will be reviewed by the Australian Radiation Protection and Nuclear Safety Agency (ARPANSA) in the near future. Table 1.3 is reproduced from the NHMRC guidelines.

The International Commission on Non-Ionizing Radiation Protection (ICNIRP) has set safety guidelines for time varying electric and magnetic fields for frequencies up to 300 GHz<sup>62</sup>. The guidelines apply to continuous wave, pulsed and modulated fields at single or multiple frequencies<sup>62</sup>. A special guideline was issued for limits on the exposure to static magnetic fields<sup>81</sup>.

**Table 1.3: Summary of exposure limits recommended by the NHMRC for occupational and general public exposures to 50/60 Hz electric and magnetic fields. The magnetic flux density is expressed in Gauss. Rms is a measure of magnetic flux density. Reproduced from<sup>69</sup>.**

### **1.7.2 RADIOWAVES AND MICROWAVES**

The Australian Protection Standard, “Maximum Exposure Levels to Radiofrequency Fields – 3 kHz to 300 GHz”<sup>82</sup> is in essence similar to the ICNIRP guidelines<sup>62</sup>. The guidelines specify six minutes as the period over which time-varying doses are to be averaged. Therefore, if the temperature does not change detectably in that period of time (on 10 g of tissue,  $\sim 10 \text{ cm}^3$ ), the exposure is considered non-thermal (athermal) as opposed to a thermal exposure in which a temperature rise can be detected<sup>83</sup>.

To understand the effect of extremely low frequency and microwaves on life forms and their complex cellular systems, it is useful to establish a basic understanding at the molecular level. Relatively little research, in a systematic order (e.g. continuous vs. pulsed vs. modulated), has been reported on *in vitro* effects of non ionising radiation.

**Table 1.4: Safety guidelines for time varying electric and magnetic fields, set by ICNIRP <sup>62</sup>. The SAR values are to be averaged over 6 minutes.**

### **1.8 EFFECTS OF EXTREMELY LOW FREQUENCY AND MICROWAVES ON PROTEINS**

There are two broad classes of ideas for the interaction of electromagnetic fields with biological systems. One of them is that the field interacts directly with the molecule and the other is that the interaction occurs via thermal processes in approximate thermal equilibrium with the surroundings.

Blank and Soo studied the effect of ELF waves (the magnetic and electric component separately) on the membrane enzyme Na,K-ATPase (the “ion pump” of cells) on the mitochondrial cytochrome oxidase redox function and on the Belousov-Zhabotinski (BZ) reaction (a redox reaction system that involves oxidation of malonic acid, and contains  $\text{Br}^-$ ,  $\text{BrO}_3^-$  and  $\text{Ce}^{3+}/\text{Ce}^{4+}$ ) <sup>84-90</sup>. They found that the magnetic and electric fields had a different effect. The magnetic field increased enzyme activity; it was argued that the magnetic field affected moving charges throughout the protein and thereby accelerated their movement. The effects became proportionally less significant as the number of charges increased. At low activation, the electric fields were comparable to the magnetic fields however at high activation, the electric field induced a reduction in enzyme activity. The effects were frequency dependent; there were different optimum frequencies for the reactions studied: ATPase (60Hz), cytochrome oxidase (800Hz), BZ (250Hz) <sup>84-96</sup>.

A “window effect” is a phenomenon that relates to an observable biological response to a magnetic or electric field that is dependent on frequency but is not proportional to the effect <sup>97</sup>.

A typical “window effect” is one in which the effect occurs most strongly in a “window”

between an upper and a lower limit of a parameter. An electric field of 15-150 Hz, with an optimum window at 45 Hz was found to increase transcription of proteins, within minutes, in human HL-60 cells. An electric field (AC) imposed by an electrode system and a window of 3 mV/m was found to have a similar effect. Magnetic field induction was about a 1000 fold lower than the electric field effect<sup>98-100</sup>.

The expression of Hsps in cells, in response to exposure of radio waves has been reported in the literature by Goodman *et al* in yeast cells<sup>101</sup>, Golfert *et al* in astrocytes<sup>102</sup> and Junkersdorf *et al* in the nematode *Caenorhabditis elegans*<sup>103</sup>. Prior exposure to magnetic field at 60 Hz has been found to protect against thermal stress<sup>104-106</sup>.

The elevated expression of Hsps, as a consequence of microwave exposure, was reported by de Pomerai *et al* in the nematode *Caenorhabditis elegans*<sup>107</sup> (CW exposure, 750 MHz, SAR 0.001 W/kg), Kwee *et al* in human epithelial amnion cells (pulsed 960 MHz, amplitude modulated, SAR 2.1 mW/kg)<sup>108</sup>, Leszczynski *et al* in a human endothelial cell line (pulsed 900 MHz, modulated, SAR 1.8-2.5 W/kg)<sup>109</sup> and Shallom *et al* in chick embryos (915 MHz, SAR 1.75-2.5 W/kg)<sup>110</sup>.

*In vitro*, two thermophilic proteins (alcohol dehydrogenase from the hyperthermophilic deep-sea Archaeon *Sulfolobus solfataricus* and  $\beta$ -galactosidase from the thermoacidophilic eubacteria *Bacillus acidocaldarius*) were exposed to 10.4 GHz (SAR 800 W/kg) and monitored by circular dichroism (CD) and fluorescence. The CD spectrum showed loss of secondary structure when exposed to microwaves and heat compared to heating only<sup>111; 112</sup>. Bohr *et al* monitored polarization of the folding and unfolding of  $\beta$ -lactoglobulin. Both the folding and unfolding kinetics were greatly enhanced by exposure to 2.45 GHz that resulted in 0.3°C temperature rise of the sample<sup>113; 114</sup>. CD was used to show the effects 2.450 GHz (CW, SAR 600 W/kg) on human erythrocyte ghost proteins. Data showed decreased  $\alpha$ -helicity<sup>115</sup> upon exposure.

The polymerization of microtubules was investigated with exposure to 2.450 GHz (CW, SAR 20 or 200 W/kg). No effect was detected using CD and light scattering techniques<sup>116</sup>.

Porcelli *et al* investigated the effect of 10.4 GHz (CW, SAR 1.5-3.1 W/kg) on two thermophilic proteins and found a decrease in enzyme activity that was time and temperature dependent<sup>117</sup>.

De Pomerai *et al* reported that, through light scattering methods, the aggregation of concentrated bovine serum albumin protein was enhanced in a time and temperature dependent way when exposed to 1.0 GHz (CW, SAR 15-20 mW/kg). Bovine insulin exposed for 24 hours formed amyloid fibrils compared to a control that did not form fibrils<sup>118</sup>.

Finally, in a computer simulation study<sup>119</sup>, the effect of a 2.450 GHz static electric field was investigated on the insulin B chain. It was found that, within the simulation timeframe, there was a thermal-like effect due to the application of static electric field of strength  $1.0 \times 10^8$  V/m. This was evidenced by the increased number of available protein conformations not normally accessible under ambient conditions. An increase of diffusion constant of water was also observed for the system under static electric field to a value close to the system under thermal stress.

## **1.9 POSSIBLE MECHANISMS OF INTERACTION**

Based on the experimental work, and theoretical calculations<sup>83; 120-123</sup>, several mechanisms have been proposed of how RF is likely to interact with tissue, cells and proteins in solutions. It is outside the scope of this project to discuss all the different proposals however two hypotheses related to direct effects of fields on proteins are discussed.

### **1.9.1 MOVING CHARGE INTERACTION (MCI)**

The Moving charge interaction (MCI) model proposes that moving electrons affect enzyme activity. The activation of genes and synthesis of stress proteins is initiated by an EM field (both electric and magnetic fields) by moving electrons. The optimal frequency dependence is related to the turnover numbers of the enzyme reaction (most are in the range of 10-100 per second)<sup>92;</sup>

<sup>94; 124-127</sup>

### 1.9.2 WRING MODES

The White theorem states that the topological link number  $L_k$  for a pair of closed curves is the sum of their twist number ( $T_w$ ) and their writhe number ( $W_r$ ):  $L_k = T_w + W_r$ <sup>128</sup>.

Bohr *et al*<sup>129-132</sup> consider that the White theorem, that applies to circular molecules, could also be valid for globular proteins because they are topologically constrained on a short time scale of less than a micro second. When proteins are exposed to microwaves, the intrinsic modes of the protein (eigen-frequencies) are excited, resulting in the acceleration of folding or unfolding.

## 1.10 PROJECT AIM AND HYPOTHESES

### AIM OF PROJECT

1. *To determine the conformational effect of pulsed microwave exposure at 2.450 GHz on a set of target proteins, in vitro, that were also stressed by temperature, reduction or chelation of an intrinsic metal ion.*
2. *To determine the effect of an applied electric field (50 Hz) on several target proteins, in vitro, that were also stressed by temperature.*

### SPECIFIC HYPOTHESES TO BE TESTED

- (i) *The initial rate of precipitation of target proteins exposed to microwave pulses once every six minutes is significantly higher than that of a control held at the same average temperature, where the average is taken over a six minute period.*
- (ii) *The sHsp,  $\alpha$ -crystallin prevents the aggregation and precipitation of target proteins under the above regimes.*
- (iii) *The initial rate of precipitation of target proteins exposed to an electric field of 50 Hz, or lower frequency, is significantly higher than that of a control held at the same average temperature.*

---

## CHAPTER 2

---

### EXPERIMENTAL

#### 2.1 SELECTION OF EXPERIMENTS

The motive of this study was to determine if pulsed microwave exposure or an applied electric field exerted a detectable and quantifiable effect on the conformation of proteins in solution.

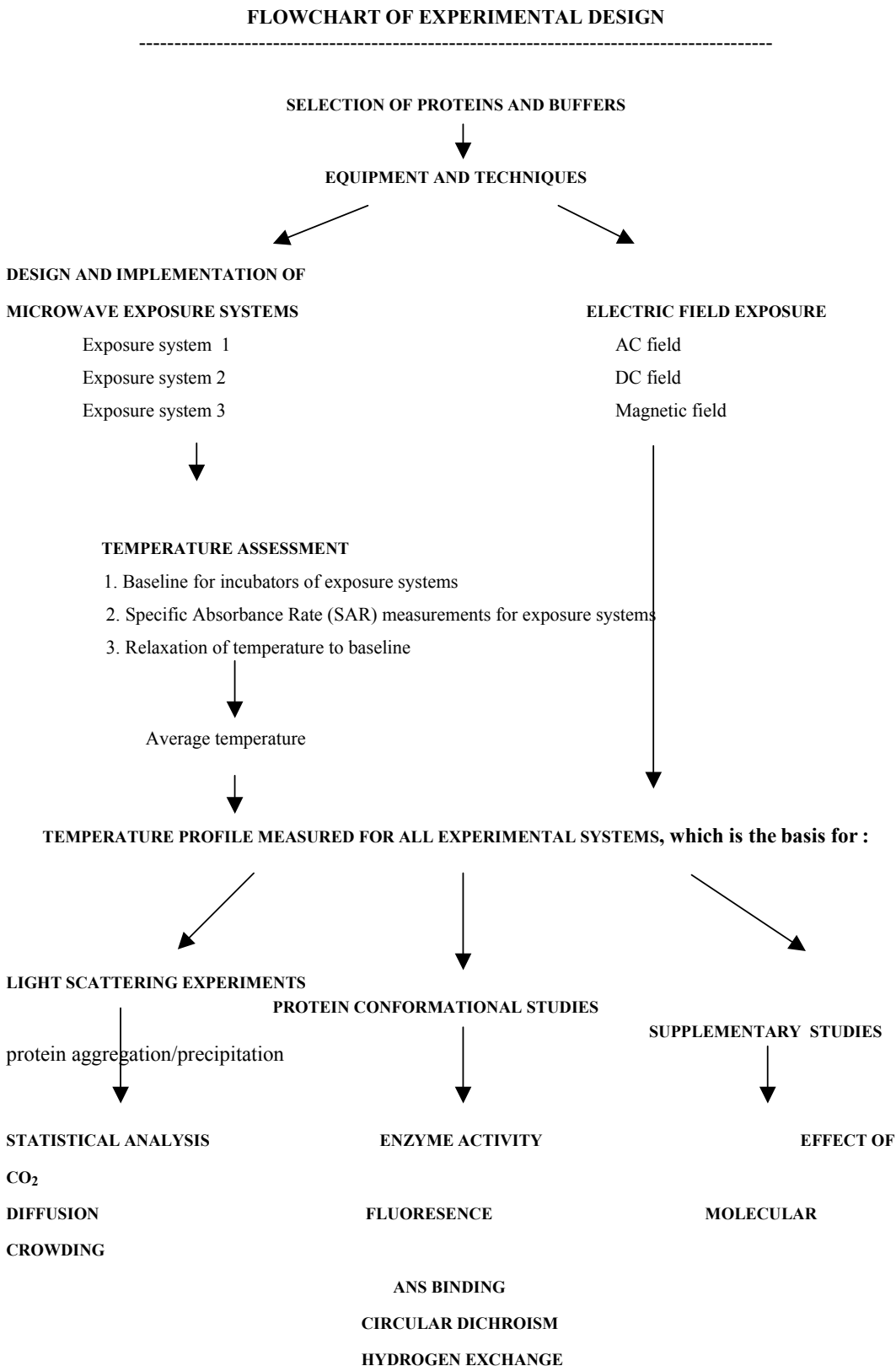
In designing the experiments, the limiting factors were the exposure equipment, instruments to detect changes in protein conformation and reliable protein assays. The microwave exposure equipment consisted of a remodelled microwave oven that gave bursts of 2.450 GHz every six minutes. For the electric field experiments, generators and a transformer were accessible.

It is common to study the aggregation and precipitation of stressed proteins in solution by monitoring light scattering at wavelengths around 360 nm. These types of experiments are also well suited to study the effect of sHsps on protein aggregation and can determine at which subunit ratios there is, if any, suppression of the aggregation and precipitation of the protein in question via the chaperone action of sHsps.

A UV/Visible spectrophotometer was readily available, therefore light scattering in tandem with microwave or electric field exposure was considered a suitable means of exploring if these exposures had an effect on protein aggregation when compared to a control (chapters 5 to 8).

To explore changes in protein conformation, experiments were undertaken on citrate synthase and alcohol dehydrogenase and are described in chapter 11.

A schematic overview of the experimental approach to the research is provided by way of a flowchart. The equipment and techniques used in the project are described in this chapter. A detailed assessment of the experimental temperature is provided in chapter 3.





## 2.2 SELECTION OF PROTEINS AND BUFFERS

### 2.2.1 TARGET PROTEINS

A total of eight proteins were selected for light scattering experiments and/or conformational studies. The choice was based on literature reports that showed how the unfolding and precipitation of these proteins could be facilitated by stress in the form of reduction, chelation of an intrinsic metal ion or by heating. It was of interest to see if the presence of a concurrent microwave exposure or the electric field could be considered an additional stress. Experimental conditions were kept similar as reported in the literature.

The following sections describe the characteristics of the proteins that were studied. The data were obtained from the ExPASy proteomics database <sup>133</sup>, unless stated otherwise. Ribbon structures based on crystallography data are reproduced from The Research Collaboratory for Structural Bioinformatics (RCSB) Protein Data Bank (PDB) and represent the assumed biological molecule <sup>134</sup>. For those proteins of which the crystal structure is not yet known, a structure of a protein from the same family has been provided.

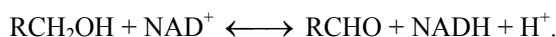
#### 2.2.1.1 Alcohol Dehydrogenase (ADH) from *Saccharomyces cerevisiae*

(baker's yeast)– P00330 <sup>133</sup>

**Figure 2.1: A ribbon structure based on X-ray diffraction data of NADP-dependent alcohol dehydrogenase from the thermophilic bacteria *Thermoanaerobium brockii*. The protein contains 4 polymer chains that bind one zinc atom each. Reproduced from the RCSB PDB database, entry 1YKF <sup>135</sup>.**

ADH is a metallo-enzyme containing four subunits that bind one zinc atoms each, the apparent mass is 146,600 Dalton (Da) <sup>136</sup>. Each chain of ADH from *Thermoanaerobium brockii* includes 17  $\beta$ -strands, 14  $\alpha$ -helices, 29  $\beta$ -turns and 3  $\gamma$ -turns (Figure 2.1) <sup>135</sup>. ADH is found in the

cytoplasm where it catalyses the conversion of acetaldehyde to acetone. The protein also acts on a variety of primary unbranched aliphatic alcohols. *In vitro* ADH catalyzes the reaction:



When ADH is incubated with the chelating agents ethylenediaminetetraacetic acid (EDTA) or 1,10-phenanthroline the intrinsic zinc ions are removed. The structure destabilizes and ADH precipitates unless Hsps are present. The unfolding process can be monitored spectroscopically

137-140

### 2.2.1.2 Bovine Serum Albumin (BSA) from *Bos taurus* (bovine) – P02769<sup>133</sup>

**Figure 2.2: A ribbon structure based on X-ray diffraction data of human serum albumin complexed with thyroxine. Reproduced from the RCSB PDB database, entry 1E78<sup>135</sup>.**

BSA is the main protein in plasma where it binds  $\text{Ca}^{2+}$ ,  $\text{Na}^+$ ,  $\text{K}^+$ , fatty acids, hormones, bilirubin and drugs. Its main function is the regulation of the colloidal osmotic pressure of blood. The protein consists of three homologous domains held together by 17 disulphide bonds and includes 31  $\alpha$ -helices, 35  $\beta$ -turns and 5  $\gamma$ -turns ; it has an apparent mass of 69,293 Da<sup>135</sup>.

*In vitro* reduction of the disulphide bonds in the presence of heat destabilizes the protein after which it aggregates and precipitates out of solution<sup>141-143</sup>.

### 2.2.1.3 Catalase from *Bos taurus* liver (bovine) - P00432<sup>133</sup>

Catalase is found in all aerobically respiring organisms and functions as a catalyst to convert hydrogen peroxide into water and oxygen:  $2\text{H}_2\text{O}_2 \rightarrow 2\text{H}_2\text{O} + \text{O}_2$

**Figure 2.3: A ribbon structure based on X-ray diffraction data of bovine liver catalase. Reproduced from the RCSB PDB database, entry 4BLC<sup>135</sup>.**

A subcellular enzyme, it is found in the peroxisome organelles in the liver. Catalase has the highest turnover number for all known enzymes (40,000,000 molecules/second<sup>4</sup>) which demonstrates the capacity of this enzyme to detoxify hydrogen peroxide and prevent the formation of carbon dioxide in blood. The protein consists of four identical chains of 506 residues with a mass each of 57,574 Da. Each chain has 12  $\beta$ -strands, 19  $\alpha$ -helices, 49  $\beta$ -turns and 7  $\gamma$ -turns (Figure 2.3)<sup>135</sup>.

At elevated temperature, *in vitro*, catalase becomes stressed and starts to precipitate out of solution. Heat assays on catalase have demonstrated the ability of heat-shock proteins to suppress aggregation<sup>144 145</sup>.

#### **2.2.1.4 Citrate Synthase from *Sus scrofa* (porcine) – P0089<sup>133</sup>**

**Figure 2.4: A ribbon structure based on X-ray diffraction data of porcine citrate synthase. Reproduced from the RCSB PDB database, entry 4CTS<sup>135</sup>.**

The enzyme citrate synthase operates in the mitochondrial matrix and is found in most cells that are capable of oxidative metabolism. Its function is to catalyze the substrate oxaloacetate and citrate from Acetyl-CoA during the tricarboxylic acid cycle (see section 2.7.1). The protein consists of two identical subunits of 437 residues each and has an apparent mass of 48,907 Da per subunit<sup>135</sup>. The structure is made up of 2  $\beta$ -strands, 23  $\alpha$ -helices, 19  $\beta$ -turns, and 4  $\gamma$ -turns (Figure 2.4)<sup>135</sup>.

Citrate synthase *in vitro* becomes unstable when heat is applied. It has been extensively used in heat assays that study the unfolding and interaction with Hsps<sup>146-148</sup>.

#### 2.2.1.5 Insulin from *Bos taurus* (bovine) – P01317<sup>133</sup>

**Figure 2.5:** A ribbon structure based on X-ray diffraction data of bovine Des-Phe B1 insulin. The protein can bind with two zinc atoms (one shown). Reproduced from the RCSB PDB database, entry 2INS<sup>135</sup>.

Insulin is a hormone secreted from pancreatic B cells in response to elevated blood concentrations of glucose. Its function is to signal cells in the body to import glucose from the blood and store it as glycogen. Insulin increases cell permeability to monosaccharides, amino acids and fatty acids. It accelerates glycolysis, the pentose phosphate cycle, and glycogen synthesis in liver. The amino acid sequence of insulin is highly conserved among vertebrates and insulin from one mammal is active in another. For example, many diabetic humans are treated with insulin extracted from pig pancreas<sup>149</sup>.

Insulin is composed of two peptide chains, A and B (Figure 2.5). They are linked together by two disulphide bonds. A third disulphide bond is formed within the A chain. The protein tends

to form dimers and hexamers due to hydrogen-bonding between the C-termini of B chains. Additionally, in the presence of zinc ions, insulin dimers associate into hexamers<sup>149</sup>. The monomer protein consists of three  $\alpha$ -helices, two in the A chain (21 residues) and one in the B chain (29 residues)<sup>135</sup>. The apparent mass of the protein is 5,700 Da.

When the disulphide bond of insulin is reduced *in vitro* by addition of DTT, the protein starts to precipitate immediately. Insulin has been used as a model protein in studies on the suppression of aggregation by Hsps<sup>139; 150</sup>.

#### 2.2.1.6 $\alpha$ -Lactalbumin from *Bos taurus* (bovine) – Q28049<sup>133</sup>

**Figure 2.6: Structure of apo bovine  $\alpha$ -lactalbumin as determined by X-ray crystallography. Reproduced from Chrysina, Brew and Acharya<sup>151</sup>.**

$\alpha$ -Lactalbumin, a subcellular protein found in the mammary gland, is the regulatory subunit of lactose synthetase that assists galactosyltransferase in the catalysis of the addition of galactose to glucose to form lactose in mammalian milk.  $\alpha$ -Lactalbumin binds several metal ions, including calcium, which is thought to play a role in the regeneration of native  $\alpha$ -lactalbumin from the reduced denatured form.  $\alpha$ -Lactalbumin also has a distinct zinc binding site that is believed to be involved in the binding of the lactose synthase complex<sup>152</sup>. The protein consists of 123 residues and has an apparent mass of 14,169 Da in the apo form. The tertiary structure (Figure 2.6) is made up of 3  $\beta$ -strands, 9  $\alpha$ -helices, 11  $\beta$ -turns and 4 disulphide bridges (entry 1F6R in PDB)<sup>135</sup>. The unfolding of  $\alpha$  lactalbumin as a result of the reduction of its disulphide bonds, has been studied extensively<sup>153; 154</sup>.

### 2.2.1.7 Lysozyme from *Gallus gallus* (chicken) – P27042<sup>133</sup>

The enzyme lysozyme is secreted in body fluids and tissue of animals and plants. The function of lysozyme is believed to be give protection against bacterial infection as the protein catalyzes the hydrolysis of polysaccharides in the cell wall structure of bacteria<sup>155</sup>. Lysozyme is secreted from the granulocyte compartment of myelomonocytic cells. Hen egg white lysozyme

**Figure 2.7: A ribbon structure based on X-ray diffraction data of hen egg-white lysozyme. Reproduced from the RCSB PDB database, entry 1LYZ<sup>135</sup>.**

is homologous with bovine  $\alpha$ -lactalbumin<sup>156</sup>. The monomeric protein consists of 129 residues with a mass of 14,296 Da. The structure (Figure 2.7) includes 3  $\beta$ -strands, 7  $\alpha$ -helices, 13  $\beta$ -turns and 4 disulphide bonds<sup>135</sup>. Lysozyme unfolding as a result of the reduction of the disulphide bonds, has been studied *in vitro* in the presence of Hsps<sup>150; 157; 158</sup>.

### 2.2.1.8 Ovotransferrin from *Gallus gallus* (chicken) – O02789<sup>133</sup>

Ovotransferrin belongs to the transferrin protein family and has a bacteriostatic function. Transferrins are iron binding transport proteins which can bind two atoms of ferric iron in association with the binding of an anion, usually bicarbonate. It is responsible for the transport of iron from sites of absorption and heme degradation to those of storage and utilization. Its concentration in avian egg is the highest concentration of any transferrin *in vivo*.

The structure of ovotransferrin which is a monomeric protein of 686 residues with a mass of 75,810 Da, consists of two domains (Figure 2.8) that include 26  $\beta$ -strands, 30  $\alpha$ -helices, 78  $\beta$ -turns, 6  $\gamma$ -turns and 15 disulphide bonds<sup>135</sup>.

**Figure 2.8: A ribbon structure based on X-ray diffraction data of hen egg-white ovotransferrin. Reproduced from the RCSB PDB database, entry 1OVT<sup>135</sup>.**

The unfolding of ovalbumin as a result of the reduction of its disulphide bonds has been studied in the presence of Hsps<sup>141; 150</sup>.

### 2.2.2 MATERIALS

The proteins and D,L-DTT were obtained from Sigma (St. Louis, MO, USA). 1,10-Phenanthroline was obtained from Ajax (Sydney, Australia) and buffer salts from Sigma or Merck (Darmstadt, Germany). Section 2.2.7 lists the concentrations used for the experiments.

### 2.2.3 BUFFERS

The buffer was 0.1 M phosphate, 0.02%  $\text{NaN}_3$  except for CS which was at 80 mM. Phosphate buffers were prepared from appropriate ratio mixtures of 0.2 M  $\text{Na}_2\text{HPO}_4$  and  $\text{NaH}_2\text{PO}_4 \cdot 2\text{H}_2\text{O}$  stock solutions that were prepared with milliQ water. Buffers were routinely filtered through a nylon membrane filter. The pH was adjusted to between pH 7.0 and pH 8.0 depending on the experiment. The preparation for the phosphate buffers and buffers used in the purification of  $\alpha$ -crystallin, are listed in Appendix 1.

#### 2.2.4 PURIFICATION OF CITRATE SYNTHASE

Citrate synthase (CS) is packed in an ammonium sulphate suspension. On arrival to the laboratory, CS was dialysed against 50mM Tris buffer, 2mM EDTA, pH 8.0 as described by Buchner *et al*<sup>148</sup>. The solution was transferred to a Centriplus-30 micro concentrator and centrifuged at 3000 x g at 4°C until the solution was ~ 30 to 40  $\mu$ M. To obtain the CS solution concentration, the absorbance was determined from the extinction coefficient of 1.78 for a 1 mg/ml solution in a quartz cuvette of 1 cm path length.

#### 2.2.5 PURIFICATION OF $\alpha$ -CRYSTALLIN

Eyeballs of freshly slaughtered cattle less than two years old were collected from Wollondilly Abattoirs Pty Ltd, Picton NSW. On return to the laboratory, the lenses were removed and stored in a freezer until ready to use. Frozen lenses, two or three at a time, were thawed and homogenized with 6 ml homogenising buffer (50mM TRIS, pH 7.2, see Appendix 1). The homogenized material was divided over six centrifuge tubes and centrifuged at 4°C, 12000 rpm for 20 minutes. The supernatants were collected and pooled into a container and then refrigerated at 4°C. A Sephacryl S-300 column, 3cm in diameter, 100 cm in length and a bed volume of ~ 1 L was equilibrated overnight with column buffer (50mM Tris, 0.04% NaN<sub>3</sub>, pH 7.5) before the refrigerated lens material was loaded. When three lenses were used, only half the lens material was loaded to the column at any given time. The column buffer was passed through the column at 20 ml per hour by use of a Masterflex L/S (Cole-Parmer Instrument Company) pump. The eluant was detected for protein content on a Single Path Monitor (Pharmacia) at 280 nm, with the sensitivity set to 0.1. Fractions were collected every 20 minutes in a Redi Frac. (Pharmacia Biotech.) fraction collector. The separation of the three crystallin proteins ( $\alpha$ ,  $\beta$  and  $\gamma$  crystallin) took about 24 hours.  $\alpha$ -Crystallin contains two subunits  $\alpha$ A and  $\alpha$ B, which eluted as one broad peak after about 10 hours, it was labelled alpha-total ( $\alpha_T$ ).  $\beta$ -Crystallin contains two subunits, Beta high ( $\beta_H$ ) and Beta low ( $\beta_L$ ) that were separated after 13 and 15 hours respectively. Two gamma fractions were collected after 18 hours. The pooled



fractions of  $\alpha_T$  were concentrated and re-loaded on the freshly equilibrated column as described above, to allow a complete separation between the high molecular weight (HMW) fraction and  $\alpha_T$ . The  $\alpha_T$  fraction was concentrated and extensively dialysed against ultra pure water with subsequent freeze-drying.  $\alpha$ -Crystallin was checked for purity by 10% SDS-polyacrylamide gel electrophoresis. The  $\beta_H$ ,  $\beta_L$  and  $\gamma$  fractions were pooled, concentrated and stored in the freezer.

## 2.2.6 PREPARATION OF $\alpha$ -LACTALBUMIN

Calcium depleted  $\alpha$ -lactalbumin (commonly called apo  $\alpha$ -lactalbumin) is a commercially available protein that contains less than 0.3 mol of calcium per 1 mol of  $\alpha$ -lactalbumin<sup>159</sup>. Pure apo  $\alpha$ -lactalbumin is obtained when apo  $\alpha$ -lactalbumin is incubated with EDTA for up to 0.5 hours after which most  $\text{Ca}^{2+}$  ions have been drawn from the protein molecules and are chelated to EDTA<sup>153; 154; 159; 160</sup>. Upon reduction of the disulphide bonds,  $\alpha$ -lactalbumin aggregates but does not precipitate from solution unless 0.1 M NaCl is added<sup>153</sup>.

Holo  $\alpha$ -lactalbumin was prepared by incubating the commercially available apo  $\alpha$ -lactalbumin in 50 mM imidazole buffer, 0.1 M NaCl that contained 5 mM  $\text{CaCl}_2$ . For CD spectra, the commercial product, holo  $\alpha$ -lactalbumin, calcium saturated, was used.

## 2.2.7 PROTEIN CONCENTRATIONS

Protein concentrations were determined at 280 nm using the extinction coefficient for 1 mg/ml solutions in a quartz cuvette of 1 cm path length<sup>161</sup> and are reported throughout the text as subunit concentrations. Concentrations used for the light scattering assays were as follows, or as described in the text:

*Thermal stress:*

- catalase (bovine liver), 0.2 mg/ml, pH 7.0, 42°C;  $A_{280\text{nm}, 1\text{cm}}^{1\%}$  12.9
- CS (pig heart), 0.2 mg/ml, pH 7.5, 42°C,  $A_{280\text{nm}, 1\text{cm}}^{1\%}$  1.78.

*Chemical-induced stress:*

- ADH (baker's yeast), 0.5mg/ml, 0.1 M NaCl, 1 mM 1,10-phenanthroline, pH 7.0, 37°C;  
 $A_{280\text{nm}, 1\text{cm}}^{1\%}$  1.26.
- BSA, 1.5 mg/ml, 20 mM DTT, pH 7.0, 45°C;  $A_{280\text{nm}, 1\text{cm}}^{1\%}$  0.71.
- insulin (bovine pancreas), 0.25mg/ml, 0.1 M NaCl, 20 mM DTT, pH 8.0, 37°C;  
 $A_{280\text{nm}, 1\text{cm}}^{1\%}$  1.0.
- $\alpha$ -lactalbumin (bovine milk), apo: 2 mg/ml, 2 mM EDTA, 20mM DTT, 0.1 M NaCl, pH 7; 37°C,  $A_{280\text{nm}, 1\text{cm}}^{1\%}$  1.95; holo: 0.5 mg/ml in 50 mM imidazole buffer, 0.1 M NaCl, 5 mM CaCl<sub>2</sub>, pH 7.2, 32°C,  $A_{280\text{nm}, 1\text{cm}}^{1\%}$  2.01.
- lysozyme (chicken egg white), (0.1 mg/ml, 20mM DTT, 0.1 M NaCl, pH 7; 30°C,  
 $A_{280\text{nm}, 1\text{cm}}^{1\%}$  0.775.
- ovotransferrin (chicken egg white), 0.2 mg/ml, 0.1 M NaCl, 20 mM DTT, pH 7.2, 45°C,  
 $A_{280\text{nm}, 1\text{cm}}^{1\%}$  1.10.

### *$\alpha$ -Crystallin*

$\alpha$ -Crystallin was used at molar subunit ratios which is reported for the individual experiments in the results section;  $A_{280\text{nm}, 1\text{cm}}^{1\%}$  0.8.

The addition of 0.1 M NaCl in most assays allowed the stabilization of the emerging aggregates thus ensuring precipitation<sup>153</sup>.

## **2.3 EQUIPMENT AND TECHNIQUES**

### **2.3.1 MICROWAVE OVEN**

A 2.450 GHz, 800-Watt domestic microwave oven was remodelled (Appendix 2) at the University of Sydney<sup>162; 163</sup>. The oven's normal controller was replaced with a customised BASIC Stamp microcontroller. The customised controller turned the oven on at six minutes

intervals for a preset time. The six minute interval was chosen because this is the period over which time varying exposures are integrated in the ICNIRP guidelines <sup>62</sup>.

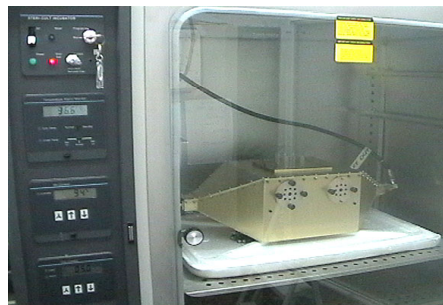
To improve circulation of the air, a fan was fitted to the door (Figure 2.9). A digital switch was installed which allowed the setting of the number of RF pulses per cycle. Each burst consisted of the typical 50 Hz modulation pulses delivered by the magnetron microwave generator of the oven. The number on the switch could be set from 10 to 250, which corresponded to microwave bursts lasting between 0.2 and 5.0 seconds. For experiments in this project, pulses lasting 3.2 or 5.0 seconds were used.



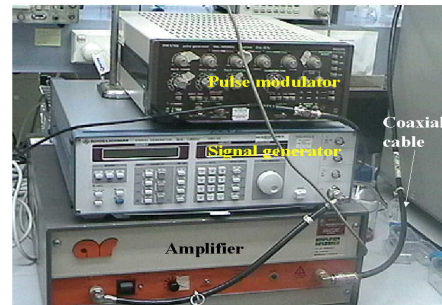
Figure 2.9: View of the remodelled oven during a pulse period (red light).

### 2.3.2 TRANSVERSE ELECTROMAGNETIC MODE (TEM) CELL

The TEM cell was custom built by Telstra Australia for the Centre for Immunology, St. Vincent's Hospital, NSW, for the purpose of applying uniform pulsed microwaves to cell culture. The cell (Figure 2.18) consisted of a microwave carrier of 900.00 MHz, pulse modulated at 217 Hz, with a 12.5% duty cycle. Pulse width was 576  $\mu$ s and the pulse period was 4.6 ms.



A



B

**Figure 2.10: TEM cell inside the incubator (A) and equipment (pulse modulator, signal generator and amplifier) to generate 900 MHz pulse moderated microwaves (B).**

The power meter reading at 20W was  $-16.4$  dBm (0 decibel m is 1 mW; 16.4 dBm is  $\sim 0.025$  mW). The free space E-field inside the TEM cell was 421 V/m at 20W forward. The cell was placed inside an incubator that was temperature controlled at  $37^{\circ}\text{C}$ ,  $\text{CO}_2$  was 5% and humidity 95%.

### 2.3.3 VISIBLE ABSORPTION SPECTROSCOPY

The turbidity (light scattering) associated with protein aggregation and precipitation was monitored at 360 nm every two minutes using a Cary-500 UV-Vis spectrophotometer. Cuvettes were placed in a multi-cell-block that was kept at the desired temperature via a circulating water bath. It took on average five minutes to reach the equilibrium temperature. The temperature of the sample buffer in the cuvettes was recorded with Luxtron 502/504 fluoroptic temperature-sensing probes at four heights in the cuvette for each of the positions in the multi-cell-block. The light beam of the spectrophotometer passed through the sample between 13 and 19 mm from the base of the cuvette.

The spectrophotometer used at the Centre for Immunology, St. Vincent's Hospital was a Shimadzu, UV-1601 UV-visible spectrophotometer.

### 2.3.4 FLUORESCENCE SPECTROSCOPY

Intrinsic tryptophan and ANS binding studies were performed on a Hitachi F-4500 fluorescence spectrophotometer with a 3 ml quartz fluorescence cuvette.

Slit widths for excitation and emission were set to 5.0 and 2.5 nm respectively. The instrument was set to 700 V. The shutter control and corrected spectra options were disabled.

Intrinsic fluorescence (tryptophan) was determined before and immediately after a light scattering experiment. Samples were excited at wavelength 295 nm and the spectrum accumulated over 260-450 nm. The scan speed was 240 nm/min. The emission of tryptophan in proteins is at 338 nm.

The Extrinsic fluorescence (ANS binding) was determined before and immediately after a light scattering experiment by adding aliquots of 10  $\mu$ l of 50 mM ANS, under constant stirring, to the protein sample. Samples were excited at wavelength 387 nm and spectra were accumulated from 450 to 520 nm. The scan speed was 6 nm/min. The emission at 479 nm was noted.

### **2.3.5 CIRCULAR DICHROISM (CD) SPECTROSCOPY**

A JASCO J-810 spectropolarimeter (Jasco, Victoria, Canada) connected to a Jasco water bath was employed for protein conformational studies. The CD resided in the Department of Physics, University of New South Wales, Sydney. Stock solutions were routinely prepared early in the morning, stored on ice and made up to the desired concentrations on arrival in Sydney. For exposure experiments, the microwave oven and block heater could be transported to Sydney so that CD spectra could be recorded during and immediately after a microwave exposure experiment. Near- and UV spectra were recorded from 240 to 320 nm and 190 to 240 nm respectively at 22°C unless otherwise stated, in a 3.0 ml cell of 10 mm pathlength. All spectra represent the average of six scans. The data were converted to molar ellipticity.

#### **2.3.5.1 CD TEMPERATURE MELTS**

The unfolding of a protein, as a result of temperature increase is usually observed by comparing the ellipticity of the  $\alpha$ -helical region in a protein that appears as a minimum at 222 nm in the folded state. Starting at 22°C, the target temperature was increased by 1.5 to 2°C at a time and equilibrated for one minute after the temperature was reached. A total of 10 scans between 220 and 225 nm were recorded and averaged, which was equivalent to 1 minute of recording for each temperature setting.

### **2.3.6 ELECTROSPRAY IONISATION MASS SPECTROMETRY**

Hydrogen-deuterium exchange mass spectra were recorded on a Platform LCZ Electrospray Mass Spectrometer which was calibrated using egg-white lysozyme. The cone was routinely cleaned before each experiment. The conditions of the electrospray were controlled to slow

down exchange to prevent excessive back exchange. The syringe and samples were kept on ice. The infusion buffer was pumped at 20  $\mu\text{L}/\text{min}$  into the injector by way of a loop that was placed inside a bucket with ice water to ensure that the temperature was always  $\sim 4^\circ\text{C}$ . Samples were introduced through a Rheodyne injector and were pumped into the electrospray interface with a fluid delivery mode. The tubing to the mass spectrometer was placed in between two ice packs as an additional cooling measure (see Figure 2.11).

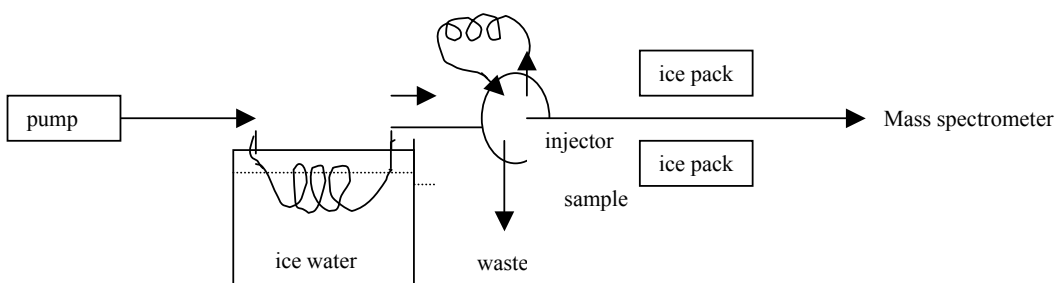


**Figure 2.11: Schematic view of the cooling conditions for hydrogen exchange experiments. The infusion buffer was pumped through a loop that was kept in a bucket with ice water. A thermometer (not shown) was kept in the bucket to monitor the temperature ( $\sim 4^\circ\text{C}$ ). Samples were introduced through an injector and the tubing to the mass spectrometer was placed in between two ice packs.**

The protocol for the hydrogen exchange experiments was adopted from <sup>164</sup>. A stock solution of apo  $\alpha$ -La was dissolved in 10%  $\text{H}_2\text{O}$ , 90%  $\text{D}_2\text{O}$  to give a concentration of to  $\sim 0.3$  mM, pH 6. The solution was left overnight, at room temperature to ensure maximum labelling. Before the experiment, a 5  $\mu\text{L}$  sample was diluted with 245  $\mu\text{L}$   $\text{D}_2\text{O}$  and injected in the mass spectrometer with  $\text{D}_2\text{O}$  as the infusion buffer to establish the mass of deuterated apo  $\alpha$ -La.

To start the hydrogen exchange, 10  $\mu\text{L}$  of stock sample was diluted with 490  $\mu\text{L}$  ice cold  $\text{H}_2\text{O}$ , pH 2. The solution was vortexed for one second and returned to the ice box. An aliquot of 20  $\mu\text{L}$  was injected into the mass spectrometer of which the infusion buffer was kept cold. Aliquots were injected at intervals of 5, 10 or 20 minutes. Spectra were collected from 1500-2000 mass/charge ratio. The experiment was repeated at least three times. The optimum results for the hydrogen exchange experiments were obtained under the following conditions: de-solvation temperature

50°C, Source block temperature 20°C, Cone voltage 40 V, retention 55, scope gain 50, scan time 2.50, inter scan 0.10, pump speed 40 µl/min.

### **2.3.7 FLUOROPTIC PROBES**

Temperature determinations were undertaken with Luxtron 502/504 fluoro optic temperature-sensing probes. The data were recorded every second. The fluoro optic measurement technique is based on a temperature sensitive phosphor material attached to the probe end of a fibre optic cable. Pulses of light excite the phosphor, causing it to fluoresce. The Digital Signalling Processing (DSP)-based electronics calculate the decay time of the fluorescence which is temperature dependent. A single optical fibre transmits both the excitation and the fluorescence signal<sup>165</sup>. The manufacturer's conversion factors for the individual probes are provided in Appendix 3.

### **2.3.8 CONDUCTIVITY METER**

A portable conductivity meter, Enviro Sensors LF 320 (WTW Wissenschaftlich, Weilheim, Germany) was used for all conductivity measurements. The meter was calibrated against 10mM NaCl which has a conductivity of 1413 µS/cm.

### **2.3.9. DRY BLOCK HEATER**

A dry block heater (Thermoline Scientific, Australia), model DB1, was modified to function as a block heater for 1.0 ml cuvettes. The aluminium block for centrifuge tubes was removed. Four aluminium cell holders were fixed to the bottom of the heater cavity with masking tape and sand was poured around the outside of the holders. For electric field experiments, two Teflon, non conducting cell holders replaced the aluminium cell holders.

## **2.4 MICROWAVE EXPOSURE**

In the course of the project, three different exposure systems were developed, a summary of which is given in Figure 2.12.

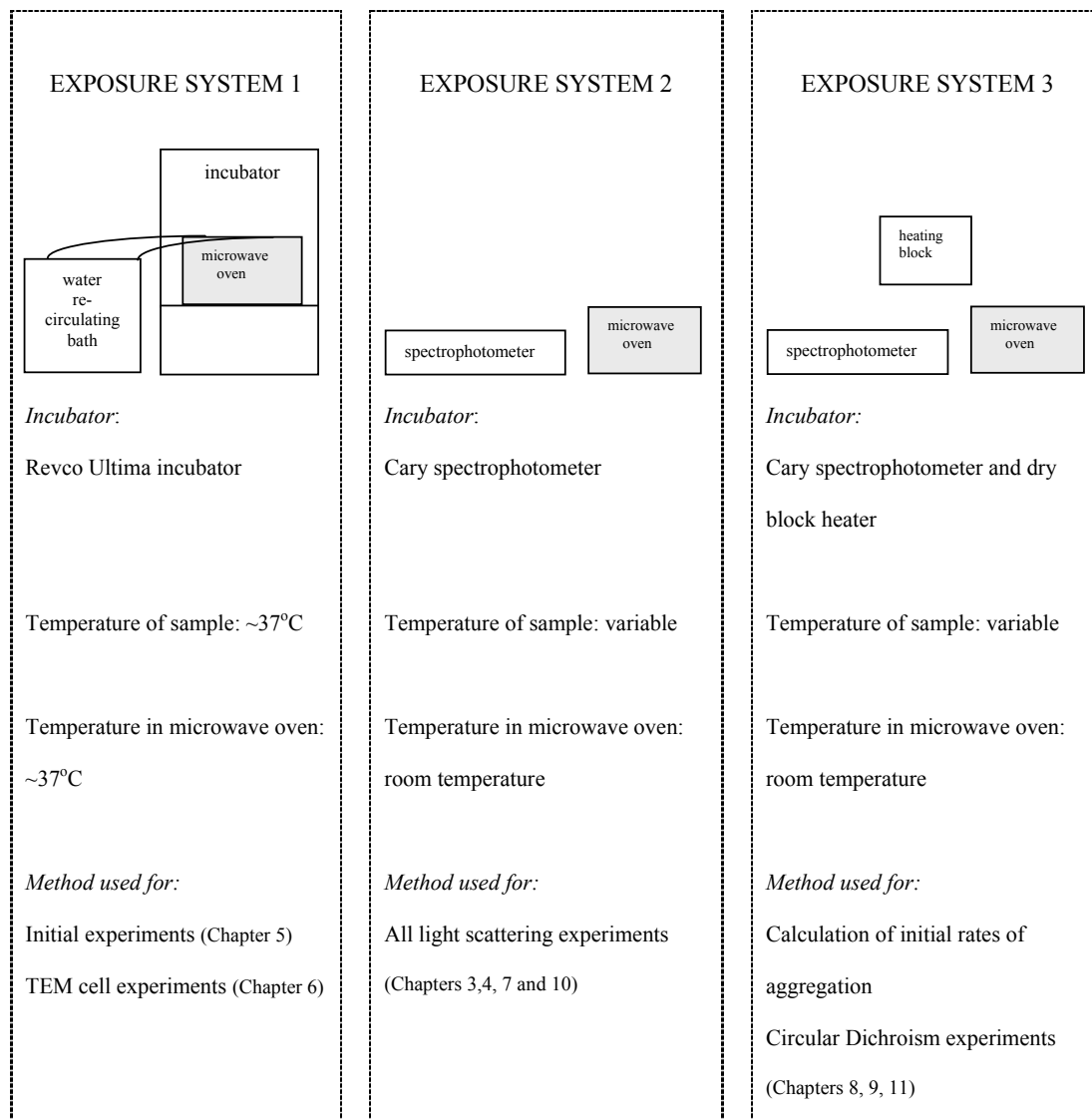


**Figure 2.12: Schematic overview of the three exposure systems employed during the project.**

*Exposure system 1* was used for the initial experiments. The temperature inside the incubator and microwave oven was determined by reading of two alcohol thermometers. One thermometer was placed in the cavity of the microwave and another one inside the incubator on the shelf underneath the microwave oven. It was assumed that the sample was at the identical temperature and the heat losses associated with taking samples out and replacing them at a later



stage was not allowed for. *Exposure system 1* proved therefore to have limitations in terms of monitoring the sample temperature. For *Exposure systems 2* and *3*, blank controls were used to establish the incubation temperature at precise locations and at several positions in the solutions, using fluoroptic probes. Detailed profiles were also made of the temperature rise and fall associated with the pulsed microwave exposure.

#### 2.4.1.1 EXPOSURE SYSTEM 1

##### *MICROWAVE OVEN*

In order to stabilize the field within the cavity of the oven and to absorb the majority of microwaves, two 1 L ethylene vinyl acetate infusion bags, each filled with water from a Julabo HC water re-circulator, were placed inside the oven (Figure 2.13).

The bags were modified to allow water from the circulating water-bath to flow into one bag, fill up and flow through a tube connecting both bags, into the second bag that was fitted with an external tube allowing water to flow back to the water-bath. Thus, water was constantly flowing from the water-bath, through the bags inside the oven, and back into the water-bath. A glass plate was placed on four cylindrical teflon supports that were affixed to the side of the oven.



**Figure 2.13:** View of cavity of the microwave oven showing the two infusion bags filled with circulating water. The bags were inter-connected by a tube. The left bag is connected to the hose of the water-bath that pumps water out into the bags and the right bag is connected to the hose that delivers the water back to the water-bath. The hoses fit through holes in the back panel of the incubator. The two incubator doors (not shown on the photograph) were closed during the experiment.

The position of the plate was marked on the supports to ensure that the glass plate was always correctly placed. The glass cover of the oven door had been removed to allow the fitting of a motorised fan that functioned as an air circulator.

The oven was placed inside a Revco Ultima incubator that was set to 37°C and to which the supply of CO<sub>2</sub> was disconnected (Figure 2.14). To ensure that the temperature inside the oven cavity was constant and similar to the temperature on the lower shelf inside the oven, the circulating water-bath, the microwave oven and the incubator were left to operate for up to 48 hours with occasional adjustments made to the temperature of the circulating water bath until the desired oven temperature was reached.

It was possible to undertake two experiments at the one time. The cuvettes containing the protein solutions that were to be exposed were placed on the marked positions on the glass plate while the control samples were placed either in the incubator under the microwave or in a dry oven that acted as the incubator.



**Figure 2.14:** View of microwave oven placed inside the incubator (door open). The circulating water-bath (on left) was connected with two water hoses that entered through the back panel of the incubator (not visible), then through two holes of the back panel of the microwave oven and the infusion bags inside the oven (see also Figure 2.13).

The microwave oven was turned on, and at regular intervals, the cuvettes as well as the controls were placed in a polystyrene container (to retain the heat) and taken to the spectrophotometer to measure light scattering. The process of transporting the cuvettes to the spectrophotometer, taking the measurements and returning the cuvettes to the oven, took on average up to four

minutes. The temperature inside the oven was noted, before and after the samples were measured.

#### ***TRANSVERSE ELECTROMAGNETIC MODE (TEM) CELL***

The TEM cell was placed in an incubator set to 37°C, with a 5% supply of CO<sub>2</sub>. For one of the experiments the CO<sub>2</sub> was turned off. The cell was calibrated to hold two flat Falcon© tissue culture flasks of volume 25 cm<sup>3</sup> in tight fitting moulds. The actual protein solution used for the experiments was 6.0 ml each for the “exposed” and “control” flasks and 6.0 ml of buffer for the second flask inside the TEM cell. The magnetic field inside the incubator was < 2 mGauss. At intervals of 20 to 60 minutes, the exposure was paused and the “exposed” and “control” flasks taken from the TEM cell and incubator. The “exposed” and “control” flasks were left at room temperature on the bench and 1.0 ml was withdrawn from both flasks into a quartz cuvette for spectroscopy measurements. The light scattering for both samples was determined at 360 nm on a Shimadzu UV-1601 UV-Visible spectrophotometer. The solutions were replaced into the flasks, that were returned to the TEM cell or incubator and exposure resumed. The temperature was measured with an alcohol thermometer, before removing and after replacing the flasks. It took on average 6 to 8 minutes to take the samples from the incubator, read the absorbance and replace them in the incubator.

#### **2.4.1.2 EXPOSURE SYSTEM 2**

*Exposure system 1* exhibited several limitations such as severe temperature loss when removing samples for light scattering measurements, the inability to accurately measure the temperature during an experiment, and the long time necessary for the incubator to reach a different temperature. Another system was therefore developed whereby the spectrophotometer acted as the incubator. Light scattering measurements were therefore *in situ* and samples were removed once every six minutes for exposure in the microwave. By placing the microwave close to the incubator (spectrophotometer), the samples lost little heat, the temperature probes were within

close proximity to both the microwave and the incubator and therefore, experiments could be undertaken at a range of temperatures.

A glass plate was glued to the cylindrical supports of the microwave oven to avoid movement during experiments and a rotating perspex plate was installed on the floor of the oven. Stoppered quartz cuvettes of 1cm path length (dimensions 46.0 x 12.5 x 12.5 mm), containing the protein solutions to be tested, were positioned in the multi-cell holder of the spectrophotometer that acted as the incubator. The cuvettes were withdrawn from the spectrophotometer for exposure every six minutes, and placed in a tight fitting cavity of a polystyrene transport box. One cuvette, named “control” was placed on the bench next to the spectrophotometer while the second cuvette, named “exposed”, was placed on a marked position on the glass plate for the duration of the exposure (typically 3.2 or 5.0 seconds). In later experiments, the box with the “exposed” sample was placed on a marked position on the glass plate of the microwave oven for the duration of the exposure. SAR calibrations were subsequently carried on the cuvette inside the box. A schematic overview of the procedure is given in Figure 2.15, while Figure 2.16 shows the experimental set-up in the laboratory.

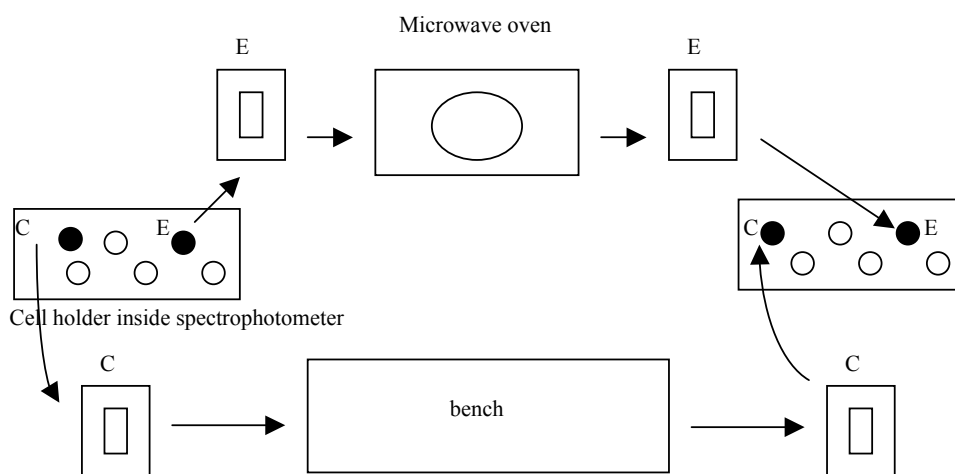


**Figure 2.15: Diagram of the experimental procedure *Exposure system 2*. Control (C) and exposed (E) samples were incubated in the cell holder of the spectrophotometer and periodically removed and placed in thermally insulated containers. The containers were either placed in the microwave oven (E) and exposed to pulsed 2.450 GHz or left on the bench (C). Both samples were returned to the cell holder within 30 seconds.**

A sealed plastic box of dimensions 11 x 8.5 x 7.0 cm, filled with water, was placed in the oven to absorb the majority of the microwaves and to stabilize the field within the cavity (Figure 2.17). The power applied to the sample could be altered by the volume of water in the plastic box.

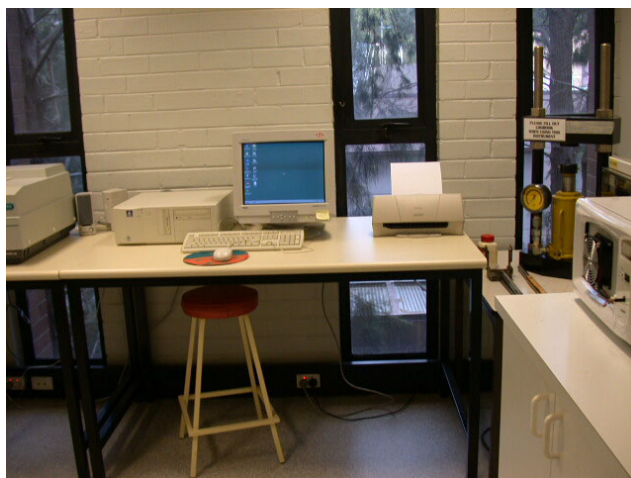


**Figure 2.16: Exposure set up *Exposure system 2*. The spectrophotometer is partly visible to left of photo. The “bench” is the table next to the spectrophotometer and the microwave oven is on the right.**



**Figure 2.17: View of the opened microwave oven as described in the *Exposure system 2*. The glass plate turns on a perplex clip. To avoid temperature loss, exposure was performed on the cuvette containing the protein solution while placed in a polystyrene box. The SAR was determined also with the cuvette placed in the box.**

### 2.4.1.3 EXPOSURE SYSTEM 3

In addition to incubating samples in the spectrophotometer, it was at times useful to have another incubation source to allow the temperature difference between samples to be in the range of 0.5 to 1.5°C and thus to enable comparison of initial rates.



**Figure 2.18: View of the microwave oven in close proximity to the dry block heater.**

Figure 2.18 shows how the block heater was adapted to function as a heating source for multiple samples. Because the block heater could be easily transported, it was a convenient incubator for the circular dichroism (CD) studies that were performed in Sydney.

## 2.4.2 ELECTRIC FIELD EXPOSURE

### 2.4.2.1 DC EXPOSURE

A 30kV Non Destructive Insulation Tester, type JP 30 (Danbridge, Denmark) was fitted with a conducting wire to expose protein samples to a DC electric field.

Two plastic cuvettes of 10 mm path length containing 1.0 ml of protein solution were wrapped with insulating tape. Two strips of aluminium foil or copper (6.0 x 1.0 cm, 0.5 cm thick), one of which acted as the electrode, were held tightly held between the cuvette and the tape, on opposite sides of cuvette. The samples were placed inside the aluminium cuvette holders of a dry block heater. DC power was obtained from the Non Destructive Insulation Tester that transferred a voltage of 5 or 10 kV via a conducting wire to the sample (exposed) by way of the

electrode. Another wire, clipped to the second electrode against the sample cuvette, acted as the earth wire. Prior to exposure, the control sample was placed in a cuvette holder directly next to the exposed sample.

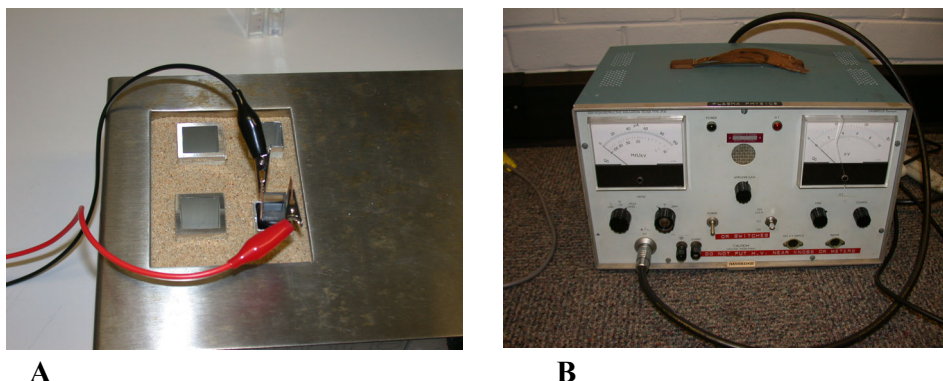


**Figure 2.19:** View of block heater and four aluminium cuvette holders in the sand filled cavity (A). DC power was obtained from a generator (B) that transferred a voltage of 5 or 10 kV (red wire on A) to the exposed sample via the electrode (copper or aluminium strip). The black wire on the second electrode is an earth wire. The covers on top of the samples were removed for the purpose of the photograph. In later experiments, for safety reasons, two Teflon, non-insulating cuvette holders were used and a cover made of insulating tape was placed over the cavity for the duration of the experiment.

Both cuvettes were covered with insulating tape. Figure 2.19 A and B shows how the experiment was set up. For later experiments two non conducting glass filled Teflon cuvette holders were designed thereby bypassing the need to wrap and unwrap the cuvettes with insulating tape. The insulating tape caused some smudging on the plastic cuvettes which was thought to interfere with the light scattering measurements. The copper strips fitted tightly between the plastic cuvette and the Teflon cuvette holder.

#### 2.4.2.2 AC EXPOSURE

A generator was connected to a voltage transformer fitted with a conducting wire to expose a protein sample to an AC electric field (Figure 2.20). Two plastic cuvettes of 10 mm path length containing 1.0 ml of protein solution were wrapped with insulating tape. Two strips of copper (6.0 x 1.0 cm, 0.5 cm thick), one of which acted as the electrode, were held tightly held between the cuvette and the tape, on opposite sides of cuvette. The samples were placed inside



aluminium cuvette holders of the dry block heater. AC power was obtained from the generator at 80 V, to the variable autotransformer that had an output of 4 kV/cm AC. The electric field was applied to the sample by way of a conducting wire that was clipped to the electrode next to the cuvette. Another wire, clipped to the second electrode against the sample cuvette, functioned as the earth wire. The control sample was placed in a cuvette holder directly next to the exposed sample.

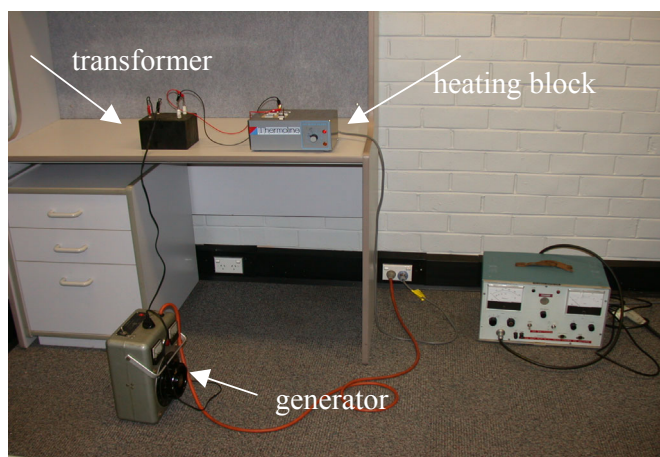


**Figure 2.20:** View of the instruments used for the AC field experiment

## 2.5 TEMPERATURE MEASUREMENTS

Microwaves deliver energy rapidly to the interior of a solution thus causing heating. It was expected that as a result of pulsed microwaves, every six minutes, the temperature of a sample solution would rise rapidly and then fall after a few seconds of exposure (Figure 2.21).

The experimental procedure that was adopted involved moving samples to and from the microwave oven every six minutes and it was therefore not possible to fit the samples with probes so that the temperature could be monitored *in situ*, for the duration of the experiment. Thus, for all experimental samples the temperature was investigated in three parts (Figure 2.21).



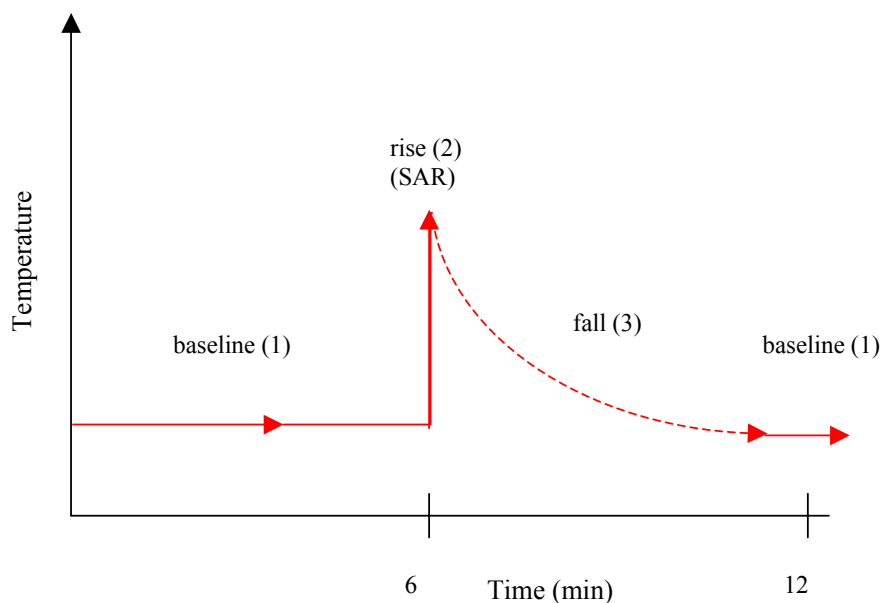


**Figure 2.21:** Diagram of the expected temperature profile over a six minute period (6 to 12 minutes) of a sample exposed to pulsed microwaves. Three parts of a typical experiment were studied separately with respect to temperature. Part 1 reflects the temperature of the sample in the incubator (baseline); part 2 relates to the temperature increase due to pulsed microwaves (the SAR was derived from the temperature rise); part 3 analyses the fall in temperature to the baseline and the time associated with it.

### 2.5.1 BASELINE (part 1 of figure 2.21)

#### 2.5.1.1 BASELINE TEMPERATURE FOR *EXPOSURE SYSTEM 1*

The temperature inside the incubator was determined by reading alcohol filled thermometers of 0.5°C gradation, one placed inside the oven cavity and the other on the lower shelf of the incubator. The temperature was read prior to taking the sample out for light scattering measurements. It was assumed that the temperature of the sample was the same as the ambient temperature. No investigation was made on the time it took for the sample to get to the baseline temperature.

#### 2.5.1.2 BASELINE TEMPERATURE FOR *EXPOSURE SYSTEMS 2 AND 3*

The multi-cell holder acted as the incubator for *Exposure system 2* (Figure 2.22) and the dry block heater for *Exposure system 3* (Figure 2.10). For our purposes, two or three samples were used per experiment. Cuvettes containing 1.0 ml of the relevant buffer were placed in labelled cells, covered with masking tape and measured for temperature at four different heights in the

solution (0, 10, 17 and 23 mm from the base of the cuvette). The temperature of the solution was measured every second for at least 20 minutes per height, using fluoroptic probes. The measurement was repeated at least twice and the average was taken to be the baseline for a particular cuvette position in the multi-cell holder or block heater. The time for the solution to reach the desired temperature was also noted.

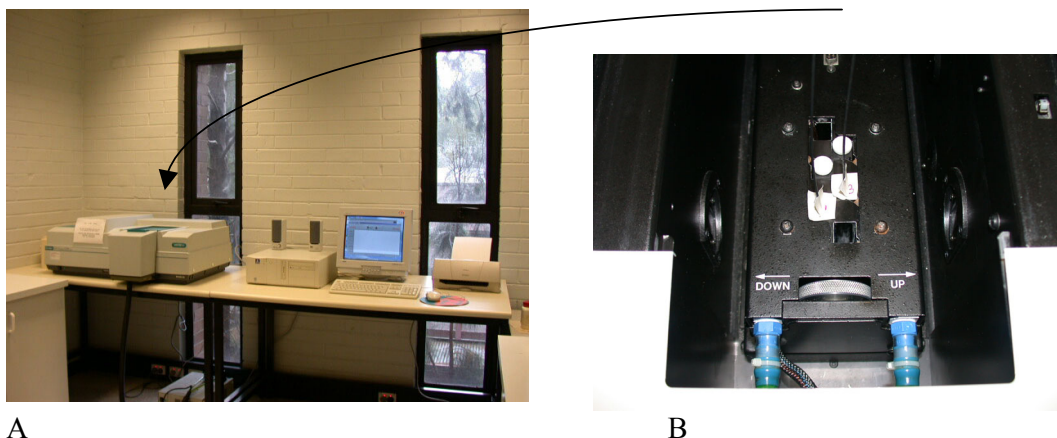


**Figure 2.22: View of the Cary spectrophotometer (A) and the multicell holder (B).** The multi-cell holder fitted a maximum of 12 cuvettes and was positioned inside the spectrophotometer under the green cover (see arrow). For the determination of the baseline of the different cell positions, a fluoroptic probe was inserted in the solution, inside the cuvette and held in place with masking tape. The temperature of the solution was monitored for at least 20 minutes at four different sample heights.

### 2.5.2 SAR MEASUREMENTS (part 2 of Figure 2.21)

The SAR was calculated for each pulse period by temperature calorimetry, using temperature measurements made with Luxtron 502/504 fluoroptic-sensing probes.

#### 2.5.2.1 SAR MEASUREMENTS FOR *EXPOSURE SYSTEM I*

The microwave oven was placed on a laboratory bench and the infusion bags inside the oven were attached to the circulating water bath that was at room temperature. Two quartz cuvettes of 1cm path length (dimensions 46x12.5x12.5 mm) were filled with 1.0 ml of buffer each and were placed on the glass plate inside the oven and the positions marked. Two fluoroptic temperature-sensing probes were inserted through the meshed door and each was placed into a cuvette. The probes, touching the bottom of the cuvettes were held into position by cellotape. Thus, the oven

door could be closed and the fan turned on while the probes were inserted into the cuvettes inside the oven. The microwave oven was turned on to emit pulses every six minutes for up to 15 minutes in total. From the numerical data, the maxima and minima were noted and the SAR for both solutions calculated, assuming that the buffer had the same specific heat capacity ( $C_p$ ) as water:

#### Calculation of SAR:

Heat delivered to 1g of water,

$$\begin{aligned} \text{per } 1^\circ\text{C temperature rise} &= \text{mass} * C_p * \Delta T \\ &= 1 \text{ g} * 4.18 \text{ Jg}^{-1}\text{K}^{-1} * 1 \text{ K} \\ &= 4.18 \text{ J} \end{aligned}$$

$$\text{Heat delivered to 1 kg} = 4180 \text{ J/kg}$$

The SAR in (W/kg), averaged over six minutes:

$$\begin{aligned} \text{SAR} &= \text{Energy delivered per kg/time of delivery} \\ &= 4180 \text{ J/kg} / 6 \text{ min.} * 60 \text{ s/min} \\ &= 11.61 \text{ W/kg per } 1^\circ\text{C temperature rise} \end{aligned}$$

#### **2.5.2.2 SAR MEASUREMENTS FOR EXPOSURE SYSTEMS 2 AND 3**

The microwave oven was placed on a laboratory bench (Figure 2.23). SAR determinations on cuvettes placed on the glass plate were the same as described for the *Exposure system 1*. However, for the cuvette in the polystyrene box, that was placed on the glass plate, procedures were as follows: One Luxtron 502/504 fluoroptic temperature-sensing probe was inserted through the meshed door and placed into the cuvette that was contained inside the polystyrene box.

It was found that the microwave field was not uniform in the solution and therefore to get a fair representation of the power distribution in the sample, the temperature was measured at four heights in the cuvette. The probe was inserted, in the middle of the solution and at 0, 10, 17 or

23 mm from the base. To hold the probe in place, the probe was led through a small hole in masking tape that covered the top of the cuvette. The microwave oven was turned on and emitted pulses every six minutes for about 30 minutes in total. In the course of the project, it was observed that the conductivity of a buffer solution affects its ability to absorb microwaves. Therefore all SAR calibrations were repeated for the various buffers (Appendix 4 and 5). The temperature determinations were repeated at least three times per height. The probe measured the temperature every second and the numerical output of the readings were saved onto a computer file from which the data could be extrapolated.

Various experimental conditions such as duration of microwave pulses, the amount of water in the plastic box inside the microwave cavity and type of buffer were explored.

The data were averaged and graphed to determine the SAR between 13 and 19 mm from the base of the cuvette as this is the area where the light beam of the spectrophotometer passed through the cuvette and detected light scattering.



**Figure 2.23: View of method of SAR calibration. Fluoroptic probes were inserted through the meshed door of the microwave oven and held in place in the cuvettes. The probes were connected to the sensor processor, which in turn was connected to a computer where the data was logged.**

### **2.5.3 FALL OF TEMPERATURE (refers to part 3 in Figure 2.21)**

#### **2.5.3.1 RELAXATION OF TEMPERATURE TO BASELINE *EXPOSURE SYSTEM 2***

The return of the temperature to its baseline value was not studied for *Exposure system 1*. Sham exposure experiments for *Exposure system 2* were carried out on buffers to monitor the temperature of the sample immediately after exposure until it had the same temperature as the baseline.

These experiments were carried out for four different heights in the solution (i.e. 0, 10, 17 and 23 mm from the base of the cuvette). The procedure for inserting the probe and keeping it in position was similar as discussed in sections 2.5.1 and 2.5.2. The sample was placed with the probe into the incubator (i.e. the multi-cell holder of spectrophotometer) until 15 seconds before exposure. The probes were then taken from the cuvettes on which lids were placed and both cuvettes were transferred to the transport box as described in *Exposure system 2*. The control box was left on the bench and the exposed box was placed in the microwave oven where the sample was exposed to either 3.2 or 5.0 seconds of pulsed microwaves. Within 15 seconds the samples were returned to the multi cell holder and the probes attached to the masking tape reinstated in the corresponding samples. The time of the return was noted and the data collected for several exposures. The experiments were carried out in triplicate. The data were collated and averaged to give:

1. the temperature of the sample after exposure and return to the multi-cell holder
2. the time of return to the multi-cell holder and
3. the time at which the sample temperature had returned to the baseline temperature.

#### **2.5.3.2 TEMPERATURE AVERAGE OVER SIX MINUTES – *EXPOSURE SYSTEM 2***

By studying the temperature in three parts it was possible to construct a profile of the temperature for a six minute period. The results of the temperature studies, referring to figure 2.21, can be summarized as follows:

<u>Part of profile</u>	<u>Experimental section</u>	<u>Description</u>
1	3.1	baseline
2	3.2	temperature rise due to microwaves
3	3.3	relaxation (fall) to baseline

For every buffer/exposure system a profile was obtained, at four heights of the cuvette, by collating the results from the above studies. The area under the graph was determined by using the Trapezoid Rule, in steps of 0.25 minutes to give an average temperature over six minutes.

### **2.5.3.3 RELAXATION OF TEMPERATURE TO BASELINE *EXPOSURE SYSTEM 3***

In principle, the same temperature modules (see figure 2.21) as for *Exposure system 2* applied to this exposure system however there were some complications that made use of this system difficult for repeat experiments. It was not possible to control the temperature other than by turning the dial and although the dial settings were marked, a slight turn of the switch could bring about a deviation in temperature. The heater was also required for electric field experiments, for which non-conducting cuvette holders were used. The cell holders in the block heater were carefully marked in order to create the same conditions as previous experiments. When *Exposure system 3* was used in association with light scattering experiments, the sample temperature was affected because of transport to and from the multi-cell holder of the spectrophotometer that had a different baseline to the block heater. Therefore all baseline measurements were performed on the same day as the experiments and sham experiments were performed to determine the loss of temperature associated with removing samples periodically.

### **2.5.3.4 TEMPERATURE AVERAGE– *EXPOSURE SYSTEM 3***

To overcome variables (2.5.3.3), the temperature was measured, in triplicate, at the conclusion of each experiment for baseline and loss of temperature due to light scattering measurements in another instrument (the spectrophotometer). The temperature was determined over 30 minutes and plotted for each six-minute period to give a slope from which the temperature for every 0.25

minutes was derived. Using the Trapezoid rule, the area under the graph was calculated and hence the average temperature.

## 2.6 LIGHT SCATTERING EXPERIMENTS

All protein and reagent solutions were prepared on the day of the experiment.

The spectrophotometer was set to the desired temperature and auto-zeroed. The experiments were carried out using pairs of samples. One sample was labelled as “exposed” and the other as “control”. The treatment of the exposed and control sample was identical, except that the exposed sample received either bursts of microwave pulses every six minutes or had an electric field applied. The light scattering was measured at  $\lambda$  360 every two minutes.

The details on the light scattering measurements are discussed individually for the different exposure systems in sections 2.4.1 and 2.4.2.

### 2.6.1 STATISTICAL ANALYSIS OF DATA

For every protein aggregation experiment that was monitored by light scattering, the point of inflection in the precipitation graph was used as a point for comparing rates of precipitation. Each profile was fitted using a sigmoidal function in SigmaPlot and the point of inflection found from the first derivative. The initial slope of the graph, calculated from this point, was determined for all exposed and control samples, expressed as the ratio of exposed over control and used as a measure of the initial unfolding rate. If the distribution of this ratio is regarded as approximately normal, then the null hypothesis states that, for a 5% confidence limit, 95% of all exposed samples have the same or a lower initial precipitation rate than the control sample. Therefore, the mean ( $\mu$ ) ratio of exposed/control was expected to be  $\leq 1$  ( $H_0: \mu \leq 1$ ).

The alternative hypothesis states that 95% of all exposed samples are likely to have a higher initial precipitation rate than the control sample (Alternative hypothesis:  $H_A: \mu > 1$ ). The  $H_0$  will be rejected if the value of  $t$ , when applying the one tailed  $t$ -test, is exceeded in random sampling and the probability  $P$  is smaller than 0.05 (Figure 2.24).

**Figure 2.24: The distribution of a normal population. By applying the  $t$ -test, there is 95% confidence that the mean of the experimental data lies between the values of  $-t_{0.05}$  and  $t_{0.05}$ <sup>166</sup>.**

### 2.6.2 DIFFUSION OF PROTEINS

The samples could not be stirred whilst in the multi-cell holder of the spectrophotometer due to the interaction of the magnetic stirrers with the microwaves. When the light scattering was measured every two minutes, the light beam passed through the cuvette between 13 and 19 mm from the base of the cuvette. As initial experiments showed that the SAR in the sample varies with sample height, it was important to examine the diffusion of proteins through the sample to be able to quantify the SAR in the light scattering experiments.

The program HYDROPRO<sup>167</sup> was downloaded<sup>168</sup> to calculate the hydrodynamic radius of the proteins. The program builds a hydrodynamic model for globular proteins from its atomic coordinates and calculates the radius of a spherical object that has the same drag coefficient, i.e. the effective hydrodynamic radius. The atomic coordinates are contained in the crystallographic data files that were downloaded from the Protein Data Bank (PDB)<sup>135</sup>. In cases where no PDB file was available for a protein, the file of a related protein was used.



## 2.7 PROTEIN CONFORMATION STUDIES

### 2.7.1 ENZYME ACTIVITY ASSAYS

#### *CITRATE SYNTHASE*

The mitochondrial enzyme citrate synthase catalyses the conversion between oxaloacetate and citrate during the tricarboxylic acid cycle (TCA) from Acetyl-CoA (Figure 2.25):

**Figure 2.25: Schematic overview of enzymatic role of citrate synthase in the TCA cycle <sup>169</sup>.**

The reaction is a useful tool in determining the enzymatic activity of citrate synthase when catalysing the formation of CoA-SH. The free cysteine in CoA-SH reacts with 5-5'-Dithio-bis-2-nitrobenzoic acid (Ellmans' reagent) in a ratio of 4 to 5 moles of  $-SH$  <sup>170</sup> per mole of CoA-SH to form the yellow thionitrobenzoic acid (TNB) residue which can be detected spectroscopically at 412 nm. The disappearance of the SH intensity is an indirect measure of citrate synthase activity (see Figure 2.16).

For the microwave exposure and thermal experiments, the following activity protocol was adapted from Buchner *et al* <sup>148</sup> :

During a typical light scattering experiment on 3.0  $\mu M$  CS, 5  $\mu l$  of the exposed and a 5  $\mu l$  of the control sample was withdrawn at several time points. The aliquots were stored on ice. To each sample, after the last aliquots were collected, was added 95  $\mu l$  of 50 mM Tris buffer, 2mM

EDTA, pH 8.0 (TE buffer). The spectrophotometer was set to  $\lambda$  412, 25°C and was zeroed using plastic 1.5 ml cuvettes filled with 1.0 ml of TE buffer.

The enzymatic reaction was started by adding 20  $\mu$ l of a diluted aliquot to a previously prepared reaction mixture that consisted of:

930  $\mu$ l of TE buffer ; 10  $\mu$ l of 10mM oxaloacetic acid in 50mM Tris (pH not adjusted); 10 $\mu$ l of 10mM DTNB (in TE buffer); 30  $\mu$ l of 5mM acetylCoA (in TE buffer).

The mixture was inverted and the absorbance read every 0.1 seconds. The linear slope of the initial increase in absorption was used to calculate the specific activity of CS. The activity, prior to exposure, was corrected to 100% activity.

## **2.8 SUPPLEMENTARY STUDIES ON PROTEINS EXPOSED TO MICROWAVES**

A series of additional experiments were carried out on protein solutions. They are listed in the following sections.

### **2.8.1 EFFECT OF CO<sub>2</sub> ON PROTEIN AGGREGATION**

For light scattering experiments in *Exposure system 2*, four 1.0 ml protein samples (ADH and CS) were transferred to quartz cuvettes. To two cuvettes, CO<sub>2</sub> was bubbled through the solution for a period of ~5 seconds each. The remaining two cuvettes were used as the controls. Of the cuvettes containing added CO<sub>2</sub>, one was exposed to pulsed microwaves and the other was kept as a control (see section 2.4.1.2 for the protocol). The experiment was repeated for the two samples that contained no added CO<sub>2</sub> and which had been kept on ice during the first experiment.

### **2.8.2 EFFECT OF MOLECULAR CROWDING ON PROTEIN AGGREGATION**

Two 1.0 ml solutions of 0.2 mg/ml ovotransferrin in 50mM phosphate buffer, 0.1 M NaCl, pH 7.0 containing 20% w/v dextran were incubated in the multi-cell holder of the spectrophotometer, *Exposure system 2*, at 45°C. After 3 minutes, both samples were withdrawn

as described in section 2.4.1.2. The exposed sample was exposed to 3.2 seconds of 2.45 GHz pulses five times at intervals of 6 minutes. The light scattering at 360 nm was measured every two minutes.

---

## CHAPTER 3

---

### TEMPERATURE ASSESSMENT

The sections in this chapter refer to parts 1, 2 and 3 in Figure 2.12, the six-minute profile for a sample exposed to pulsed microwaves in *Exposure systems 1, 2 and 3*. The calibration of the TEM cell with regards to SAR was not undertaken.

#### 3.1 BASELINE TEMPERATURE OF INCUBATORS (refers to part 1 in figure 2.21)

##### 3.1.1 BASELINE EXPOSURE SYSTEM 1

For *Exposure system 1*, the ambient temperature was noted from reading the alcohol thermometers close to the position of the cuvettes, which was set at 37 °C. No measurements were taken of the solution inside the cuvettes.

##### 3.1.2 BASELINE EXPOSURE SYSTEM 2

For *Exposure system 2*, a detailed study was undertaken not only of the temperature at different heights of the solutions but also of temperature variations between positions of the multi cell holder (spectrophotometer). No difference was found between baseline temperatures of 50 mM and 0.1 M buffer solutions or buffers containing 0.1 M salt. However considerable differences in temperature were found with respect to the height of the solution and between cells of the multi-cell holder. Appendix 7 summarizes the data for each position in the multi-cell holder. Cells 5 and 6 of the multi-cell holder were on average warmer over the full height than the other cells, with cell 6 being the warmest. The temperature of the solution between 13 and 19mm was of particular interest as this is the region that was sampled in light scattering experiments. In general, controls were always placed in the cells that were warmer than others. When the control was placed in cell 6 and the exposed in cell 2, the difference in average temperature

(taking the average values of 13 and 19mm height) was 0.8°C. Thus, to minimize the difference in average temperature (over a 6 minute period), a control would be placed in cell 6 or cell 5 while the sample that was to be exposed would occupy any of the other cells. Figure 3.1 shows graphs of the three temperature regimes that were adopted for this project. The data represent the temperature of samples in the six cells of the multi-cell holder of the spectrophotometer, over four different sample heights.

Table 3.1 provides a summary of the buffers and exposure conditions that were studied in detail with respect to SAR and position of the cells in the multi-cell holder. For clarity the buffer/exposure conditions have been given a systematic Roman number.

Buffer	Amount of water in plastic box in microwave cavity (ml)	Duration of microwave pulses (s)	Buffer/exposure conditions – systematic number	Temperature (multi-cell holder) °C	Cells used in incubator
80mM phosphate buffer, pH 7.5	550	3.2	I	42	2,3,4,5
0.1M phosphate buffer, pH 7.0	550	5.0	II	42	2,3,4,5
0.1M phosphate buffer, 0.1M NaCl, pH 7.0	650	5.0	III	37	2,3,4,5,6
0.1M phosphate buffer, 0.1M NaCl, pH 7.2	650	5.0	III	45	3,4,5,6
0.1M phosphate buffer, 0.1M NaCl, pH 7.0	500	5.0	IV	45	3,4,5,6

**Table 3.1: Overview of buffer and exposure conditions that were used in experiments. For simplicity, the listed temperatures are arbitrary. In general, the software was set 1°C higher in order for the cells to get to the required temperature. Furthermore, the temperature differed with sample height (Figure 3.1).**

The time to reach the baseline (temperature equilibrium) was determined by placing a cuvette containing 1.0 ml of milli-Q water with a fluoroptic probe in the spectrophotometer (the top was covered with masking tape). The temperature was measured for up to 20 minutes. Figure 3.2 shows the temperature profile of two such solutions where the probe was placed 10 mm from the base of the cuvette. One cuvette was placed in cell 5 and the other in cell 6 of the spectrophotometer of which the temperature was set to be 42°C. The baseline of these cells (Appendix 7) at this position is  $41.81 \pm 0.11$  for cell 5 and  $42.03 \pm 0.06$  for cell 6.

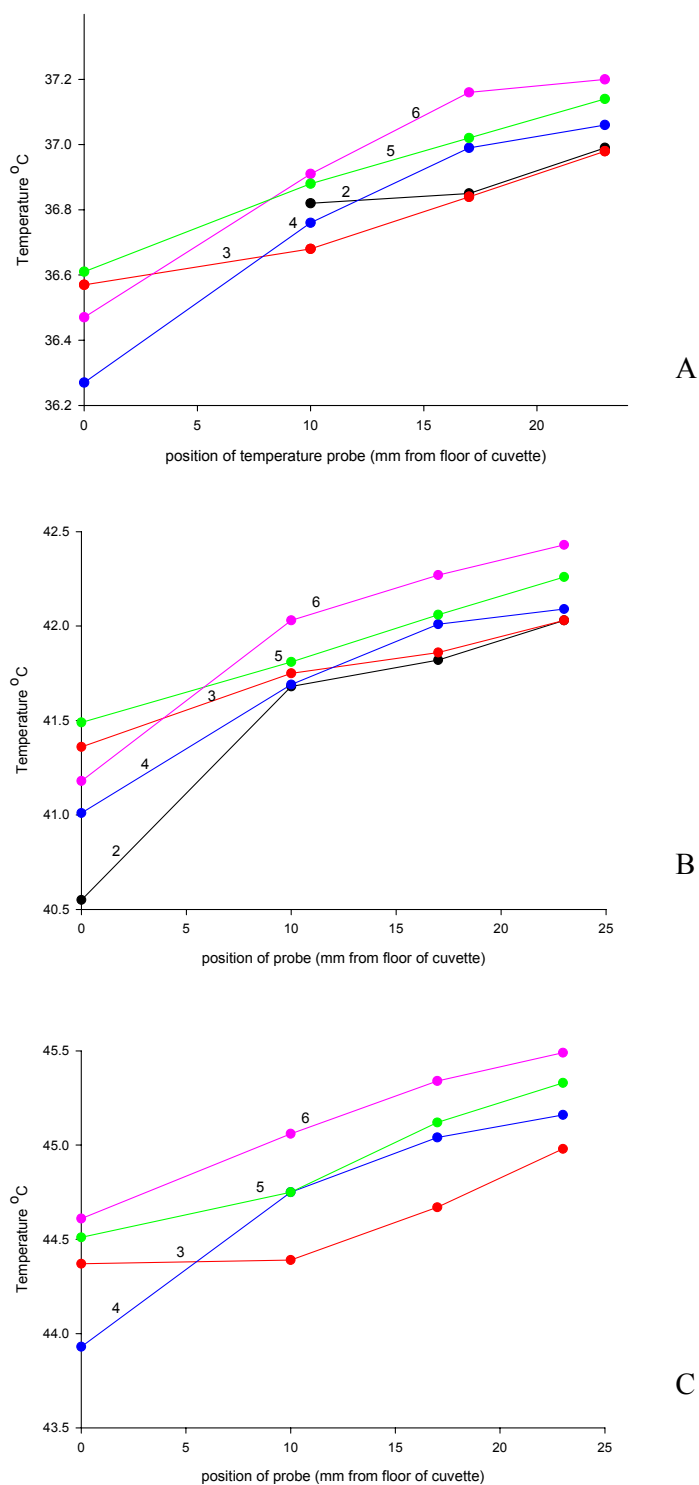
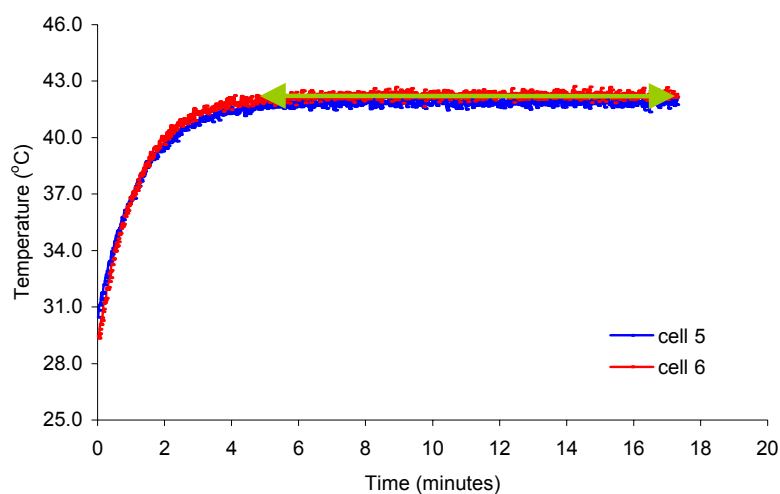


Figure 3.1: Temperature of 1.0 ml of 0.1 M phosphate buffer pH 7 in a quartz cuvette placed in positions 2, 3, 4, 5, or 6 of the multi-cell holder of the spectrophotometer (data are reported in Appendix 7). For clarity, the error bars have not been inserted. The temperature was measured at 0, 10, 17 and 23 mm from the base of the cuvette. The setting of the temperature software was 38°C (A), 43°C (B) and 46°C (C).

From Figure 3.2 it can be deduced that it took on average 5 minutes for the samples in the spectrophotometer to reach equilibrium. It was found to be similar for samples in the other cell.



**Figure 3.2:** Profile of baseline temperature for cells 5 and 6 in the multi-cell holder when the software temperature was set to 43°C. The temperature was measured 10 mm from the base of the cuvette. The green arrow represents the equilibrium temperature that was reached at ~5 minutes.

### 3.1.3 BASELINE EXPOSURE SYSTEM 3

An initial baseline determination of two cells in the block heater is shown in Figure 3.3. The temperature fluctuates in sets of twenty minutes. This pattern was at first attributed to the instrument. However on further investigation, it was found that the ceiling fans in the instrument room caused the “bumping” effect and when the fans were turned off, the samples in the block heater showed a regular temperature profile (Figure 3.3 B). Figure 3.3 B shows that it took at least 20 minutes for samples to get to the baseline temperature. Therefore it was not possible to compare aggregation rates of proteins if some samples were heated in the heating block while others were heated in the spectrophotometer, which takes on average 5 minutes for samples to get to the baseline temperature. To overcome this problem, samples were initially equilibrated in the spectrophotometer for 2 to 6 minutes. It was not possible to make this time longer as some proteins started to aggregate within several minutes. For an initial 2 minute incubation, the time to reach the baseline was thus reduced to 10 minutes (Figure 3.3 C).

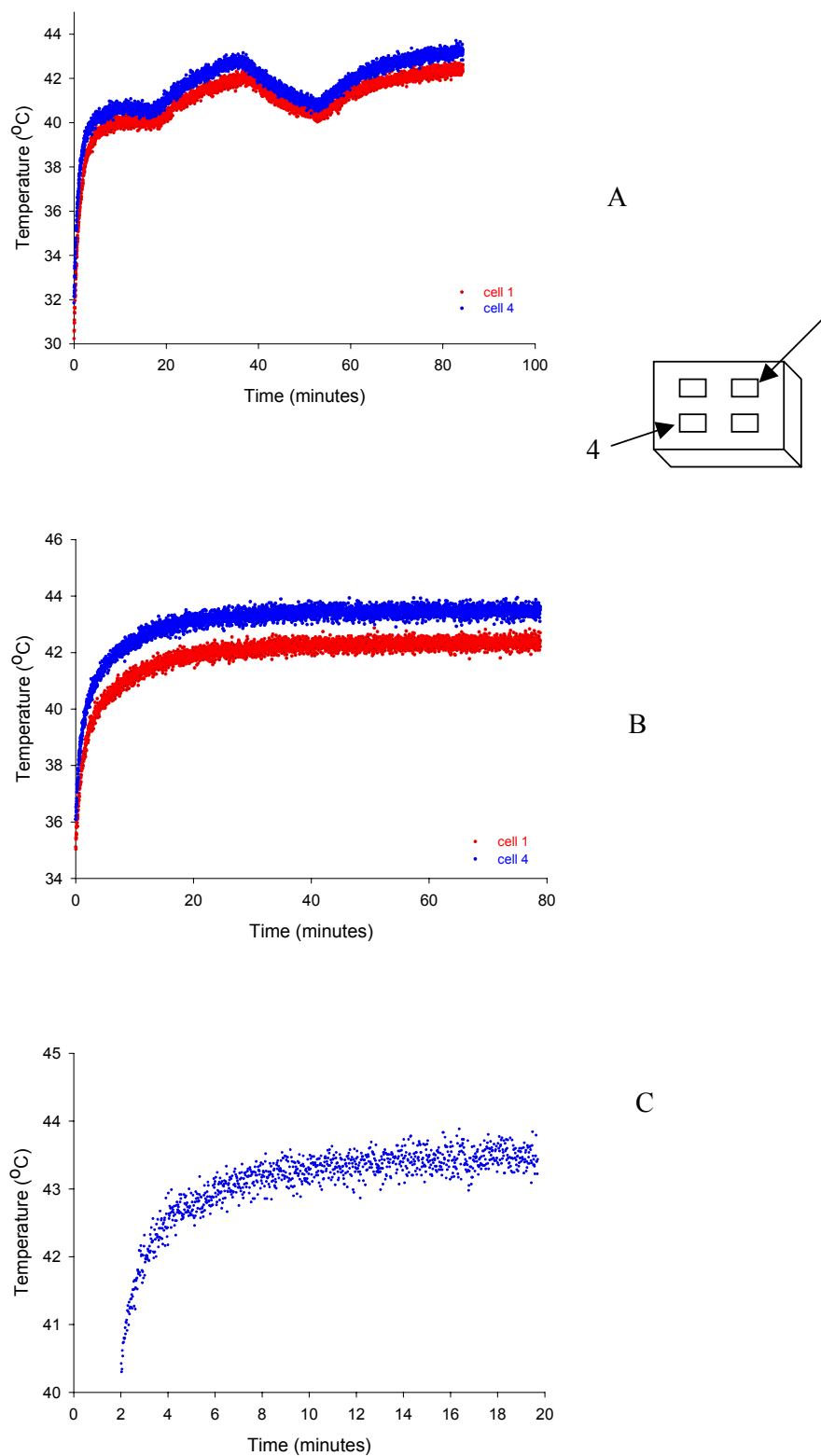


**Figure 3.3: Profile of temperature of 1.0 ml of milliQ water 10 mm from the base of cuvette in cells 1 and 4 of heating block when the temperature dial was set to “50°C” with the ceiling fan on (A) and off (B) in the instrument room. The diagram of the heating block is viewed from top showing the positions of the cells. C is the temperature profile of the sample incubated for 20 minutes in the multi-cell holder of the spectrophotometer (C).**



### 3.2 SAR MEASUREMENTS (refers to part 2 in figure 2.21)

The SAR measurements in the TEM cell were calibrated by Telstra for similar volumes as used in this project. They are reported as an average SAR value in Chapter 6.

Following are the experimental results for SAR measurements in *Exposure systems 1, 2 and 3*:

A burst of microwave pulses caused a transient temperature increase in the buffer solutions that were measured with fluoroptic probes. The temperature increase was found to be dependent on the type of buffer. Figure 3.4 is a typical plot of a temperature profile of a buffer over a period of exposure. The data, imported to Microsoft Excel, were graphed (grey colour) and the trendline (moving average of 5) is shown in red. The maxima and average minima of each exposure period were recorded from the trendline and the SAR was calculated from the difference between them using the equations given in section 2.5.2.1. Table 3.2 presents the data for the 8 pulse periods in Figure 3.4.

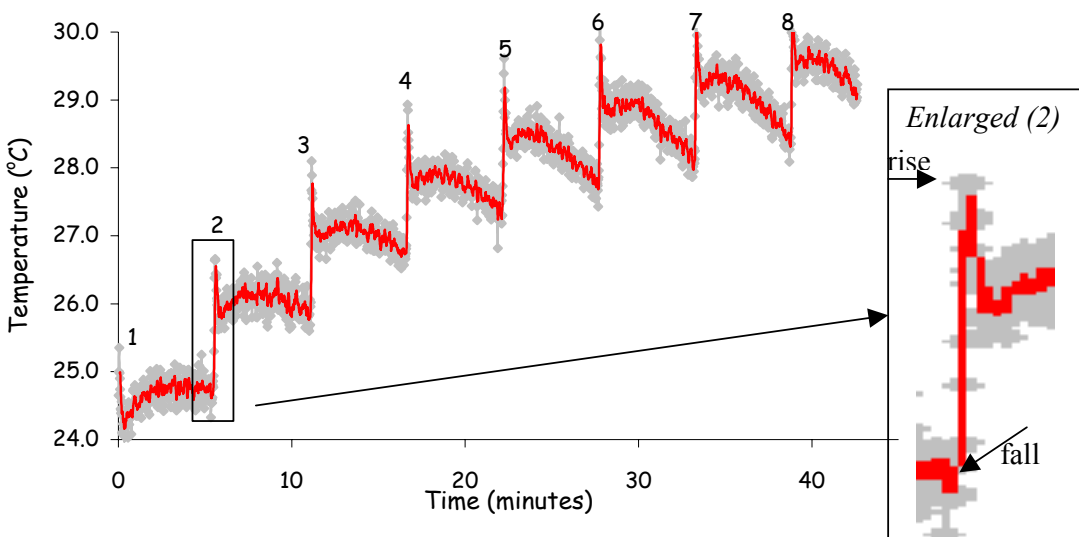


**Figure 3.4:** Temperature of a buffer solution exposed to pulsed microwaves during a 50 minute period. 1.0 ml of 50mM phosphate buffer, 0.1M NaCl, pH 7.0 initially at room temperature, was exposed to 8 periods of pulsed 2.45 GHz. Microwave bursts of 5 seconds were applied every 6 minutes. The plastic box in the microwave oven contained 550 ml water. The temperature was measured with a fluoroptic probe that was positioned at the bottom of the cuvette. The cuvette was placed inside a polystyrene box as described in section 2.4.1.2. Inset: Pulse period 2, enlarged. The difference in temperature between the rise and fall was noted as the change in temperature.

Pulse period	Average temperature prior to exposure (minima) in °C	Maximum temperature after exposure (maxima) in °C	Temperature difference in °C	SAR (W/kg)
1				
2	24.70	26.56	1.86	
3	25.85	27.77	1.92	
4	26.74	28.62	1.88	
5	27.35	29.18	1.83	
6	27.75	29.81	2.06	
7	28.10	30.20	2.10	
8	28.35	30.50	2.15	
$\Delta T$			$1.97 \pm 0.13$	$22.89 \pm 1.50$

**Table 3.2 : Data for the temperature rise and fall of the 8 pulse periods in Figure 3.4.**

Table 3.2 indicates that the difference between the maximum and minimum temperature became larger as the temperature increased. The SAR values reported in this project are based on sampling at room temperature only therefore values are an estimated only. See also section 7.10.1.

### 3.2.1 RELATIONSHIP BETWEEN CONDUCTIVITY AND SAR

It was found that the SAR of buffers containing 0.1 M NaCl was higher than the buffers without salt which prompted an investigation of the conductivity of all buffers. Figure 3.5 shows how the SAR increases for solutions of higher conductivity and Figure 3.6 shows a mathematical correlation by fitting the data points with a quadratic polynomial curve. From these data it was apparent that the SAR of a solution of 50 mM phosphate buffer containing 0.1M NaCl was at least double the SAR for a 50 mM buffer that did not contain salt. The box inside the microwave cavity contained 550 ml of water and the pulse (250) duration was 5 seconds.

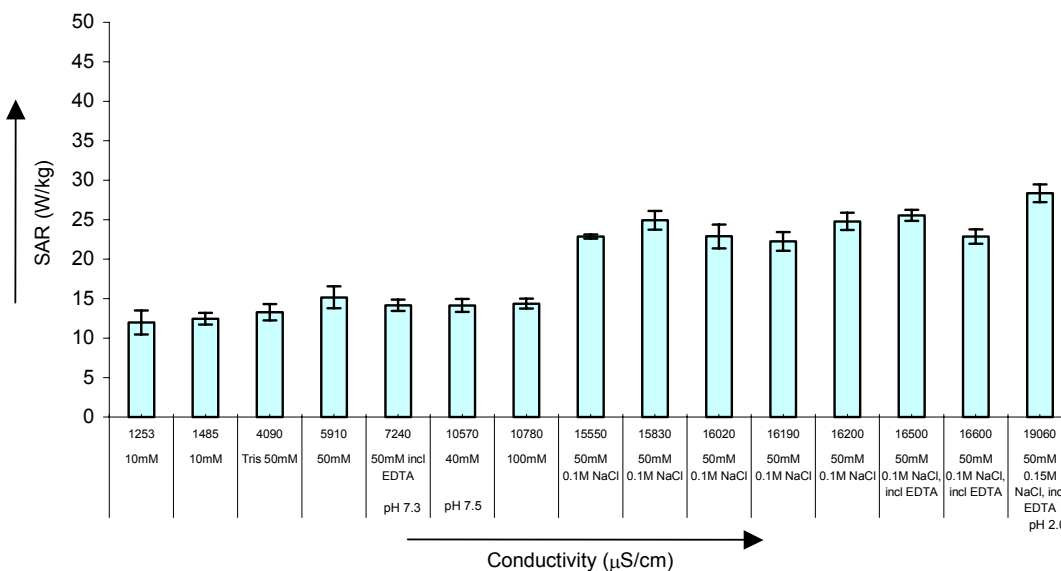


**Figure 3.5: Relationship between conductivity (numbers under the bars) and SAR.** The buffers were exposed to 5 seconds of bursts of 2.450 GHz at six-minute intervals for at least twenty minutes. Unless stated, the samples were 1.0 ml phosphate buffer, pH 7 of various concentrations (as indicated under the bars). All solutions were initially at room temperature. The temperature was measured at the bottom of the cuvette with fluoroptic probes.

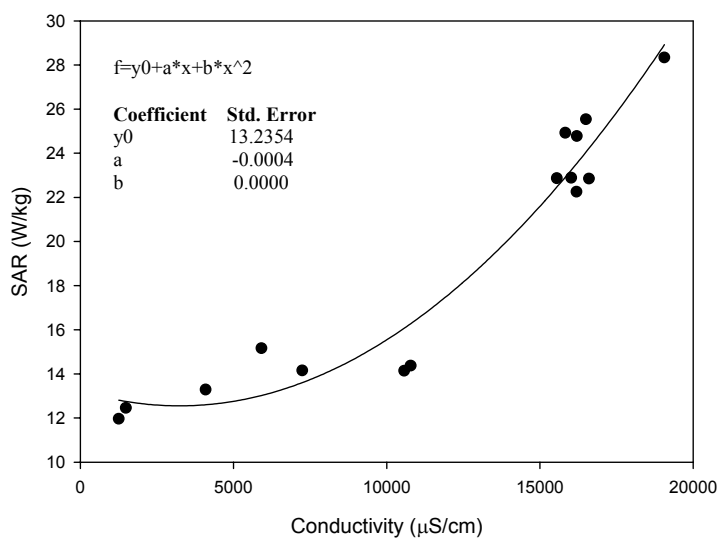


**Figure 3.6: Relationship between conductivity and SAR.** The data points (Figure 3.5) were fitted with a quadratic polynomial curve, using SigmaPlot.

### 3.2.2 RELATIONSHIP BETWEEN SAMPLE HEIGHT AND SAR

The SAR was established at four different heights in the cuvette (for each buffer), at the base of the cuvette (0mm), as well as at 10mm, 17mm and 23 mm from the base. The light beam of the spectrophotometer passes through the cuvette between 13 and 19 mm from the base of the cuvette (Figure 3.7). To calculate the SAR of the layer in the sample where sampling took place, the SAR was derived from the slopes of graphs, by assuming that the SAR between the 10 and 17 mm, as well as the SAR between 17 and 23 mm followed a straight line (Figure 3.8 A-D). The variation over a period of months was examined for every buffer system and the SAR was found to vary only slightly by 2 to 4 %.

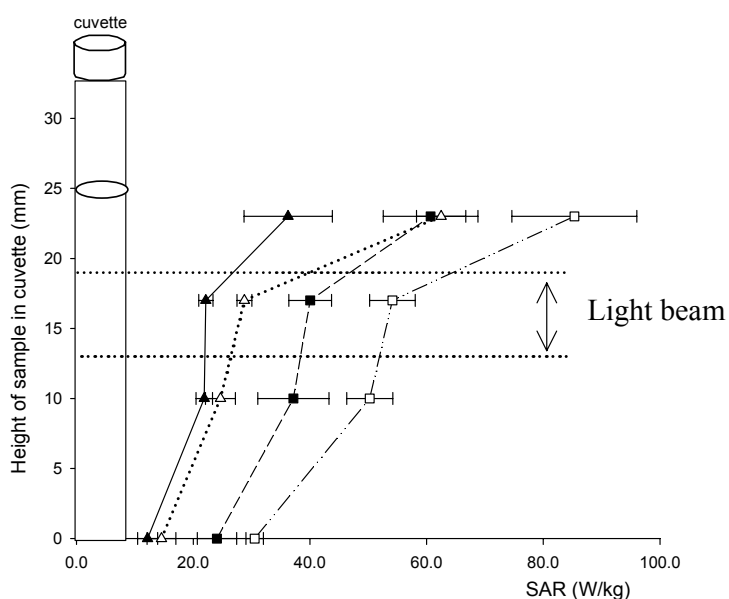


**Figure 3.7:** The specific absorbance rate (SAR) of the various buffer systems as a function of sample height. The SAR of the buffers was calculated as described in section 2.5.1.1. The dotted area on the graph corresponds to the area of the cuvette through which the light beam of the spectrophotometer passes. Key: 80 mM phosphate buffer, pH 7.5, 550 ml water box, 3.2 seconds per pulse period (pp) (—); 0.1 M phosphate buffer, pH 7.0, 550 ml water box, 5.0 seconds per pp (---); 0.1 M phosphate buffer, 0.1 M NaCl, pH 7.0, 650 ml water box, 5.0 seconds pp (.....); 0.1 M phosphate buffer, 0.1 M NaCl, pH 7.0, 500 ml water box, 5.0 seconds pp (-.-.-.-.).

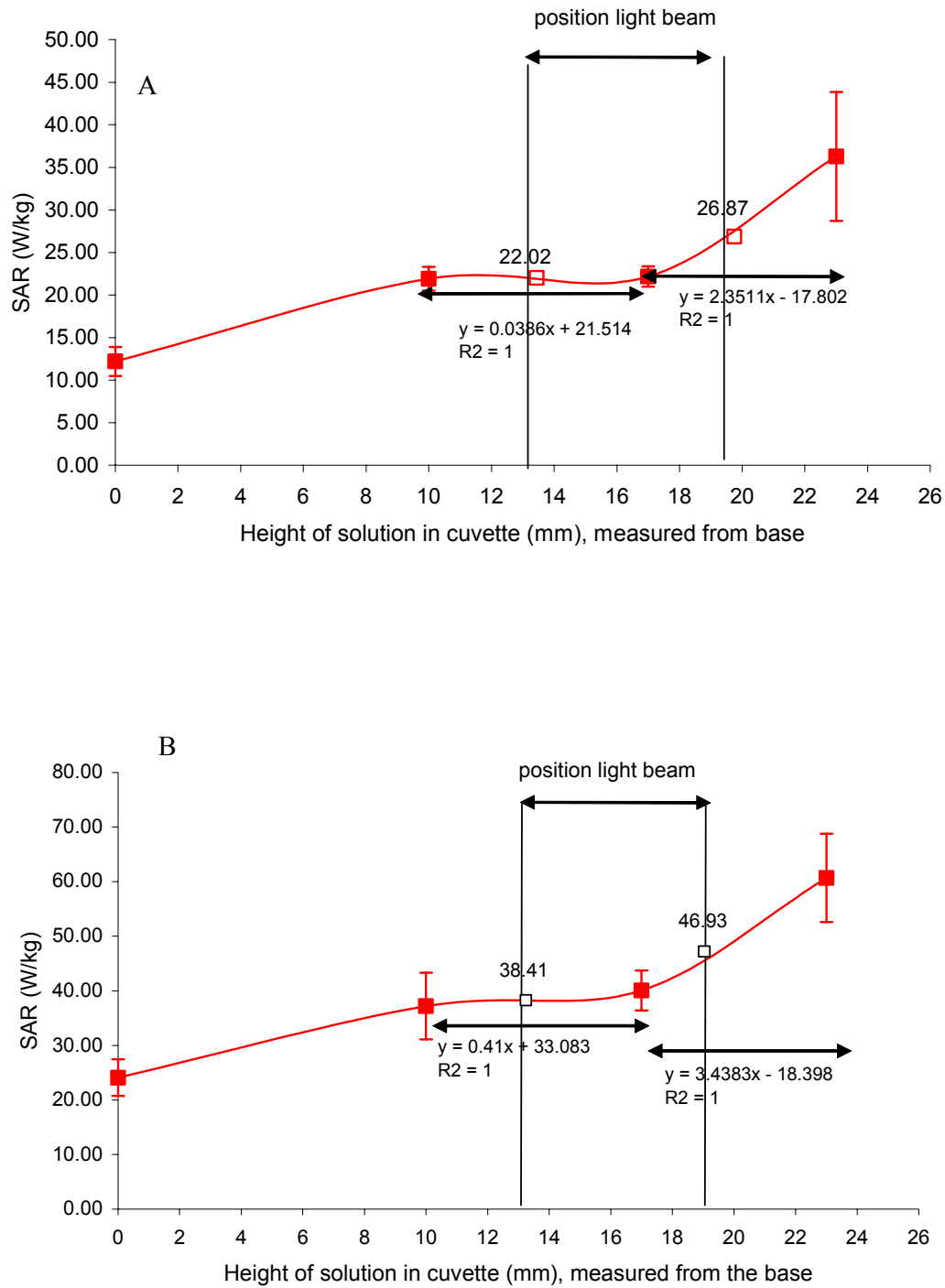
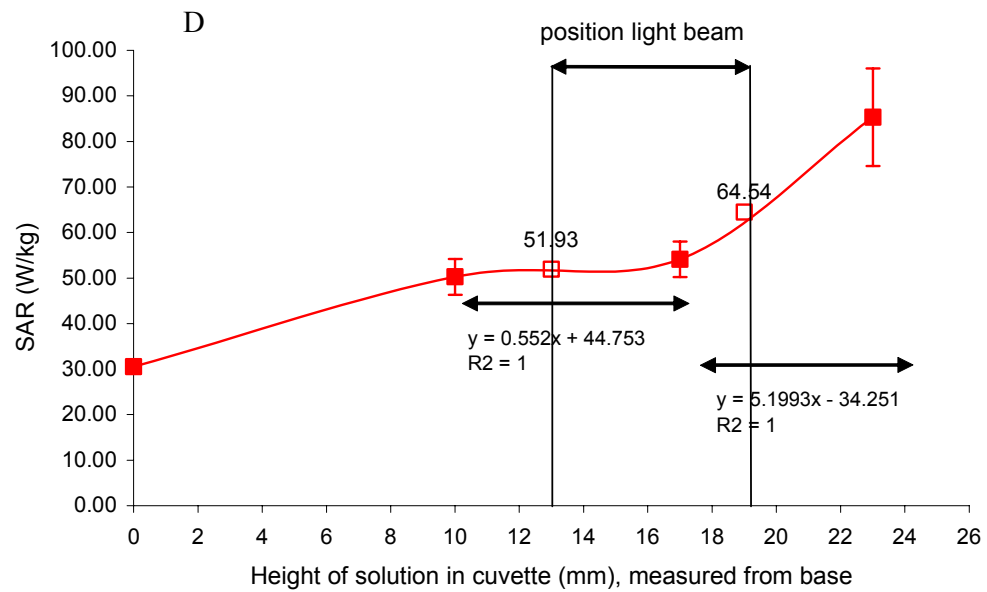
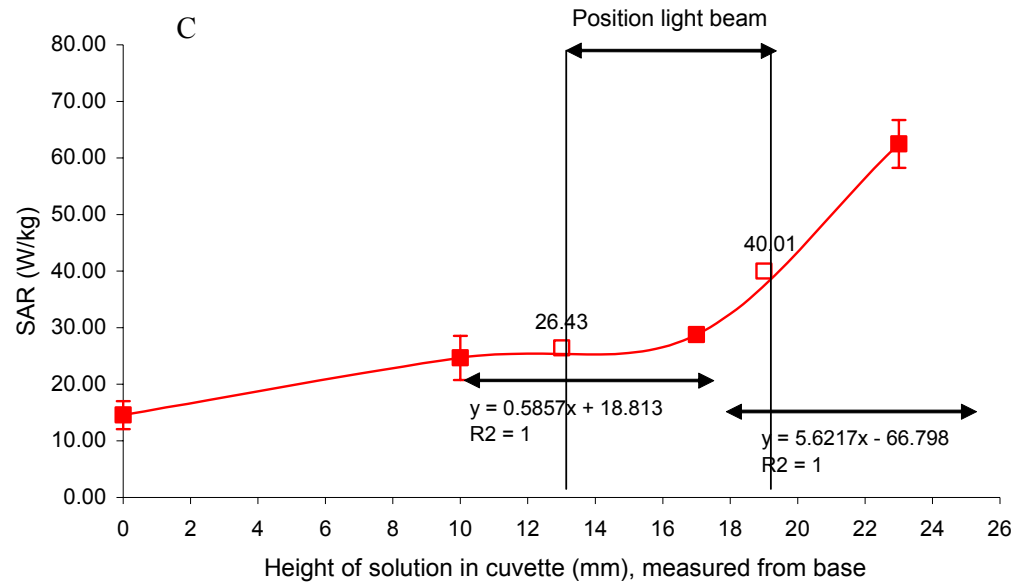


Figure 3.8: SAR at the position of the light beam (13-19 mm from base of cuvette). Buffer and exposure conditions I (A) and II (B)



**Figure 3.9: SAR at the position of the light beam (13-19 mm from base of cuvette). Buffer and exposure conditions III (C) and IV (D)**

### 3.3 RELAXATION OF TEMPERATURE TO BASELINE (refers to part 3 of figure 2.21)

#### 3.3.1 EXPOSURE SYSTEM 2 -EXPERIMENTALLY DERIVED TEMPERATURES

The temperature and the time (in seconds) of the return of the sample into the incubator (after exposure) were established from exposure experiments with buffer solutions. These experiments also determined the time it took for the sample to return to the baseline temperature. Determinations, in triplicate, were carried out for all buffer/exposure conditions at four different heights in the cuvette. Figure 3.10 shows the plot of one set of temperature determinations for an exposed and control sample immediately after a pulse of microwaves when the samples were being replaced in the multi-cell holder. The data were recorded every second from the time that the sample was placed in the multi-cell holder (grey for control sample and blue for exposed sample) and were plotted using the Excel program. The data points were fitted to a trendline with a moving average of 5 periods (green line for control sample and red line for exposed sample).

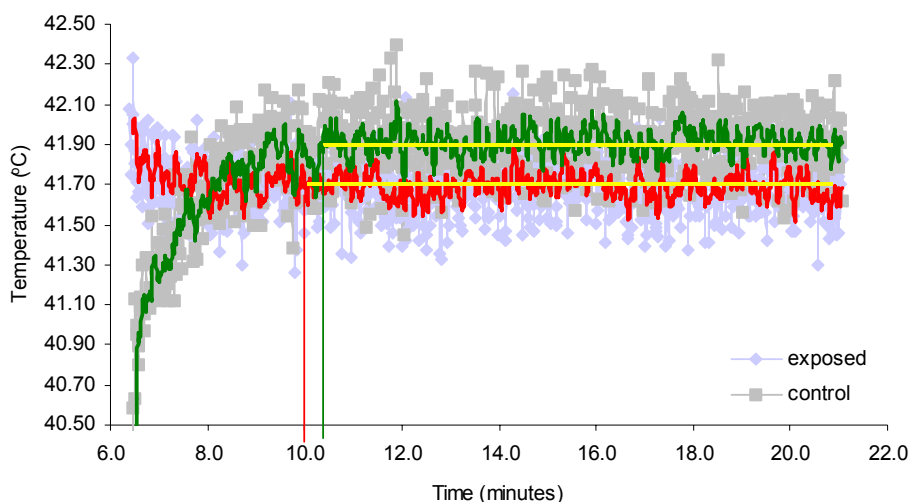


**Figure 3.10:** Temperature profile of an exposed and control sample of 1.0 ml sample of 80mM phosphate buffer that was returned to the incubator after one exposure of microwave pulses. The red and green trendline (see text) refer to the exposed and control data respectively. The horizontal red (exposed) and green (control) lines refer to the time at which the sample was considered at the baseline temperature. The yellow lines on the trendline refer to the baseline examined 10 mm from the base of the cuvette.

The time at which the sample had returned to the baseline temperature was that point where the

baseline was considered stable (yellow lines on graph with corresponding drop lines to the time points). The temperature and time of the return of the samples to the incubator were noted and averaged (this is the “Temperature after sample was returned to cell” in Table 3.3).

It was observed that the temperature had remained stable for the 15 seconds that it took for the sample to be taken from the incubator, placed into the transport box and positioned into the microwave oven. Therefore, no correction needed to be made for this step in the experiment. (See Table.3.3 “temperature at time zero, immediately prior to exposure”).

<b>Exposed sample</b>	<b>°C</b>	<b><u>Time/min</u></b>
Baseline temperature (1)	41.69	5.90
Temperature at time zero, immediately prior to exposure (1)	41.69	6.00
Temperature immediately after exposure (2)	43.58	6.05
Temperature after sample was returned to cell 4 (3)	42.23	6.53
Baseline temperature (1)	41.69	10.94
 <b>Control sample</b>	 <b>°C</b>	 <b><u>Time/min</u></b>
Baseline temperature (1)	41.81	5.90
Temperature at time zero, immediately prior to exposure (1)	41.81	6.00
Temperature after sample was returned to cell 6 (2)	40.99	6.53
Baseline temperature (1)	41.81	10.00

**Table 3.3: Experimental temperatures at specific time points of a 1.0 ml solution of 80mM phosphate buffer, pH 7.5, exposed to 3.2 seconds of 2.450 GHz pulses at the start of a six minute period. The numbers in brackets refer to the modules in Figure 2.12.**

It should be noted that in these experiments, the temperature of the sample was assumed to be at the temperature of the baseline from the start of the experiment. This assumption is valid for the comparison of samples that were incubated in the spectrophotometer only and thus, the fact that a sample takes 5 minutes in the spectrophotometer to get to the baseline temperature, was not deemed important in the six minute average calculations as all samples were affected in the same way.



Table 3.3 tabulates the experimentally derived temperature for a 1.0 ml sample of 80mM phosphate buffer, pH 7.5 that was exposed to 3.2 seconds of 2.450 GHz pulses at the start of a six minute period. The cuvette to be exposed was incubated in cell 4 of the multi-cell holder and the control cuvette was incubated in cell 5. The temperature was examined at 10 mm from the base of the cuvette (see Figure 3.10). The section numbers in brackets refer to the modules in Figure 2.12. The period of examination was 6.0 to 12.0 minutes.

### 3.3.2 EXPOSURE SYSTEM 2 – COMPUTATIONALLY DERIVED TEMPERATURES

The experimentally derived temperatures (Table 3.3) were plotted in SigmaPlot and fitted with an exponential decay function thus enabling the mathematical determination of temperatures every 0.25 minutes.

### 3.3.3 EXPOSURE SYSTEM 2 – AVERAGE TEMPERATURE OVER SIX MINUTES

Table 3.4 presents all the temperature data in periods of 0.25 minutes. The experimental data are in red and the mathematically derived temperature is in black. The temperature was measured at a height of 10 mm from the base of the cuvette, for a blank exposed and control sample of buffer/exposure condition I (see Table 3.1). The data were plotted in Figure 3.12 and the area under the graph was calculated using the Trapezoid Rule. For example, the area for the exposed sample at 6.05 minutes was:  $/2 = 8.623$ . The data were summed to give an average temperature per minute of 41.86 (exposed) and 41.60 (control) °C/min.

Calculations and temperature plots were established for all the buffer/exposure conditions for four heights in the solution in different cells in the incubator to give an average temperature per minute based on a six minute exposure period.

Figures 3.12 to 3.14 present the temperature profiles for samples of four different buffer/exposure conditions incubated in cells 4 (exposed) and 5 (control) of the incubator. The red and orange lines represent the temperature at the four heights in a sample exposed to microwave pulses. The blue and green curves represent the temperature at the four heights in a control sample.

EXPOSED				CONTROL		
minutes	°C	area		minutes	°C	area
5.5	41.69	10.423		5.50	41.81	10.453
5.75	41.69	10.423		5.75	41.81	10.453
6	41.69	2.132		6.00	41.81	10.383
6.05	43.58	8.623		6.25	41.25	11.514
6.25	42.65	11.883		6.53	40.99	9.030
6.53	42.23	9.275		6.75	41.10	10.289
6.75	42.08	10.508		7.00	41.21	10.315
7	41.98	10.487		7.25	41.31	10.337
7.25	41.91	10.473		7.50	41.39	10.357
7.5	41.87	10.463		7.75	41.46	10.373
7.75	41.83	10.455		8.00	41.52	10.388
8	41.81	10.449		8.25	41.58	10.400
8.25	41.79	10.444		8.50	41.62	10.411
8.5	41.77	10.440		8.75	41.66	10.420
8.75	41.75	10.437		9.00	41.70	10.428
9	41.74	10.434		9.25	41.73	10.435
9.25	41.73	10.432		9.50	41.75	10.441
9.5	41.72	10.430		9.75	41.78	10.448
9.75	41.72	10.428		10.00	41.81	10.453
10	41.71	10.427		10.25	41.81	10.453
10.25	41.70	10.425		10.50	41.81	10.453
10.5	41.70	10.424		10.75	41.81	10.453
10.75	41.69	7.921		11.00	41.81	10.453
10.94	41.69	2.501		11.25	41.81	10.453
11	41.69	10.423		11.50	41.81	10.453
11.25	41.69	10.423		11.75	41.81	10.453
11.5	41.69	10.423		12.00	41.81	
11.75	41.69	10.423				
12	41.69				sum	249.590
	sum	251.182			per minute	41.60
	per minute	41.86				

**Table 3.4:** Experimental (data in red) and mathematically derived (data in black) temperatures over a six minute period of a 1.0 ml sample of 80mM phosphate buffer, pH 7.5 that was exposed to 3.2 seconds of 2.450 GHz at 42°C (buffer and exposure condition I) compared to a control sample.

The graphs present data over a typical six minute period, starting at 15 seconds before the time that the samples were withdrawn from the incubator. It was assumed that the solutions were at the baseline temperature. In general it took about 5 minutes to reach this temperature when samples, initially at room temperature, were placed in the incubator.

After the samples were taken from the incubator and placed in a polystyrene transport box to either be exposed to pulsed microwaves (exposed sample) or to be placed on the bench (control sample), it took about 25 seconds before the samples were returned.

The pulsed microwaves induced a short and sharp excursion in temperature. The temperature returned to the baseline temperature before the next pulse period.

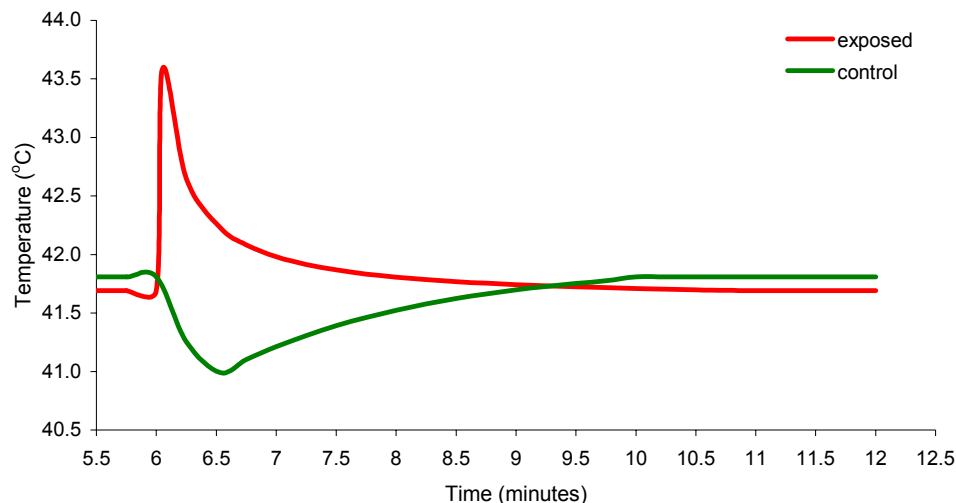


**Figure 3.11:** Temperature profiles of two 1.0 ml 80mM phosphate buffer solutions over a six minute exposure period. The temperature was measured at 10 mm from the base of a cuvette. One sample (red line) was exposed to pulsed microwaves once (at 6 minutes) and the control sample was left on the bench for the duration of the exposure (buffer/exposure condition I).

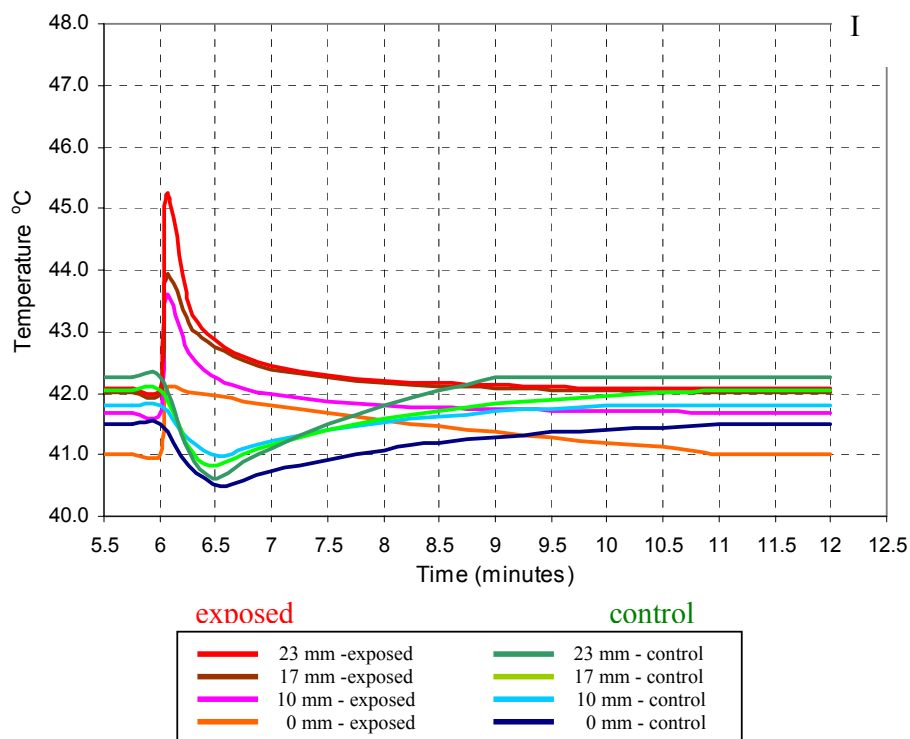


**Figure 3.12:** Six minute temperature profile of two 1.0 ml buffer solutions (buffer/exposure condition I) that were incubated in cell 4 (exposed samples) and cell 5 (control samples).

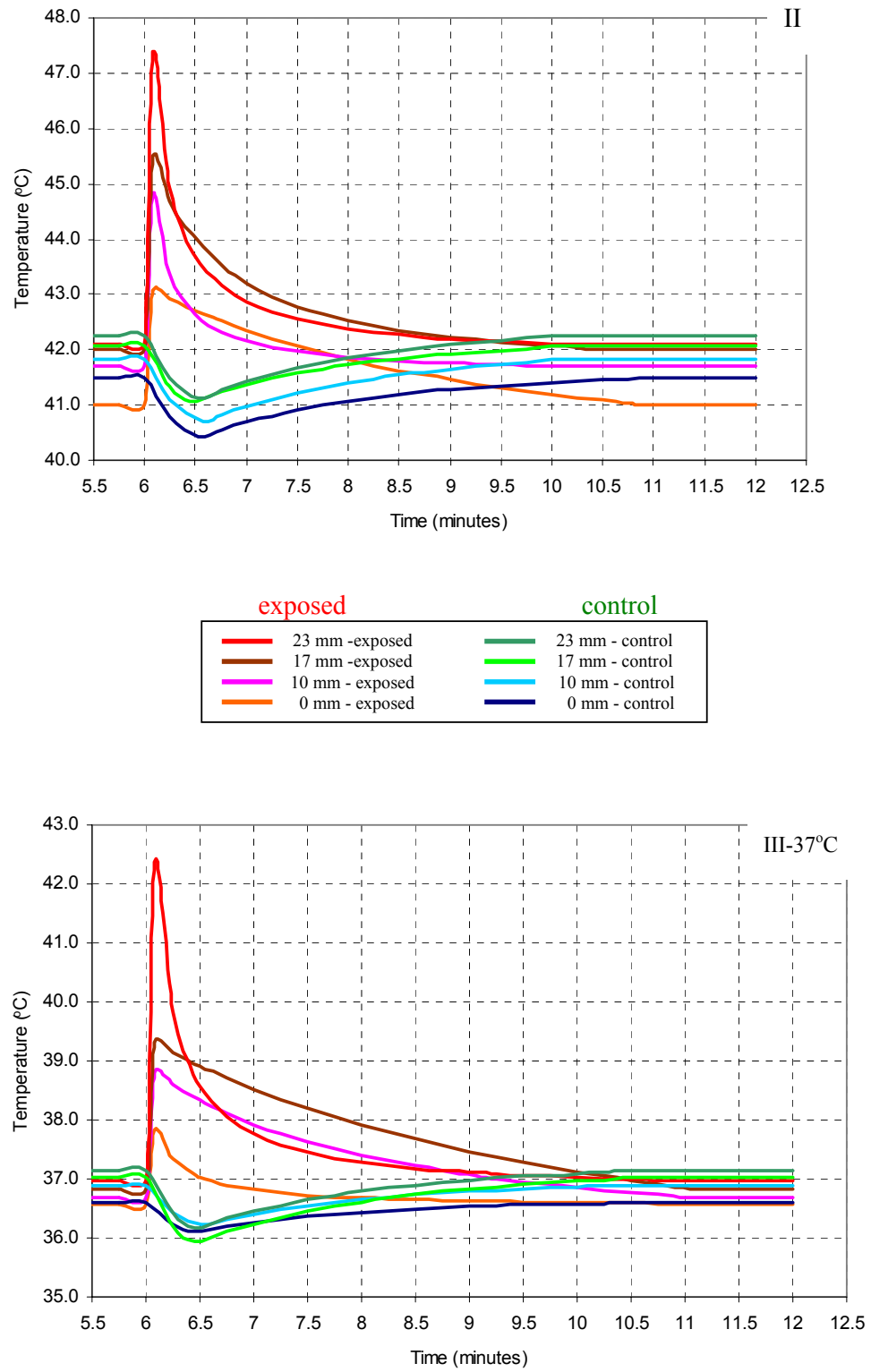


Figure 3.13: Six minute temperature profile of two 1.0 ml buffer solutions (buffer/exposure condition II and III-37°C) that were incubated in cell 4 (exposed samples) and cell 5 (control samples).

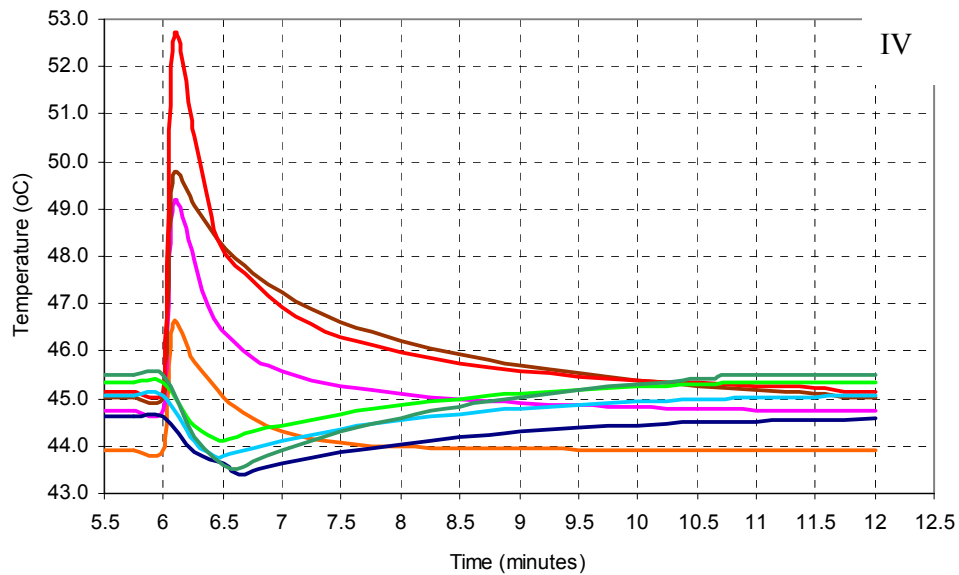
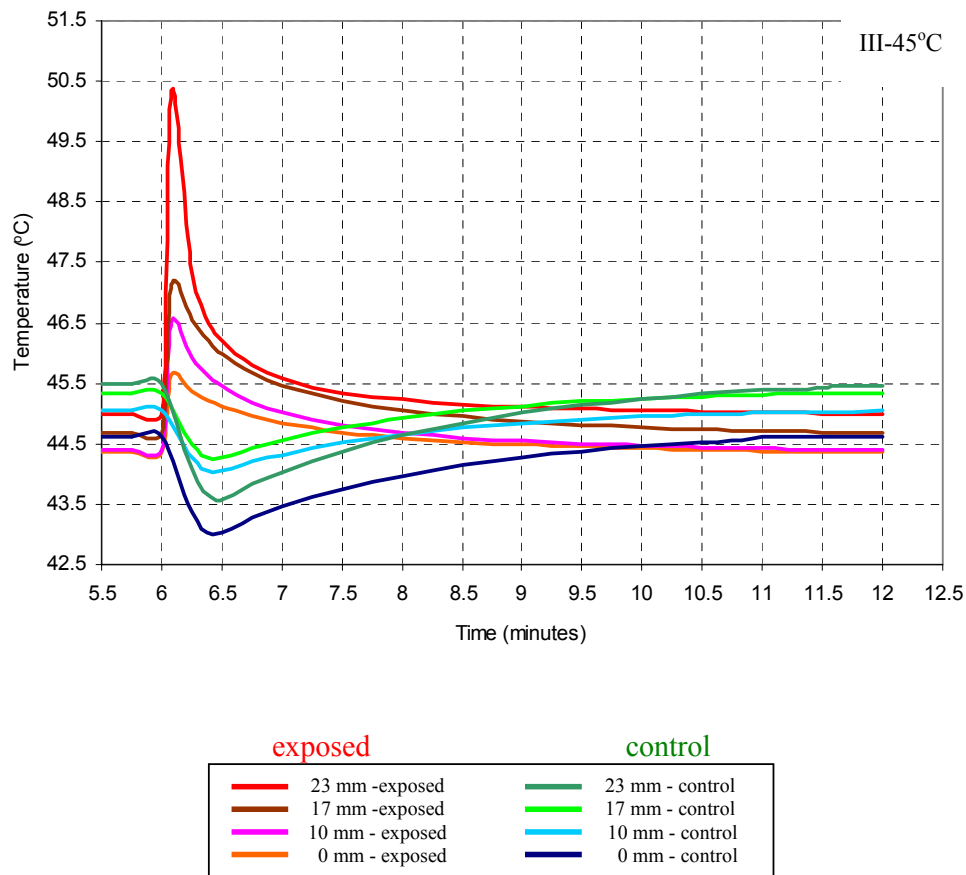


Figure 3.14: Six minute temperature profile of two 1.0 ml buffer solutions (buffer/exposure condition III-45°C and IV) that were incubated in cell 4 (exposed samples) and cell 5 (control samples).

---

## CHAPTER 4

---

### PREPARATIVE EXPERIMENTS

During the course of the project, it became apparent that protein solutions, at times, gave conflicting results. For example, new batches of protein stock did not have the same extent of precipitation under identical conditions as earlier batches, or when a stock solution was stored on ice, it did not precipitate as much as the previous sample. Some of these findings have been included in this chapter to highlight the difficulty in comparing results. There were also day to day discrepancies which lead to the decision to compare results between experiments in terms of the initial ratio (exposed/control) of initial rate of precipitation (see 1.10 and 2.6.1.1).

#### 4.1 ALCOHOL DEHYDROGENASE (ADH)

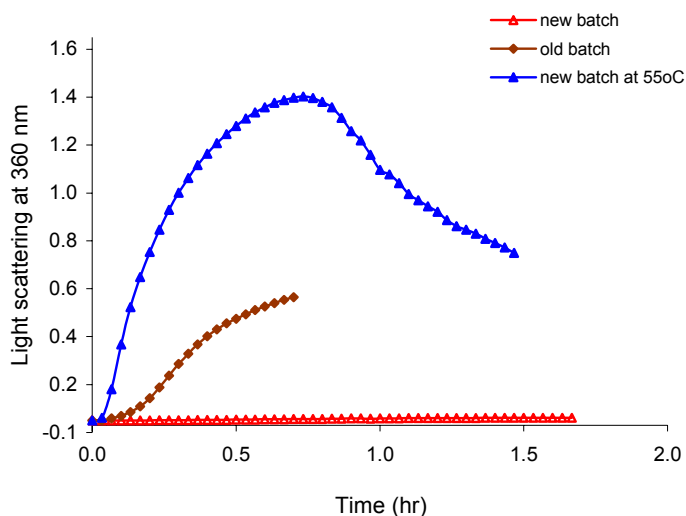


**Figure 4.1:** Effect of storage on ADH unfolding. Two samples of different batches of 0.5 mg/ml ADH, (1mM 1,10 phenanthroline in 0.1 M phosphate buffer, 0.1 M NaCl, pH 7) were incubated at 37°C, in the multi cell holder of the spectrophotometer (pink and brown lines). Only when the protein sample containing the new batch was heated to 55°C, did precipitation occur.

It was observed that when a newly purchased batch of ADH was used, the results of aggregation experiments differed from previous work. In Figure 4.1 are shown the precipitation profiles of

two batches of ADH at 37°C, prepared on the same day. The solution made from the new batch did not precipitate. However, when the solution was heated to 55°C, precipitation occurred.

## 4.2 BOVINE SERUM ALBUMIN (BSA)

The extent of BSA precipitation was sensitive to the age of the lyophilized protein stock and the length of time a concentrated solution in buffer was stored (mostly on ice).

In a preparative experiment, two 1.5 mg/ml samples made from a batch of BSA that had been stored in the fridge for more than one year and a batch of BSA that had been stored in the fridge for less than a month, were incubated at 45°C, in the presence of 20 mM DTT with or without 0.1 M NaCl (Figure 4.2).

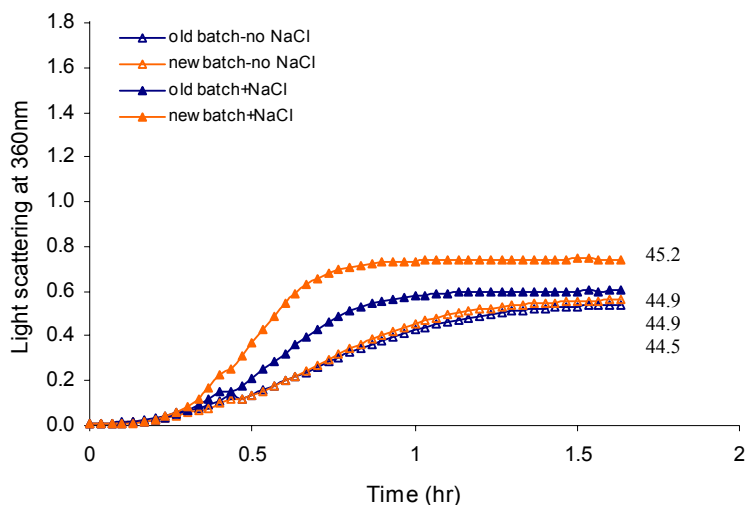


**Figure 4.2: Effect of storage on BSA unfolding.** Comparison of the precipitation of an “old” and a “new” batch of 1.5 mg/ml BSA, 20mM DTT in 0.1 M phosphate buffer, pH 7 that was incubated at 45°C, without or in the presence of 0.1 M NaCl. The average temperature of the solutions, during the experiment, is listed on the plots.

The precipitation of the new batch of BSA was enhanced only in the presence of salt compared to the old batch. When no salt was added to the samples, the precipitation was equal for both the old and new batches of BSA. Temperature variation between samples (0.3°C and 0.4°C) was not considered to contribute to the differences in aggregation.

### 4.3 INSULIN

When a concentrated stock solution was prepared from lyophilized powder and stored on ice, the extent of precipitation was reduced over time.

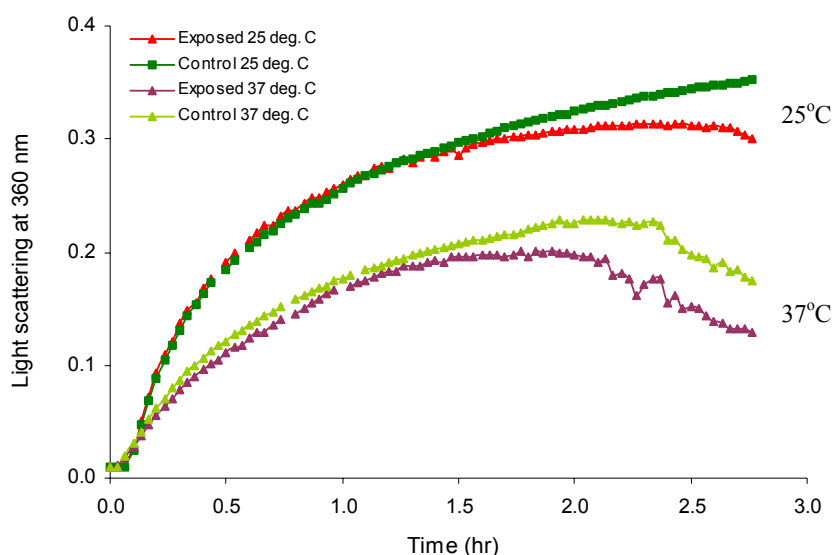


**Figure 4.3: Effect of storage on insulin unfolding.** 0.25 mg/ml insulin, 20mM DTT in 0.1 M phosphate buffer, 0.1 M NaCl, pH 8 exposed to 15 pulses of 2.450 GHz at 25°C and at 37°C as indicated on the graph. The SAR was 33.22 W/kg (at the position of the light beam).

Figure 4.3 shows the precipitation profile of a sample exposed to pulsed 2.450 GHz at 25°C and a sample exposed 90 minutes later at 37°C. The samples were freshly made up to the right concentration just before the experiment when DTT was also added. Generally the extent of aggregation is greater at higher temperatures as hydrophobic interactions in a protein are strongly temperature dependent<sup>171</sup> therefore it was concluded that the stability of the protein was affected in a relatively short time.

### 4.4 PURIFICATION OF $\alpha$ -CRYSTALLIN

Of the five protein separation experiments undertaken during this project, an average of 75.7  $\pm$  42.5 mg of  $\alpha_T$  was recovered from a 2 lens homogenate. For good separation the column needed to be well equilibrated with buffer and at times the column had to be repacked to give



well defined peaks. Figure 4.3 shows the profile of individual crystallins after separation of the lens homogenate on a Sephacryl S-300 size exclusion column. The HMW and  $\alpha_T$  were passed through the column a second time to give a better separation which is represented in Figure 4.4.

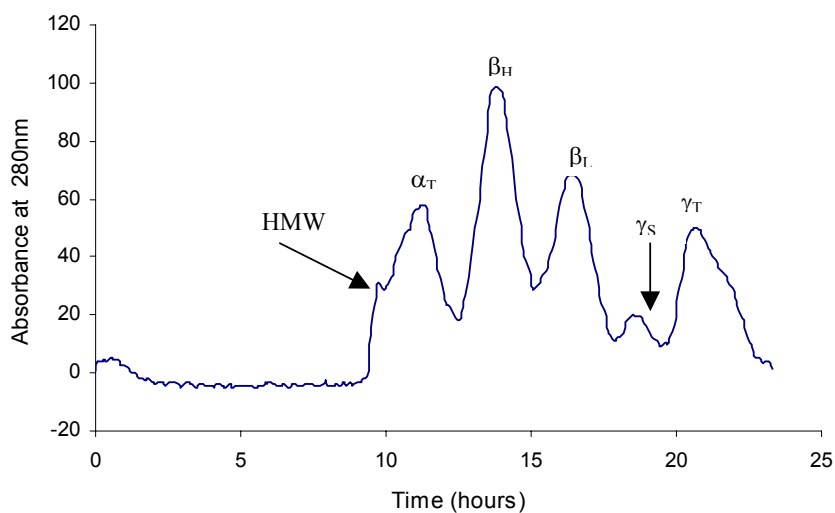


**Figure 4.4:** Typical separation of crystallin proteins (2 calf lenses) by size exclusion chromatography. The profile was obtained after the lens homogenate had passed through a size exclusion column once. For conditions see section 2.2.5.

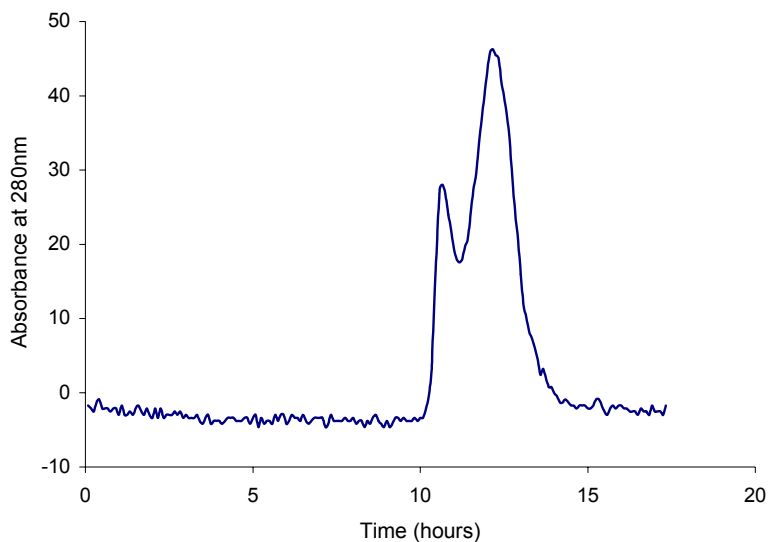


**Figure 4.5:** Separation of  $\alpha$ -crystallin on a size exclusion column. The HMW and  $\alpha_T$  fractions of Figure 4.4 were pooled and re-loaded on the column to give a better separation.

#### 4.4.1 STABILITY OF $\alpha$ -CRYSTALLIN

The age of stock solutions of  $\alpha$ -crystallin and their ability to suppress protein precipitation was investigated by incubating 1.5 mg of BSA with three solutions of  $\alpha$ -crystallin at a subunit molar ratio of 1:0.1 prepared from different stock solutions in buffer (Figure 4.5). The stock solutions had been stored in the fridge until preparation. BSA was partially suppressed by all samples. However, the sample prepared from the one day old solution was less effective after 24 minutes and the sample prepared from the two week old stock solution was least effective after this time.  $\alpha$ -Crystallin by itself precipitated to an insignificant extent (Figure 4.5).

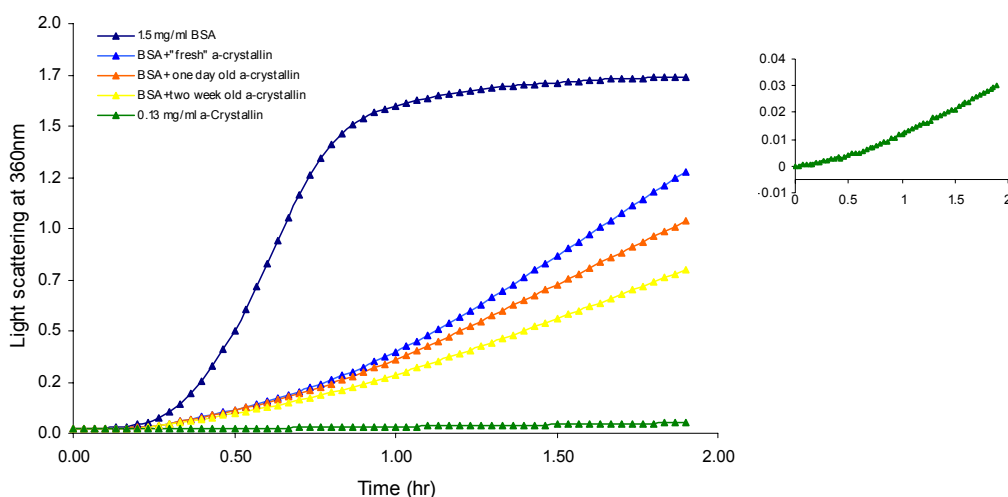


**Figure 4.6:** Suppression of 1.5 mg/ml BSA, 20 mM DTT in 0.1 M phosphate buffer, 0.1 M NaCl by  $\alpha$ -crystallin at the subunit molar ratio of 1:0.1, incubated at 45°C. The suppression of freshly prepared  $\alpha$ -crystallin (light blue) was compared to solutions of one day old (orange) and two weeks old (yellow) stock solutions of  $\alpha$ -crystallin.  $\alpha$ -Crystallin (0.13 mg/ml) incubated by itself did not precipitate. Inset:  $\alpha$ -crystallin with scale reduced.

$\alpha$ -Crystallin is thermally stable at temperatures up to 90°C and its chaperone action increases at higher temperatures<sup>139,160</sup>.

#### 4.5 LIGHT SCATTERING PROFILES

Three types of scattering profiles were observed (Figure 4.6) while studying the aggregation and precipitation of unfolding proteins as a result of exposure to pulsed microwaves in combination with heat, reduction or chelation of an intrinsic metal ion. To avoid a repetitious discussion of

the profiles for each reported experiment, a general description of the process of aggregation/precipitation is presented in this section.

The optical property of a solution is characterized by its refractive index. Light passes through a pure solution. However, when the solution contains solid particles or bubbles<sup>172</sup> the refractive index changes and light hitting the particles will scatter in all directions<sup>173</sup>. The intensity of the scattering can be measured spectroscopically.

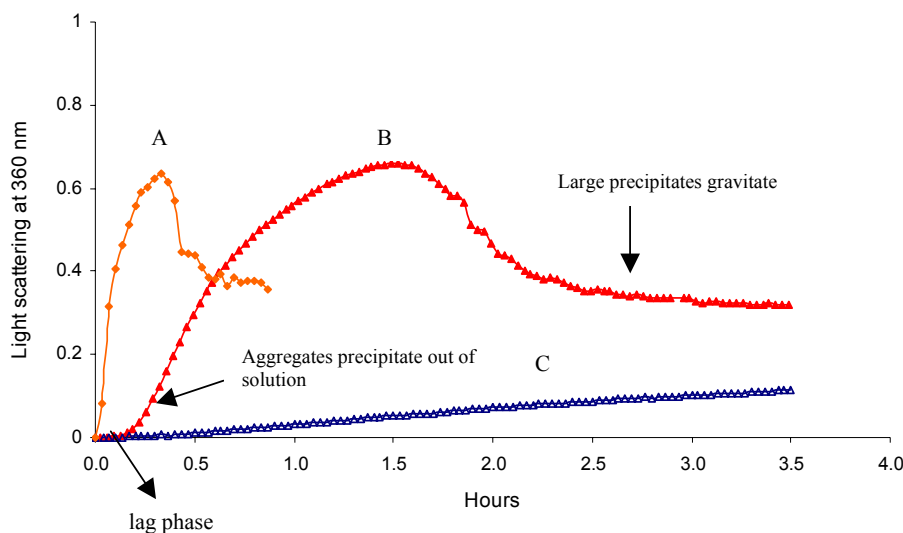
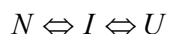


**Figure 4.7:** Examples of precipitation profiles of three different proteins that were unfolded by temperature, reduction or chelation of an intrinsic metal ion. Letters are discussed in the text.

Protein aggregation as a result of stress, e.g. heat, involves the following stages<sup>174</sup>:

1. *The initial unfolding of protein molecules:*



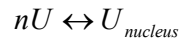
where N is the native state, I the intermediate states  $I_1$  and  $I_2$  and U the unfolded protein (see section 1.4).

2. *Nucleation*

Nucleation is a thermodynamically unfavourable process because it results in a loss of configuration energy (i.e. decreased entropy) as shown by a positive  $\Delta G$  in Figure 4.8.

However, when a sufficient number of stable nuclei are formed, the system reaches a

critical stage that favours aggregation and leads to a decrease in the system's free energy (negative  $\Delta G$  in Figure 4.8) <sup>174; 175</sup>:



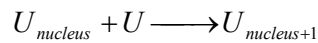
where  $nU$  is the number of unfolded protein molecules participating in the formation of a nucleus ( $U_{nucleus}$ ).

**Figure 4.8** Free energy change,  $\Delta G$ , as a function of time,  $t$ , for the initial stages of protein aggregation. Reproduced from Kurganov <sup>174</sup>.

This stage of nucleation is termed the lag phase and is presented in Figure 4.7 as the time period in which no light scattering is observed:

### 3. Aggregation

At the end of the lag phase, nucleation and aggregation become thermodynamically favourable:



Nucleation continues <sup>175</sup> and aggregation increases exponentially causing larger particles and an increase in light scattering (sigmoidal curves for proteins A and B, Figure 4.7).

Protein A in Figure 4.7 starts precipitating immediately which suggests that the lag phase was too short to observe. This is conceivable under conditions whereby the hydrophobic collapse of secondary structure occurs in seconds<sup>171</sup> The lag phase for protein B was about 6 minutes. Both graphs are sigmoidal. After the maximum absorbance, the precipitated particles become too heavy and gravitate to the bottom of the sampling cuvette, hence the decrease in absorbance as shown on the graph. Protein C aggregates very slowly and the kinetics of this process are different from the nucleation-growth model for proteins A and B. The kinetics for protein C most likely fit the multimeric polymerization model where growth of the aggregates is by association of multimers<sup>171</sup>.

---

## CHAPTER 5

---

### LIGHT SCATTERING EXPERIMENTS

#### 5.1 MICROWAVE EXPOSURE IN *EXPOSURE SYSTEM 1*

*Exposure system 1* presented severe limitations which are discussed in section 2.4.1.2 (page 41).

The results of the work carried out in this system have been included in this thesis to highlight the shortcomings and to provide a basis for the later experiments.

Experiments in *Exposure system 1* (see section 2.4.1.1) were conducted at 37°C. The temperature of the samples could not be monitored during an experiment however the ambient temperature close to the samples was recorded by reading a thermometer when samples were withdrawn and returned from the incubator. Alcohol dehydrogenase (ADH), catalase, citrate synthase (CS) and  $\alpha$ -lactalbumin were exposed in this system. The samples were taken from the incubator at periodic intervals to measure the light scattering at 360 nm.

##### 5.1 APO ALCOHOL DEHYDROGENASE (ADH)

Figure 5.1 is representative of experiments on 0.5 mg/ml ADH exposed to pulsed microwaves in *Exposure system 1* at 37°C. The rate of initial precipitation of the exposed sample in this particular experiment ( $0.45 A_{360}\text{hr}^{-1}$ ) was much greater than the control ( $0.04 A_{360}\text{hr}^{-1}$ ) and the extent of precipitation was greater compared to the control.

A sham exposure on 0.5 mg/ml ADH, 1mM 1,10 phenanthroline in 0.1 mM phosphate buffer, 0.1 M NaCl, pH 7 showed that the control precipitated at a faster rate than the sham exposed (Figure 5.2). The temperature inside the microwave oven was found to be  $\sim 1^\circ\text{C}$  higher than in the incubator.

In comparing the sham experiment with a typical exposure and considering that the sham exposed sample was at least  $1^\circ\text{C}$  warmer, the difference between the exposed and

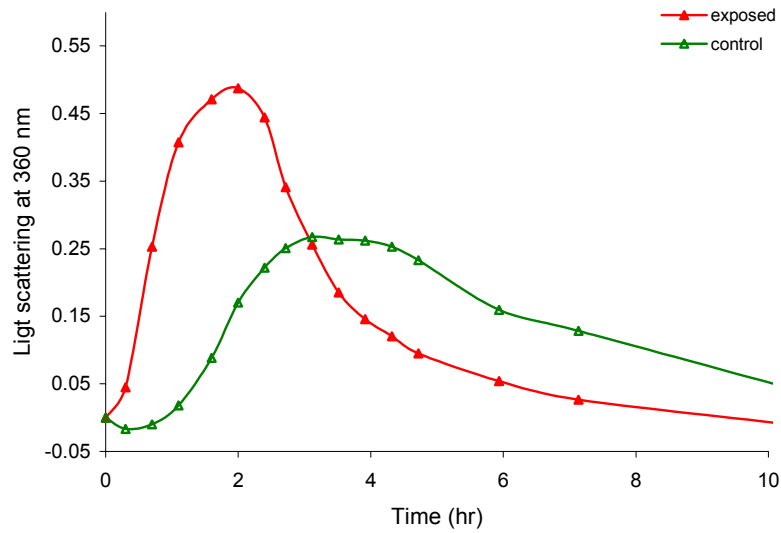


Figure 5.1: Exposure of 0.5 mg/ml ADH at 37°C (0.1 M phosphate buffer, 0.1 M NaCl, 1mM 1,10 phenanthroline, pH 7) to 3.2 seconds of pulsed 2.450 GHz every 6 minutes, for 20 hours at 37°C. For clarity, data for only the first 7 hours are shown.

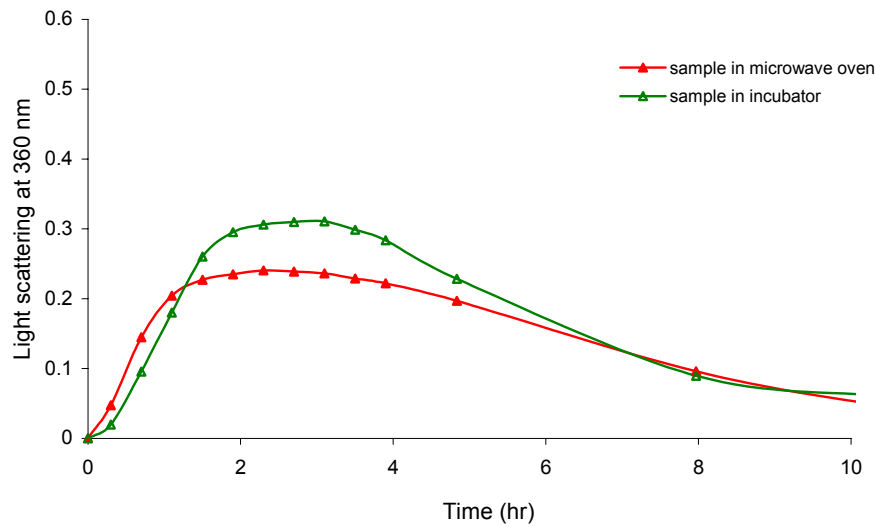
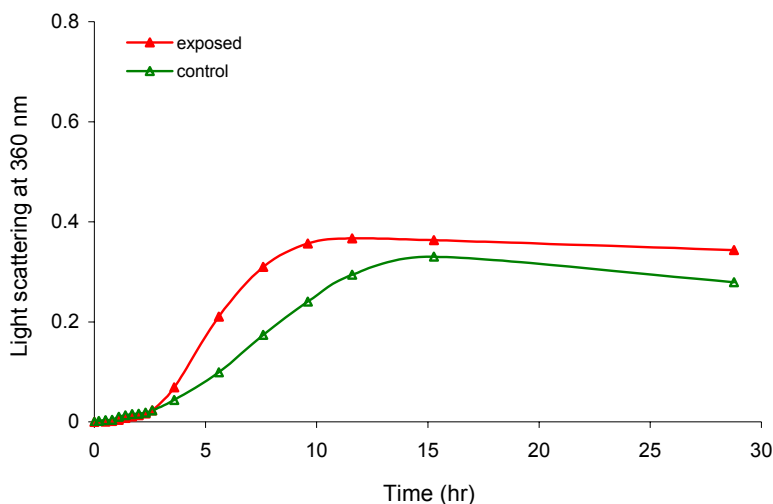


Figure 5.2: Sham exposure experiment on 2 x 1.0 ml of 0.5 mg/ml ADH in 0.1 M phosphate buffer, 0.1 M NaCl, 1mM 1,10 phenanthroline, pH 7 at 37°C. One sample was placed in the non-operational microwave oven while another sample was placed in the incubator on the shelf beneath the microwave oven. Temperature readings showed that the environment of the sample in the microwave oven was on average 1°C warmer than the "control".

control sample with respect to initial rate of precipitation and the extent of precipitation was much greater than in the sham experiment. The ratios of the initial rate were 0.50 (exposed/control) for the sham experiment (control/exposed 1.99) compared to 10.5 for the exposure experiment (exposed/control). The SAR for this particular experiment was calculated to be 10.3 W/kg. Therefore, the effect of the microwave exposure was considered significant.

## 5.2 CATALASE

When catalase, at a concentration of 0.4 mg/ml, was exposed to pulsed 2.450 GHz for up to 30 hours, the exposed sample started to precipitate more than the control after four hours (Figure 5.3). The extent of precipitation was also increased. The SAR was estimated to be 10.33 W/kg.



**Figure.5.3:** Exposure of 0.4 mg/ml catalase in 0.1 M phosphate buffer, pH 7 at 37°C to 3.2 seconds of pulsed 2.450 GHz every 6 minutes, for 30 hours.

As the temperature inside the microwave oven was  $\sim 1^{\circ}\text{C}$  higher than in the incubator (section 5.1) the enhancement of precipitation was likely to be due to the temperature difference.

When the concentration was almost doubled to 0.8 mg/ml, the precipitation increased gradually over hours, no plateau was reached after 30 hours (Figure 5.4). It had been anticipated that aggregation would occur faster because of the two fold concentration. Two samples were simultaneously exposed; the SAR was estimated to be 10.33 and 11.03 W/kg. The initial rate



and extent of the exposed samples were significantly greater than the control samples. The rate of aggregation/precipitation of the sample that was exposed to 10.33 W/kg accelerated sharply after 18 hours. This sample and the control were taken from the incubator every 36 minutes for light scattering measurements while the sample exposed to 11.03 W/kg was withdrawn every 18 minutes. The amount of precipitation of the two control samples was similar. The only difference between the two exposed samples was the rate of withdrawal of the cuvettes for spectroscopic measurements and a difference of 1.00 W/kg in SAR.

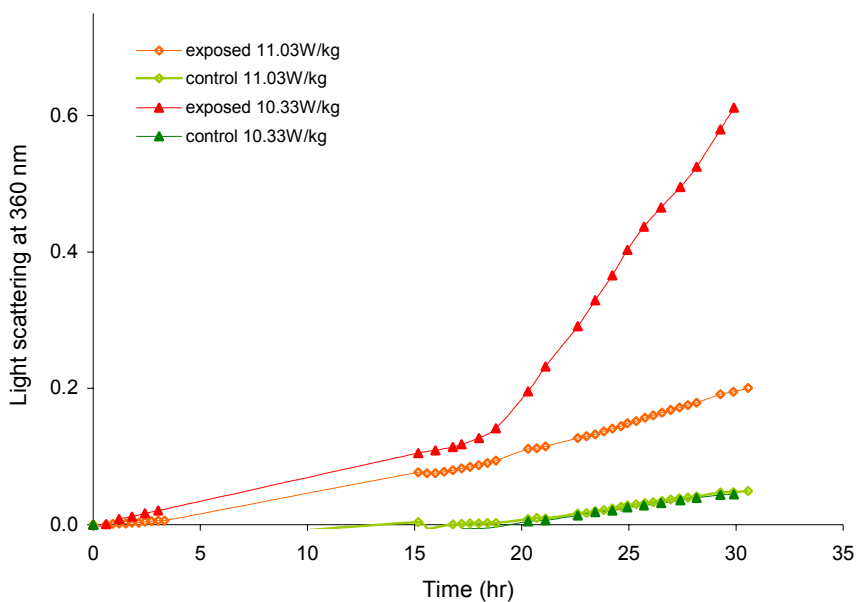


**Figure 5.4:** Exposure of 0.8 mg/ml catalase in 0.1 M phosphate buffer, pH 7 at 37°C to 3.2 seconds of pulsed 2.450 GHz every 6 minutes, for 30 hours. The sample exposed to 10.33 W/kg and the corresponding control were withdrawn from the oven every 36 minutes compared to the exposed at 11.03 W/kg and its corresponding control that were withdrawn every 18 minutes.

The calculation of the SAR was based on a one off calibration (see section 2.5.2.1) and it seems therefore plausible that one sample was exposed to more energy than initially calibrated especially as the precipitation of the controls was identical and they were treated in a similar way to the exposed samples.

### 5.3 CITRATE SYNTHASE (CS)

Citrate synthase incubated at 37°C and at a concentration of 0.2 mg/ml and 0.4 mg/ml showed an enhanced aggregation/precipitation in the exposed samples as compared to the controls. Sham experiments (Figure 5.5) showed that this enhancement was due to temperature differences in the sample environment.

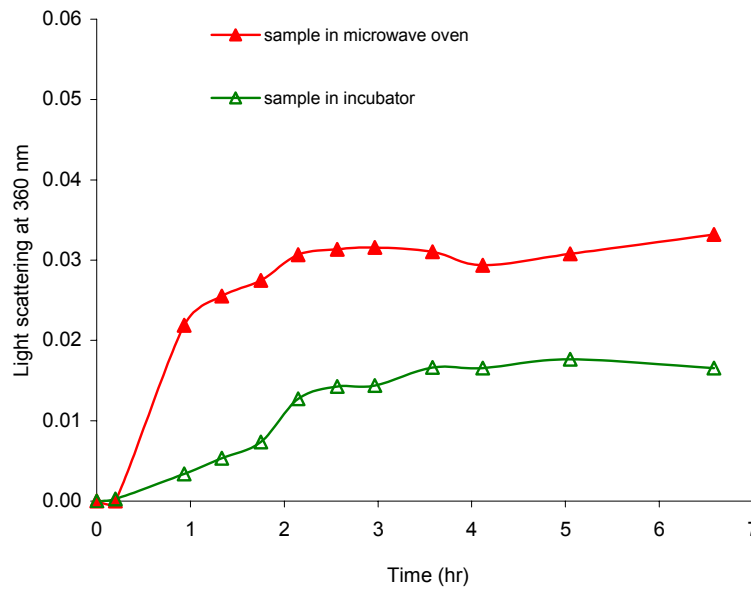


**Figure 5.5:** Sham exposure experiment on 2 x 1.0 ml of 0.2 mg/ml CS at 37°C. One sample was placed in the non-operational microwave oven inside the incubator while another sample was placed in the incubator on the shelf below the microwave oven. Temperature readings showed that the sample in the microwave oven was on average 1°C warmer than the control.

Figure 5.6 A shows the aggregation profile of a 1.0 ml sample of 0.2 mg/ml citrate synthase maintained at 37°C that was measured for light scattering every 20 minutes for 8 hours. The result for a sample at double this concentration is presented in Figure 5.6 B. The activity assay for the 0.4 mg/ml CS concentration shows that the exposed sample had lost 25% more activity than the control sample (Figure 5.7). After 90 hours the difference was even more profound. The activity of the control sample was 77% compared to the exposed sample of 8% activity. The SAR for the 0.2 mg/ml experiment was estimated to be 10.33 W/kg and for the 0.4 mg/ml sample 11.03 W/kg, which would suggest a transient temperature increase in the exposed sample of 0.9°C every six minutes.

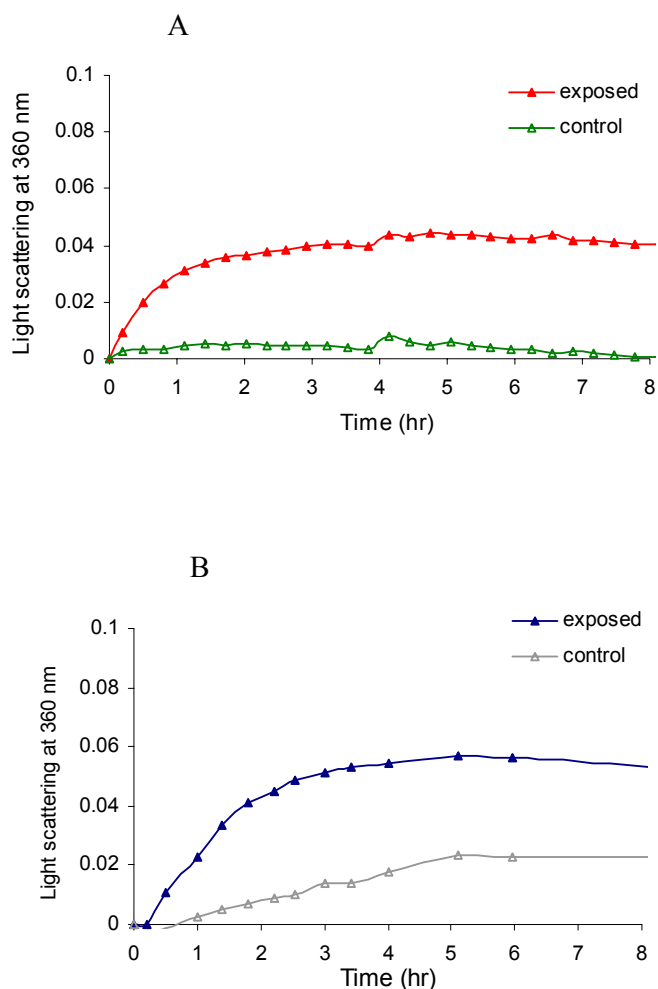


**Figure 5.6:** 1.0 ml of 0.2 mg/ml (A) and 0.4 mg/ml (B) CS in 80mM phosphate buffer was exposed to pulsed microwaves of 3.2 seconds duration every six minutes for 43 hours (A) and 92 hours (B). The exposed sample was kept in the microwave oven that was placed in an incubator at 37°C and the control sample was incubated in a dry oven also at 37°C. The temperature was measured by reading a thermometer that was placed directly next to the cuvette. A variation of up to 1°C between incubators may have occurred. For clarity only the first eight hours are shown

An activity assay on the 0.4 mg/ml exposed and control sample of Figure 5.6 B showed that the activity of the control sample at 37°C was 86% after 4 hours compared to 60% for the exposed. The data suggest that the difference in precipitation and enzyme activity between exposed and control samples was due to the difference in temperature alone. The low absorbance values indicate that only a small percentage of proteins precipitated.

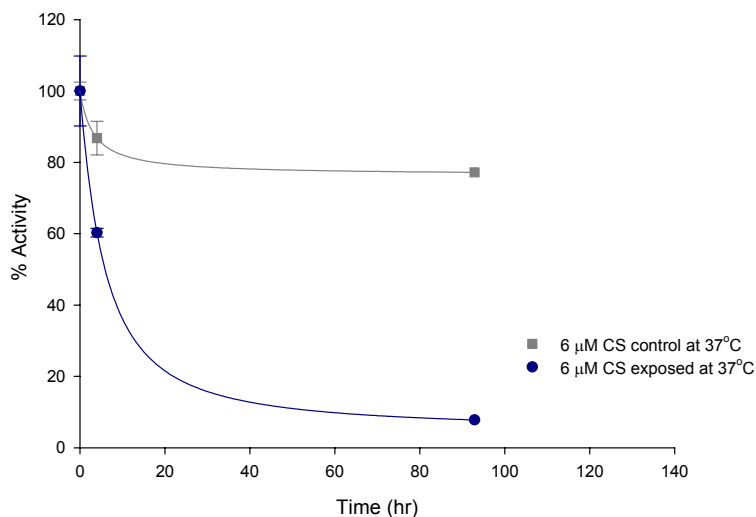


Figure 5.7: The enzymatic activity of 0.4 mg/ml CS samples (Figure 5.6B) at 37°C.

#### 5.4 REDUCED APO A-LACTALBUMIN

Figure 5.8 shows the precipitation profile of a 1 mg/ml sample of reduced apo  $\alpha$ -lactalbumin that was exposed to pulsed 2.450 GHz for 25 hours at 37°C. No EDTA was used and the buffer did not contain salt (see section 2.2.6). The experiment was repeated with similar results on 2 mg/ml apo  $\alpha$ -lactalbumin.

The average temperature in the microwave oven was 36.9°C and in the incubator where the control sample was placed, 36.7°C. The SAR was estimated to be 11.03 W/kg (at the base of the cuvette). The initial rate and extent of precipitation were both enhanced for the exposed sample. The microwave exposure caused a transient increase in temperature (base of cuvette) of  $\sim 1^\circ\text{C}$  which most probably caused the enhancement of precipitation (SAR 11.03 W/kg).

In an acidic solution at pH 2,  $\alpha$ -lactalbumin exists in a molten globule conformation that has significant secondary structure but no tertiary structure<sup>176; 177</sup>. Two samples of  $\alpha$ -lactalbumin, 3 mg/ml and 6 mg/ml were incubated at 37°C and exposed to pulsed 2.450 GHz. Light scattering at 360 nm was measured every 2 hours for the first 7 hours and after this only periodically until 47 hours after the experiment (Figure 5.9). The cuvettes were inverted prior to light scattering measurements.

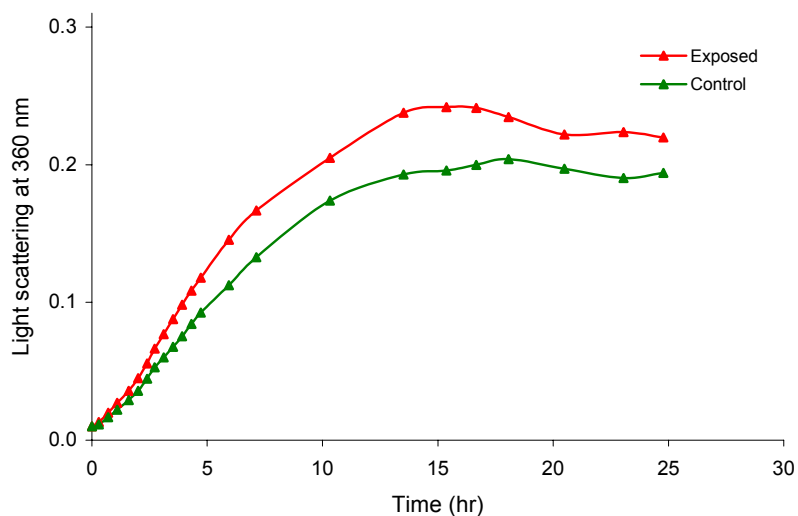


Figure 5.8: 1 mg/ml apo  $\alpha$ -Lactalbumin (no EDTA) in 50 mM phosphate buffer, 20 mM DTT, pH 7 exposed to pulsed 2.450 GHz at 37°C.

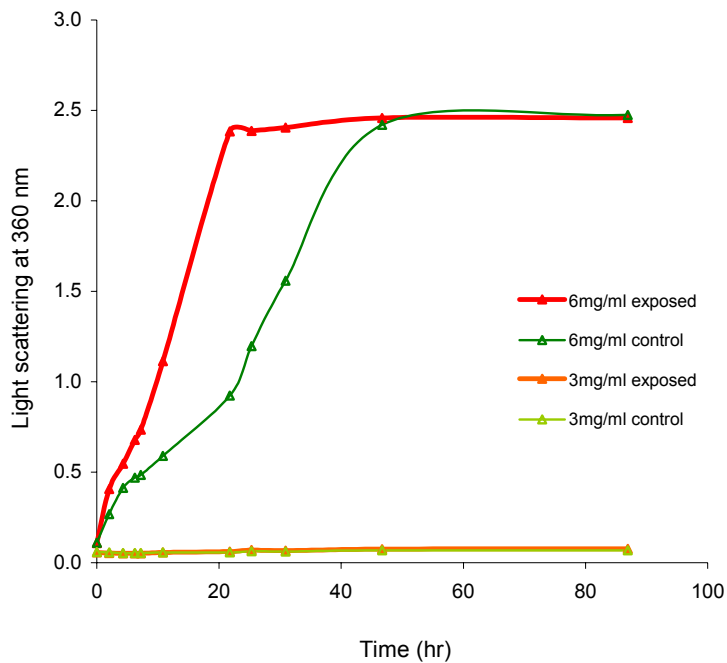


Figure 5.9: 3 and 6 mg/ml  $\alpha$ -Lactalbumin, in 0.1 M HCl, 0.1 M NaCl, pH 2 was exposed to pulsed 2.450 GHz, every 6 minutes for 45 hours. Cuvettes were inverted prior to light scattering measurements at 360 nm.

The exposed sample of 6 mg/ml precipitated at a much faster rate than the control sample. The transient temperature rise ( $2.7^{\circ}\text{C}$  at the base of the cuvette) in the exposed sample was effective in enhancing the precipitation. After 20 hours the precipitation had peaked whereas the maximum for the control sample was only reached after 45 hours. The extent of precipitation for both samples was similar. The 3 mg/ml samples did not precipitate even after 45 hours. The transient temperature rise was  $2.0^{\circ}\text{C}$  at the base of the cuvette. The SAR for the exposed sample containing 3 mg/ml was  $23.6 \pm 0.6$  W/kg and  $31.0 \pm 0.5$  W/kg for the 6 mg/ml sample (base of the cuvette).

## 5.5 SUMMARY OF RESULTS

The main limitations of *Exposure system 1* were the temperature difference between the oven cavity and the incubator and the uncertainty about the temperature of the samples during the experiment. For example, it was not established how long it took a sample to reach the ambient temperature of the oven environment; what the temperature loss was after a sample was measured for light scattering, or the increase in temperature from a pulse period of exposure.

Nevertheless following sham experiments which corrected for temperature difference, it could be demonstrated, that exposed ADH precipitated faster and to a larger extent than the control sample. The SAR was believed to be 10.3 W/kg which converts to an increase in temperature every six minutes of  $0.9^{\circ}\text{C}$ .

The enhancement in precipitation of the exposed samples of catalase, citrate synthase and reduced apo  $\alpha$ -lactalbumin (no EDTA) was attributed mainly to the difference in temperature between the oven cavity and the incubator.

The experiments in this chapter were important in that they underpinned the shortcomings of *Exposure system 1*. The experimental results have been included in this thesis as a comparison to the experiments undertaken in the other exposure systems.

---

## CHAPTER 6

---

### LIGHT SCATTERING EXPERIMENTS

#### MICROWAVE EXPOSURE IN THE TRANSVERSE ELECTROMAGNETIC MODE (TEM) CELL

The use of this exposure system was granted for a limited period during the project. It provided an opportunity to expose samples to pulsed microwaves with very low energy that at most elevated the temperature of a sample by 0.05°C at every pulse.

Alcohol dehydrogenase (ADH) solution was exposed to pulsed microwaves of 900 MHz, for 576  $\mu$ s, every 4.6 ms in a transverse electromagnetic mode (TEM) cell at 37°C. The experimental details are described in section 2.3.2 .

#### 6.1 APO ALCOHOL DEHYDROGENASE (ADH)

The TEM cell was designed to hold two Falcon© tissue culture flasks of volume 25 ml into a mould inside the cavity of the cell. Experiments in the laboratory at the Centre of Immunology, St. Vincent's Hospital, were routinely executed on 6.0 ml of buffer and SAR calibrations on this volume were well established in a collaboration with Telstra Research Laboratories.

To monitor samples for light scattering measurements, the exposure system needed to be paused, the screws on the TEM cell undone, the flasks removed and 1.0 ml aliquots withdrawn for spectroscopic analysis. This procedure introduced many variables such as significant temperature fluctuations and physical disturbance of the solutions. Figure 6.1 shows the result of a mock experiment in the laboratory when a solution of 6.0 ml of 0.5 mg/ml ADH contained in a flask was exposed in the microwave oven (*Exposure system I*) to pulsed 2.450 GHz. At intervals of half an hour, 1.0 ml was withdrawn and measured at 360 nm, in the spectrophotometer. The aim of the experiment was to examine if the variables of temperature and sample disturbance had much of an effect on the precipitation of the unfolding protein.

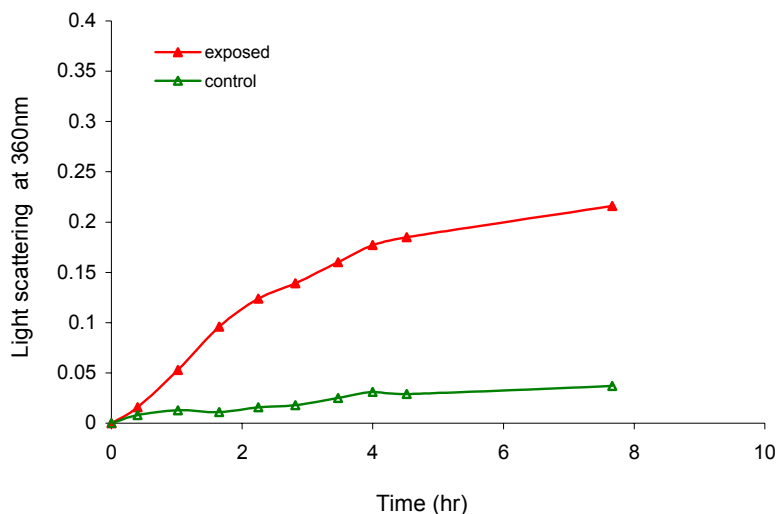


**Figure 6.1:** Exposure of large volume of ADH to pulsed microwaves (*Exposure system I*). 6.0 ml of 0.5 mg/ml ADH (1mM 1,10 phenanthroline in 0.1 M phosphate buffer, 0.1 M NaCl, pH 7) was placed in a 25 ml flask that was exposed to pulsed 2.450 GHz at 37°C for 7 hours. The microwave pulses were of 3.2 seconds duration. An identical solution was kept in the incubator. At half an hour intervals, 1.0 ml was withdrawn from the solutions and placed into quartz cuvettes. The samples were taken to a spectrophotometer to measure the light scattering in the solutions. The aliquots were then returned to the flasks and the exposure was resumed.

The SAR was not determined for the mock experiment. The control sample did not precipitate much as can be seen from the low absorbance at 360 nm, however the exposed sample precipitated significantly. Compared to the experiments of Figure 5.1 a slower precipitation rate was observed.

For the TEM cell experiments, two 6.0 ml solutions of 0.5 mg/ml ADH in 0.1 M NaCl, 1 mM 1,10 phenanthroline, 0.1 mM phosphate buffer, pH 7, were transferred to separate tissue flasks. The depth of the volume was 4 mm. One solution, the “exposed”, was exposed in the TEM cell for four hours to pulsed 900 MHz (pulses occurred every 4.6 ms that lasted 576  $\mu$ s) while the “control” was placed inside the same incubator underneath the TEM cell. Figure 6.2 shows the precipitation of the ADH solutions over time as measured by light scattering.

Every hour the exposure was paused and 1.0 ml was withdrawn from the solutions for light scattering measurements. Thereafter, aliquots were returned to the flasks and the exposure was resumed. This procedure took on average six to eight minutes.



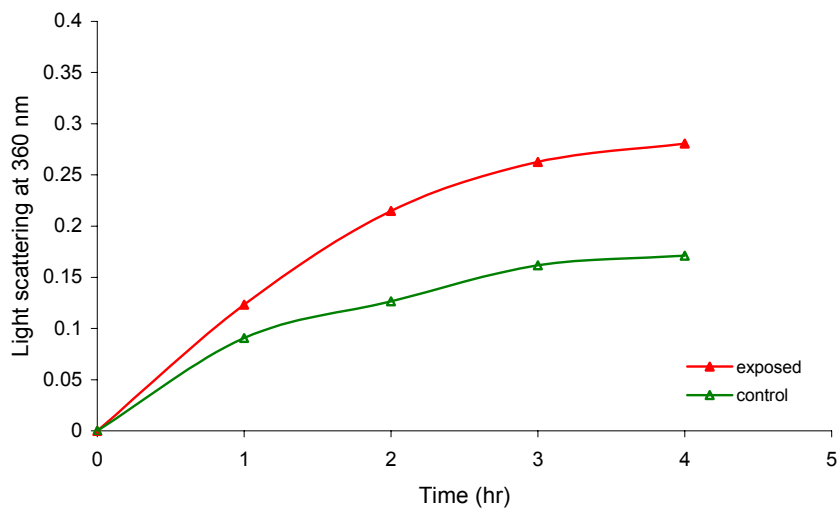


**Figure 6.2:** Exposure of ADH in TEM cell. 6.0 ml of 0.5 mg/ml ADH (1mM 1,10 phenanthroline in 0.1 M phosphate buffer, 0.1 M NaCl, pH 7) to pulsed 900 MHz in a TEM cell at 37°C for 4 hours. An identical solution was incubated at 37°C (control).

The pH of the solutions was measured after termination of the experiment and was found to be pH 6.9 for exposed as well as for control. The SAR of the solution was calculated from the formula in reference <sup>178</sup> to be 0.50 W/kg on the bottom and middle of the dish or 0.21 W/kg average throughout the solution.

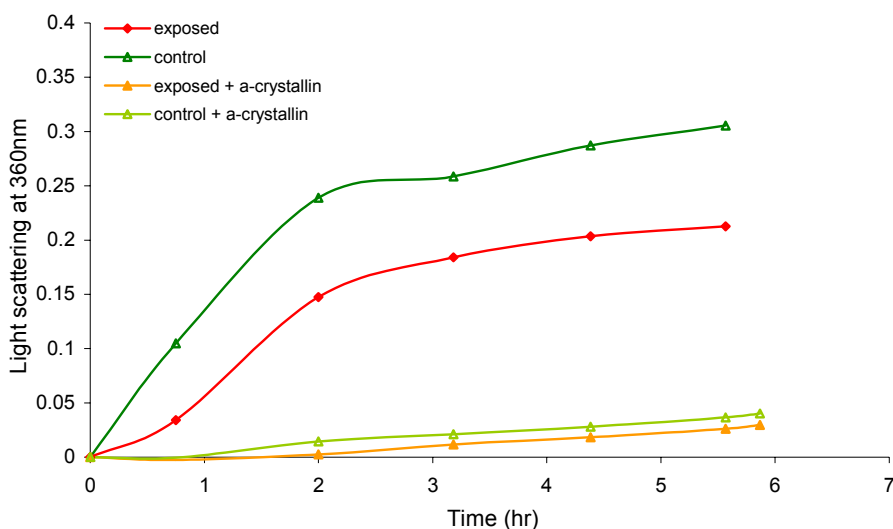


**Figure 6.3:** Exposure of 6.0 ml of 0.5 mg/ml ADH (1mM 1,10 phenanthroline in 0.1 M phosphate buffer, 0.1 M NaCl, pH 7) to pulsed 900 MHz at 37°C for 6 hours. An identical solution was incubated at 37°C. The experiment was repeated in the presence of  $\alpha$ -crystallin at a subunit molar ratio of 1: 2. The CO<sub>2</sub> supply to the incubator was disconnected.

The experiment was repeated and followed by an experiment on ADH in the presence of a 1: 2 subunit molar ratio of  $\alpha$ -crystallin (Figure 6.3). The experimental conditions were identical with the exception that the CO<sub>2</sub> source was turned off to keep to the same conditions the same as in *Exposure system I* (see 2.4.1.1). A thermometer was placed in the incubator and the temperature was read before the flasks were removed and when they were returned. The temperature of the incubator dropped at times 1.5°C, however, the temperature of the solutions was not monitored (Figure 6.4).

The difference in initial rate and the extent of precipitation between an exposed and control sample was completely reversed when the CO<sub>2</sub> was turned off.

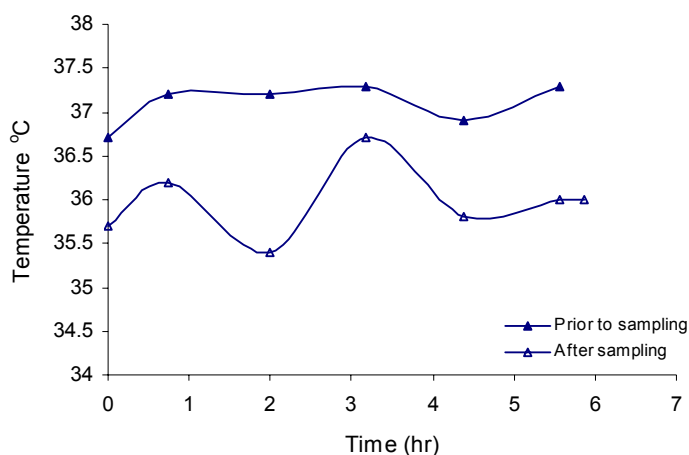


**Figure.6.4:** Profile of temperature in the incubator. The temperature was read before (closed triangles) removing the flasks for spectroscopic measurements and after (open triangles) they were returned.

$\alpha$ -Crystallin significantly suppressed precipitation of ADH for exposed and control samples.

The exposed sample had precipitated marginally more than the control.

A sham experiment was performed to establish the aggregation/precipitation profile of the protein under non-exposure conditions in the TEM cell and the incubator. The amplitude, pulse and signal generators were turned off and all other conditions were equal to the previous experiment (no CO<sub>2</sub> supply). Figure 6.5 shows the result of the sham experiment. The sample in

the incubator precipitated faster than the sample in the TEM cell which was the opposite result as found in Figure 6.2 but similar to Figure 6.3

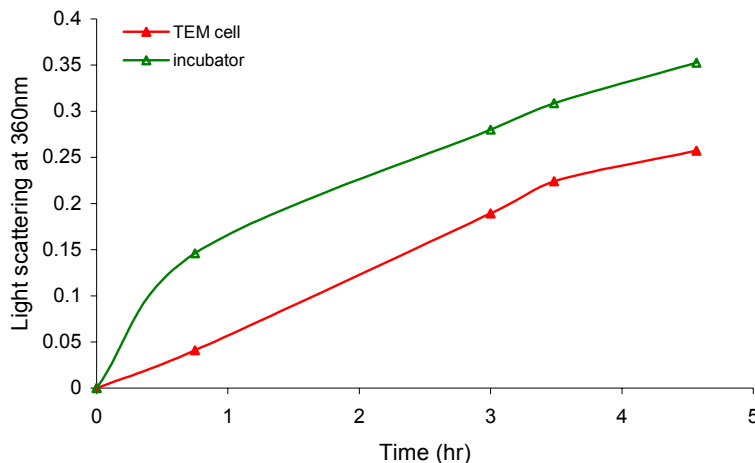


**Figure 6.5:** Sham experiment in which one sample of 6.0 ml of 0.5 mg/ml ADH, 1mM 1,10 phenanthroline, in 0.1 M phosphate buffer, 0.1 M NaCl, pH 7 was placed inside the TEM cell (not operational) and another in the incubator below the TEM cell, at 37°C for 4.5 hours. The CO<sub>2</sub> supply to the incubator was disconnected.

For exposed samples, the SAR at the bottom of the flask was estimated to be 0.5 W/kg which corresponds to a temperature increase of 0.04 °C. The temperature increase, every 4.6 ms was considered insignificant in enhancing the aggregation and precipitation of ADH. The sham experiment established that a sample in the incubator (control) precipitates faster than a sample in the TEM cell (exposed) and therefore the result of the experiment in Figure 6.2 was inconsistent (see also Figure 6.3 and 6.5).

It was speculated that the presence of CO<sub>2</sub> gas may have interfered with the microwave exposure and amplified the effect.

In chapter 10 are presented the results on the aggregation of ADH solutions through which CO<sub>2</sub> was bubbled.

## 6.2 SUMMARY OF RESULTS

The experimental arrangements of the TEM cell were not specifically designed for light scattering experiments as proposed in this project. One of the drawbacks was that each time the samples needed to be taken out for light scattering measurements, the door of the incubator had to be opened for at least a few minutes as the tiny screws of the TEM cell were undone. Following this procedure the exposed and control samples were both taken to the bench and an aliquot was withdrawn from both samples for spectroscopic analysis. Therefore, the temperature fluctuations in the incubator (Figure 6.1) and of the samples were substantial and they were not studied.

The results of the experiments in the TEM cell can therefore not be analysed in a quantitative manner. The unexpected finding that an exposed sample of ADH, which was placed in a cooler environment than the control (Figures 6.3 and 6.5), precipitated faster than the control (Figure 6.2) was attributed to the CO<sub>2</sub> gas in the incubator which had accidentally been left on for that experiment. The possibility that a mutual effect of CO<sub>2</sub> and microwaves increased the kinetics of protein unfolding was further investigated in Chapter 9.

---

## CHAPTER 7

---

### LIGHT SCATTERING EXPERIMENTS

#### MICROWAVE EXPOSURE IN *EXPOSURE SYSTEM 2*

The experimental conditions for *Exposure system 2* are described in section 2.4.1.2. This system enabled a range of experimental temperatures to be utilised. The choice of temperature was based on the response of the target protein to the applied stresses in terms of time.

The following proteins were studied in *Exposure system 2*: Alcohol dehydrogenase, Bovine serum albumin, catalase, citrate synthase, insulin,  $\alpha$ -lactalbumin, lysozyme and ovotransferrin. Experimental results are presented and discussed for each protein.

The statistical analyses of the results are presented in section 7.10. Small differences in the average temperature between exposed and control samples are discussed in section 7.11.

#### 7.1 ALCOHOL DEHYDROGENASE (ADH)

Each of the four chains of ADH covalently binds a  $\text{Zn}^{2+}$  ion (section 2.2.1.1). Experiments were performed on two forms of ADH with respect to the binding of zinc. When the zinc atom is chelated (by 1,10 phenanthroline), the protein is in the apo form while holo ADH relates to the  $\text{Zn}^{2+}$  bound form of the protein.

##### 7.1.1. APO ADH AT 37°C

To study the effect of small temperature differences between cells in the incubator (see section 3.1.2), four samples of 0.5 mg/ml apo ADH were incubated at 37°C in the multi-cell holder of the spectrophotometer (Figure 7.1).

The initial rate of precipitation (section 2.6.1.1) of the four samples is presented in Table 7.1. The ratio of the largest over the lowest rate was 1.42. Although the temperature of the solution

in, for example, cell 6 was 0.3°C higher than in cell 4, this difference did not correspond to a higher initial rate of precipitation. In fact it was lower (Table 7.1).

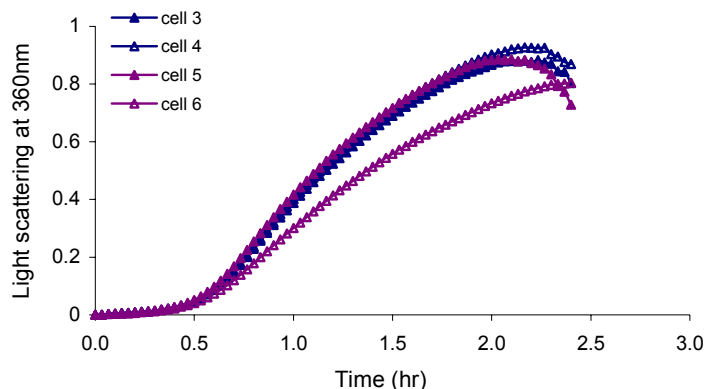


**Figure 7.1:** Incubation of four 1.0 ml samples of 0.5 mg/ml ADH (1mM 1,10 phenanthroline in 0.1 M phosphate buffer, 0.1 M NaCl, pH 7) at 37°C. The samples were placed in four different positions in the multi-cell holder of the spectrophotometer.

Cell	Initial rate of ppt. ( $A_{360}\text{hr}^{-1}$ )	Average temperature (°C) at 13.5 mm from base of cuvette
3	0.36	$36.83 \pm 0.07$
4	0.37	$36.76 \pm 0.12$
5	0.41	$36.95 \pm 0.12$
6	0.29	$37.04 \pm 0.20$

**Table 7.1:** Temperature of samples in cells 3,4,5 and 6 of spectrophotometer and the initial rate of precipitation of the 0.5 mg/ml ADH samples that were incubated in these cells.

In repeat experiments, the variations between cells in terms of ratios (initial rate of precipitation) was around 1.20 (highest rate/ lowest rate). This indicates that the initial nucleation in the aggregation of ADH is subject to random variation.

Figure 7.2 represents routine experiments on 0.5 mg/ml ADH, 1 mM 1,10 phenanthroline, in 0.1 M phosphate buffer, 0.1 M NaCl, pH 7 at 37°C exposed to 3.2 seconds of pulsed 2.450 GHz, every six minutes. The SAR for the experiment was 33.2 W/kg (at the position of the light beam of the spectrophotometer, where the sampling occurs, see section 3.2.2).

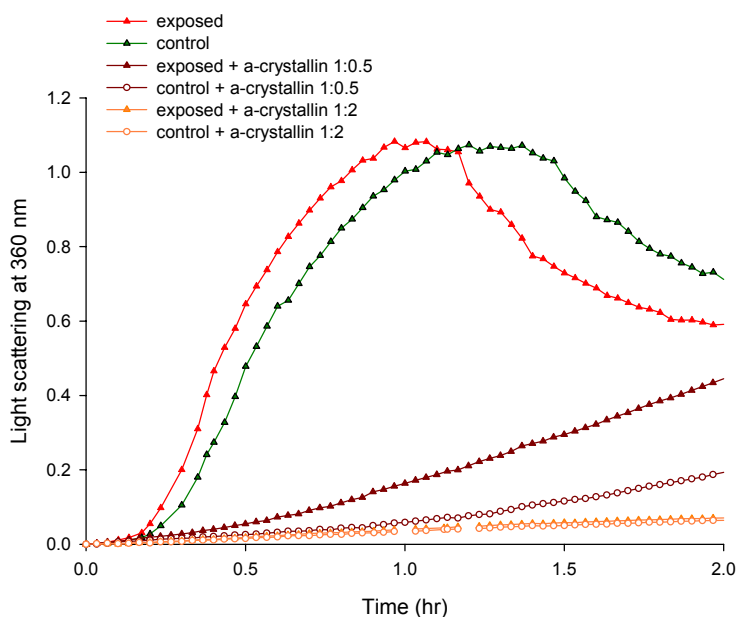


**Figure 7.2:** 0.5 mg/ml ADH (1mM 1,10 phenanthroline, in 0.1 M phosphate buffer, 0.1 M NaCl, pH 7) incubated at 37°C and exposed to 12 pulse periods (5 seconds duration) at 6 minutes intervals of 2.450 GHz with or without the presence of  $\alpha$ -crystallin at the indicated subunit molar ratios. The average temperature over six minutes was 37.6°C (exposed) and 36.8°C (control) and for the  $\alpha$ -crystallin experiments, molar ratio 1.0 : 0.5, 37.5°C (exposed) and 36.7°C (control). The pulse duration for the experiment on ADH in the presence of  $\alpha$ -crystallin at 1: 2 ratio was 3.2 seconds (no temperature profile available).

The average temperature of the samples, measured at the position of the light beam, was 37.6°C and 36.8°C for exposed and control respectively and the ratio of exposed/control (initial rate of precipitation) was 1.14 for this particular experiment.  $\alpha$ -Crystallin suppressed precipitation of ADH at the subunit molar ratio of 1:2 for both exposed and control samples. When the ratio was 1:0.5, the precipitation was partly suppressed; however, the control was more suppressed than the exposed.

Of the eleven exposure experiments performed in *Exposure system 2* with ADH, the average ratio exposed/control (initial rate of precipitation) was 1.52. Statistical analysis showed that the ratio exposed/control was  $> 1$  ( $P < 0.0005$ ).

### 7.1.2 EFFECT OF NUMBER OF PULSE PERIODS ON PRECIPITATION

As ADH aggregates and precipitates fast under the conditions used, the rate of precipitation was calculated within the first thirty minutes of the experiments. Usually, the sample was calibrated

in the incubator for two minutes prior to exposure. Therefore, there were only four pulse periods in the first thirty minutes. To establish if the number of pulse periods had an effect on the initial rate of precipitation, ADH was exposed to three different pulse periods. Figure 7.3 shows the precipitation of apo ADH exposed to 2, 8 and 15 pulse periods compared to a control. The SAR was not calculated for this experiment (for 5 second duration of pulse periods the SAR was 33.2 W/kg (measured at the position of the light beam)).

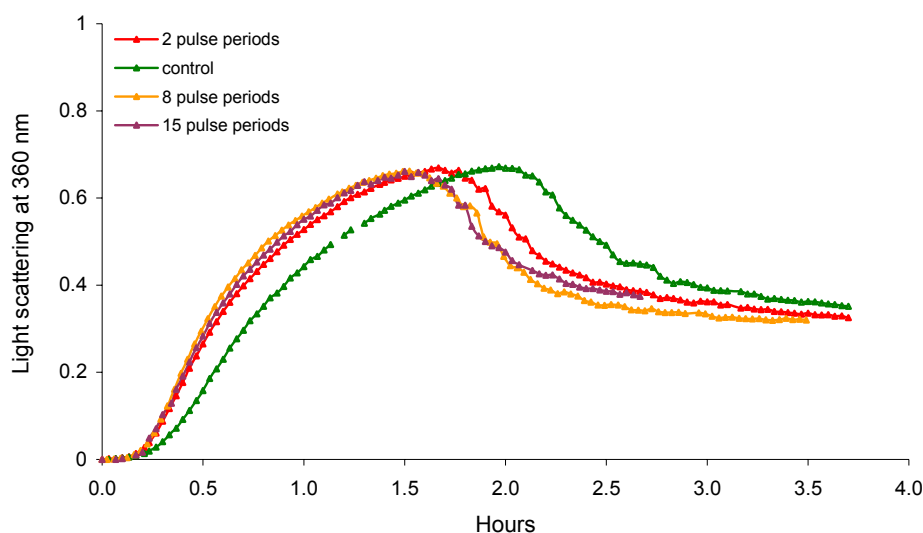


**Figure 7.3:** Exposure of 0.5 mg/ml ADH (1mM 1,10 phenanthroline in 0.1 M phosphate buffer, 0.1 M NaCl, pH 7) to 2, 8 or 15 pulse periods (each of 3.2 seconds duration) at 6 minutes intervals of 2.450 GHz at 37°C.

The ratios of the initial rates of precipitation (exposed/control) were 1.31, 1.39 and 1.38 for the 2, 8 and 15 pulse periods respectively. The initial rate was calculated within the first thirty minutes of the experiment (four pulse periods). After this time, the samples exposed to 8 and 15 periods of 2.450 GHz pulses, precipitated faster than the sample exposed to only 2 periods of pulses. Therefore, it can be concluded that, in terms of initial rate of precipitation, 2 pulse periods were sufficient to cause the difference between exposed and control samples.

### 7.1.3 HOLO ADH AT 45°C AND 60°C

To determine if the native form of yeast ADH (with bonded Zn atom) could be affected by a transient temperature increase compared to a control at constant temperature, a 0.5 mg/ml



solution of holo ADH in 0.1 M phosphate buffer, pH 7 was exposed to pulsed microwaves at 45°C and 60°C (Figures 7.4 and 7.5). The SAR was not calculated for these experiments.

The average temperature over six minutes was 44.9°C for the exposed sample, 44.3°C for the first control and 45.2°C for the second control. The ratio exposed/control 1 was 1.81 and for exposed/control 2 the ratio was 1.02.

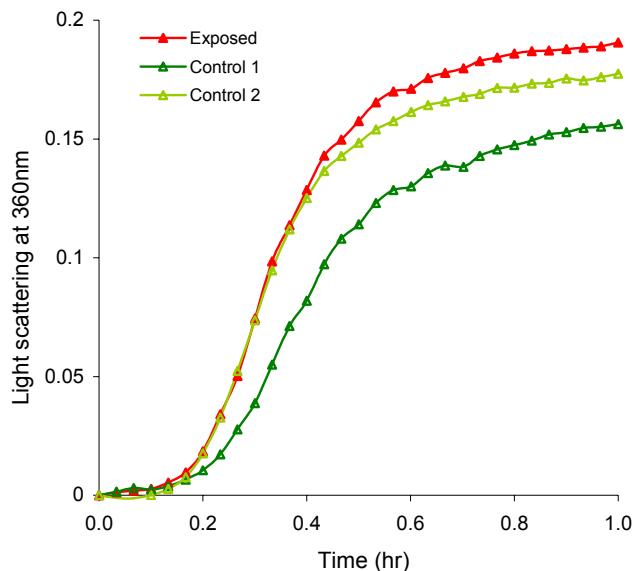


**Figure 7.4:** Exposure of 0.5 mg/ml ADH in 0.1 M phosphate buffer, pH 7 to 7 pulse periods at 45°C (4 seconds duration) of 2.450 GHz. The average temperature over six minutes was 44.9 (exposed), 44.3 (control 1) and 45.2°C (control 2).

The difference in temperature between the two controls was 0.9°C, which may explain the significant difference exposed/control ratio. Precipitation at 60°C was rapid and almost immediate (Figure 7.5). The average temperature over six minutes was not established for this experiment but as the same cell holders were used as in the experiment at 45°C, it may be assumed that there was a similar temperature difference between control 1 and 2. The ratio exposed/control 1 was 1.07 and the exposed/control 2 ratio was 0.95.

The increase in temperature from 45°C to 60°C increased the kinetics of unfolding (as demonstrated by the rate and extent of precipitation) but the microwave induced temperature incursion did not make a significant difference in the rate of precipitation compared to the control at a similar average temperature.

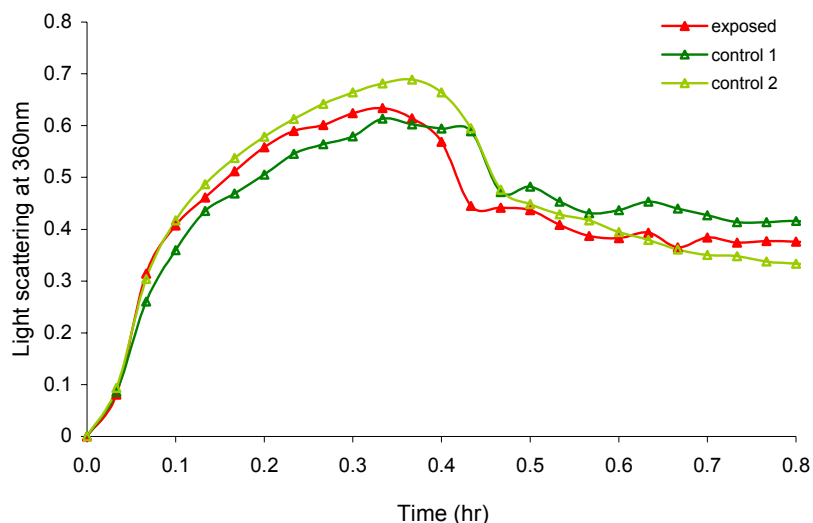


**Figure 7.5:** Exposure of 0.5 mg/ml ADH in 0.1 M phosphate buffer, pH 7 to 4 pulse periods (4 seconds duration) at 6 minutes intervals of 2.450 GHz at 60°C.

It can therefore be concluded that although holo ADH was destabilised by increasing the temperature, the microwave exposure, in this particular experiment had no effect.

## 7.2 BOVINE SERUM ALBUMIN (BSA)

The structure of BSA is severely weakened when the disulphide bonds, of which BSA has seventeen, are reduced. The experiments carried out on this protein were on both forms: oxidised BSA and reduced BSA.

### 7.2.1 REDUCED BSA AT 45°C

To study the effect of small temperature differences between cells in the incubator (see section 3.1.2), four samples of 1.5 mg/ml BSA were incubated at 45°C in the multi-cell holder of the spectrophotometer (Figure 7.6). The initial rate of precipitation of the four samples is presented in Table 7.2. The ratio of the largest over the lowest rate was 1.14. The difference between the highest (cell 6) and lowest temperature (cell 3) was 0.7°C; however, the rates do not correlate with the variation in solution temperature (Table 7.2). Figure 7.7 represents routine experiments on 1.5 mg/ml BSA, 20 mM DTT in 0.1 M phosphate buffer, 0.1 M NaCl, pH 7 at 45°C exposed

to pulsed 2.450 GHz, every six minutes. The SAR for this particular set of experiments was 58.2 W/kg (position of the light beam). The ratio of the exposed over the control sample in terms of initial rate of precipitation was 1.16 for the sample that contained BSA only.

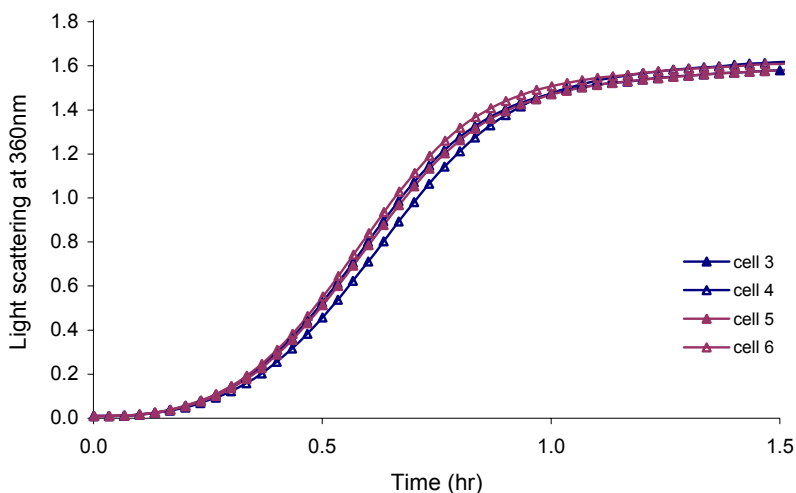


**Figure 7.6:** Incubation of four 1.0 ml samples of 1.5 mg/ml BSA, 20 mM DTT in 0.1 M phosphate buffer, pH 7 at 45°C. The samples were placed in four different positions in the multi-cell holder of the spectrophotometer.

Cell	Initial rate of ppt ( $A_{360}\text{hr}^{-1}$ )	Average temperature (°C) at 13.5 mm from base of cuvette
3	2.59	44.51 $\pm$ 0.25
4	2.36	44.87 $\pm$ 0.21
5	2.71	44.93 $\pm$ 0.24
6	2.55	45.20 $\pm$ 0.17

**Table 7.2:** Temperature of samples in cells 3, 4, 5 and 6 of the spectrophotometer and the initial rate of precipitation of the 1.5 mg/ml BSA samples that were incubated in these cells.

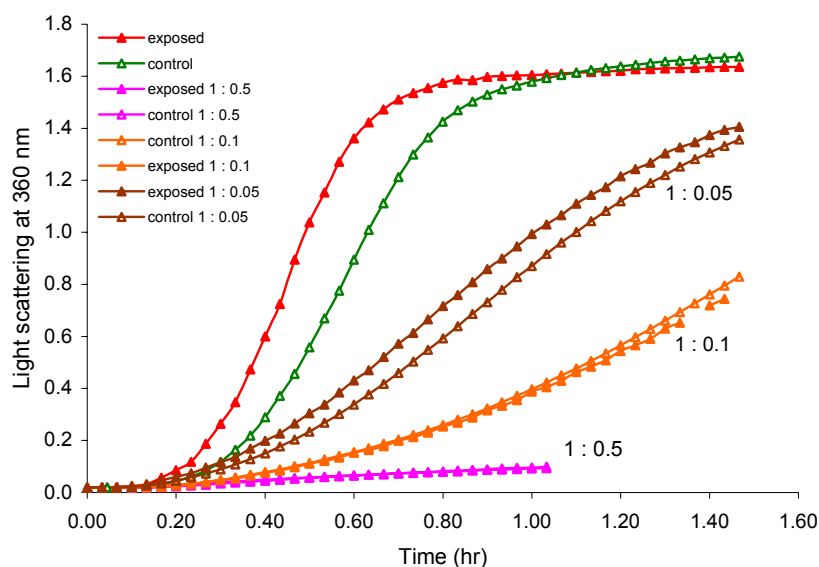


**Figure 7.7:** 1.5 mg/ml BSA, 20mM DTT in 0.1 M phosphate buffer, 0.1 M NaCl, pH 7 incubated at 45°C and exposed to pulsed 2.450 GHz at six minute intervals without or in the presence of  $\alpha$ -crystallin in subunit molar ratios as indicated on the graph. The pulse periods lasted 5 seconds each; a total of 10 pulse periods (BSA, no  $\alpha$ -crystallin), 15 pulse periods (ratios 1.00: 0.05 and 1.0: 0.1) and 11 pulse periods (ratio 1.0: 0.5) were applied to the “exposed” sample.

Statistical analysis on the ratios of the five experiments indicated that the ratio exposed/control was not significantly greater than 1 ( $P>0.25$ ) hence microwave exposure under the conditions set out above, did not enhance the rate of precipitation of BSA (1.5 mg) at 45°C.  $\alpha$ -Crystallin suppressed precipitation significantly but at the molar ratio of 1.00: 0.05, the control was more suppressed than the exposed sample. The ratio exposed/control was 1.28 in this case. However, at the molar ratio BSA:  $\alpha$ -crystallin, 1.0: 0.1 the suppression for the control and exposed sample was equal. At a molar ratio of 1.0: 0.5 precipitation was wholly suppressed for control and exposed samples. The average temperature (see section 3.3.3) over a six minute period was: 45.3°C (exposed) and 44.6°C (control).

### 7.2.2 REDUCED BSA AT HIGH CONCENTRATION, 37°C

de Pomerai *et al* reported<sup>118</sup> that exposure of high concentrations of BSA (75 mg/ml) to continuous wave 1.0 GHz at 37, 40 and 45°C caused a significant enhancement in light scattering compared to shielded samples. The high concentration was chosen so that it would increase the chances of collision between partly unfolded molecules that would lead to

irreversible aggregation and thus to increased light scattering. It was therefore of interest to determine if pulsed microwaves would have a similar effect.

When 50 mg/ml BSA, 20 mM DTT in 0.1 M phosphate buffer, 0.1 M NaCl, pH 7, was incubated at 37°C and exposed to five pulse periods of 2.450 GHz, at a SAR of 33.2 W/kg, the sample precipitated greatly after 9 minutes and by 28 minutes the exposed sample had turned to a gel (Figure 7.8). The control sample did not precipitate at that stage. No repeat experiments were performed.

Thus, by reducing the disulphide bonds of BSA and increasing the concentration more than 30 fold over previous experiments, the exposed sample rapidly precipitated out of solution at 37°C. The control however did not start to precipitate until after 0.5 hours and the extent was much smaller than the experiment in Figure 7.7 at 45°C.

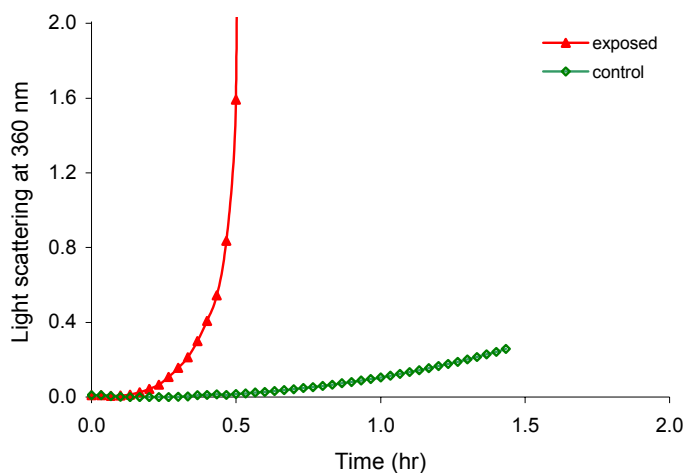


**Figure 7.8:** Exposure of 50 mg/ml BSA, 20mM DTT in 0.1 M phosphate buffer, 0.1 M NaCl, pH 7 at 37°C to 5 pulse periods of 2.450 GHz at 6 minute intervals. Each pulse period lasted 5 seconds.

### 7.2.3 OXIDISED BSA AT HIGH CONCENTRATIONS, 50°C AND 60°C

Two experiments were carried out on 45 mg/ml BSA in 0.1 M phosphate buffer, pH 7. In one experiment, the exposed sample, incubated at 50°C (Figure 7.9) was subjected to fifteen pulse periods at six minute intervals. The SAR was not determined for these experiments but was expected, on the basis of the conductivity of the buffers (section 3.2.1), to be smaller than the

samples in Figure 7.7. BSA proved to be quite stable in the non-reduced form even when samples were more than 30 times as concentrated as in section 7.2.1. At 50°C only a small population of BSA molecules aggregated as can be deduced from the aggregation profile in Figure 7.9. At 60°C aggregation was much more enhanced but there was no difference between the exposed and control samples (Figure 7.10) indicating that the transient temperature incursions did not have an effect on the aggregation of non-reduced BSA at high concentrations.

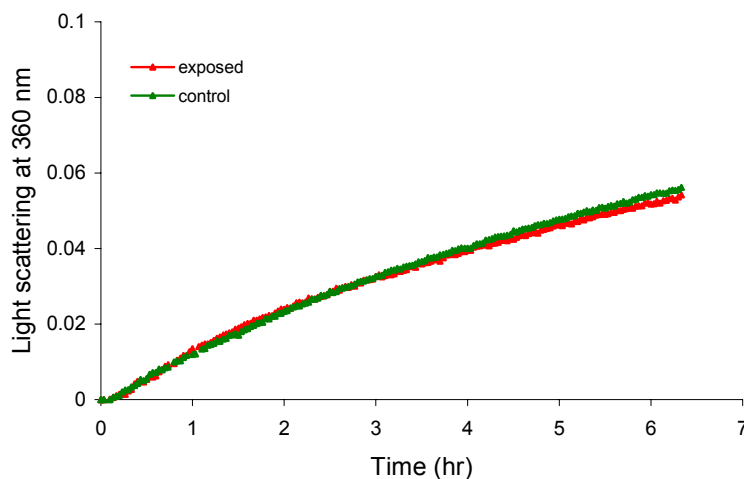


**Figure 7.9:** Exposure of 45 mg/ml BSA in 0.1 M phosphate buffer, pH 7 at 50°C to 15 pulse periods of 2.450 GHz at 6 minute intervals. Each pulse period lasted 5 seconds. The water box inside the microwave oven contained 650 ml water.

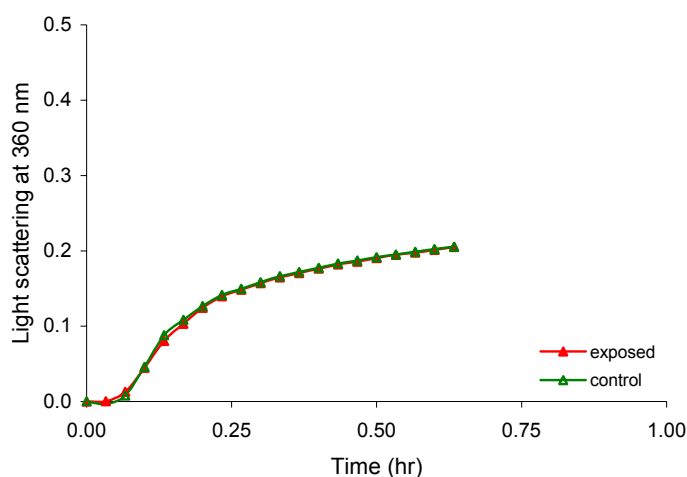


**Figure 7.10:** Exposure of 45 mg/ml BSA in 0.1 M phosphate buffer, pH 7 at 60°C to six pulse periods of 2.450 GHz at 6 minute intervals. Each pulse period lasted 3.2 seconds. The water box inside the microwave oven contained 750 ml water as opposed to 500 ml in other experiments on BSA.

In comparing reduced and oxidised BSA at high concentrations, the most profound difference was found in the reduced samples at 37°C. Reduction of BSA at the lower concentration of 1.5 mg/ml at 45°C (Figure 7.7) resulted in considerable light scattering (an absorbance of 1.6 after one hour). The oxidised samples (Figures 7.9 and 7.10) precipitated much less. The absorbance after one hour was ~0.1 at 50 °C and ~0.2 at 60°C respectively. It was expected that the control sample of the experiment on a high concentration of BSA at 37°C, would have caused an increase in light scattering similar or more so than the light scattering shown in Figure 7.7 (at 45°C). However, very little protein had precipitated after one hour. The formation of a gel in the exposed sample at 37°C, compared to the formation of particles in other samples, is curious.

It may appear that there was not a sufficient excess of DTT molecules to reduce the many disulphide bonds in the highly concentrated protein sample (there was a 10 mole excess of DTT compared to a 340 mole excess in the less concentrated samples ). Therefore, the secondary structure of most protein molecules was stable. This would explain the low absorbance of the control sample. Precipitation of the exposed sample started after 7 minutes (Figure 7.8), therefore one period of a 2.9°C temperature increase (pulse period) seemed sufficient to force the aggregating molecules into a matrix that favoured gelation. Gelation is an orderly aggregation of proteins which may still exhibit some secondary structure, into a three dimensional network<sup>179</sup>. Formation of disulphide bonds are known to be involved in the initial step of coagulation<sup>180, 181</sup>. It is therefore conceivable that because of the lack of sufficient DTT and the occasional temperature spike, disulfide bonds were able to re-form randomly intra- and intermolecularly in the crowded environment thus resulting in gel formation.

### 7.3 CATALASE

#### 7.3.1 CATALASE AT 42°C

To study the effect of small temperature differences between cells in the incubator (see section 3.1.2), four samples of 0.2 mg/ml catalase were incubated at 42°C in the multi-cell holder of the spectrophotometer (Figure 7.11). The initial rate of precipitation of the four samples is

presented in Table 7.3. The ratio of the largest over the lowest rate was 1.14. The difference between the highest (cells 4 and 5) and lowest temperatures (cell 2) was 0.2°C; however, as the highest temperature corresponded to the lowest rate, it was concluded that the temperature variations did not affect the initial rate of precipitation in this particular experiment.

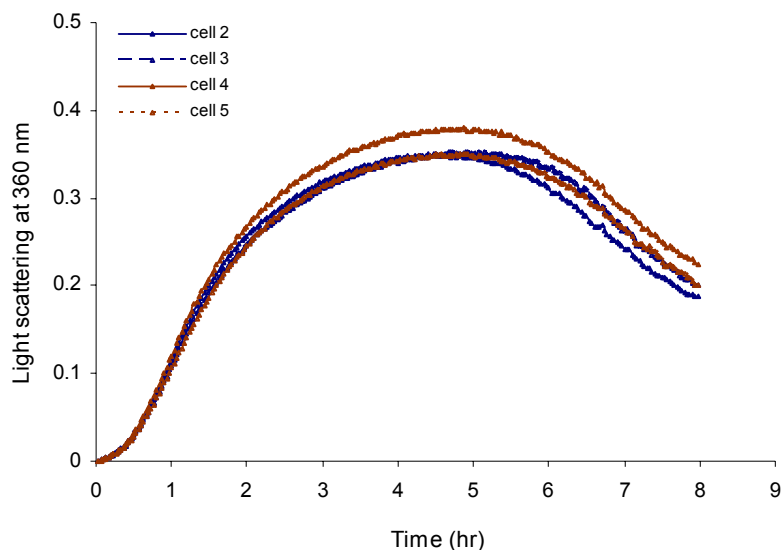


**Figure 7.11:** Incubation of four 1.0 ml samples of 0.2 mg/ml catalase in 0.1 M phosphate buffer, pH 7 at 42°C. The samples were placed in four positions in the multi-cell holder of the spectrophotometer.

Figure 7.12 represents routine experiments on 0.2 mg/ml catalase, in 0.1 M phosphate buffer, pH 7 at 42°C exposed to pulsed 2.450 GHz, every six minutes. The SAR for this particular set of experiments was 42.7 W/kg at the position of the light beam.

Cell	Initial rate of ppt ( $A_{360}\text{hr}^{-1}$ )	Average temperature (°C) at 13.5 mm from base of cuvette
2	0.19	41.75 $\pm$ 0.21
3	0.18	41.80 $\pm$ 0.23
4	0.20	41.93 $\pm$ 0.20
5	0.17	41.93 $\pm$ 0.16

**Table 7.3:** Temperature of samples in cells 2,3,4 and 5 of spectrophotometer and the initial rate of precipitation of the 3.2  $\mu\text{M}$  catalase samples that were incubated in these cells.



The ratio of the initial rate of precipitation (exposed/control) for the assay containing only catalase was 1.84 which is well above the ratio caused by temperature variations between the cells (see Figure 7.11).

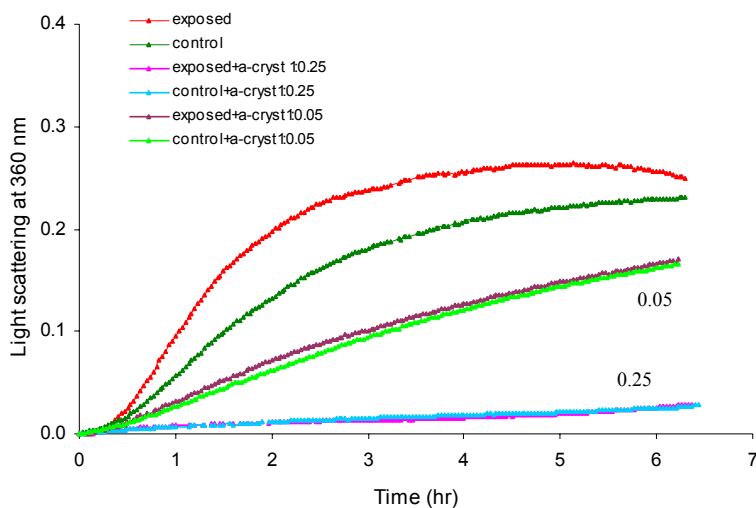


**Figure 7.12:** 0.2 mg/ml catalase in 0.1 M phosphate buffer, pH 7 incubated at 42°C and exposed to pulsed 2.450 GHz at six minute intervals without or in the presence of  $\alpha$ -crystallin at the subunit molar ratios as indicated. The pulse periods, 20 in total, lasted 5 seconds each.

The temperature, averaged over six minutes (see section 3.3.3), was 42.3°C for the exposed and 41.7°C for the control samples. The extent of precipitation was enhanced for the exposed sample as compared to the control.

Of the six experiments on catalase under exactly the same conditions, the initial rate of the precipitation of the exposed samples was significantly greater than the control. ( $0.005 < P < 0.01$ ).  $\alpha$ -Crystallin suppressed precipitation partially at the ratio of 1.00 : 0.05 and fully at the ratio of 1.00 : 0.25 (Figure 7.12).

## 7.4 CITRATE SYNTHASE (CS)

### 7.4.1 CS AT 37°C

Experiments on CS, using the multi-cell holder of the spectrophotometer as the incubator, were performed at 37 °C concentrations of 0.2 mg/ml and in the presence of  $\alpha$ -crystallin. The effect

of either 8 or 15 pulse periods on precipitation was studied and the results are shown in Figures 7.13 and 7.14. The ratio of the initial rate of precipitation of exposed/control was 0.99 for the sample exposed to 15 pulse periods and 1.09 for the sample exposed to 8 pulse periods of 2.450 GHz.

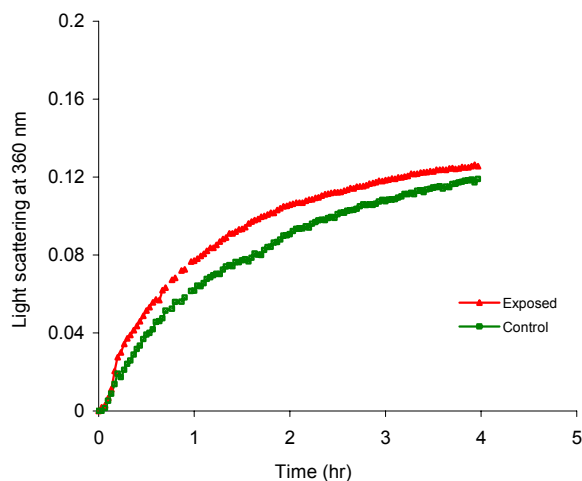


**Figure 7.13:** 0.2 mg/ml CS incubated at 37°C and exposed to 15 pulse periods of 3.2 seconds of 2.450 GHz. The SAR for this sample was < 22.09 W/kg in the region where the light beam passes through the sample.

In the presence of  $\alpha$ -crystallin at a subunit molar ratio of 1.0: 0.5, no difference was found between exposed and control in terms of the initial rate of precipitation.

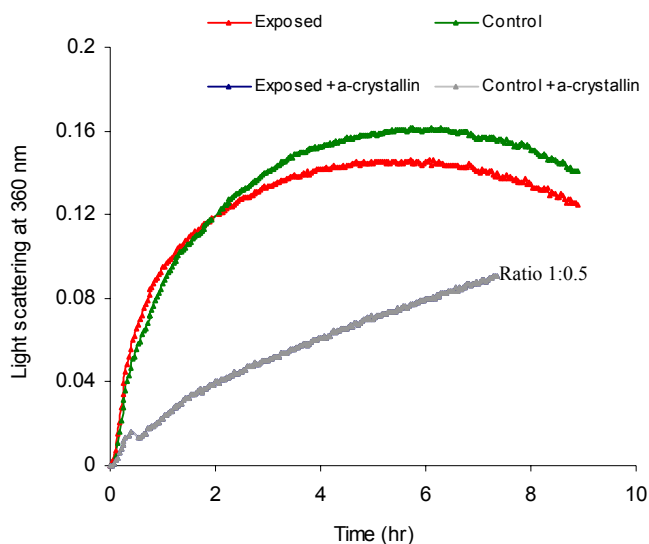


**Figure 7.14:** 0.2 mg/ml CS incubated at 37°C and exposed to 8 pulse periods of 3.2 seconds of 2.450 GHz (red and green) and in the presence of a ratio of 1: 0.5  $\alpha$ -crystallin (blue and grey, superimposed). The SAR for this sample was < 22.09 W/kg in the region where the light beam passes through the sample.

It can be concluded that although the initial rate of precipitation was almost equal for exposed and control samples, a longer exposure of 15 pulse periods compared to 8 (Figure 7.13), resulted in more precipitation. The ratio exposed/control for CS experiments at 37°C, under the exposure conditions of  $\sim 22$  W/kg were statistically not larger than 1 ( $0.10 < P < 0.25$ ). The samples exposed to 15 pulse periods (Figure 7.13) were measured for fluorescence emission (see section 9.2).

#### 7.4.2 CS AT 42°C

In order to establish if the small temperature differences between the positions in the cell block would have a corresponding effect on CS aggregation, a 0.2 mg/ml sample was divided in 4 x 1.0 ml samples that were placed in four stoppered cuvettes in positions 2, 3 4 and 5 of the cell block. Figure 7.15 shows the profile of the light scattering for these samples. The initial rate of precipitation was calculated for each sample and is shown in Table 7.4. The ratio of the highest rate over the lowest rate was 1.11 and the ratio of the highest two rates was 1.04. Hence the initial rate of precipitation was similar in the four cells.

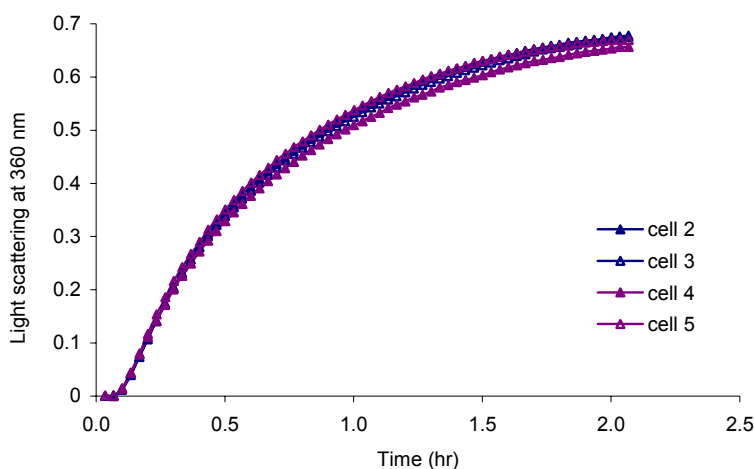


**Figure 7.15:** Effect of small temperature differences on CS aggregation. Four samples of 1.0 ml 0.2 mg/ml CS were placed in positions 2, 3, 4 and 5 of the multi cell holder of the spectrophotometer and incubated at 42°C. The light scattering was monitored over 2 hours.

Cell	Initial rate of ppt. ( $A_{360}0hr^{-1}$ )	Average temperature ( $^{\circ}C$ ) at 13.5 mm from base of cuvette
2	0.97	$41.75 \pm 0.21$
3	1.00	$41.80 \pm 0.23$
4	0.94	$41.89 \pm 0.20$
5	1.04	$41.93 \pm 0.16$

**Table 7.4:** Temperature of samples of 0.2 mg/ml CS in cells 2,3,4 and 5 of spectrophotometer and the initial rate of precipitation of the samples that were incubated in these cells.

Figure 7.16 is representative of a typical CS thermal experiment performed at  $42^{\circ}C$ . The initial rate of precipitation for the exposed sample was higher than the control; the ratio of exposed/control was 1.63.

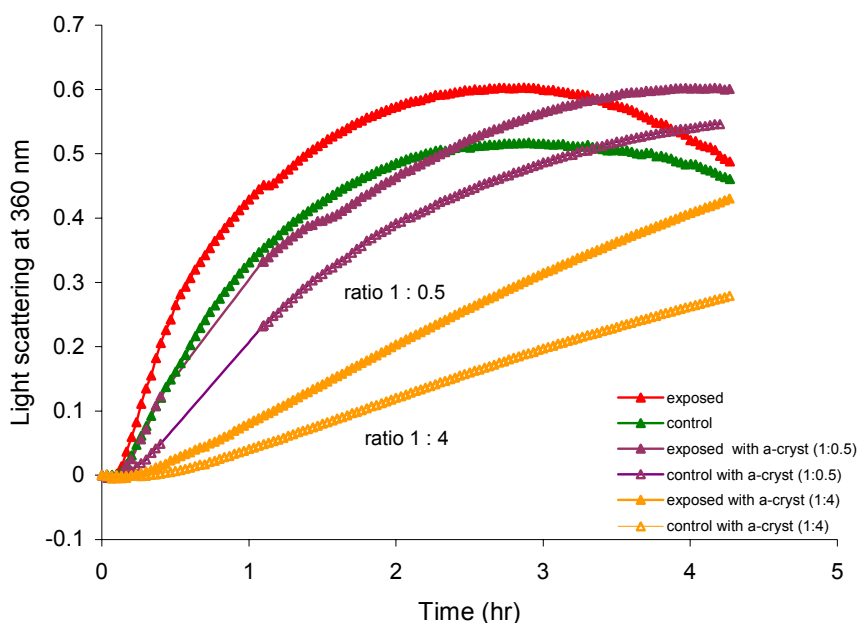


**Figure 7.16:** 0.2 mg/ml CS incubated at  $42^{\circ}C$  and exposed to 6 pulse periods (3.2 seconds duration) at 6 minute intervals of 2.450 GHz with or without the presence of  $\alpha$ -crystallin in subunit molar ratios as indicated on the graph. The SAR was 24.4 W/kg. The average temperature over six minutes was  $42.0^{\circ}C$  (exposed) and  $41.7^{\circ}C$  (control) and for the  $\alpha$ -crystallin experiments, ratio 1.0 : 0.5,  $42.0^{\circ}C$  (exposed) and  $41.7^{\circ}C$  (control); ratio 1 : 4,  $41.9^{\circ}C$  (exposed) and  $41.6^{\circ}C$  (control).

The precipitation of the exposed sample was enhanced over the entire length of the experiment compared to the control. On average, over a six minute period, the exposed sample was just 0.3°C warmer (measured at the position of the light beam) than the control sample. In the light of the results of the experiment in which aggregation was measured of samples held at small temperature differences (see Figure 7.15 and Table 7.4), this is a significant difference. Under the conditions described above, the ratio (initial rate of precipitation) exposed/control was greater than 1 for all experiments ( $0.005 < P < 0.01$ ). In the presence of  $\alpha$ -crystallin (the ratio was expressed as subunit moles of target protein : sHsp), the aggregation was suppressed to a greater extent in the control samples than in the exposed samples.

By increasing the incubation temperature from 37°C to 42°C, the difference between the exposed and control samples with respect to the initial rate of precipitation increased significantly. This is discussed in more detail in section 7.9.2.

## **7.5 INSULIN**

### **7.5.1 REDUCED INSULIN**

To study the effect of small temperature differences between cells in the incubator (see section 3.1.2), four samples of 0.25 mg/ml insulin, 20mM DTT in 0.1 M phosphate buffer, 0.1 M NaCl, pH 8 were incubated, in two different experiments, at 19 and 25°C, in the multi-cell holder of the spectrophotometer (Figure 7.17).

The initial rate of precipitation of the four samples of both experiments is presented in Table 7.5. The ratio of the largest over the lowest rate was 1.82 and 1.10 for 19 and 25°C respectively. The temperature deviations at 19 and 25°C were not studied in depth for the multi cell holder (Figure 3.1).

It is possible that the cooling of the cell block to 19°C, which was below room temperature, could have brought about a larger variation in the cells than the temperature variations observed when the cell block was heated. Pulsed microwave experiments undertaken on insulin at 37°C did not cause a significant difference in the initial rate of precipitation or the extent of precipitation between exposed and control samples (not shown).

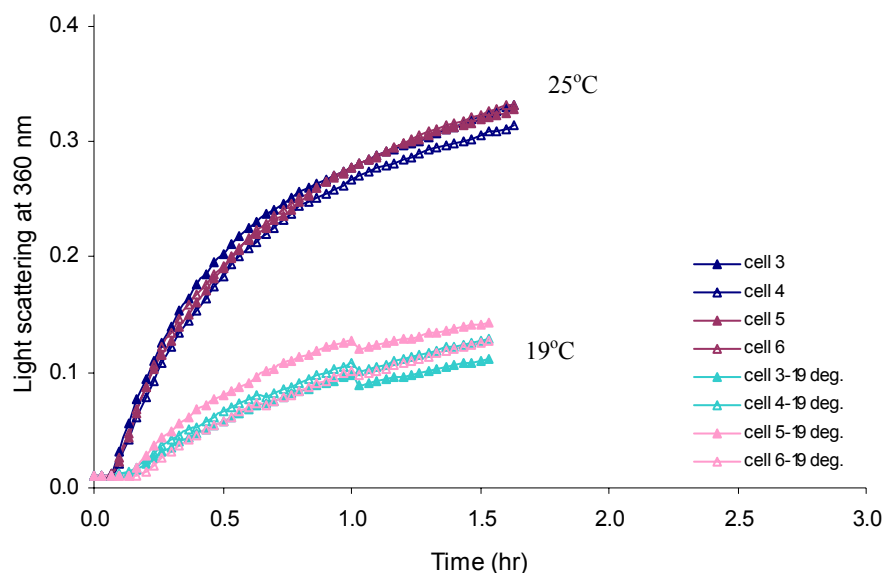


**Figure 7.17:** Incubation of four 1.0 ml samples of 0.25mg/ml insulin, 20 mM DTT in 0.1 M phosphate buffer, 0.1 M NaCl, pH 8 at 19 and 25°C. The samples were placed in four positions in the multi-cell holder of the spectrophotometer.

Cell	Initial rate of ppt at 19°C ( $A_{360}\text{hr}^{-1}$ )	Initial rate of ppt at 25°C ( $A_{360}\text{hr}^{-1}$ )
3	0.15	0.64
4	0.17	0.58
5	0.26	0.63
6	0.18	0.61

**Table 7.5:** Initial rate of precipitation of 0.25 mg/ml insulin at 19 and 25°C in cells 3, 4, 5 and 6 of the spectrophotometer.

Therefore, experiments were performed also at 25°C and 19°C in order to slow down the kinetics of the aggregation. In Figure 7.18 are shown the results of experiments on exposed insulin at 19°C and 25°C. The ratio exposed/control (initial rate of precipitation) was 1.16 in Figure 7.18 A (25°C). The SAR for this experiment was 58.24 W/kg (position of the light beam) which corresponds to a transient temperature increase every six minutes of 5.0°C. After 1.5 hour the extent of the precipitation of the control was slightly enhanced. At that time the exposure

was completed (57 minutes).  $\alpha$ -Crystallin at the molar ratio of 1 : 1 (A) suppressed precipitation up to 100 minutes (when the experiment was stopped). The ratio exposed/control in Figure 7.18 B (19°C) was 1.06, the extent of the precipitation was enhanced compared to the control. The microwave power in B was much higher than in A. The SAR was not calibrated but was considered to be higher than in Figure 7.18 A as the box in the microwave oven contained half the amount of water than in A. Furthermore, only three pulse periods were applied (the exposure was stopped after 15 minutes into the experiment).

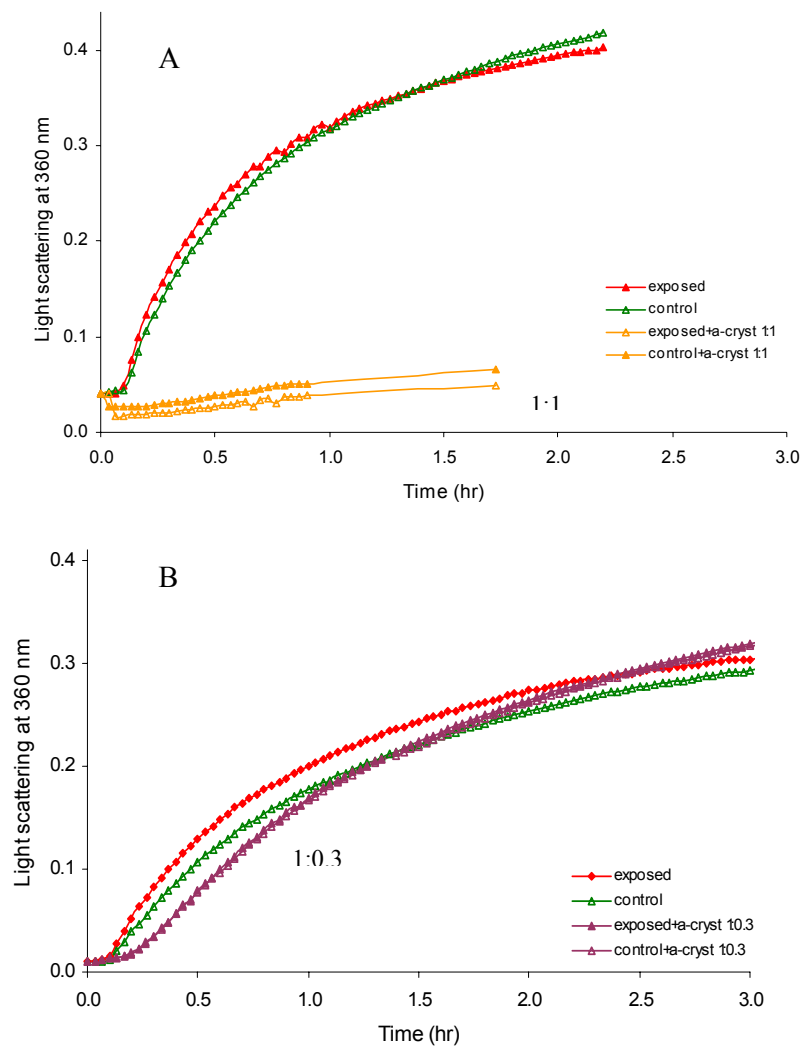


**Figure 7.18:** 0.25 mg/ml insulin, 20mM DTT in 0.1 M phosphate buffer, 0.1 M NaCl pH 8 incubated at 25°C and exposed to pulsed 2.450 GHz at six minutes intervals without or in the presence of  $\alpha$ -crystallin in subunit molar ratios as indicated on the graphs. In one experiment (A) the pulse periods lasted 5 seconds each; a total of 10 pulse periods were applied and the SAR was 58.24 W/kg (at the position of the light beam). In the second experiment (B) the pulse periods lasted 5 seconds; a total of 3 (no  $\alpha$ -crystallin) or 10 (with  $\alpha$ -crystallin) pulse periods were applied. The SAR was not calibrated and was expected to be higher than in A. The box in the microwave oven contained 250 ml water as opposed to 500 ml in A.

When  $\alpha$ -crystallin was added at a subunit molar ratio of 1 : 0.3, the precipitation was not suppressed and no difference in the initial rate and extent of precipitation between the exposed and control sample was observed. The samples that contained  $\alpha$ -crystallin were exposed under the same conditions as the samples without  $\alpha$ -crystallin except that they were exposed to 10 pulse periods of 2.450 GHz instead of three.

An experiment was undertaken to compare the initial rate of precipitation for a sample exposed to 10 pulse periods at 6 minutes interval to a sample exposed to two pulse periods, two minutes apart (Figure 7.19). The SAR was 58.24 W/kg.

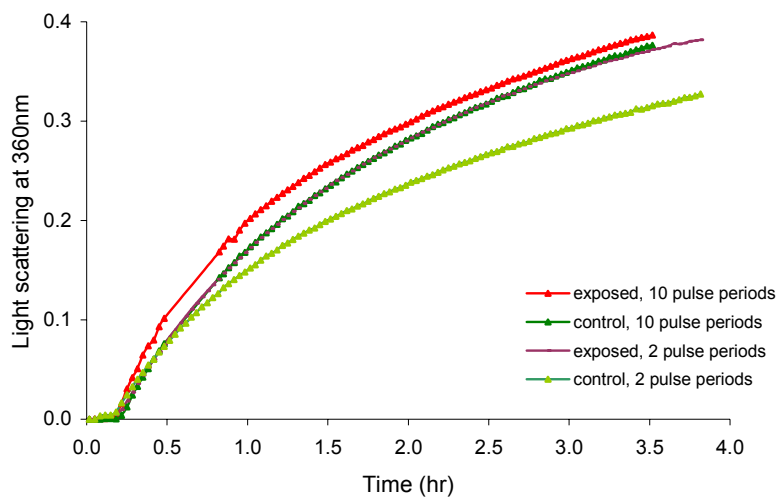


**Figure 7.19:** 0.25 mg/ml insulin, 20mM DTT in 0.1 M phosphate buffer, 0.1 M NaCl pH 8 exposed to 10 pulse periods of 6 minutes interval or 2 pulse periods of 2 minutes interval at 19°C. The pulse periods lasted 5 seconds and exposure was to 2.450 GHz. The SAR was 58.24 W/kg (at the position of the light beam). Note that the plots of the exposed (2 pulse periods) and control (10 pulse periods) are superimposed.

The ratios of the initial rate of precipitation (exposed over control) was 1.17 for the samples exposed to 10 pulse periods and 1.09 for the samples exposed to 2 pulse periods. However, the extent of precipitation was different for the two sets of experiments. The sample exposed to 10 pulse periods precipitated slightly more compared to the control. In comparison, the sample exposed to two pulse periods, precipitated considerably more than the control.



## 7.6 $\alpha$ -LACTALBUMIN

During the course of the project, the precipitation experiments on  $\alpha$ -lactalbumin often gave contradictory results. At times, either no precipitation occurred or the precipitation was so severe, that the absorbance at  $\lambda$  360 went off-scale. It was noted that most light scattering experiments on  $\alpha$ -lactalbumin reported in the literature, that used 2 mg/ml<sup>153; 154; 182; 183</sup>, were performed on a plate reader whereas the experiments in this project were performed inside a quartz cuvette of 1.4 ml volume. Different concentrations, buffer solutions, and temperatures were used to identify the problem but there did not seem to be a clear reason for the behaviour of the protein. Protein solutions were always freshly made up and buffers were normally made fresh at least every second week. At the time of the experiments it was not considered to measure light scattering at 500 nm in order to allow larger particles to be measured.

### 7.6.1 REDUCED APO $\alpha$ -LACTALBUMIN

When 2 mg/ml apo  $\alpha$ -lactalbumin, 2 mM EDTA, 20 mM DTT, 0.1 M NaCl in 0.1 M phosphate buffer, pH 7 was exposed to pulsed 2.450 GHz at 36°C, no significant difference was found between the exposed and control sample as is shown in Figure 7.20.

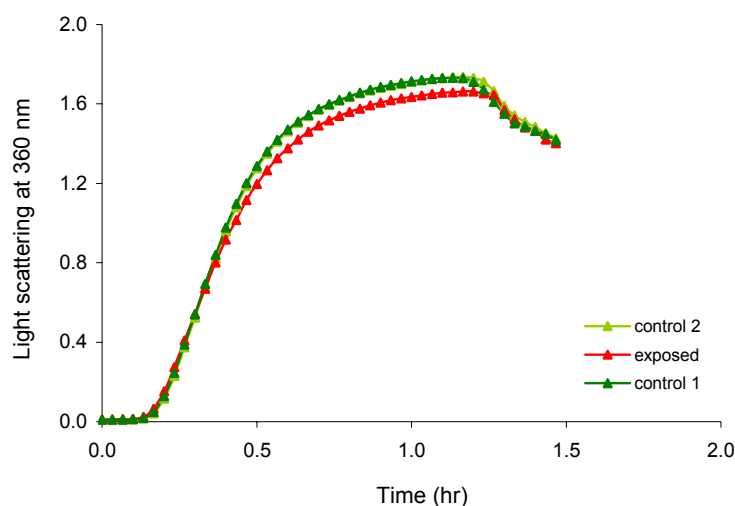
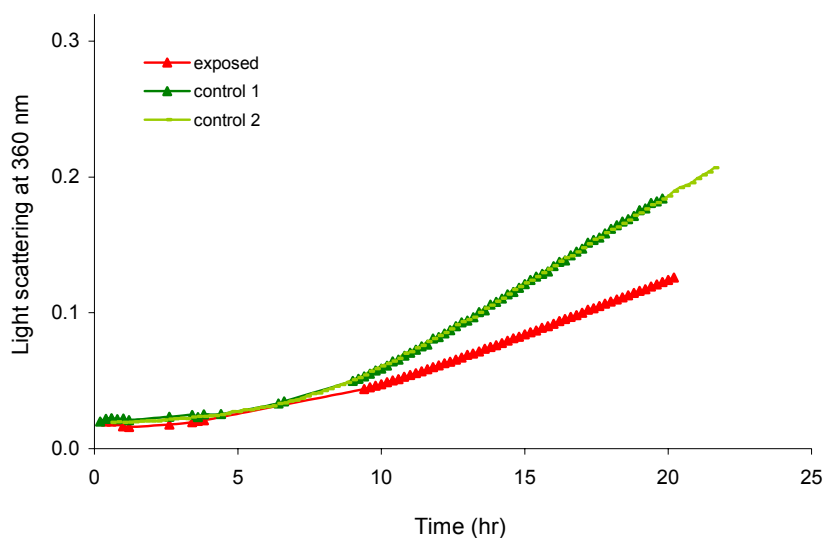


Figure 7.20: 2 mg/ml apo  $\alpha$ -Lactalbumin, 2 mM EDTA, 20 mM DTT in 0.1 M phosphate buffer, 0.1 M NaCl, pH 7 exposed to 5 pulse periods of 2.450 GHz at 36°C. The two controls are superimposed on each other. The SAR was 33.2 W/kg at the position of the light beam.

Control 1 was taken out of the spectrophotometer for the duration of the exposure and was returned at the same time as the exposed sample. The temperature, averaged over a six-minute period, for this sample was 35.9°C. The temperature for the exposed sample was 35.6°C and 35.9°C for the second control that remained in the multi-cell holder for the term of the experiment. The SAR at the position of the light beam was 33.2 W/kg. The ratio exposed/control 1(initial rate of precipitation) was 1.01 and for exposed/control 2 it was 1.04.

To study the effect of heating, an experiment was conducted at room temperature. 0.5 mg/ml reduced  $\alpha$ -lactalbumin, 2 mM EDTA, was exposed to pulsed microwaves, every six minutes, for 9 hours (Figure 7.21). The precipitation of the two controls was similar (ratio control 2/control 1 was 1.06) but the exposed sample was slower in precipitating..

One control remained on the bench and light scattering was measured together with the exposed sample, every 12 minutes. The second control was left in the multi-cell holder of the spectrophotometer and was measured for light scattering every 2 minutes. After 9 hours all samples were placed in the multi-cell holder. The ratio exposed/control 1 (initial rate of precipitation) was 0.73 and for exposed/control 2 was 0.69. The SAR for this experiment was not calculated but was estimated from similar experimental conditions to be ~58 W/kg.



**Figure 7.21:** 0.5 mg/ml apo  $\alpha$ -Lactalbumin, 2 mM EDTA, 20 mM DTT in 0.1 M phosphate buffer, 0.1 M NaCl, pH 7 was exposed to pulsed 2.450 GHz every six minutes for 9 hours at room temperature. The SAR was estimated to be 58 W/kg.

A 5°C transient temperature increase every six minutes failed to enhance the precipitation of 0.5 mg/ml  $\alpha$ -lactalbumin when samples were maintained at room temperature. While the initial rate of precipitation was similar for the exposed and control samples, after 6 hours the controls precipitated faster than the exposed sample.

## 7.6.2 REDUCED HOLO $\alpha$ -LACTALBUMIN

Reduced holo  $\alpha$ -lactalbumin was exposed to pulsed microwaves at concentrations of 0.5 and 1 mg/ml. Figure 7.22 shows the result of an exposure of 5 pulse periods of 2.450 GHz on holo  $\alpha$ -lactalbumin compared to a control sample.

The ratio exposed/control 1 and exposed/control 2 was 0.96 and 0.91 respectively. The extent of precipitation was largest for control 2, the sample that had remained in the spectrophotometer at all times.

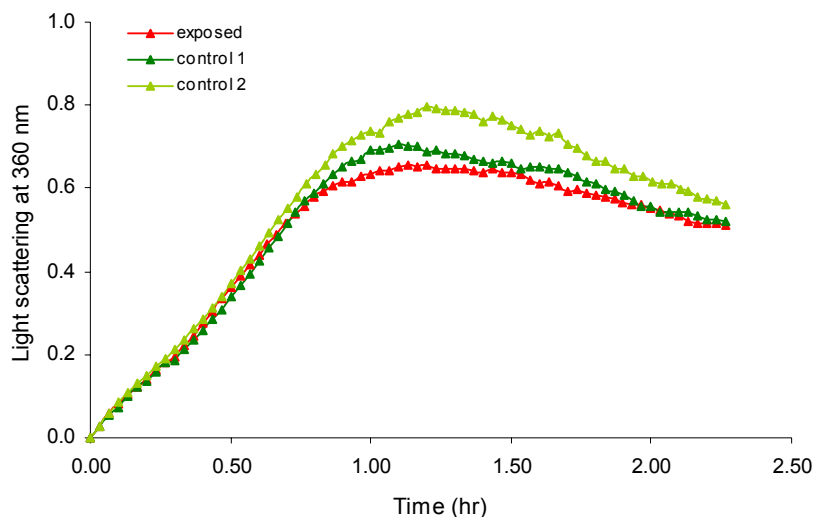


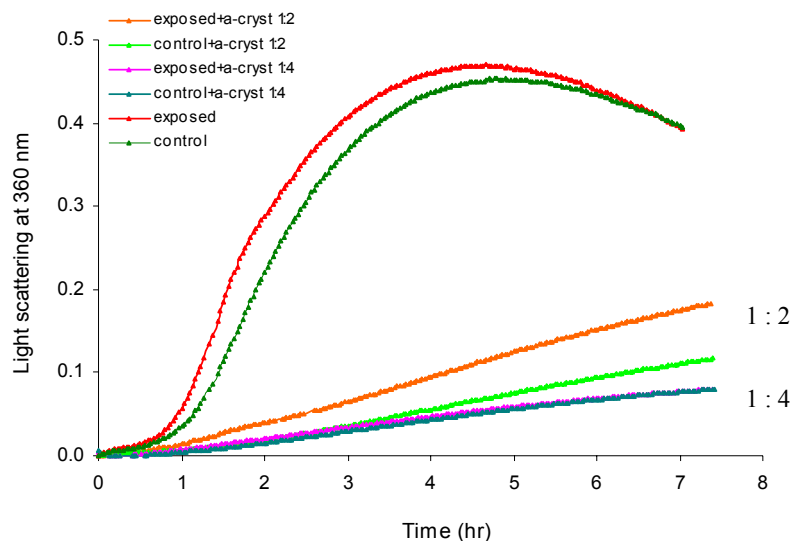
Figure 7.22: 0.5 mg/ml holo  $\alpha$ -lactalbumin in 50 mM imidazole buffer, 0.1 M NaCl, 5 mM  $\text{CaCl}_2$ , 20 mM DTT, pH 7.2 was exposed at 32°C to 5 pulse periods of 2.450 GHz. The SAR was estimated to be 11.5 W/kg.

## 7.7 LYSOZYME

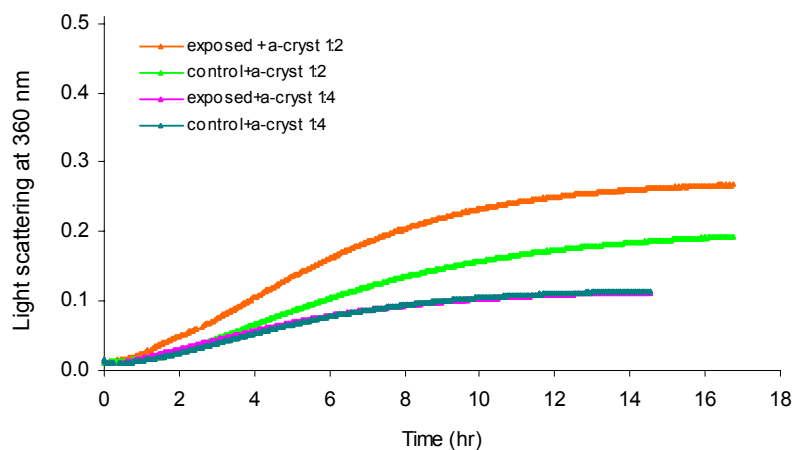
### 7.7.1 REDUCED LYSOZYME

Figure 7.23 represents routine experiments on 0.1 mg/ml lysozyme, 20 mM DTT in 0.1 M

phosphate buffer, 0.1 M NaCl, pH 7 that was exposed to pulsed 2.450 GHz. In this particular experiment, the ratio exposed/control (initial rate of precipitation) was 1.19.



**Figure 7.23:** 0.1 mg/ml Lysozyme, 20mM DTT in 0.1 M phosphate buffer, 0.1 M NaCl, pH 7 exposed to 15 pulse periods of 2.450 GHz at 30°C in the presence of various ratios of  $\alpha$ -crystallin. The SAR (measured at the base of the cuvette) was  $22.8 \pm 8$  W/kg.



**Figure 7.24:** The light scattering measurements for samples incubated with  $\alpha$ -crystallin (Figure 7.23) was continued until 16 hours after the start of the experiment. Exposure was terminated after 93 minutes.

The extent of precipitation of the exposed sample was enhanced compared to the control.  $\alpha$ -Crystallin at the molar ratios 1:2 (lysozyme: $\alpha$ -crystallin) and 1:4, partially suppressed the

precipitation of lysozyme, with the ratio 1:4 being the most effective (Figures 7.25 and 7.26). At the ratio 1:2 the exposed precipitated more than the control.

Statistical analysis on six experiments performed in *Exposure system 2* with reduced lysozyme, established that exposure significantly enhanced protein precipitation ( $0.025 < P < 0.05$ ).

## 7.8 OVOTRANSFERRIN

### 7.8.1 REDUCED OVOTRANSFERRIN

To study the effect of small temperature differences between cells in the incubator (see section 3.1.2), four samples of 0.2 mg/ml ovotransferrin, 20mM DTT in 0.1 M phosphate buffer, 0.1 M NaCl, pH 7.2 were incubated at 45°C in the multi-cell holder of the spectrophotometer (Figure 7.25). The initial rate of precipitation of the four samples of both experiments is presented in Table 7.6. The ratio of the largest over the lowest rate was 1.76 (or 0.57 for the lowest/largest rate). The maximum rate corresponded with the highest temperature (cell 6) and the difference between the cell of lowest (cell 3) and highest temperature was 0.7°C.

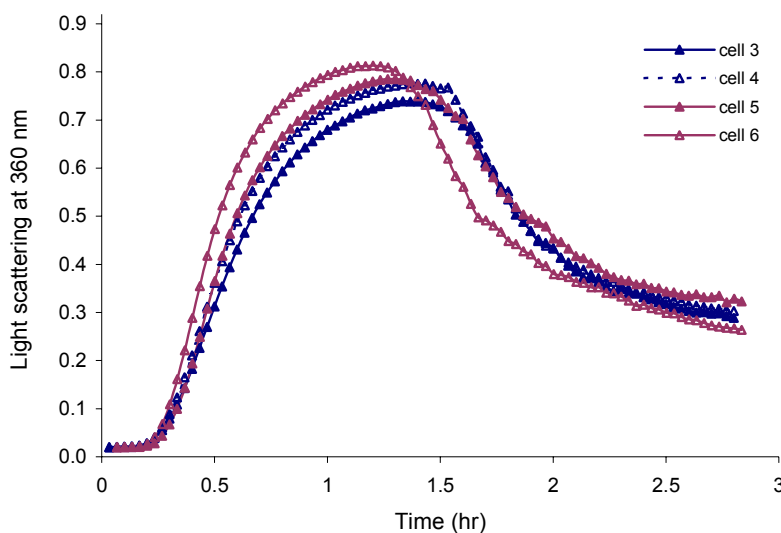


Figure 7.25: Incubation of four 1.0 ml samples of 0.2mg/ml ovotransferrin, 20 mM DTT in 0.1 M phosphate buffer, 0.1 M NaCl, pH 7.2 at 45°C. The samples were placed in cells 3 to 6 in the multi-cell holder of the spectrophotometer.

When the initial rates of precipitation in Table 7.6 were plotted against the temperature of the samples in the four cells, the data were fitted to a straight line ( $R^2 = 0.90$ , Figure 7.26).

Therefore, the initial rate was considered to be dependent on small temperature variations.

Cell	Initial rate of ppt $A_{360}\text{hr}^{-1}$	Temperature ( $^{\circ}\text{C}$ ) at 13.5 mm from base of cuvette
3	1.10	$44.51 \pm 0.25$
4	1.30	$44.87 \pm 0.21$
5	1.57	$44.93 \pm 0.24$
6	1.94	$45.20 \pm 0.17$

**Table 7.6: Initial rate of precipitation of 0.2 mg/ml reduced ovotransferrin at  $45^{\circ}\text{C}$  in cells 3, 4, 5 and 6 of the spectrophotometer.**

Of seven exposure experiments performed under similar conditions on 0.2 mg/ml reduced ovotransferrin, only one ratio exposed/control (initial rate of precipitation) was  $< 1$ . The controls were mostly  $\sim 0.5^{\circ}\text{C}$  cooler than the exposed, measured over a six minute average. In two experiments (not shown) however when the temperature was identical for exposed and control, the ratio exposed/control was  $> 1$ .

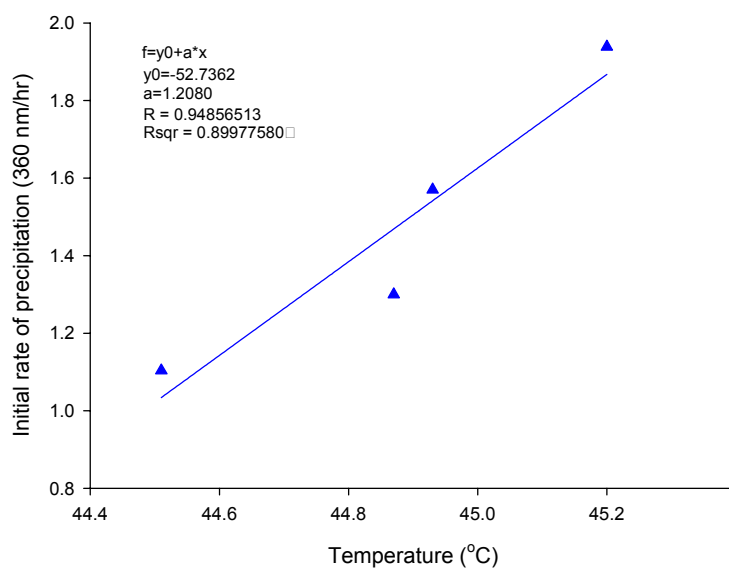


**Figure 7.26: The initial rate of precipitation ( $A_{360}\text{hr}^{-1}$ ) of four samples of 0.2 mg/ml reduced ovotransferrin in Table 7.7 plotted against the temperature of the samples.**

In Figure 7.27 are presented three sets of samples of reduced 0.2 mg/ml ovotransferrin exposed to pulsed 2.450 GHz at 45, 50 and 60°C.

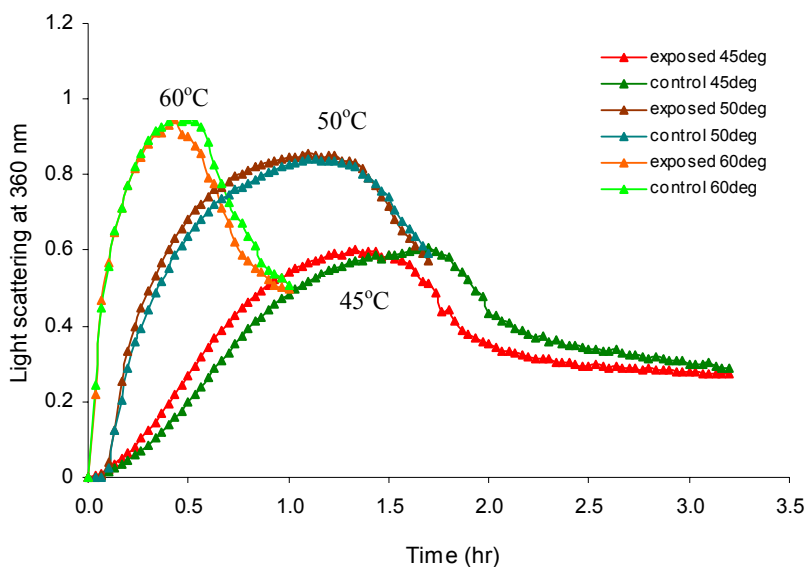


**Figure 7.27:** 0.2 mg/ml ovotransferrin, 20 mM DTT in 0.1 M phosphate buffer, 0.1 M NaCl, pH 7.2 exposed to 15 (45°C), 6 (50°C) and 5 (60°C) pulse periods of 2.450 GHz. The SAR was 33.22 W/kg (measured at the position of the light beam).

Experiment	Initial rate of ppt. $A_{360} \text{hr}^{-1}$	Ratio exposed/control (initial rate of ppt.)	Average temperature over 6 minutes (°C)
Exposed 45°C	0.43		45.4
Control 45°C	0.31	1.37	44.9
Exposed 50°C	3.05		N.D.
Control 50°C	2.59	1.18	N.D.
Exposed 60°C	2.05		N.D.
Control 60°C	2.13	0.96	N.D.

**Table 7.7:** Initial rate of precipitation and average temperatures of experiments in Figure 7.27. The average temperature for the 50 and 60°C experiments was not determined (N.D.)

The temperature profiles were not calculated for the 50 and 60°C exposure, however the exposed samples were placed in the cell that was on average warmer than the cell of the control samples (see section 3.1.2). Table 7.7 summarises the initial rate of precipitation for the experiments in Figure 7.27 and the ratio (initial rates) of exposed/control.

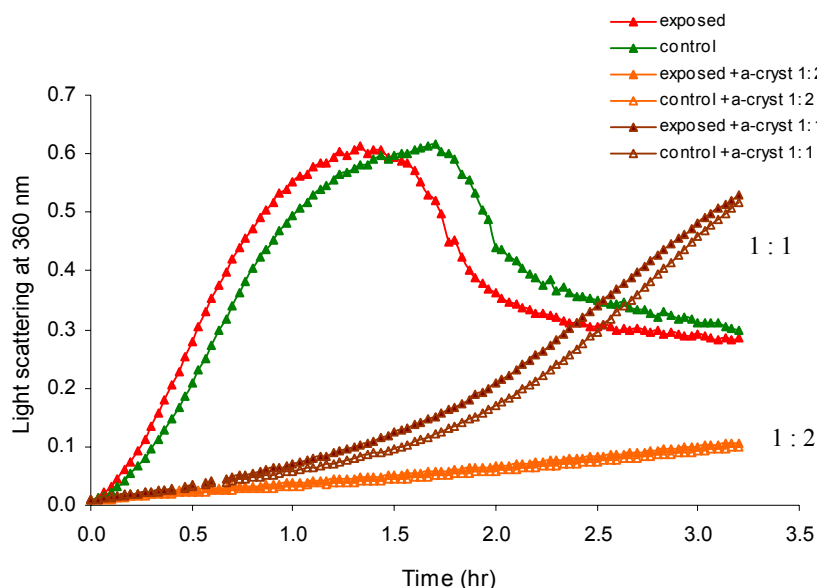


**Figure 7.28:** 0.2 mg/ml Ovotransferrin, 20mM DTT in 0.1 M phosphate buffer, 0.1 M NaCl, pH 7.2 incubated at 45°C and exposed to pulsed 2.450 GHz at six minute intervals without or in the presence of  $\alpha$ -crystallin in subunit molar ratios as indicated on the graph. The pulse periods lasted 5 seconds each; a total of 15 pulses were applied to the “exposed” samples. The estimated SAR was 33.22 W/kg at the position of the light beam.

When ovotransferrin was incubated with  $\alpha$ -crystallin and subsequently exposed to pulsed 2.450 GHz, precipitation was partially suppressed at the molar subunit ratio (ovotransferrin: $\alpha$ -crystallin), 1:1 and more so at the ratio 1:2. The exposed samples (both ratios) were not suppressed to the same extent as the control sample (see Figure 7.28).

### 7.8.2 OXIDISED OVOTRANSFERRIN

Thermal denaturation of non-reduced ovotransferrin was not observed at temperatures under 60°C. When the protein in solution was incubated at 65°C and exposed to 8 pulse periods of 2.450 GHz, the initial rate of precipitation of the exposed was greater than the controls (Figure 7.29). The ratio of exposed/control-1 and exposed/control-2 was 1.02 and 1.40 respectively. The ratio of the two controls was: control-1/control-2, 1.37. Control 1 was kept in the incubator for the duration of the experiment while control 2, like the exposed sample, was withdrawn every six minutes. Therefore, the difference between the initial rate of precipitation of the exposed and control samples was within the expected range for this experiment.



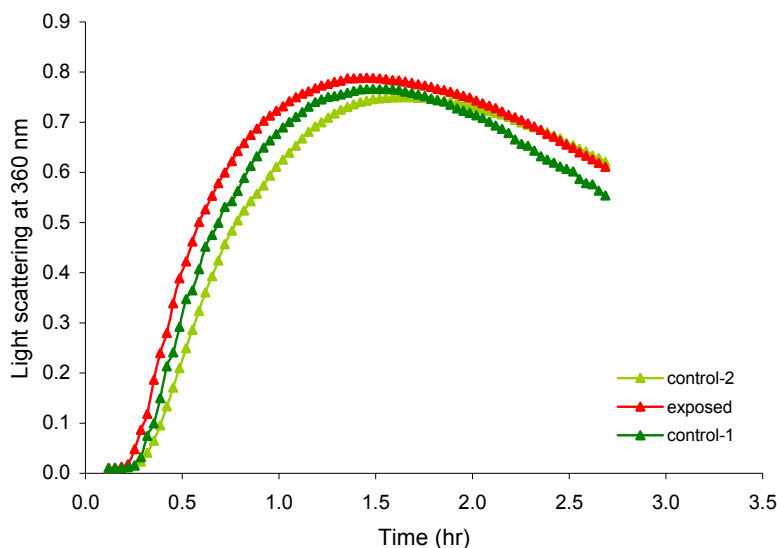


**Figure 7.29:** 0.5 mg/ml ovotransferrin in 0.1 M phosphate buffer, pH 7.2 exposed to 8 pulse periods of 2.450 GHz at 65°C. The SAR was not established for this experiment; it was estimated to be ~ 24.4 W/kg (at the position of the light beam).

## 7.9 SUMMARY AND INTERPRETATION OF RESULTS

A summary of the experimental results of the microwave exposure experiments in *Exposure system 2* is provided in Table 7.8. In general, microwaves did not have an effect on the initial rate of precipitation of a protein unless the protein was already stressed. Proteins were stressed by temperature (catalase, citrate synthase), reduction of S-S bonds (BSA, ovotransferrin) or by chelation of an intrinsic metal ion (ADH ). Enhancement of the initial rate of precipitation was not observed when the temperature was not favourable for unfolding as was seen for CS at 37°C (where microwaves had no significant effect on initial rate of precipitation) versus CS at 42°C (where microwaves enhanced the initial rate of precipitation) or when the temperature was too high so that the microwave exposure could not contribute to the rate of the rapidly unfolding protein (e.g. in assays of reduced insulin and ovotransferrin at 60°C).

The sHsp  $\alpha$ -crystallin suppressed the precipitation of proteins at specific subunit molar ratios however at certain ratios, depending on the protein and experimental conditions, more  $\alpha$ -

crystallin was needed to suppress the microwave exposed protein compared to the control to achieve the same suppression.

Protein	Temp.(°C)	Additional stress	Effect of microwaves on light scattering on initial rate of ppt.	Effect of $\alpha$ -crystallin on light scattering: 1. Did exposed sample require more $\alpha$ -crystallin for suppression of ppt ? 2. Was ppt suppressed at specific subunit molar ratios ?	Was the effect of microwave on initial rate of ppt. significant ?
Apo ADH 0.5 mg/ml	37	Chelation of $Zn^{2+}$	enhanced	1. yes, 2. yes	yes
Holo ADH 0.5 mg/ml	45, 60		not enhanced	not undertaken	not tested
BSA 1.5 mg/ml	45	reduced	enhanced	1. yes, 2. yes	no
50 mg/ml	37	reduced	enhanced: gel	not undertaken	not tested
BSA 45 mg/ml	50, 60		not enhanced	not undertaken	not tested
Catalase 0.2 mg/ml	42		not enhanced	1. yes, 2. yes	yes
CS 0.2 mg/ml	37		inconclusive	1. no, 2. yes	no
0.2 mg/ml	42		enhanced	1. yes, 2. yes	yes
Insulin 0.25 mg/ml	19, 25	reduced	enhanced	1. no, 2. yes	no
Apo $\alpha$ -Lactalbumin 2 mg/ml	36	reduction and chelation of $Ca^{2+}$ as above	not enhanced	not undertaken	not tested
0.5 mg/ml	RT		not enhanced	not undertaken	not tested
Holo $\alpha$ -Lactalbumin 0.5 mg/ml	32	reduced	not enhanced	not undertaken	not tested
Lysozyme 0.1 mg/ml	30	reduced	enhanced	1. yes, 2. yes	yes
Ovotransferrin 0.2 mg/ml	45, 50 60	reduced reduced	enhanced not enhanced	45°C: 1. yes, 2. yes 50, 60°C not undertaken	45°C: yes not tested
Ovotransferrin 0.5 mg/ml	65		enhanced	not undertaken	not tested

**Table 7.8: Summary of light scattering experiments on selected proteins in tandem with microwave exposure in *Exposure system 2*. The statistical analysis of the ratio of the initial rate of precipitation (exposed/control) is discussed in section 7.10. The experimental details for the individual protein assays are described in the text. Ppt is precipitate and RT is room temperature.**

### 7.9.1 THE EFFECT OF PULSED MICROWAVES ON TEMPERATURE

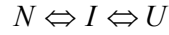
In Chapter 3 it was established that pulsed microwaves of 3.2 or 5.0 seconds, applied every six minutes, caused a transient temperature jump of 2.1°C (to a solution of CS) to 5°C (to a solution of BSA) under exposure/buffer conditions summarised in Table 3.1.

A relationship was established between conductivity of the buffer and the temperature incursion (and hence the SAR). The transient temperature increase lasted less than a second, the smallest unit of measurement, and fell back to the baseline temperature within six minutes before the next pulse period (Figure 3.13 and 3.14). In this respect, the thermal nature of microwaves can be understood as a temperature jump. “Temperature jump” is a widely used rapid kinetics technique applied in the study of protein folding and unfolding<sup>184-186</sup>. A short pulse of current at high voltage, a laser beam or a burst of microwaves induces a temperature rise of a few degrees within a few microseconds. The sudden temperature incursion shifts the “folding-unfolding” equilibrium (Figure 1.4) to an increase in intermediately folded states until the protein sample has reached a new equilibrium value.

Samples in *Exposure system 2* reached temperature equilibrium in approximately 5 minutes (see figure 3.2). This resulted in faster initial precipitation rates and also a greater extent of precipitation than assays exposed in *Exposure system 1*. For example, ADH started to precipitate at 0.5 hours (compared to 1 hour in *Exposure system 1*), the extent of which was at least three fold compared to controls (see figures 5.1 and 7.2). CS at 37°C precipitated immediately in both systems but the extent of precipitation was at least four fold compared to *Exposure system 2* (Figures 5.6 and 7.14).

Thus, it can be concluded that the rate of aggregation and therefore the proportion of intermediately folded proteins is dependent on the method of temperature delivery. If it is fast (*Exposure system 2*), aggregation will be faster and more aggregation and precipitation occurs. This can be explained in terms of the Gibbs free energy changes ( $\Delta G$ )<sup>187</sup>. In solution, proteins

are in equilibrium between the native folded, the intermediately folded and the unfolded conformations (Figures 1.3 and 1.4).



$$K_{unf} = K[I]/[N] + K[U]/[I]$$

(where K is the equilibrium constant)

The stability of the protein in the native state is dependent on the free energy ( $\Delta G$ ) which is related to enthalpy ( $\Delta H$ ) that is a measure of hydrophobic interactions and hydrogen bonding and entropy ( $\Delta S$ ) that comprises conformational freedom and solvation:

$$\Delta G_{unf} = \Delta H_{unf} - T\Delta S_{unf}$$

$$\Delta G_{unf} = -RT \ln K_{unf}$$

(where T is the temperature in Kelvin and R is the ideal gas constant)

With increasing temperature (T), weak electric forces and hydrogen bonding will be disrupted leading to a change in enthalpy initially and as the temperature climbs,  $T\Delta S$  increases, resulting in a negative  $\Delta G$ . The equilibrium will now shift from the folded state to the unfolded state. This can be demonstrated from experiments on for example the proteins ADH and citrate synthase. When solutions of ADH and CS were heated rapidly regardless if microwaves were applied the extent of precipitation increased compared to slower heating (*Exposure system 11* vs. *Exposure system 2*).

Protein unfolding is a cooperative process which means that when one region of a protein starts to unfold, the unravelling of the whole proteins follows<sup>187</sup> possibly in the order of micro seconds<sup>173</sup>. The results presented in this chapter show that proteins which were already on the protein unfolding pathway, unfolded and aggregated faster and to a greater extent when they also experienced a transient increase in temperature by way of pulsed microwaves in *Exposure system 2*. Thus, the equilibrium between protein conformations can be altered by transient temperature jumps such as delivered by pulsed microwaves.

The average temperature of exposed and control samples was determined over a six minute period and, in general, the exposed samples were warmer than the controls; ranging from 0.3°C (CS at 42°C) to 0.7°C (ADH, BSA). However, this may have only had an effect on the results in the case of ovotransferrin as this protein was found to be sensitive to temperature differences (Table 7.7).

## 7.10 STATISTICAL ANALYSIS OF RESULTS AND TESTING OF HYPOTHESES

In order to demonstrate that the results obtained from light scattering experiments in tandem with microwave exposure in *Exposure system 2* were significant, the ratio of the initial rate of precipitation of the exposed over the control samples was analysed statistically.

The initial rate of precipitation was calculated (see also section 2.6.1.1) for samples of experiments that were carried out at least in triplicate under similar conditions. The protein  $\alpha$ -lactalbumin was not tested as it proved difficult to obtain consistent light scattering profiles.

The one tailed  $t$  test was applied to the data to test for the hypothesis:

$H_0: \mu \leq 1$  (null hypothesis, stating that for a 5% confidence limit, 95% of all exposed samples have the same or a lower precipitation rate than a control sample)

and

$H_A: \mu > 1$  (alternative hypothesis, stating that for a 5% confidence limit, 95% of all exposed samples have a larger precipitation rate than a control sample).

The null hypothesis is rejected if the calculated  $t$  value is larger than  $t_{0.05}$ .

	Apo ADH	Reduced BSA	Reduced insulin	Reduced lysozyme	Reduced ovotransferrin
n	12	5	6	5	4
$\sum X_i$	18.27	5.29	5.90	7.06	4.55
$\sum X_i^2$	29.64	5.83	6.02	10.72	5.18
$\bar{X}$	1.52	1.06	0.98	1.41	1.14
SS	1.82	0.24	0.23	0.74	0.01
$s^2$	0.17	0.06	0.05	0.18	0.004
s	0.41	0.24	0.21	0.43	0.06
$s(\bar{x})$	0.12	0.11	0.09	0.19	0.03
t	4.33	0.53	-0.20	2.15	4.88
$t_{0.05(1),v}$	1.812	2.132	2.015	2.132	2.353
$H_0$	Reject	Accept	Accept	Reject	Reject
P	0.0005<P P<0.001	P>0.25	P>0.25	0.025<P P<0.05	0.005<P P<0.01

**Table 7.9: One-tailed t test for the hypothesis  $H_0: \mu \leq 1$  and  $H_A: \mu > 1$  for light scattering experiments on chemically stressed proteins that were also exposed to pulsed microwaves. One sample was exposed to pulsed microwaves and another sample was kept as a control.**

Symbols: n is number of experiments;  $\sum X_i$  is the sum of data;  $\sum X_i^2$  is the sum of squared values;  $\bar{X}$  is mean of data; SS is sum of squares of the deviations from the mean;  $s^2$  is the sample variance; s is the standard deviation;  $s(\bar{x})$  is the sample variance of the mean; t is the value of the t distribution; P is the probability.

	catalase	CS-37°C	CS-42°C
n	6	6	6
$\sum X_i$	9.16	6.59	8.03
$\sum X_i^2$	14.53	7.66	11.03
$\bar{X}$	1.53	1.10	1.34
SS	0.54	0.43	0.29
$s^2$	0.11	0.09	0.06
s	0.33	0.29	0.24
s(x)	0.13	0.12	0.10
t	3.93	0.82	3.45
t,0.05(1),v	2.016	2.015	2.015
H <sub>0</sub>	Reject	Accept	Reject
P	0.005<P P<0.01	0.10<P P<0.25	0.005<P P<0.01

**Table 7.10: One-tailed *t* test for the hypothesis H<sub>0</sub>:  $\mu \leq 1$  and H<sub>A</sub>:  $\mu > 1$  for light scattering experiments on thermally stressed proteins that were also exposed to pulsed microwaves. One sample was exposed to pulsed microwaves and another sample was kept as a control. Symbols are defined in Table 7.10.**

The results of the statistical analysis (Tables 7.9 and 7.10) show that the null hypothesis was rejected for five proteins: apo ADH, lysozyme, ovotransferrin, catalase and CS, (42°C), at the conditions reported earlier. In other words, there is a probability of less than 5% that from a pool of experiments, the ratio of the initial rate of precipitation of the exposed over the control is smaller or equal to one. The null hypothesis was accepted for the proteins BSA, insulin and CS (37°C) under the conditions reported in this chapter. Therefore the pulsed microwaves did not have a significant effect on the initial rate of precipitation for these three proteins under the specific conditions. These findings will be discussed in the light of current knowledge about unfolding of these proteins.

Table 7.11 is a summary of the experiments that were analysed statistically.

Experiment	Buffer/exposure system	T (°C)	Duration of pulses (sec)	Number of pulse periods	Start of ppt.(min)	$\Delta T$ (°C) position	SAR (W/kg) position	light beam	t-test	Average temp. over 6 minutes Exp. Contr.
<b>Apo ADH</b> 0.5 mg/ml 1mM 1,10-phenanthroline	III	37	5.0	10	2.4	2.9	33.2		P<0.0005 n=11	37.6 36.9
<b>Reduced BSA</b> 1.5 mg/ml 20mM DTT	IV	45	5.0	10	Imm.	5.0	58.2		P>0.25 n=5	45.3 44.6
<b>Catalase</b> 0.2 mg/ml	II	42	5.0	20	3.6	3.7	42.7		0.005<P<0.01 n=6	42.36 41.7
<b>CS</b> 0.2 mg/ml	I	37	3.2	6	Imm.	2.1	24.4		0.10<P<0.25 n=6	37.5 36.9
CS 0.2 mg/ml	I	42	3.2	6	Imm..	2.1	24.4		0.005<P<0.01 n=6	42.0 41.7
<b>Reduced insulin</b> 0.25 mg/ml 20 mM DTT		19- 37	3.2 or 5.0	10-15	4.2	2.1 or 2.9	24.2 or 33.2		0.05<P<0.10 n=10	n.a.
<b>Reduced lysozyme</b> 0.1 mg/ml 20 mM DTT		30	5.0	2-15	9	2.0	22.8		0.025<P<0.05 n=6	n.a.
<b>Ovotransferrin</b> 0.2 mg/ml 20mM DTT	III	45	5.0	15	1.8	2.9	33.2		0.005<P<0.01 n=4	45.4 44.9

**Table 7.11: Summary of microwave experiments in *Exposure system 2* that were statistically analysed.**  $\Delta T$  refers to the average temperature change of the sample after a pulse period, calculated at the position where the light beam of the UV-Vis spectrophotometer passes through. The average temperature of the exposed and control samples, over a six minute period, relates to the average of at least three experiments. Ppt: precipitation; imm.: immediately; exp.: exposed, contr.: control, n.a.: not available. The t-test for insulin was taken over a series of experiments at temperatures of 19, 25 and 37°C.

### 7.10.1 ANALYSIS OF REDUCED BSA (1.5 mg/ml)

In Figure 7.7, reduced BSA exposed to pulsed microwaves at 45°C precipitated faster than the control sample; the ratio of the initial rate of the exposed sample over the control sample was larger than 1. However when pooling the results of four similar experiments on BSA, the statistical test rejected the significance of a ratio of initial rates greater than 1.

BSA is intrinsically a stable protein, e.g. in its fully oxidised native state its structure is stable to 80°C<sup>142</sup>. The unfolding of a protein can be followed by monitoring the ellipticity at 224 nm



which is a measure of the  $\alpha$ -helicity in a protein as a function of temperature in steps of one or more degrees <sup>188</sup>. At 30°C the structure of BSA is in the folded form. The full CD spectrum shows a negative dip in the spectrum at 224 nm <sup>189</sup>. The slope of unfolding (ellipticity vs temperature) of oxidised BSA (Figure 7.30 A) is gradual up to ~ 60 °C after which the slope increases at a faster rate per °C. This indicates that oxidised BSA is relatively stable up to about 60°C after which  $\alpha$ -helix structure is being lost at a fast rate.

**Figure 7.30: Thermal unfolding of oxidised BSA (A) and reduced BSA (B) as determined by ellipticity at 224 nm as a function of temperature (Figure A adapted from Arakawa and Kita <sup>142</sup>). The concentration in A was 1.2 mg/ml in 20 mM Tris, pH 7.2 and in B was 0.07 mg/ml in 10mM phosphate buffer, pH 7.0, 0.7mM DTT.**

When BSA is reduced, the same pattern is observed (Figure 7.30 B) which demonstrates that the protein is relatively stable until about 70°C. To quantify these observations, the slopes were calculated from the graphs and they are summarised in Table 7.12.

Between 40 and 50°C, according to Table 7.11 the slope of change in  $\alpha$ -helicity was 0.9 ( $[\theta] \times 10^{-3}/^{\circ}\text{C}$ ). This increased to 1.6 ( $[\theta] \times 10^{-3}/^{\circ}\text{C}$ ) for temperatures between 50-60°C, suggesting that temperature excursion between 50 and 60°C would have more effect on  $\alpha$ -helicity than between 40 and 50°C. Indeed, when reduced BSA (1.5 mg/ml) was heated to 45°C and exposed to microwaves that caused the samples to experience a 5°C transient temperature

increase, every six minutes (section 7.2.1), the initial rate of precipitation, was considered equal to or lower than the control sample (Table 7.9). In other words, the transient temperature incursion had no effect on the unfolding of the protein.

Temperature (°C)	BSA oxidised slope ( $[\theta] \times 10^{-3}/^{\circ}\text{C}$ )	BSA reduced slope ( $[\theta] \times 10^{-3}/^{\circ}\text{C}$ )
40-50	0.9	0.5
50-60	1.6	1.5
60-70	3.0	3.2

**Table 7.12: Slope of temperatures between 40 and 70 °C calculated from the graphs in Figure 7.34.**

If the protein had been exposed to a higher dose of pulsed microwaves, it would be expected that the protein would unfold more rapid than a control sample. For temperatures over 60°C, when the slope increases three fold compared to the 40-50°C region, temperature excursions of much less than 5°C are expected to have a significant effect on the unfolding rate of reduced BSA.

#### 7.10.2 ANALYSIS OF CS AT 37°C COMPARED TO CS AT 42°C

From thermal denaturing studies<sup>190</sup> it can be shown that CS is stable between 20 and ~ 40°C which corresponds to optimum enzyme activity. The change in ellipticity at 222 nm is a measure of  $\alpha$ -helicity. Above this temperature the protein unfolds rapidly.

The slope, in  $[\theta] \times 10^{-3}$  (degree-cm<sup>2</sup>-dmol<sup>-1</sup>)/°C), was deduced from Figure 7.31 to be 0.7 for temperatures between 40 and 45°C. The activity of CS between 40 and 50°C falls from ~100% to ~60%. Therefore, the observation that a periodic temperature increase of 2.1°C to a sample maintained at 37°C has no significant impact on the rate of precipitation compared to a control sample can be understood in this context. As the slope of unfolding increases dramatically (and

$\alpha$ -helix structure is lost) after  $\sim 40^{\circ}\text{C}$ , small temperature excursions for samples maintained at  $42^{\circ}\text{C}$  would be expected to escalate unfolding.

**Figure 7.31: Reproduced from Zhi *et al*<sup>190</sup>. The thermal unfolding of 0.1 mg/ml pig heart citrate synthase. The change in ellipticity at 222 nm and the percent activity remaining were measured as a function of temperature in 5.0 mM Tris-HCl, pH 7.5. Thermal denaturation was measured in steps of  $1.5^{\circ}\text{C}$ .**

This was indeed observed for the experiments of CS at  $42^{\circ}\text{C}$ . The increase to  $44.1^{\circ}\text{C}$  lasting only a few seconds, every six minutes, resulted in a significant enhanced precipitation rate compared to the controls ( $0.005 < P < 0.01$ ).

### 7.10.3 ANALYSIS OF INSULIN (reduced)

Reduced insulin did not show a difference in the rate of precipitation between exposed and control samples. Computer simulation of the unfolding of insulin has shown that, upon reduction of the three disulphide bonds with DTT, the small B chain unfolds very rapidly, i.e. within two nanoseconds of simulation time<sup>191</sup>, prior to its aggregation and subsequent precipitation (the A chain remains in solution). Consequently, upon reduction, the unfolding of the B chain occurs too fast to respond to temperature transients of less than a few seconds duration as applied by pulsed microwaves.

## 7.11 CONTROLLING FOR SMALL DIFFERENCES IN AVERAGE TEMPERATURE BETWEEN EXPOSED AND CONTROL SAMPLES

The hypothesis tested in section 7.10 refers to exposed and control samples being kept at the same average temperature over a six-minute period. As shown in Table 7.11, there were small differences between the average temperatures for exposed and control in most cases. These small temperature differences between samples were unavoidable because of the design of the temperature-controlled multicell holder. In all cases where the control was cooler than the exposed, it was necessary to ensure that the conclusion concerning the hypothesis was not altered by the presence of these small differences. Therefore, in a separate set of experiments on CS at 42°C, ADH and catalase, four identical samples were incubated at slightly different temperatures and monitored for light scattering. One of the samples was taken out, as described previously, every six minutes, and exposed to pulsed microwaves. The average temperature over a six-minute period was calculated for each of the samples and plotted against the initial rate of precipitation.

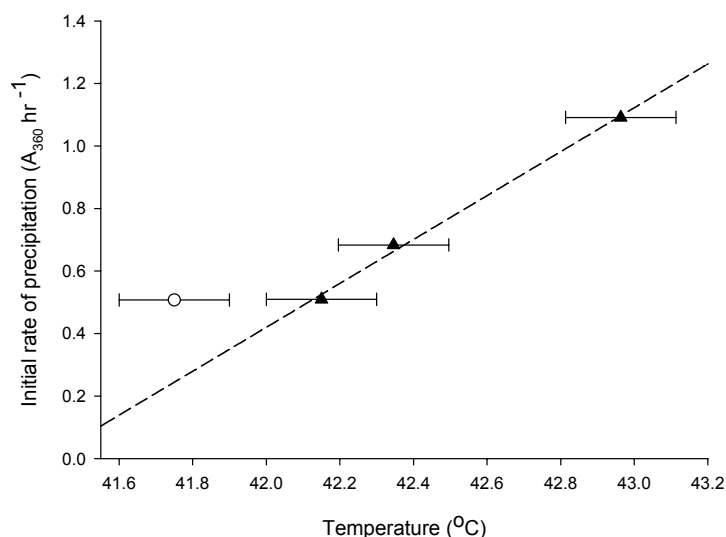


**Figure 7.32:** The initial rate of precipitation for CS at a nominal incubation temperature of 42°C is shown as a function of the actual measured temperature, averaged over six minutes as discussed in the text. The exposed point (open circle) lies above the trend line created by the controls (black triangles), showing that the hypothesis is sustained.

Figure 7.32 shows such a plot for CS. In these experiments, the exposed sample was cooler than the control samples over the six-minute averaging time yet its point on the plot lies above the trend line created by the controls, i.e. its initial rate of precipitation is faster than that expected if it were simply exposed to a constant temperature of 41.8°C. Thus these data are consistent with the hypothesis.

In order to allow for the effects of small differences between the average temperatures of the exposed and control samples, the dependence of the precipitation rate ratio on temperature for CS at 42°C was examined in detail. The difference in initial rate per 1°C was calculated from the trend line in Figure 7.32. As a result, when the t-test was applied, the probability was increased by 10% to a confidence limit of  $0.0005 < P < 0.001$ .

## 7.12 DIFFUSION OF PROTEIN MOLECULES DURING EXPERIMENTS

One of the drawbacks in utilising light scattering for the visualisation of protein precipitation is that the detector of the spectrophotometer only samples part of the assay. When pulsed microwaves are applied to a sample, the energy is unevenly distributed (section 3.2.2) and the question arises: are the protein molecules that were detected in the light scattering experiment the same as the molecules that were exposed (and for which the SAR was calculated at the height of the detector (section 3.2.2) ? In other words, is it possible that protein molecules diffused through the sample so that the measurements were not representative?

In order to establish how fast molecules moved through the solution, the diffusion of the target proteins was calculated (see also section 2.6.1.2).

### 7.12.1 CALCULATION OF TRANSLATIONAL MOVEMENT

The diffusion constant <sup>1</sup>,  $D$ , for different temperatures and buffer compositions can be derived from the Stokes-Einstein equation:

$$D = K_B.T / f \quad (1)$$

where  $K_B$  is the Boltzmann's constant,  $f$  the frictional coefficient and  $T$  the absolute temperature.

Fick's second law relates  $D$  to the mean-squared distance travelled,  $\overline{x^2}$ , per unit time,  $t$

$$D = \overline{x^2} / 2t \quad (2)$$

$$i.e. \quad \overline{x^2} = (K_B / f).T.2t \quad (3)$$

The frictional coefficient,  $f$ , can be determined if the viscosity of the solution,  $\eta$ , and the hydrodynamic radius,  $r$ , of the protein are known:

$$f = 6 \pi \eta r \quad (4)$$

Thus, the mean distance (in mm), travelled per minute by one molecule of protein is given by:

$$\overline{x} = \sqrt{(K_B.T.t)/(3 \pi.\eta.r)} \quad (5)$$

The program HYDROPRO<sup>167</sup> was used to calculate,  $r$ , for each target protein. The viscosity data for solutions were obtained from<sup>192</sup>.

By using equation 5, the translational movement arising from diffusion for each protein was calculated at the experimental temperature (Table 7.12).

Because the experimental protein solutions were not stirred, the temperature was not uniform in the sample. The temperature distribution in the samples was described in detail in Chapter 3. The SAR corresponding with the region in the sample that was sampled for light scattering (height between 13 and 19 mm from the base of the cuvette) was derived from SAR determinations at four positions in the sample (see Figure 3.7).

Some mixing between regions of higher and lower SAR occurred but as the precipitation increased, and the aggregates increased in size, the diffusion of the large aggregates slowed down. Therefore, the SAR (Table 11) should be used as an estimate only.

Protein	PDB file	Radius ( $10^{-7}$ cm)	$\bar{x}$ (mm/min)
ADH	1ykf	4.45	0.71
BSA	1e78	5.12	0.72
Catalase	4blc	4.98	0.71
CS	4cts	3.81	0.82
Insulin	2ins	1.88	1.09
Ovotransferrin	1ovt	3.72	0.84

**Table 7.13: Calculated hydrodynamic radius of proteins.** The hydrodynamic radii for target proteins was calculated using the HYDROPRO program and the mean distance travelled (in mm) per minute ( $\bar{x}$ ) was calculated, using equation 5.

---

## CHAPTER 8

---

### LIGHT SCATTERING EXPERIMENTS

#### MICROWAVE EXPOSURE IN *EXPOSURE SYSTEM 3*

##### 8.1 CONSTANT TEMPERATURE VS PERIODIC TEMPERATURE EXCURSIONS

To establish if the initial rate of precipitation of a sample exposed to pulsed microwaves was similar to a sample incubated at a constant temperature, experiments were undertaken in which four protein samples were incubated at different temperatures utilising the temperature variability of the cells in the heating block (see section 3.1.3).

###### 8.1.1 REDUCED APO ALCOHOL DEHYDROGENASE (ADH)

Four 1.0 ml samples of 0.5 mg/ml ADH were incubated at different temperatures. One of the samples was also exposed to 7 pulse periods of 2.450 GHz at six minute intervals (the pulses were of 5 seconds duration). The SAR for the exposed sample was 26.8 W/kg (measured at the position of the light beam) which equated to a transient temperature maximum of 2.3 °C every six minutes. The results of one such experiment are plotted in Figure 8.1. The averaged temperatures (see section 3.3.3) for the controls 1, 2 and 3, over six minutes, were 45.2, 45.9 and 46.5°C respectively. The average temperature for the exposed sample was 44.9°C.

The baseline temperature for the exposed cell (average of measurements at 10 and 17 mm from the base of the cuvette) was 44.5°C. The expected initial rate of precipitation at a temperature of 46.8°C ( $44.5 + 2.3^{\circ}\text{C}$ ) was calculated from the slope of Figure 8.2 to give an initial rate of 0.71 ( $A_{360} \text{ h}^{-1}$ ). The initial rate for the exposed sample was 0.60 ( $A_{360} \text{ h}^{-1}$ ).



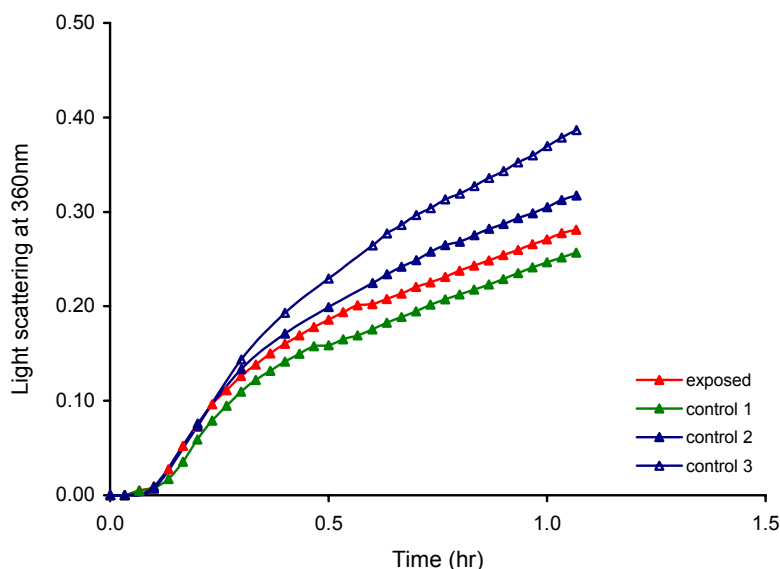


**Figure 8.1:** The effect of constant temperature compared to a transient microwave induced temperature increase every six minutes on the aggregation and precipitation of 0.5 mg/ml ADH in 1 mM phenanthroline in 0.1 M phosphate buffer, 0.1 M NaCl, pH 7, at 45°C. Samples were incubated in the multi-cell block of the spectrophotometer for 2 minutes. The temperature was averaged over a six minute period as discussed in section 3.3.3. Control 1 was kept in the multi-cell holder of the spectrophotometer (cell 6) and controls 2 and 3 were kept in the block heater. They were removed at six minute intervals for spectroscopy. After 7 pulse periods all samples were left in the spectrophotometer.

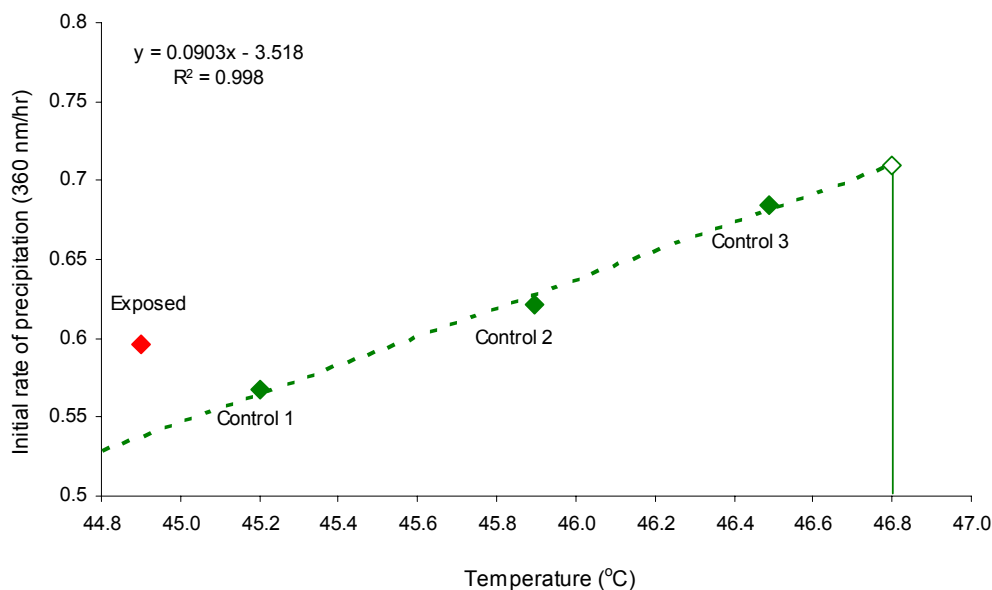


**Figure 8.2:** The effect of temperature on the initial rate of precipitation for the four 1.0 ml samples of 0.5 mg/ml ADH in 1 mM phenanthroline in 0.1 M phosphate buffer, 0.1 M NaCl, pH 7, at 45°C incubated in either the spectrophotometer or the heating block (See also Figure 8.1). The rate of precipitation of the exposed lies above the trendline of samples incubated at a constant temperature. The expected initial rate of precipitation for a temperature of 46.8°C was 0.71 ( $A_{360}hr^{-1}$ ) (green line).

Therefore, the initial rate of precipitation of a 0.5 mg/ml sample of reduced apo ADH, incubated at a temperature of 44.5°C that transiently increased to 46.8°C for less than a few seconds, every 6 minutes, was 16% lower than a 0.5 mg/ml ADH sample incubated at a steady temperature of 46.8°C. The experiment was repeated three times with very similar results.

### 8.1.2 CITRATE SYNTHASE (CS)

SAR calibrations established that for buffer/exposure system I, exposure to pulsed 2.450 GHz led to a transient temperature increase of 1.0 to 3.1°C (Figure 3.7), every six minutes (measured between 0 and 23 mm from the base of the cuvette).

To establish if the initial rate of precipitation of an exposed sample under the conditions described above was similar to a sample incubated at a constant temperature of 42°C plus the increment determined by the pulse. An increment of 2.1°C or 24.38 W/kg (between 10 and 17 mm from the base of the cuvette) was chosen.

In Figure 8.3 are plotted the results of one such experiment where controls 1, 2 and 3 were incubated at averaged temperatures (over six minutes) of 42.0, 42.8 and 43.4°C respectively. The average temperature of the exposed sample was calculated to be 41.9°C.

The baseline temperature for the exposed cell (average of measurements at 10 and 17 mm from the base of the cuvette) was 41.8°C. The expected initial rate of precipitation at a temperature of 43.9°C ( $41.8 + 2.1^{\circ}\text{C}$ ) was calculated from the slope of Figure 8.4 to give  $0.79 \text{ A360hr}^{-1}$ . The initial rate for the exposed sample was  $0.62 \text{ A360hr}^{-1}$ . The initial rate of precipitation of a 0.2 mg/ml CS sample, incubated at a temperature of 41.8°C that transiently increased to 43.9°C for less than a few seconds, every 6 minutes was 27% lower than a 0.2 mg/ml CS sample incubated at a steady temperature of 43.9°C. The experiment was repeated three times with similar results.

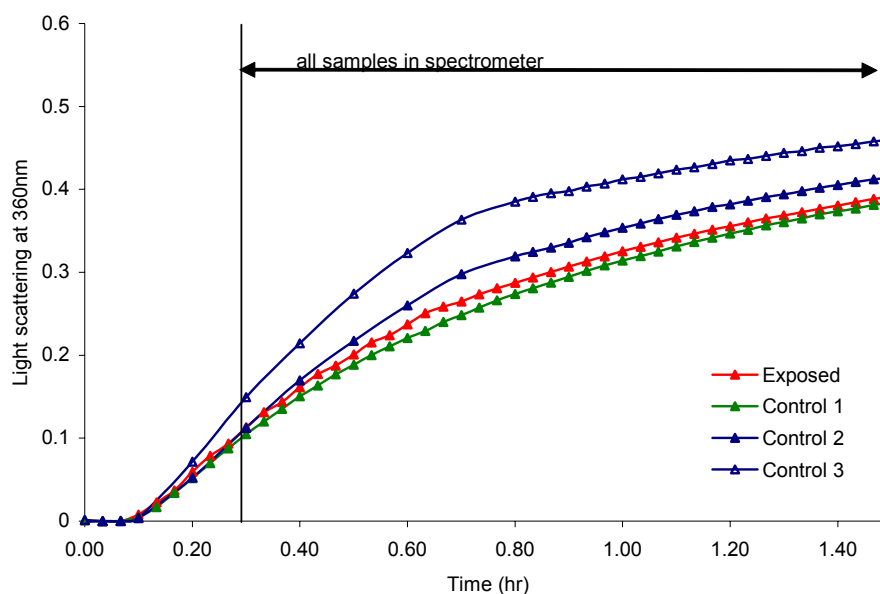


**Figure 8.3:** The effect of constant temperature compared to transient temperature increases every six minutes, on the aggregation and precipitation of 0.2 mg/ml CS. Samples were incubated in the multi-cell block of the spectrophotometer for 6 minutes thereby ensuring that all samples reached their baseline temperature at the same time. The temperature was averaged over a six minute period as discussed in section 3.3.3. The control (1) was kept in the multi-cell holder of the spectrophotometer as opposed to experiments where the control was taken out each time every six minutes similar to the exposed sample. Controls 2 and 3 relate to cells 1 and 3 in the heating block, they were removed initially every six minutes for light scattering measurements. The associated temperature loss is reflected in the average temperature over six minutes. After 7 pulse periods all samples were left in the spectrophotometer.

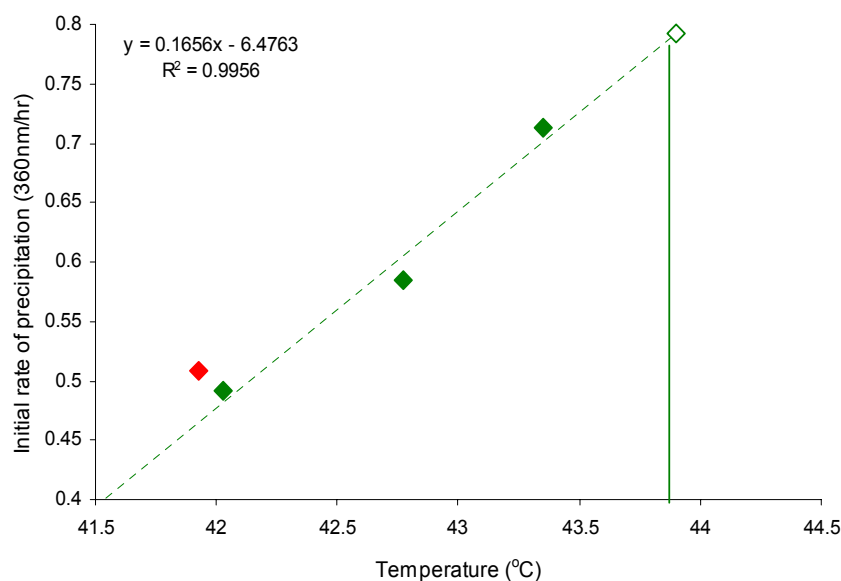


**Figure 8.4:** The effect of temperature on the initial rate of precipitation for the four 1.0 ml samples of 0.2 mg/ml CS incubated in either the spectrophotometer or the heating block (See also Figure 8.3). Exposure caused a transient temperature increase of 2.1°C. The average temperature of the sample was 41.8 The rate of precipitation of the exposed lies above the trendline of samples incubated at a constant temperature. The expected initial rate of precipitation for a temperature of 46.8°C was 0.79 ( $A_{360}hr^{-1}$ ) (green line).

### 8.1.3 SUMMARY OF RESULTS

The results of the experiments in sections 8.1.1 and 8.1.2 indicate that when the proteins ADH and CS are heated at a constant temperature of “x”, these proteins proportionally unfold faster (green lines in Figures 8.2 and 8.4) than if they would have been exposed to pulsed microwaves that transiently, for less than one second, increased the temperature of “x” every six minutes (red triangles in Figures 8.2 and 8.4).

However, when comparing temperatures over a six minute period, the initial rate of unfolding for exposed proteins is significantly larger than control samples that have the same average temperature (red triangles lie outside the trendline in Figures 8.2 and 8.4).

---

## CHAPTER 9

---

### PROTEIN CONFORMATIONAL STUDIES

#### MICROWAVE EXPOSURE IN *EXPOSURE SYSTEMS 2 AND 3*

In the past chapters the effect of pulsed microwaves on protein unfolding and precipitation was presented in terms of kinetics. In this chapter the conformation of the proteins in solution is probed by spectroscopical methods. The secondary structure of catalase, citrate synthase and  $\alpha$ -lactalbumin was monitored during microwave experiments. The intrinsic and extrinsic fluorescence of citrate synthase was measured before and after a microwave experiment and the conformational changes of  $\alpha$ -lactalbumin, where they occurred, were established by hydrogen exchange mass spectrometry.

#### 9.1 CIRCULAR DICHROISM STUDIES

Amino acids are chiral with a left handed configuration (L-form), which rotates the plane of polarisation clockwise. Proteins are therefore optically active and their conformation can be studied by circular dichroism spectroscopy (CD). CD measures the differential absorption of the left and right circularly polarised components of plane polarised radiation<sup>193</sup>. Data are recorded in degrees of ellipticity,  $\Theta$  and converted to either molar ellipticity,  $[\Theta]$  or residue ellipticity,  $[\Theta]_{MRW}$ <sup>194</sup> (conversion calculations are given in Appendix 8).

CD measurements in the far-UV region (typically 180 nm to 240 nm) detect transitions involving the peptide chromophore and therefore give information about the overall secondary structure of the protein<sup>188</sup>. The ellipticities at 208 and 222 nm are double minima that are characteristic of  $\alpha$ -helical structure<sup>193</sup>. Unstructured regions have been reported to have ellipticity at 205 nm<sup>195</sup>. In section 7.10 the temperature melt of BSA and CS were discussed as a function of the disappearance of signal at 222 nm ( $\alpha$ -helicity) respectively. Measurements in the near-UV region (250 to 350 nm) provide information about aromatic groups in proteins, i.e.

phenylalanine, tyrosine and tryptophan <sup>193</sup>. It is therefore a method of examining tertiary structural features of proteins.

CD was considered an ideal tool to study conformational changes in proteins that were exposed to pulsed microwave radiation and to compare these with control samples. The advantage of CD spectroscopy was that only small aliquots (2 to 6 µl) are required during the course of a microwave exposure experiment. The withdrawal of such small amounts was not considered to have an effect on the SAR.

Proteins that were readily destabilised by heat, catalase and CS, were studied. As CD studies on the unfolding of  $\alpha$ -lactalbumin have been extensively reported, the conformation of this protein was investigated also. In the following sections, “exposed” refers to the microwave exposed sample, “control” to the control sample incubated at the same temperature as the “exposed” with “native” referring to the native state of the protein prior to addition of DTT and application of heat. The heating block (*Exposure system 3*) was used as the incubator for the CD experiments. The heating block relies on conductive heat transfer which takes place at a smaller rate than applies in *Exposure system 2* (section 3.1) used for light scattering experiments. It therefore took a longer time for the target proteins to reach the baseline temperature. The average of 6 CD scans at 22°C was recorded prior to, during and after the experiments.

### 9.1.1 CATALASE

Catalase was monitored by far-UV CD spectroscopy during a microwave exposure experiment. The block heater was utilised as an incubator (*Exposure system 3*). The temperature of the samples was established by placing a thermometer inside a cuvette containing 1.0 ml of water after the block heater had been equilibrated for 45 minutes. The temperature of the cell of the “exposed” sample was 43.3°C and of the “control” sample 44.0°C. Two samples containing 0.2 mg/ml catalase in 50 mM phosphate, pH 7 were incubated in the block heater for two minutes after which the “exposed” sample was exposed (Buffer/exposure system II) to a pulse period of 5 seconds duration. The SAR was measured to be 42.7 W/kg which corresponds to a

temperature elevation of 3.7°C at each pulse period. The exposure was repeated every six minutes. When the “exposed” sample was taken out for exposure, the control sample was placed in a transport box and left on the bench during exposure. For far-UV CD spectroscopy, aliquots of 1 µl were withdrawn at the start of the experiment and after 1, 3, 5 and 8 pulse periods. To this aliquot was added 1.0 ml of water after which the spectra were obtained.

The far-UV CD spectrum of the native conformation (Figure 9.1) is in accordance with a previously reported CD spectrum of catalase at pH 7 and shows characteristic  $\alpha$ -helix double minima at around 208 and 222 nm<sup>196</sup>.

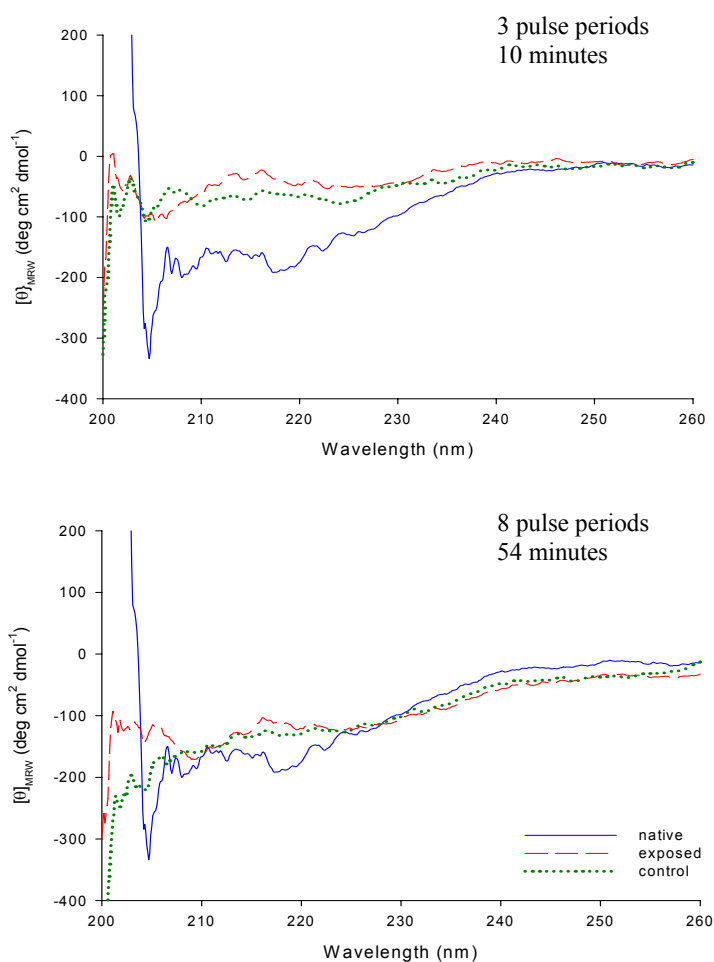


**Figure 9.1:** Far UV CD spectra of catalase at 22°C after exposure to 3 and 8 pulse periods of pulsed 2.450 GHz. The exposed sample was incubated at 43.3°C and the control sample at 44.0°C in a heating block. The SAR was 42.7 W/kg.

The structure of catalase (section 2.2.1.3) is rich in  $\alpha$ -helices in containing four identical chains that have 19 helices each. After 1 pulse period a difference with respect to ellipticity can be seen between the exposed and control sample (not shown). After three pulse periods, the exposed and control samples lost significant secondary structure compared to the native protein; this is shown by the loss of helicity at 192 nm (only the right shoulder of the peak is visible), 208 nm and at 222 nm (Figure 9.1).

After 54 minutes (8 pulse periods), not all the protein molecules have unfolded and most of the population is likely to be in intermediate folded states as can be seen from the light scattering spectrum (Figure 7.12) and comparing it to the reported CD spectrum of unfolded catalase at pH 11.5<sup>196</sup>.

### 9.1.2 CITRATE SYNTHASE (CS) AT 42°C

The far-UV CD spectrum of thermally unfolded CS has been reported (section 7.10) in the literature<sup>190; 197</sup>. The spectrum of native CS shows double minima at 210 and 222 nm which is characteristic of a protein with considerable  $\alpha$ -helical content (CS has 23  $\alpha$ -helices in its secondary structure; section 2.2.1.4)<sup>190; 197</sup>. The spectrum obtained prior to the exposure experiment was similar to the spectra reported in the literature with the exception of a broad minimum from ~220 to 228 nm compared to a reported minimum of 222 nm.

The temperature of the experimental samples was established by placing a thermometer inside a cuvette containing 1.0 ml of water after the block heater had been equilibrated for 45 minutes. Samples of 1.0 ml of 0.2 mg of CS in 80mM phosphate buffer, pH 7.5 were incubated at an temperature of 41.17°C (exposed) and 41.39°C (control) in the block heater and, every six minutes, one cuvette (exposed) was withdrawn and placed in a polystyrene transport box that was exposed to 3.2 seconds of microwave bursts (Buffer/exposure system I); the second sample (control) remained in the heater. The SAR was estimated to be ~23 W/kg (~2.0°C temperature increase) which was based on previous studies on similar concentrations. The first pulse period was delivered prior to placing the samples in the incubator.



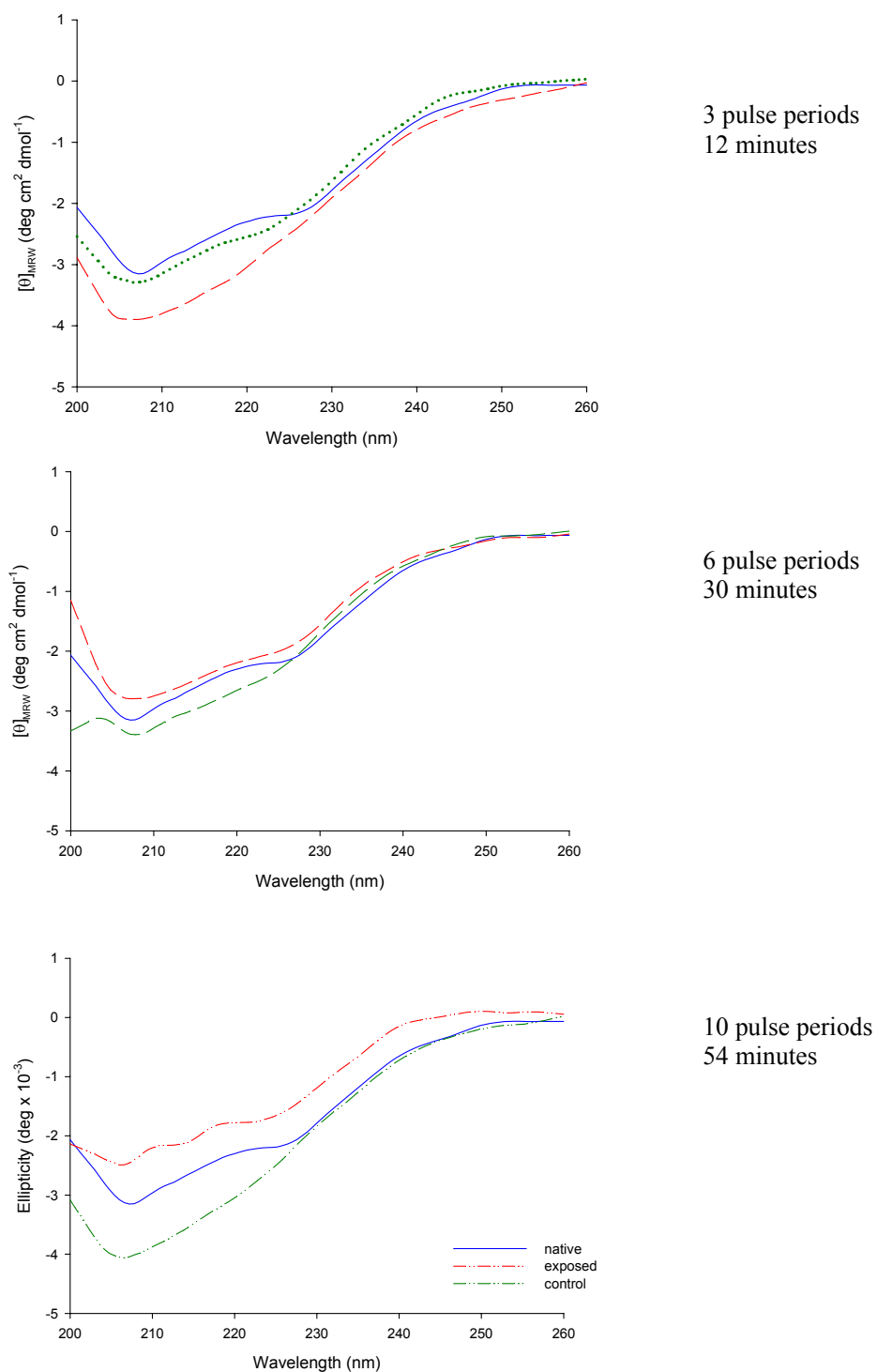


**Figure 9.2:** Far UV CD spectra of CS (smoothed) at 22°C. Sample cuvettes were inverted prior to the withdrawal of a 6  $\mu$ l aliquot. To this was added 3.0 ml of 10mM phosphate buffer, pH 7.5.

Aliquots (6  $\mu$ l) for CD experiments were taken from the middle of the solution prior to incubation as well as after 3, 6 and 10 pulse periods. The aliquots were then diluted with 3.0 ml of 10mM phosphate buffer, pH 7.5.

After three pulse periods (12 minutes into the experiment), the exposed sample showed one broad minimum at 206-208 nm while the control sample still exhibited minima at 208 and 222 nm (Figure 9.2) indicating that the protein in the exposed sample was more unfolded.

After six pulse periods, the control sample had regained ellipticity while the exposed now showed less ellipticity than before incubation. The minimum at 206 nm became broader for both samples and a broad second minimum at  $\sim$  228 nm was observed for both samples.

After ten pulse periods the exposed sample had lost a significant amount of structure as was deduced from the three minima at 206, 215 and 225 nm and reduced ellipticity. The control sample showed a similar profile and ellipticity as the exposed sample after three pulse periods, it had gained in ellipticity compared to six pulse periods. The CD spectrum still shows considerable structure as compared to a reported structure of thermally unfolded CS<sup>190</sup> (Figure 9.2).

The CD results for CS complement the light scattering experiments. The results for light scattering experiments presented in Figure 7.16 demonstrate that after one hour (i.e. after 10 pulse periods), exposed samples significantly aggregated and precipitated more than controls. Notwithstanding the slower rate of heat delivery in the heating block compared to the incubator used for light scattering experiments, the CD spectra show that not all protein molecules had unfolded and most of the population of the exposed sample lost  $\alpha$ -helical structure faster than the control (as indicated by loss of minima at 210 and 222 nm and increase in ellipticity at 205 nm, especially after 12 minutes) and was generally more unfolded than the control sample (loss in ellipticity). The average temperature of the samples over a six minute period, based on baseline temperature and SAR, was calculated to be 41.3°C (exposed) and 41.2°C (control).

### 9.1.3 $\alpha$ -LACTALBUMIN

The structure of  $\alpha$ -lactalbumin and its destabilisation by denaturation<sup>198</sup> reduction of its four disulphide bonds<sup>199-202</sup>, proteolytic removal of a subdomain<sup>203</sup>, fibrillation<sup>30</sup>, its molten globule structure<sup>204; 205</sup> and its chaperone action with  $\alpha$ -crystallin<sup>159; 183</sup> have been extensively studied spectroscopically. Therefore  $\alpha$ -lactalbumin was selected as a target protein for study by CD spectroscopy.

Protein	Buffer	Exposure conditions	ID
Apo $\alpha$ -La 2 mg/ml	2.5 mM EDTA 20mM DTT in 50 mM phosphate buffer, pH 7	550ml water in box 7 pulse periods of 4 seconds average temp (pos. light beam): exposed 38.1°C, control 38.1°C	A
Apo $\alpha$ -La 5 mg/ml	20mM DTT in water	550ml water in box 10 pulse periods of 5 seconds average temp (base of cuvette): exposed 37°C, control 38.5°C	B
Apo $\alpha$ -La 5 mg/ml	20mM DTT in 10 mM ammonium buffer, pH 7	550ml water in box 15 pulse periods of 5 seconds average temp (base of cuvette): exposed 37°C, control 38.5°C	C
Holo $\alpha$ -La 5 mg/ml	20mM DTT in water	550ml water in box 10 pulse periods of 5 seconds average temp (base of cuvette): exposed 37°C, control 38.5°C	D
Holo $\alpha$ -La 5 mg/ml	20mM DTT in 10 mM ammonium buffer, pH 7	550ml water in box 10 pulse periods of 5 seconds average temp (base of cuvette): exposed 37°C, control 38.5°C	E

**Table 9.1: Summary of exposure experiments of  $\alpha$ -lactalbumin that were monitored by CD spectroscopy. The experiments have been given an identity (ID) letter for easy reference.**

A variety of experimental conditions were applied. One of the experiments was performed in phosphate buffer containing EDTA, another experiment was performed in water and a set of experiments was performed at higher concentration (5mg/ml vs. 2 mg/ml) in ammonium acetate

buffer to keep experimental conditions similar to hydrogen exchange experiments (section 9.3). Under these conditions, in the absence of salt, the protein does not precipitate out of solution during the time of the experiment.

Apo  $\alpha$ -lactalbumin, from here on abbreviated as *apo- $\alpha$ -La*, was commercially obtained and contains small amounts of calcium (section 2.2.6). To completely remove all calcium ions, 2.5 mM EDTA was added to the buffer. Holo  $\alpha$ -lactalbumin, from here on abbreviated as *holo- $\alpha$ -La*, was commercially obtained; it has been saturated with calcium. Table 9.1 summarises the thermal unfolding experiments performed on  $\alpha$ -lactalbumin that were monitored by CD spectroscopy also. The experimental conditions have been listed and each experiment has an identity letter (from A to E) for easy reference. The SAR was not established for the buffer systems, however from data in Figure 3.5 it is estimated to be  $\sim 13$  W/kg (1.1°C temperature increase) at the bottom of the cuvette.

### 9.1.3.1 REDUCED APO $\alpha$ -LACTALBUMIN

The experiments, concentrations, buffers and exposure conditions are listed in Table 9.1. The SAR was not established for the water or buffer systems but was estimated to be  $\leq 13$  W/kg, at the base of the cuvette, as estimated from the conductivity of the solvents (Figure 3.6). The estimated SAR equates to about 1°C temperature increase in the solution every six minutes, lasting less than one second.

#### FAR-UV CD SPECTROSCOPY (FIGURE 9.3)

The structure of  $\alpha$ -La is destabilised somewhat by the addition of the chelating agent EDTA which removes the bound  $\text{Ca}^{2+}$  ion<sup>206</sup>. Thus, at physiological pH and at room temperature,  $\alpha$ -La in the presence of EDTA, forms a molten globule state<sup>207</sup>. CD spectra of molten globule states have shown that they retain secondary structure (far-UV) but loose tertiary structure (near-UV)

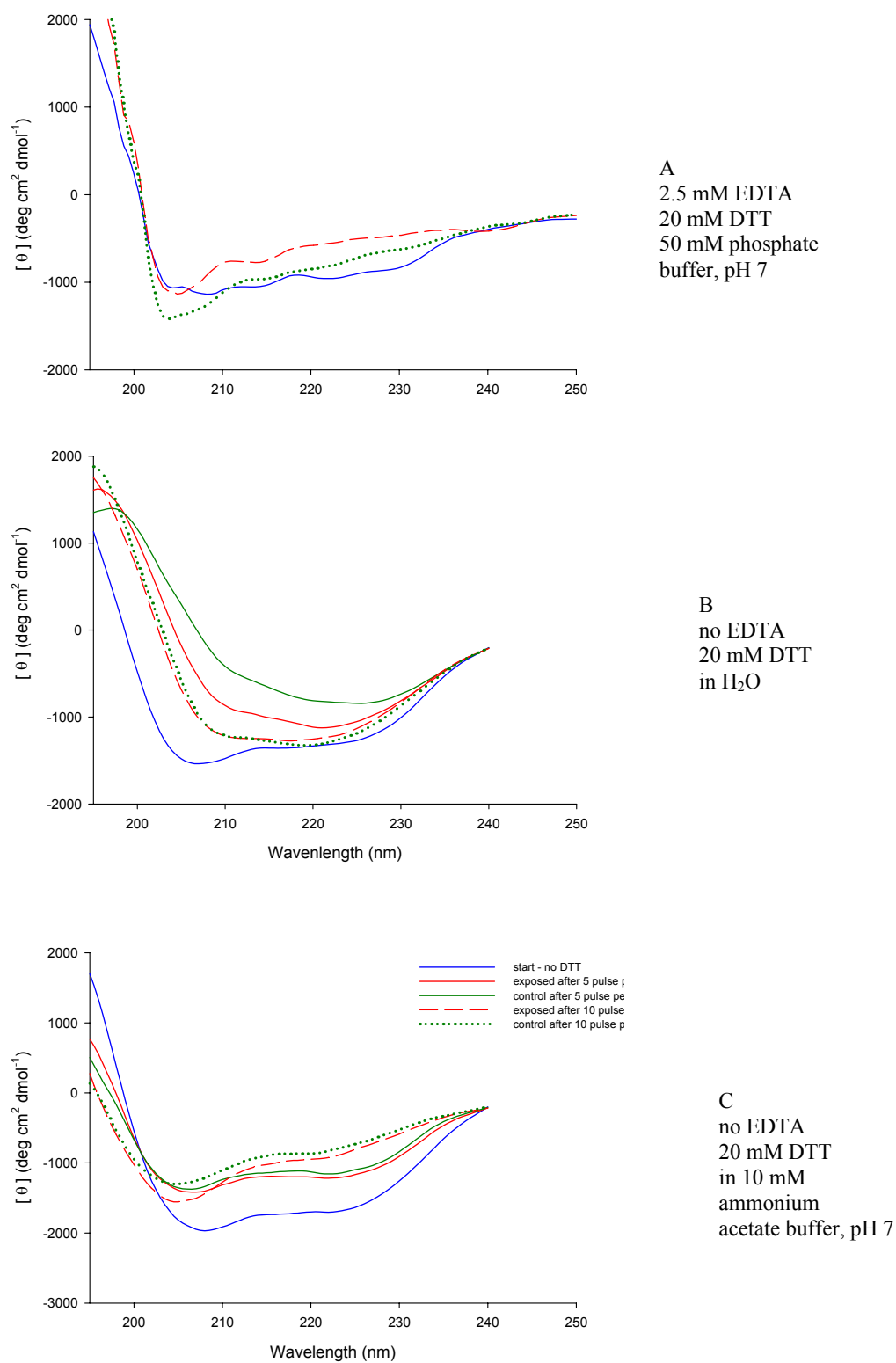


**Figure 9.3:** Far UV spectra of apo- $\alpha$ -lactalbumin (smoothed) before and after reduction and exposure to pulsed 2.450 GHz under conditions in Table 9.1. Aliquots of 6  $\mu$ l were withdrawn from samples and diluted with 2.0 ml 10 mM buffer, pH 7 (A and C), or 1.5 ml water (B). Smoothed spectra are on the right.

The far-UV spectrum of  $\alpha$ -La in Figure 9.3(A) at the start of the experiment is indicative of a molten globule conformation with faint minima at 208 and 222 nm. and is in good agreement with the spectrum of wild-type human  $\alpha$ -La in the presence of EDTA<sup>207</sup> and of the pH-induced molten globule state of bovine  $\alpha$ -La at pH 2<sup>205</sup>.

$\alpha$ -La in water and apo  $\alpha$ -La in ammonium acetate buffer (without addition of EDTA), prior to the start of the experiment, showed similar spectra in the far UV that showed two well defined minima at 208 and 222 nm (Figure 9.4 B and C) which is in agreement with a reported spectrum of apo  $\alpha$ -La<sup>208</sup>.

#### **5 PULSE PERIODS (~30 MINUTES)**

Upon reduction of the disulphide bonds, simultaneous heating at 37°C and 5 pulse periods of microwave exposure the protein lost some of its secondary structure (Figure 9.3 B and C). In B, the characteristic minima, as compared to the native protein were less distinct. This was likely to be the result of the addition of DTT to the water which would have caused a change in pH (not measured). In water, the control was more reduced in intensity than the exposed sample. The exposed and control samples in ammonium acetate buffer (C) lost a similar amount of ellipticity after 5 pulse periods.

#### **10 PULSE PERIODS (~60 MINUTES)**

At the conclusion of the experiment, the molten globule structure of the microwave exposed sample was more unfolded than the control in 50 mM phosphate buffer containing EDTA. pH 7 (Figure 9.3 A). Samples in phosphate buffer and ammonium buffer showed a distinct minimum at 205 nm which was not observed in the molten globule conformation of the apo form of the protein. An *increase* at 205 nm is indicative of random coil formation<sup>195</sup>.

Both the control and exposed samples in ammonium buffer had lost more ellipticity compared to the sampling after 5 pulse periods. The control had lost more than the exposed. The profile of the CD spectrum (Figure 9.3 C) was similar to the molten globule profile of the samples reduced and heated in the 50 mM phosphate buffer (Figure 9.3 A).

## NEAR UV CD SEPCTROSCOPY (FIGURE 9.4)

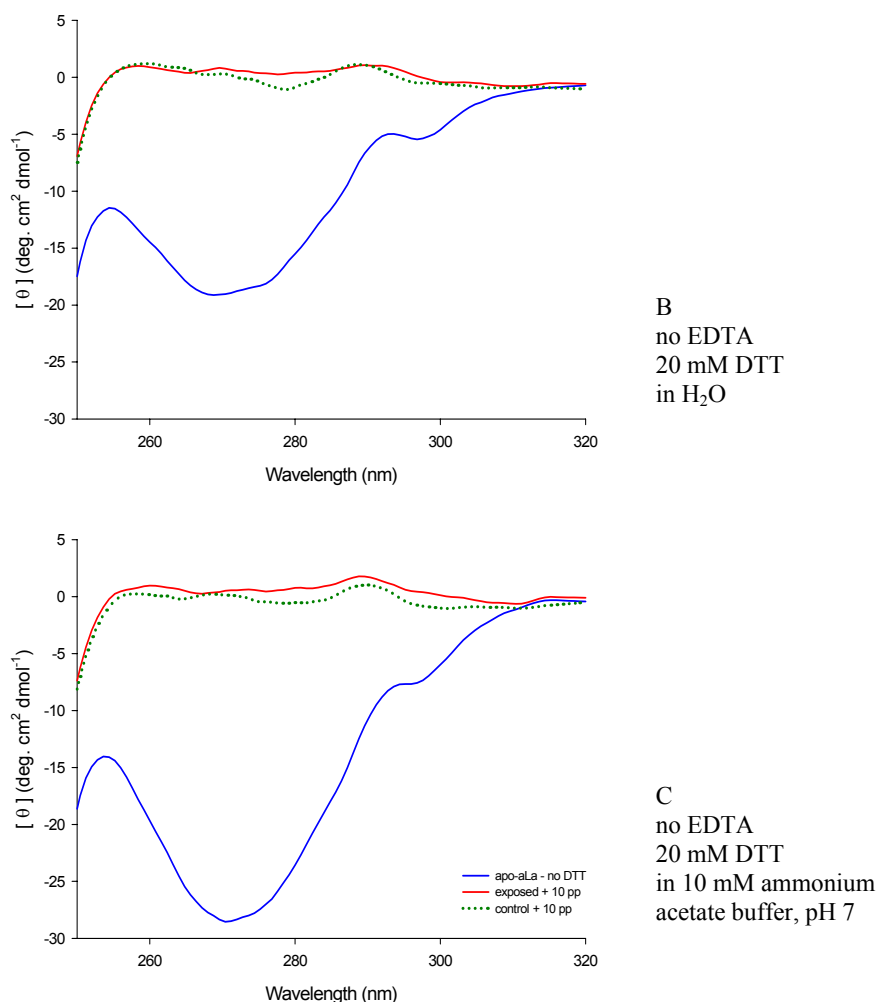


**Figure 9.4:** Near-UV spectra of apo- $\alpha$ -lactalbumin (smoothed) exposed to pulsed 2.450 GHz as per conditions in Table 9.1. Aliquots of 100  $\mu$ l were withdrawn from samples after exposure and diluted with 1.0 ml of water (B) or 1.0 ml of 10 mM buffer, pH 7 (C).

The near-UV spectra of samples B and C (Table 9.1) was obtained prior to the start of the experiment and after the last pulse period. No spectrum was recorded in phosphate buffer (A).

The spectrum of native  $\alpha$ -La in buffer was more distinct than the spectrum of  $\alpha$ -La in water, both were in agreement with a recorded near-UV spectrum of apo  $\alpha$ -La<sup>199</sup>. Tertiary structure was almost completely lost at termination of the experiments ( $\sim$  1 hour) as can be demonstrated

from the loss of ellipticity. Even so, a difference was observed between the exposed and control sample where the exposed was more collapsed than the control.

In summary, it can be concluded that at the completion of the experiments, the buffered samples, according to the far and near UV spectra, were in molten globule states. In phosphate buffer, as deduced from the far UV spectra, the exposed sample had lost more structure and in the ammonium buffer the control had lost more structure compared to the exposed. A slight difference was observed in ellipticity (far UV) between exposed and control samples in water at the conclusion of the experiment. The proteins in water were not buffered therefore difference may have arisen from pH fluctuations.

Light scattering experiments with reduced  $\alpha$ -La failed to show a significant difference in initial rate and extent of precipitation between microwave-exposed and control samples. Usually these experiments were conducted at a higher concentration and in buffer containing salt which therefore increases the SAR (section 3.2.1). As the effect of microwave exposure on secondary structure was reversed for samples in the two different buffers, it would be of interest to explore this phenomenon in more detail.

#### **9.1.3.2 REDUCED HOLO $\alpha$ -LACTALBUMIN**

Holo  $\alpha$ -La was reduced and exposed to pulsed microwaves in water and 10 mM ammonium acetate. Conditions are described in Table 9.1. The results for far-UV CD are presented in Figure 9.5 and for near-UV in Figure 9.6.

##### **FAR UV CD SPECTROSCOPY (FIGURE 9.5)**

Holo  $\alpha$ -lactalbumin (with bound calcium) dissolved in water or ammonium acetate buffer gave a similar far-UV CD spectrum (Figure 9.6) and was comparable to reported spectra in the literature<sup>200; 203</sup>.

##### **5 PULSE PERIODS (~30 MINUTES)**

After reduction, simultaneous heating at  $\sim 37^\circ\text{C}$  and 5 pulse periods of microwaves, the protein samples had lost ellipticity however the minimum at 208 nm was still observed and it was more preserved in the exposed sample in 10 mM ammonium acetate. Minima at 208 and 222 nm are



indicative of  $\alpha$ -helical structure<sup>193</sup>. In both sets of experiments (water and ammonium acetate), the exposed had lost slightly more ellipticity than the control.

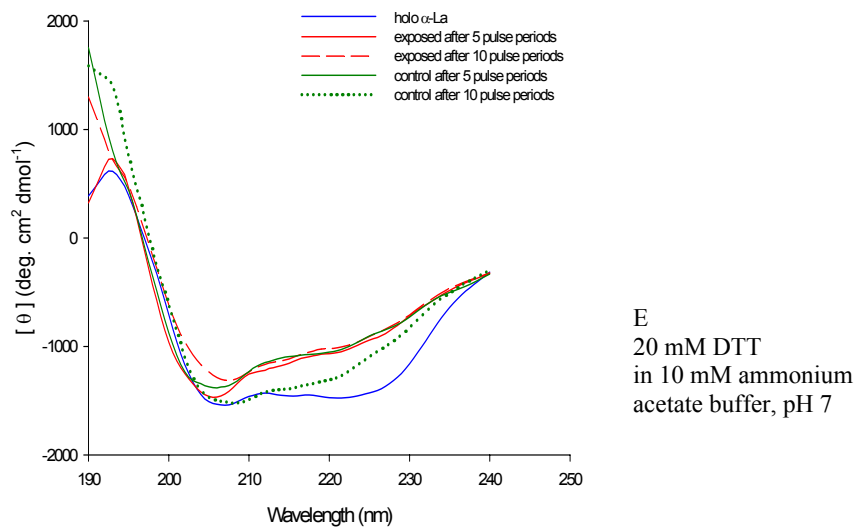
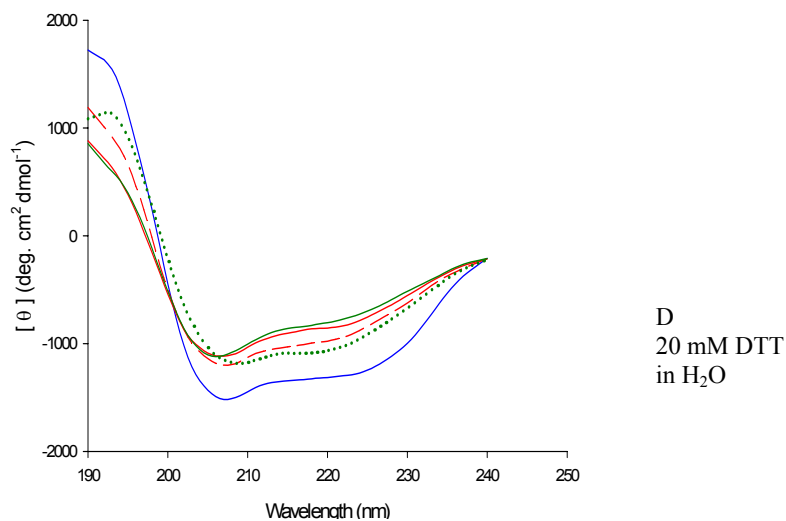


**Figure 9.5:** Far UV CD spectra of holo- $\alpha$ -lactalbumin (smoothed) before and after, reduction and exposure to pulsed 2.450 GHz as per conditions in Table 9.1. Aliquots of 6  $\mu\text{l}$  were withdrawn from samples and diluted with 1.5 ml water (D) or 2.0 ml 10 mM buffer, pH 7 (E).

**10 PULSE PERIODS (~60 MINUTES)**

After 10 pulse periods, the ellipticity had recovered compared to the loss of signal after 5 pulse periods, for all samples except the exposed sample in 10 mM ammonium acetate buffer (Figure 9.5). The exposed samples showed a decrease in molar ellipticity compared to the controls. The spectra indicate that holo  $\alpha$ -La still has secondary structure and is in accordance to the far-UV CD spectrum of fully reduced holo- $\alpha$ -La reported in the literature<sup>202</sup>.

**NEAR UV CD SPECTROSCOPY**

After reduction, heating at 37°C for 60 minutes and exposure to 10 pulse periods of microwaves, the tertiary structure of reduced holo  $\alpha$ -lactalbumin was lost. The signals of the exposed and control samples overlapped for both sets of experiments in the near UV. The near-UV CD spectrum of the fully reduced holo- $\alpha$ -La (see far-UV)<sup>202</sup> is similar to the spectra in Figure 9.6.

Light scattering experiments on reduced holo  $\alpha$ -lactalbumin did not show a difference in initial rate or extent of precipitation between exposed and control samples (section 7.6.2). These experiments were at concentrations of 1 mg/ml in imidazole buffer containing  $\text{CaCl}_2$  and at a slightly lower temperature than experiments carried out in tandem with CD spectroscopy. The far-UV spectra show that the secondary structure for the exposed samples in both water and ammonium acetate have lost more ellipticity than the controls with respect to the native structure under similar conditions to the light scattering experiments. The far-UV spectrum of the exposed sample in ammonium acetate buffer shows a distinct minimum at ~209 nm which is indicative of a more unfolded structure. The fact that all samples, after reduction and heating still have a measure of secondary structure but no tertiary structure (near UV) confirms that the conformations are in a molten globule state. Reduced holo- $\alpha$ -La was found to be more unfolded in ammonium acetate buffer than in water compared to the control sample.

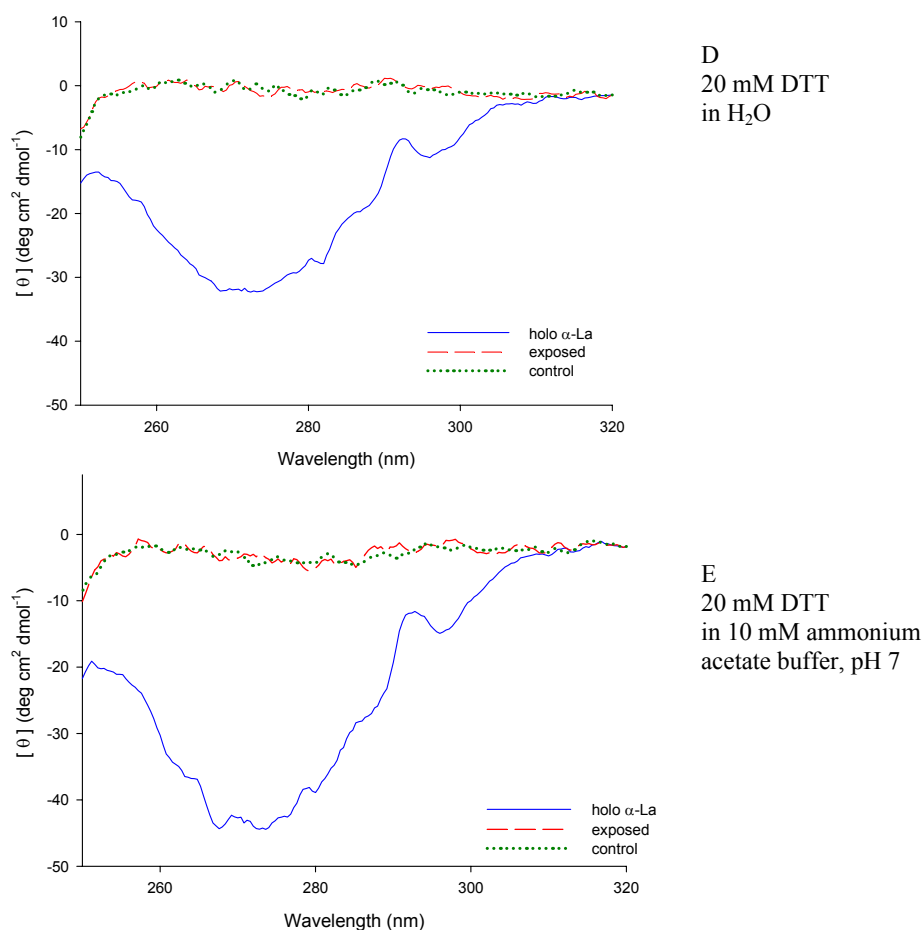


**Figure 9.6:** Near UV CD spectra of holo- $\alpha$ -lactalbumin exposed to pulsed 2.450 GHz as per conditions in Table 9.1. Aliquots of 100  $\mu$ l were withdrawn from samples after exposure and diluted with 1.0 ml of water (D) or 1.0 ml of 10 mM buffer, pH 7

## 9.2 FLUORESCENCE STUDIES

Proteins containing one or more tryptophan residues emit fluorescence when excited. Changes in protein conformation may lead to the burying or increased exposure of tryptophan residues which results in a decrease or increase of fluorescence intensity<sup>209</sup>. The fluorescence can be measured spectroscopically and is referred to as *Intrinsic Fluorescence*.

The hydrophobic dye, 8-anilino-1-naphthalene sulfonate (ANS) binds to exposed and clustered hydrophobic areas on the unfolding proteins and emits fluorescence when excited<sup>210</sup>. ANS also binds to aggregates and is able to penetrate into the aggregates where it binds to the hydrophobic regions within<sup>211</sup>. It is therefore a convenient method to probe the unfolding of a

protein as exposed hydrophobicity increases as the protein unfolds. The fluorescence, referred to as *Extrinsic Fluorescence* is measured by titration with ANS.

Citrate synthase contains 9 tryptophan residues in each subunit (2) and is easily destabilised by heat. The protein was therefore considered a good choice in probing, by fluorescence techniques, the conformational changes with temperature.

### 9.2.1 INTRINSIC FLUORESCENCE CITRATE SYNTHASE AT 37 °C

Two samples of 1.0 ml of 0.2 mg/ml CS in 80 mM phosphate buffer, pH 7.5 were incubated at 37°C. One sample was exposed to 15 pulse periods of 2.450 GHz (pulse duration was 3.2 seconds). The SAR for this sample was 22.1 W/kg in the region where the light beam passes through the sample. The intensity at the tryptophan emission maximum wavelength of 338 nm was compared before exposure and at the termination of the light scattering measurements (Figure 9.7), which was four hours later. From the inset in Figure 9.7 it can be seen that the protein started to precipitate immediately when heated and that the precipitation peaked at ~ 4 hours

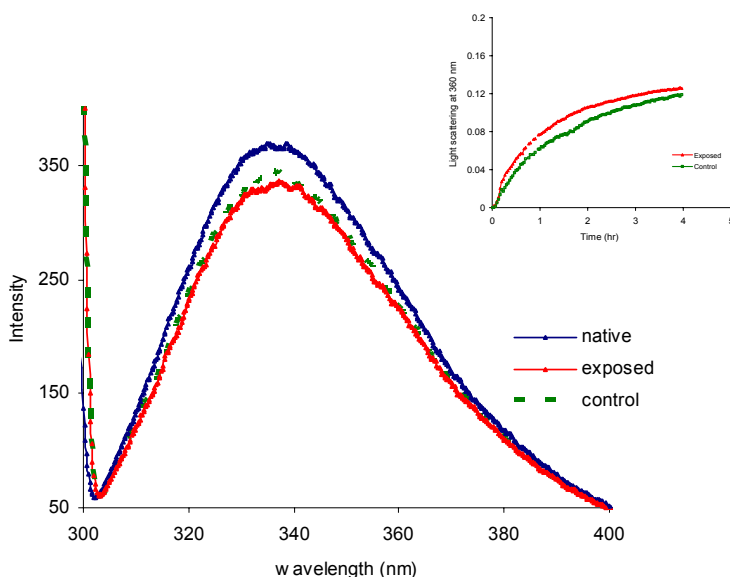


**Figure 9.7:** Tryptophan fluorescence of two 1.0 ml samples of 0.2 mg/ml CS in 80 mM phosphate buffer, pH 7.5. One sample was exposed to 15 pulse periods of 2.450 GHz at 37°C and the other sample was incubated at 37°C (control). The fluorescence was measured before and after the experiment (4 hr). The samples were excited at wavelength 295 nm and the emission accumulated over 260–450 nm. Inset: The light scattering profile, measured at 360 nm, of the sample.

Thus, Figure 9.7 is a reflection of the remaining soluble population of CS proteins. In this particular experiment (Inset Figure 9.7), the initial rate of precipitation was larger than the control. Compared to CS at the start of the experiment, both control and exposed samples lost similar fluorescence intensity with the control sample losing 6.5 % intensity compared to the exposed sample which lost 8.4 % intensity. When the SAR was considerably increased (by lowering the volume of water inside the plastic box in the microwave cavity from 500 ml to 300 ml) and the incubation temperature increased to 40°C, the difference between exposed and control was found to be more distinct. The aggregation and precipitation of the exposed protein was greatly enhanced (Figure 9.8 inset). Figure 9.8 shows the tryptophan fluorescence emission before and after exposure to pulsed microwaves. The SAR was not calculated for this particular experiment. The control lost 24.8% intensity and the exposed 44.4% intensity in tryptophan emission.

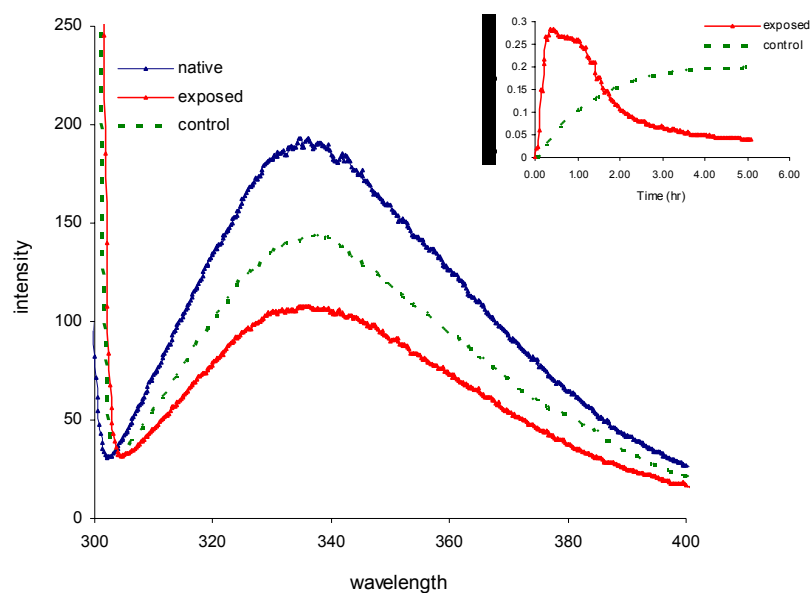


**Figure 9.8:** Tryptophan fluorescence of two 1.0 ml samples of 0.2 mg/ml CS incubated at 40°C. One sample was exposed to 5 pulse periods (5 seconds in duration) of 2.450 GHz (300 ml water box ) compared to a control sample incubated at the same temperature. The fluorescence was measured before and after the experiment (5 hr). The samples were excited at wavelength 295 nm and emission accumulated over 260-450 nm. Inset: aggregation profile of the same samples.

Of the nine tryptophan residues in CS, seven are exposed to the external environment as deduced from modelling data from the protein data bank <sup>135</sup>. Studies on the temperature dependence of tryptophan fluorescence have shown that increasing temperature causes a red shift (shift to longer wavelengths) in the fluorescence emission maximum which is accompanied by a decrease in fluorescence intensity <sup>209; 212; 213</sup>. The red shift is not noticeable at 37°C but can be detected in the assay at 40°C thus confirming that tryptophan residues are increasingly exposed which is consistent with greater unfolding of the protein. At the higher temperature and higher SAR, the protein precipitated out more than at 37°C as can be seen from the absorbance. Therefore less protein remains in solution at 40°C which accounts for a larger decrease in fluorescence than at 37°C. Thus, the light scattering experiments supplemented the fluorescence studies.

### 9.2.2 EXTRINSIC FLUORESCENCE CITRATE SYNTHASE AT 37.5 °C

In an experiment at 37.5°C comparable to the experiment at 37°C in section 9.2.1 (same conditions) in which one sample of CS was exposed to 15 pulse periods of 2.450 GHz compared to a control, the exposed hydrophobicity of CS protein molecules, before and after microwave exposure, was probed by ANS binding and fluorescence.

The heated samples bound more ANS than the native sample (prior to the start of the experiment) and the exposed sample bound slightly more ANS than the control sample (Figure 9.9). The data for the experimental samples reflect proteins after 4 hours when the light scattering measurements were terminated. These results are in accordance with literature reports that measured ANS fluorescence intensity as a function of temperature and in the presence of aggregates <sup>210; 211</sup>.

The observation that the microwave exposed samples exhibited less intrinsic fluorescence compared to a control (Figures 9. 7 and 9.8) and exhibited more ANS binding (Figure 9.9) supports the finding from light scattering experiments on CS that the initial rate and extent of aggregation, precipitation (and hence unfolding) was enhanced for the microwave exposed samples compared to controls. In terms of the change in protein conformation, it can be

concluded that protein samples exposed to heat as well as pulsed microwaves are structurally more altered than control samples.

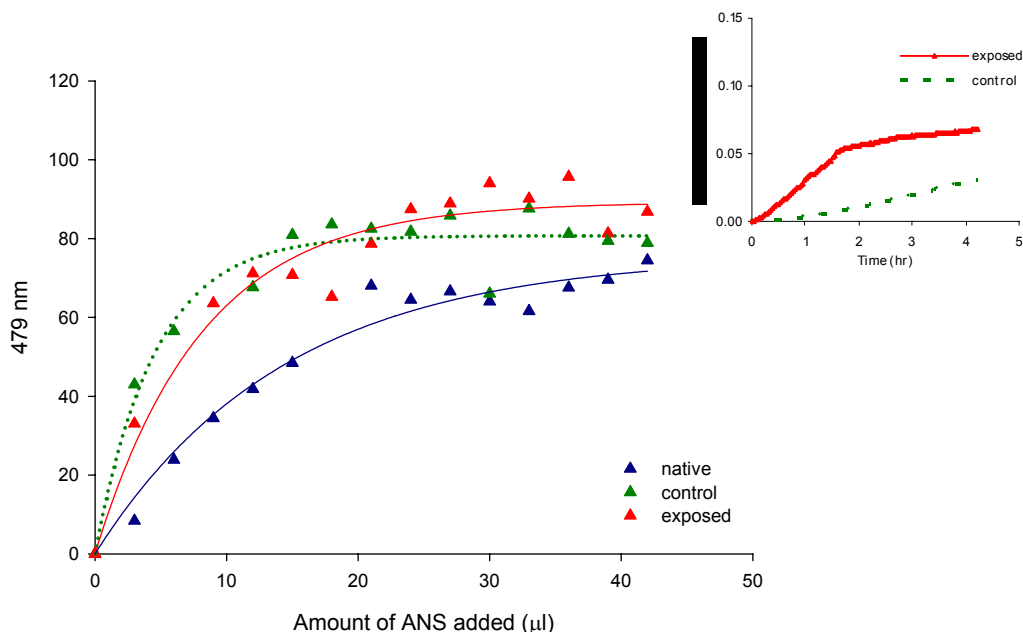


**Figure 9.9:** ANS binding of two 0.2 mg/ml CS samples in 80 mM phosphate buffer, pH 7.5. One sample was exposed to 15 pulse periods of 2.450 GHz at 37.5°C and the control was incubated at the same temperature. After the experiment the samples were titrated with 10 mM ANS and excited at wavelength 387 nm; the emission was monitored at 479 nm. The SAR for this sample was not determined. Inset: Light scattering profile at 360 nm of the same sample.

The decrease in intrinsic fluorescence shows that tryptophan residues in the microwave exposed samples become *more* accessible to the aqueous environment and the increased extrinsic fluorescence shows that the microwave exposed samples exhibit more exposed hydrophobicity than the control samples due to structural destabilisation.

### 9.3 ELECTROSPRAY MASS SPECTROMETRY

Hydrogen–deuterium exchanges in proteins have been explored as far back as the 1950s by Linderström-Lang and collaborators<sup>214</sup>. It was proposed that the amide hydrogens in the peptide backbone exchange with the surrounding solvent as a function of the intrinsic dynamics of the protein. Globular proteins exist in a range of conformations due to structural fluctuations (see section 1.4, figure 1.4). During the brief opening of a protein, when the hydrogen bond acceptor and donor are temporarily separated, the peptide group is attacked either by a  $\text{H}_3\text{O}^+$  or  $\text{OH}^-$  ion

<sup>214</sup>. Hydrogen exchange can be monitored by NMR spectroscopy and mass spectrometry (MS). NMR monitors the average exchange at individual amide sites over the distribution of protein molecules <sup>215</sup> and is therefore a very powerful technique for monitoring the conformation at individual sites in the protein. Electrospray ionisation (ESI) is particularly useful as it is a gentle technique that produces multiply-charged ions from the protein of interest with minimal fragmentation and can be applied to study large weakly associated protein aggregates in solution <sup>215-217</sup>. MS gives gross information on the solvent accessibility of all the NH groups in the proteins. Robinson *et al* <sup>164</sup> published findings on the hydrogen exchange kinetics of a three-disulphide reduced derivative of  $\alpha$ -lactalbumin ( $\alpha$ -Lac) bound to the molecular chaperone GroEL using electrospray mass spectrometry. Initially, apo  $\alpha$ -Lac was deuterated in D<sub>2</sub>O and hydrogen exchange initiated by dilution into H<sub>2</sub>O, pH 5 at 4°C. The exchange was plotted and showed an exponential decrease in exchange over 100 minutes. Following this, the three-disulphide derivative of  $\alpha$ -Lac bound to the molecular chaperone GroEL was deuterated followed by incubation with GroEL in D<sub>2</sub>O. The complex was diluted into water pH 5 and monitored for hydrogen exchange using ESI-MS. The technique enabled the monitoring of the protein-chaperone complex and give a quantitative ratio of the binding of  $\alpha$ -Lac with GroEL <sup>164</sup>. It was reasoned that this method could be adapted to the microwave exposure experiments to see differences between exposed and control samples in the early stages of aggregation with respect to the number of exchangeable hydrogens. This could improve understanding about the conformation of the proteins, e.g.  $\alpha$ -Lac, at the different stages of unfolding after exposure to pulsed microwaves. The method was envisaged to also include experiments in the presence of the sHsp,  $\alpha$ -crystallin, in order to probe the differences between exposed and control samples in terms of protein-chaperone complexes.

The hydrogen exchange experiments started relatively late in the course of the project and therefore the results are preliminary. The reason that this section has been included in the thesis is to provide a foundation for future work.



### 9.3.1 APO A-LACTALBUMIN

The hydrogen exchange experiment in which deuterons in apo  $\alpha$ -Lac are exchanged by hydrogen atoms <sup>164</sup> was performed several times with good reproducibility. In Figure 9.10 the results are compared.

Prior to the exchange, an aliquot of  $\alpha$ -lactalbumin was diluted 1:100 into D<sub>2</sub>O (pH 6) and injected into the mass spectrometer with D<sub>2</sub>O being also the running buffer. This gave the molecular mass of the deuterated protein (14433 Da). Therefore, 255 hydrogens were exchanged overnight for deuterons, at room temperature. Hydrogen exchange was initiated by the 100 fold dilution of the deuterated protein in ice cold H<sub>2</sub>O made acidic to pH 2 by formic acid. The hydrogen exchange was monitored by observing the reduction in mass via ESI-MS.

**Figure 9.10: Hydrogen exchange of apo  $\alpha$ -lactalbumin in ice cold H<sub>2</sub>O, pH 2. Initial incubation was in D<sub>2</sub>O, 10% H<sub>2</sub>O to ensure complete exchange of hydrogens to deuterons. Dilution into H<sub>2</sub>O, pH 2 was 1 : 100 (v/v) on ice. Results are compared with Robinson *et al* <sup>164</sup>.**

Within the first minute upon dilution, under conditions of 0-4 °C, a total of 171 deuterons were exchanged (Figure 9.10). The exchange, up to 60 minutes, for sample 2 (Figure 9.10) followed second order kinetics as the plot of the inverse of the number of deuterons exchanged against time could be fitted with a straight line (Figure 9.11) according to the formula:

$$\frac{1}{[A]_t} = kt + \frac{1}{[A]_0} \quad (1)$$

Where  $[A]_t$  is the concentration at a time point (y axis),  $[A]_0$  is the initial concentration,  $k$  is the rate constant (slope) and  $t$  is the time in minutes (x axis).

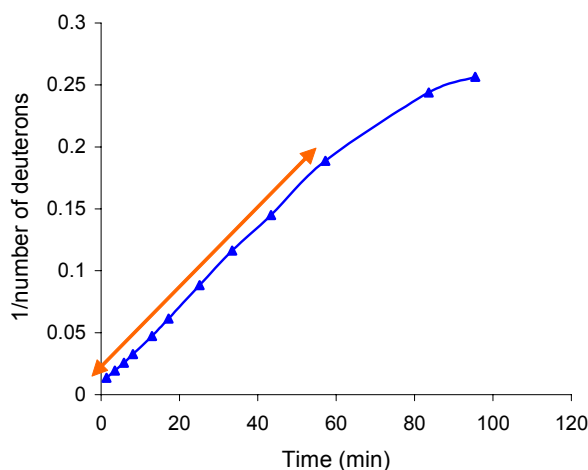


**Figure 9.11:** Plot of formula 1 applied to sample 2 in Figure 9.10. Sample 2 followed second order kinetics up to 60 minutes (the arrow indicates the straight line) after exchange was initiated.

Hydrogen exchange was monitored in another way by diluting a sample of  $\alpha$ -Lac prepared in aqueous buffer with  $D_2O$  and measuring the increase of molecular mass over time by ESI-MS. At specific time points, the reaction was quenched by dilution into ice cold  $H_2O$ , pH 2. Figure 9.12 shows the result of two experiments in which apo  $\alpha$ -lactalbumin was dissolved in 0.1 M ammonium acetate buffer and diluted into  $D_2O$ .

The hydrogen exchange experiment was used to determine if a difference could be detected in exchangeable hydrogens of two samples of reduced apo  $\alpha$ -Lac, one sample of which was exposed to pulsed microwaves. Figure 9.13 shows the result of two samples of 5 mg/ml  $\alpha$ -lactalbumin dissolved in 1.0 ml of  $D_2O/10\%$   $H_2O$  each and left overnight to exchange at room temperature. The samples were reduced by addition of 20 mM DTT and incubated in the block heater at  $\sim 37^\circ C$  and one sample was exposed for 10 periods to pulses of 2.450 GHz. The SAR was estimated from conductivity measurements (section 3.2.1) to be  $\sim 10$  W/kg at the base of the cuvette (which equates to a transient temperature increase of  $0.9^\circ C$ ).

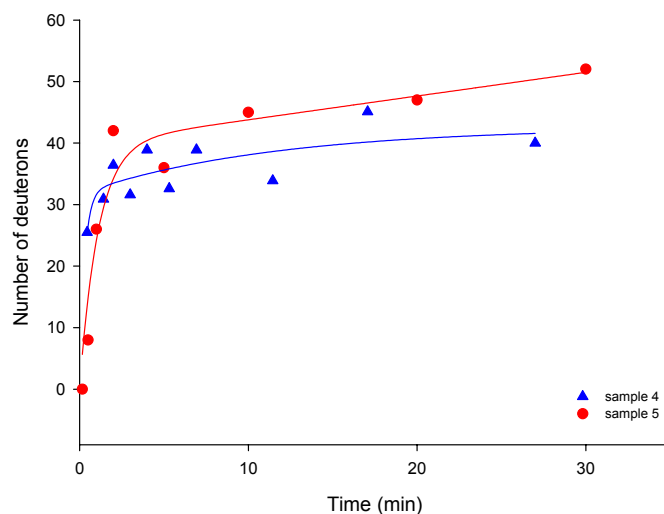


**Figure 9.12:** Hydrogen exchange of apo  $\alpha$ -lactalbumin examined by electrospray mass spectrometry. An aliquot of 2 mg/ml (sample 4), 5 mg/ml (sample 5) in 0.1 M ammonium acetate buffer, pH 7 was diluted into  $D_2O$ , 1:10 (sample 4) or 1:20 (sample 5) at room temperature. At time points indicated on the graph, aliquots were quenched by dilution into ice cold  $H_2O$ , pH 2.5: 1:10 (sample 4) or 1:4 (sample 5) and a sample was immediately injected into the electrospray source.

At the conclusion of the experiment, an aliquot was removed of each sample and diluted 1 : 30 into  $H_2O$ , pH 7 at room temperature and stored on ice. At designated time points, an aliquot of the dilution was quenched 1:1 with ice cold  $H_2O$ , pH 2.

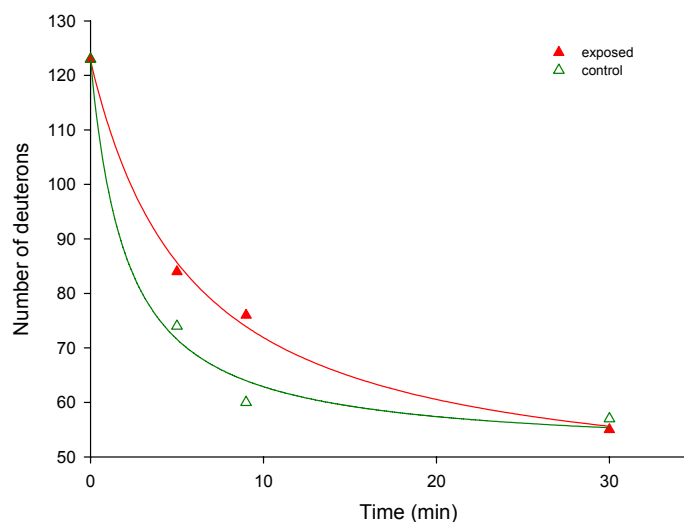


**Figure 9.13:** Comparison of hydrogen exchange of two samples of reduced deuterated 5 mg/ml  $\alpha$ -lactalbumin that were incubated at  $\sim 37^\circ C$  of which one was exposed to 10 pulse periods of 2.450 GHz.

The number of deuterons (124) that exchanged prior to exposure, after DTT was added, was determined by dilution into H<sub>2</sub>O, pH 2 (1: 30) followed by dilution 1:1 in ice cold H<sub>2</sub>O, pH 2.

After 5 minutes of exchange into water, the control sample had exchanged 10 more deuterons than the exposed; after 9 minutes the difference was 6 deuterons. At 30 minutes, there was no significant difference between the hydrogen exchange of the exposed and control samples. These results were from a single exchange determination.

#### 9.4 INTERPRETATION OF RESULTS ON PROTEIN CONFORMATIONAL STUDIES

In section 7.9, it was concluded that when proteins were exposed to a stress in tandem with pulsed microwaves, the kinetics of unfolding was increased as compared to a control sample. The effect was dependent on specific conditions of buffer, temperature and exposure dosage. Light scattering provides information about the relative quantity of aggregated particles, i.e. proteins that have come out of solution. The results presented in this chapter provide information about how the conformation of an “exposed” protein differed to a “control” protein. The measurements refer to soluble protein populations often in intermediately folded conformations which may be present as soluble aggregates.

The secondary structure of catalase was probed only by far-UV CD. The spectrum shows that the protein still had considerable secondary structure after exposure to microwave radiation at 42°C but it had a distinct shoulder at 208 nm which is characteristic of random coil formation. The  $\alpha$ -helical region was more reduced for the exposed sample compared to the control. The CD results therefore complement the light scattering experiments and it is concluded that the exposed protein unfolded and aggregated faster in solution and therefore precipitated out at a faster rate than the control sample.

The secondary structure of CS was probed by far-UV CD at 42°C. The spectrum showed that over time, the exposed protein lost secondary structure faster than the control as judged by increased loss of  $\alpha$ -helicity compared to the control. This complemented the fluorescence studies which indicated that tryptophan fluorescence decreased more for the exposed than for

the control. The exposed sample bound more ANS, a probe for hydrophobicity, than the control sample thus confirming that the exposed protein sample was more unfolded than the control.

Reduced apo and holo  $\alpha$ -Lac did not precipitate out of solution during the experiments. Light scattering experiments using higher concentrations of  $\alpha$ -La in different buffer systems showed no difference between the initial rate nor in the extent of precipitation of an exposed and control sample. Reduced apo and holo  $\alpha$ -La, at 37°C exist as molten globule states, showing secondary structure (UV-far CD) and no tertiary structure (near-UV CD)<sup>202</sup>. After 54 minutes, when some of the protein population has already precipitated (Figures 7.20 and 7.22), the remaining soluble protein adopted a molten globule state as can be deduced from the far-UV and near-UV CD spectra. The secondary structure of the exposed holo  $\alpha$ -La was slightly more unfolded than the control in water as well as in ammonium acetate. Apo  $\alpha$ -La in phosphate and ammonium acetate buffer gave conflicting results as the exposed sample lost more ellipticity in phosphate buffer and the control sample lost more ellipticity in ammonium acetate buffer. An initial hydrogen exchange experiment on  $\alpha$ -La, which was exposed to pulsed microwaves in water, showed that the exposed protein sample exchanged hydrogens slower than the control sample. It could be speculated that the exposed protein population is on average more aggregated and therefore more restricted in exchanging with the hydrogens of the surrounding solvent. However, the far-UV CD spectrum for apo  $\alpha$ -La in water (Figure 9.3B) did not show a difference in secondary structure between the exposed and control.

In future experiments it would be useful to obtain near-UV spectra at time points during the exposure in order to gain understanding on the changes occurring in the tertiary structure. This requires re-evaluation of the SAR as aliquots of ~ 100  $\mu$ l are needed for each spectrum.

Analyses of exposed and control samples by deuterium exchange electrospray mass spectrometry may prove to be a promising tool in further research.

---

## CHAPTER 10

---

### ADDITIONAL STUDIES

In this chapter are grouped the results of a series of experiments that were not finalised due to restraints in time. The experiments were the results of questions that arose from earlier experiments: why does a sample containing CO<sub>2</sub> unfold faster in presence of pulsed microwaves compared to a non-exposed sample and what are the effects of pulsed microwaves on more concentrated samples that mimic conditions in a living cell ?

The findings provide supplementary data that are useful for the interpretation of results discussed in earlier chapters and could be the basis of future studies.

#### 10.1 EFFECT OF CO<sub>2</sub> ON UNFOLDING

The supposition that CO<sub>2</sub> had an effect on the unfolding of ADH when exposed to pulsed 900 MHz at a SAR of 0.21 W/kg (Section 6.1) was investigated by bubbling CO<sub>2</sub> through protein solutions and monitoring light scattering at 360 nm. Samples were heated and exposed to pulsed microwaves in similar experiments as described in Chapter 7. For this experiment ADH and ovotransferrin were selected as the exposure conditions at which they precipitated had been well studied (sections 7.1 and 7.8). The SAR for the exposures was estimated from the SAR of previous experiments under the same conditions of buffer, temperature and exposure parameters.

##### 10.1.1 ALCOHOL DEHYDROGENASE

Two solutions of 1.0 ml of 0.5 mg/ml ADH, 1 mM 1,10 phenanthroline, in 0.1 M phosphate buffer, 0.1 M NaCl, pH 7 were prepared on ice. A glass pipette was attached to a hose attached to a CO<sub>2</sub> cylinder and the gas was regulated to a slow flow. The pipette was placed inside the solutions, one at a time, to allow the gas to bubble through the solutions for less than 3 seconds. One sample was exposed to 10 periods of pulsed 2.450 GHz, of 3.2 seconds duration each and

the second sample was the control. The SAR was estimated, from similar experiments, to be ~ 19 W/kg. The results were compared to a pair of 1.0 ml solutions that were treated identically with the exception that they did not contain CO<sub>2</sub> (Figure 10.1).

In Table 10.1 are listed the pH of the samples after exposure, average temperature of the solutions and the initial rate of precipitation. The ratio of the exposed/control (initial rate of precipitation) was 6.43 for the samples containing added CO<sub>2</sub> and 10.9 for the samples without CO<sub>2</sub>. The difference between the temperatures of the exposed and control was similar in both sets of experiments.

Dissolved CO<sub>2</sub> decreases pH in aqueous solutions according to the following equation:

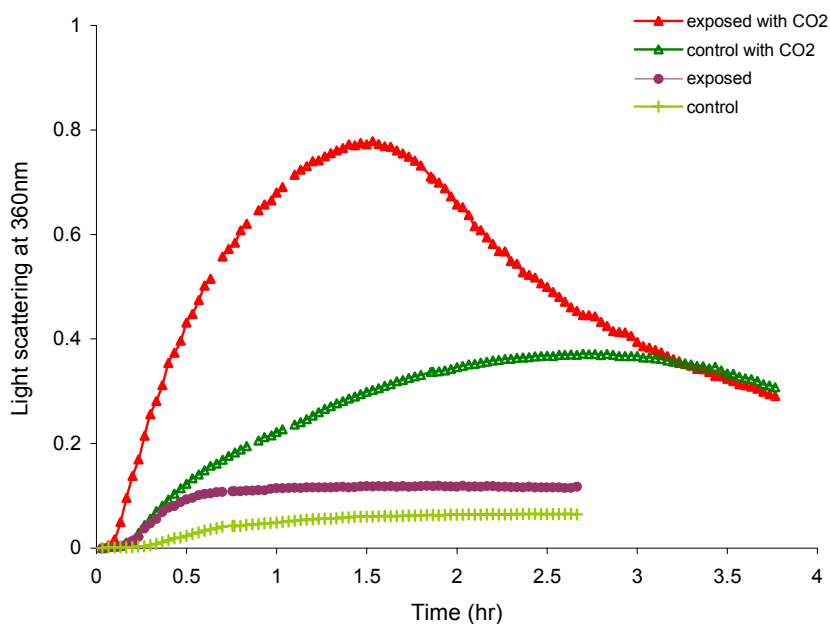
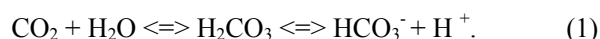


**Figure 10.1:** Exposure of 0.5 mg/ml ADH, 1mM 1,10 phenanthroline in 0.1 M phosphate buffer, 0.1 M NaCl, pH 7 to 10 pulse periods of 2.450 GHz at 37°C. The duration of the pulse periods was 3.2 seconds and the pulses were applied every six minutes. CO<sub>2</sub> was bubbled through one pair of samples (exposed and control with CO<sub>2</sub>) and the other pair contained no added CO<sub>2</sub> (exposed and control). The SAR was ~19 W/kg.

It was found that bubbling of CO<sub>2</sub> through the samples took the pH from 7 to pH 6.4 (Table 10.1). The difference in pH may have contributed to an increased precipitation of ADH by destabilising the protein to a greater extent than removing the zinc ion by chelation with 1,10 phenanthroline. Apart from the initial rate of precipitation, the extent of precipitation (maximum absorbance) for the exposed sample containing CO<sub>2</sub> was much greater compared to the control sample.

Sample	pH at conclusion of experiment	Average temp.	Initial rate
Exposed+ CO <sub>2</sub>	6.34	37.8	1.1819
Control + CO <sub>2</sub>	6.40	36.8	0.1838
Exposed	6.69	37.5	0.1428
Control	6.68	36.7	0.0131

**Table 10.1: Experimental data for experiment in Figure 10.1. The temperature profile for this particular experiment (pulse period of 3.2 seconds) was not undertaken therefore, as this was a comparative study only, the average temperatures for a pulse period of 5.0 seconds was presented.**

In section 7.1.1 it was reported that the average ratio of the exposed/control (initial rate of precipitation) was 1.52. With the addition of CO<sub>2</sub>, it was found to be 6.4. The samples that did not contain added CO<sub>2</sub> did not precipitate to the extent that was normally observed for ADH under the chosen conditions. The samples were stored on ice for 3.5 hours prior to the start of the experiment which may have caused this behaviour.

### 10.1.2 OVOTRANSFERRIN

The results obtained in the previous section (10.1.1) showed that the protein ADH, in the presence of a chelating agent, excess CO<sub>2</sub> and exposed to mild heating and pulsed microwaves, unfolded and precipitated more rapidly than a control that was not exposed to microwaves. It was of interest to know how a protein would behave if one of the stress factors was removed and the temperature excursion as a result of microwave exposure was negligent. Therefore, an



experiment was undertaken on ovotransferrin at room temperature; the pulse duration was set to 0.2 seconds to minimize heating.

Two samples of 0.2 mg/ml ovotransferrin, 20 mM DTT in 0.1 M phosphate buffer, 0.1 M NaCl were flushed with CO<sub>2</sub> as described in section 10.1.1. DTT was added to the samples prior to the start of the experiment after the CO<sub>2</sub> had been bubbled through. One sample was positioned in the microwave oven and exposed at room temperature to a burst of microwaves of 0.2 seconds duration, every six minutes, for 40 hours. The control was placed on the bench nearby. The samples were inverted before light scattering measurements.

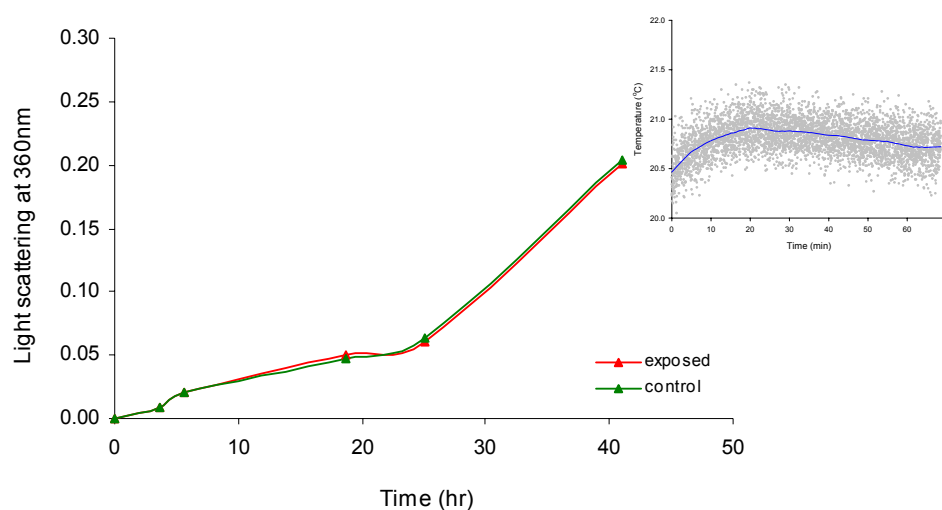


**Figure.10.2:** 0.2 mg/ml Ovotransferrin, 20 mM DTT in 0.1 M phosphate buffer, 0.1 M NaCl, pH 7.2 at room temperature. CO<sub>2</sub> was bubbled through both samples. One sample was exposed every six minutes to pulsed 2.450 GHz (bursts of 0.2 seconds), the control sample remained on the bench also at room temperature. Inset: Plot of temperature, measured every second, of a 1.0 ml sample containing buffer only and exposed to pulse periods of 0.2 seconds duration every six minutes. The trendline (blue) is drawn over the data points (grey).

The pH of the samples had dropped to pH 6.42 after bubbling with CO<sub>2</sub> but prior to addition of DTT. An insignificant difference was observed in precipitation between control and exposed samples therefore CO<sub>2</sub> did not have an effect, at room temperature, on the unfolding and precipitation of reduced ovotransferrin (Figure 10.2). Future work will need to determine if ovotransferrin in the presence of CO<sub>2</sub> behaves similarly to ADH when also heated and exposed to pulsed microwaves. Furthermore, it was not possible to detect a change in solution temperature as a result of an applied pulse. The plot in Figure 10.2, inset, shows the temperature

of the solution over a 70 minute period exposed to 0.2 seconds of 2.450 GHz every six minutes. No temperature escalation as demonstrated in Figure 3.4 could be observed. At the start of the experiment the sample was cold and it took up to 20 minutes to get to room temperature after which the temperature slightly dropped. This occurrence was considered to be independent of the exposure. For a better scientific approach, a control should have been monitored for temperature also.

Essentially this microwave exposure can be considered to be athermal (section 1.6.2) as no temperature change could be detected from the exposure. In this context it is interesting to recall the results illustrated in Figure 7.22 where reduced apo  $\alpha$ -lactalbumin exposed to pulses of athermal 2.450 GHz was shown to precipitate slower than the two control samples.

The synergy between dissolved CO<sub>2</sub> and microwave exposure should be further explored as intriguing observations have been reported in the literature over the last few years on this topic. Spilimbergo *et al*<sup>218</sup> studied the synergistic effect of high pressure CO<sub>2</sub> and pulsed electric field on the inactivation of bacteria as an alternative to pasteurization of thermally labile compounds. It was shown that a synergy existed which depended on the electrical field strength and number of pulses. Temperature variations were not explored.

Ishikawa *et al*<sup>219</sup>, using CD spectroscopy, found that the protein myoglobin was irreversibly unfolded by heating and addition of gaseous CO<sub>2</sub> compared to the reversible unfolding of the protein by heat, pH-lowering or addition of a denaturant.

In an unrelated study on the quenching of phosphorescence of fully buried tryptophan in proteins, Wright *et al*<sup>220</sup> showed that small uncharged molecules (e.g. H<sub>2</sub>S, CS<sub>2</sub>) were most effective in penetrating the interior of target protein molecules, amongst which was ADH. They argued that H<sub>2</sub>O and CO<sub>2</sub> resemble H<sub>2</sub>S, CS<sub>2</sub> in size and would show similar diffusion behaviour. This would explain the results observed in the TEM cell (Chapter 6). The penetration of CO<sub>2</sub> into the protein molecules prevents the proteins from refolding as was observed in myoglobin<sup>219</sup>. By applying microwave exposure, and therefore, temporarily increasing the temperature of the solution, more molecules will be shifted in the unfolding pathway to the

partially unfolded state (reversible; see Figure 1.4). In so doing, they will absorb CO<sub>2</sub> into their interior and as a result the unfolding would potentially become irreversible. Therefore, more unfolding will occur compared to control samples as was observed in the TEM cell and in the experiment with ADH in section 10.1.

## 10.2 EFFECT OF MOLECULAR CROWDING ON OVOTRANSFERRIN PRECIPITATION

The rates of biochemical processes in the living cell are very different from rates determined by *in vitro* studies<sup>221</sup>. Cells are crowded with high concentrations of macromolecules. To mimic conditions in the cellular environment, non-labile crowding agents such as glycerol and dextran are often dissolved in tandem with the proteins of interest<sup>221; 222</sup>.

As most of the experiments undertaken in this project were of relatively low concentrations of proteins, it was of interest to determine the effect of pulsed microwaves on the rate of aggregation of a protein that was incubated with a crowding agent. The target protein for this experiment was ovotransferrin.

A sample of 0.2 mg/ml ovotransferrin, 20 mM DTT in the presence of 20% of dextran (w/v) in 0.1 M phosphate buffer, 0.1 M NaCl, pH 7.2, was investigated at 45°C.

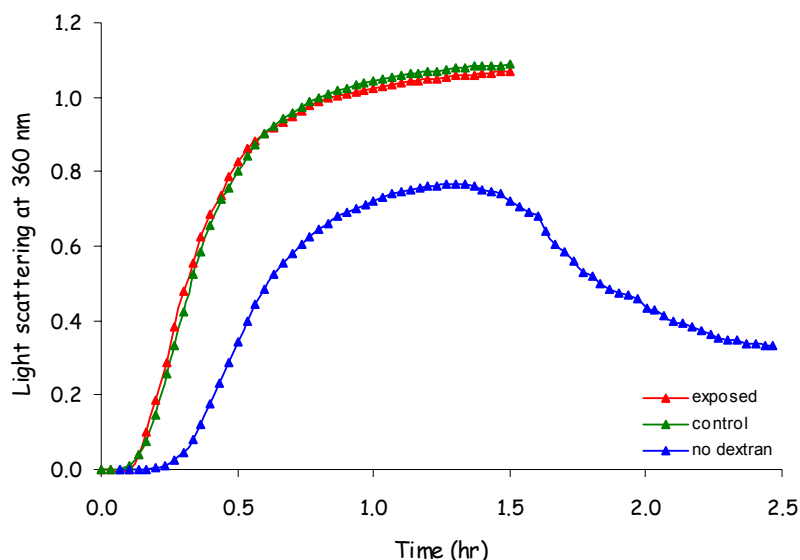


**Figure 10.3:** 0.2 mg/ml Ovotransferrin, 20 mM DTT, 20% dextran in 0.1 M phosphate buffer, 0.1 M NaCl, pH 7.2 was exposed to 5 pulse periods of 2.450 GHz at 45°C. The SAR was estimated to be 14.0 W/kg (measured at the base of the cuvette). The control sample of Figure 7.25, cell 5 (no dextran) has been included for reference to show the increase in precipitation due to the crowding agent.

The sample was exposed to five pulse periods of 2.450 GHz and the SAR was estimated to be  $14.0 \pm 1.6$  W/kg (measured at the base of the cuvette). The results are plotted in Figure 10.3.

The ratio exposed/control (initial rate of precipitation) was 1.08. The temperature of the exposed, averaged over a six minute period, was  $\sim 44.9^\circ\text{C}$  compared to the control that was  $44.3^\circ\text{C}$ . The initial rate of precipitation and the extent was enhanced for both the exposed and control samples when compared to a reference control (Figure.10.3). This is in agreement with an earlier study where protein aggregation was found to be enhanced in a crowded environment<sup>223</sup>. However, in this study the exposure to pulsed microwaves did not have a significant effect on protein aggregation in the presence of a crowding agent (Figure 10.3). This is likely to be due to the fact that the SAR in the experiment was 14 W/kg, which equates to a transient temperature increase of  $1.2^\circ\text{C}$  every six minutes. In a similar experiment without the presence of a crowding agent, the exposed sample precipitated faster than a control when the SAR was 33.2 W/kg, equating to a  $2.9^\circ\text{C}$  temperature increase every six minutes. It is therefore likely that a temperature threshold exists below which the equilibrium between native and unfolded protein, via the intermediate states, is not disturbed. This still needs to be clarified and tested without *and* in the presence of a crowding agent.

---

## CHAPTER 11

---

### ELECTRIC FIELD EXPOSURE

*In vivo*, cells are known to maintain electric fields of 100-500 kV cm<sup>-1</sup> across membranes <sup>224</sup>. These huge field potentials are important to the proper functioning of specific proteins and enzymes and are the more remarkable when compared to the dielectric breakdown of pure water that occurs at an electric field of ~ 100kV cm<sup>-1</sup>. Findings that radio waves caused increased enzyme activity <sup>85; 87; 89; 92</sup> and that static electric field exerted a thermal-like effect on insulin in molecular dynamics studies <sup>119</sup>, led to the speculation that electric fields could act as a stress on proteins that were already destabilised by, for example, temperature. Two target proteins were investigated: citrate synthase (CS), a protein that was destabilized by heat and alcohol dehydrogenase (ADH), a protein that was stabilised by chelation of its intrinsic zinc atom. In contrast to microwave exposure, which was found to be temperature inducing under conditions described in Chapters 7 to 10, an electric field exposure of 5 to 10 kV cm<sup>-1</sup> was considered to have a non-thermal impact on the solution.

#### 11.1 APPLICATION OF DC ELECTRIC FIELD

##### 11.1.1 CITRATE SYNTHASE

Citrate synthase was used as the target protein in the electric field experiments as this protein was readily unfolded by application of heat only (sections 5.3 and 7.4). The concentration and buffer system are described in section 2.6. The light scattering at 360 nm was noted for two identical samples of CS in the spectrophotometer after which they were transferred to the heating block. One sample was exposed to an electric field of 5 or 10 kV cm<sup>-1</sup> for ten minutes, the second sample was held as the control. After the exposure both samples were placed in the multi-cell holder of the spectrophotometer to monitor light scattering at 360 nm.

The samples had not reached the baseline temperature at ten minutes into the experiment (see Figure 3.3). Therefore, temperature measurements are reported as average temperatures. In the first electric field experiment performed in the laboratory, where cuvettes were wrapped with insulating tape (see Experimental section), the average temperature, measured at 17 mm from the base of the cuvette, over the first ten minutes of the experiment was 32.9°C for the exposed sample and 34.2 °C for the control sample. After the application of 5 kV cm<sup>-1</sup> for ten minutes, the insulating tape was removed and the cuvettes placed in the multi-cell holder of the spectrophotometer. The exposed was placed in cell 5 (the baseline temperature at 17 mm was 42.1°C) and the control in cell 6 (the baseline temperature at 17 mm was 42.3°C). Therefore the temperature of the control was on average 1.3°C warmer than the exposed in the first ten minutes.

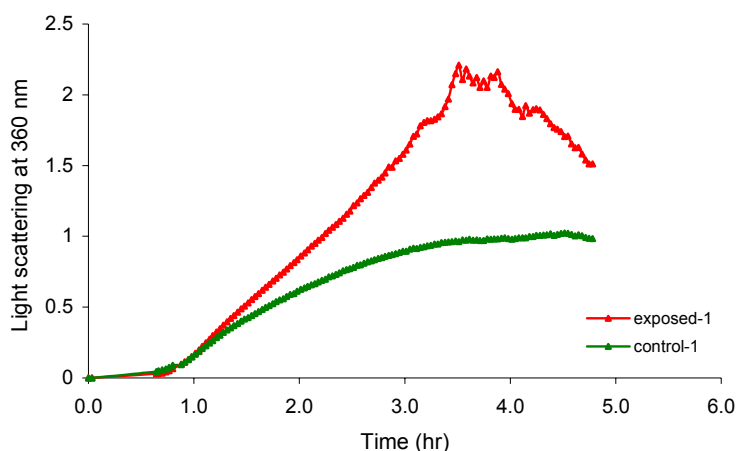


**Figure 11.1:** Exposure of 1.0 ml of 3  $\mu$ M CS in 80mM phosphate buffer, pH 7.5 to 10 minutes of 5kV cm<sup>-1</sup> DC at an average temperature of 32.9°C compared to a control that was held at an average temperature of 34.2°C. After the exposure, the samples were placed in an incubator with a temperature of 42°C. All temperatures were measured at 17 mm from the base of the cuvette.

The small difference in time it took both samples to reach the baseline temperature once they were placed in the multi-cell holder was not accounted for. The initial rate of precipitation of the control sample (Figure 11.1) was larger than the exposed (ratio exposed/control is 0.85) however after one hour, the precipitation of the exposed became much more enhanced than the

control and after three and a half hours, the precipitates started to fall to the bottom of the cuvette as can be seen from the drop in light scattering (Figure 11.1).

In subsequent experiments, the exposed and control samples were incubated in the multi-cell holder of the spectrophotometer at  $\sim 42^{\circ}\text{C}$  for 6 or 10 minutes followed by incubation and exposure in the heating block. For electric field exposures of 5, 8 or  $10\text{ kV/cm}$  the ratio of exposed/control (initial rate of precipitation) was either  $<1$ ,  $>1$  or  $\sim 1$ ; no pattern could be observed in the aggregation. In Figure 11.2 is shown the results of an exposure experiment of 5 and  $10\text{ kV}$ .

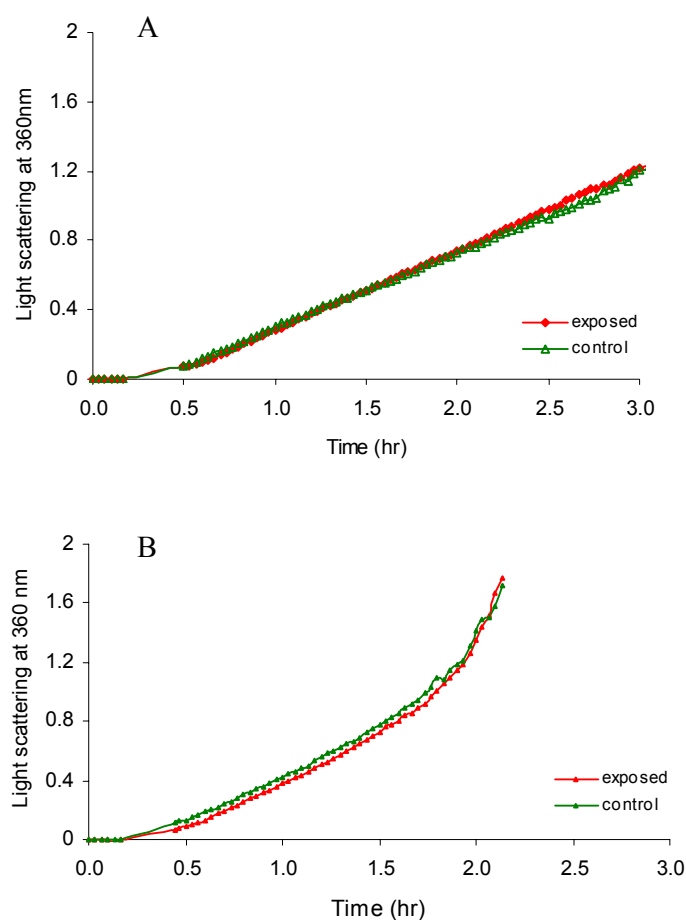


**Figure. 11.2:** Exposure of  $1.0\text{ ml}$  of  $3\text{ }\mu\text{M}$  CS in  $80\text{ mM}$  phosphate buffer, pH 7.5 to 10 minutes of  $5\text{ kV cm}^{-1}$  DC (A) and  $10\text{ kV cm}^{-1}$  DC (B). The samples were firstly incubated for 6 and 10 minutes in the multi-cell holder at  $42^{\circ}\text{C}$  followed by incubation and exposure for 10 minutes in the heating block that was  $40.5$  and  $40.7^{\circ}\text{C}$  for exposed and control respectively. After exposure the samples were replaced in the multi-cell holder.

The ratios of the initial rate of incubation (exposed/control) are 0.76 and 0.81 for the experiments in Figure 11.4 A and B respectively. In the heater, the exposed sample was on average 40.5°C and the exposed 40.7°C (average of measurements between 10 and 17 mm from the base of the cuvette). Therefore it can be concluded that the samples were at the same average temperature for the duration of the experiment (see also Figure 3.1 that shows the variability between cells in the multi-cell holder).

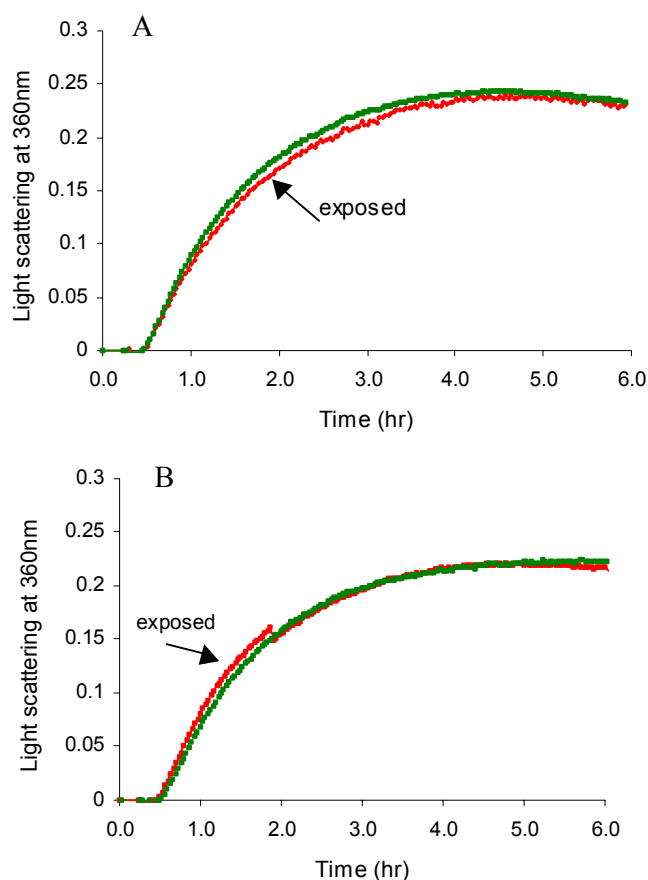


**Figure.11.3:** Exposure of 1.0 ml of 3  $\mu$ M CS in 80 mM phosphate buffer, pH 7.5 to 10 minutes of 5kV cm<sup>-1</sup> DC (A) and 10 kV/cm DC (B) at room temperature. After exposure the samples were placed in the multi-cell holder at 42°C.

It was postulated that the unfolding of CS was induced too rapidly by temperature alone while being exposed to an electric field at 42°C compared to ~ 34°C as in the first experiment (Figure 11.1).



Figure 11.3 shows the results of samples that were exposed to an electric field at room temperature after which they were incubated in the multi-cell holder at 42°C. The ratios of the initial rates of precipitation (exposed/control) were 0.92 for 5 kV cm<sup>-1</sup> and 1.08 for 10 kV cm<sup>-1</sup>. These values are not significant enough to demonstrate a difference between the exposed and control samples.

An ANS binding study was undertaken on CS immediately after a 10 minute exposure to a 10 kV cm<sup>-1</sup> exposure at ~ 27°C. The temperature of both samples after exposure was 28.9°C (measured 13 mm from the base of the cuvette). The samples showed a low fluorescence intensity of which the control sample showed slightly more hydrophobicity than the control (Figure 11.4). Thus, the exposed hydrophobicity of CS was not affected greatly by electric field exposure, implying that the electric field did not alter the conformation of the protein. This confirms observations from light scattering experiments (section 7.10.2) which established that only a small population of CS unfolds at this temperature

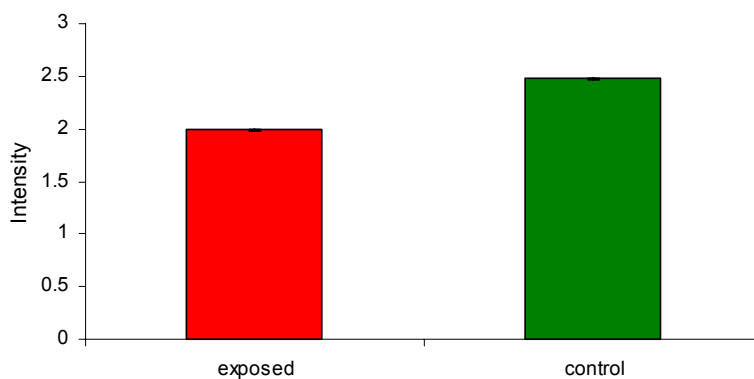


**Figure 11.4:** Binding of 60 µl 10mM ANS by two samples of 3 µM CS in 80mM phosphate buffer, pH 7.5. One sample was exposed to 10 kV cm<sup>-1</sup> DC for 10 minutes at ~ 27°C (measured at 13 mm from the base of the cuvette). The second sample was the control. The bar graph represents the detected intensity (average) of 479-480.8 nm.

In repeat experiments on CS when samples were incubated and exposed at temperatures of ~ 35°C, the results did not support the findings of the first experiment, as is shown in Figure 11.5. The ratio exposed/control (initial rate of precipitation) was 0.98 and 1.19 for exposed/2<sup>nd</sup> control. After about two and a half hour the light scattering of the exposed sample increased

significantly in an almost linear fashion. For the experiment represented in Figure 11.5 B, the ratio of exposed/control was 1.08, however the extent of precipitation of the control sample, after two hours was greater than for the control.

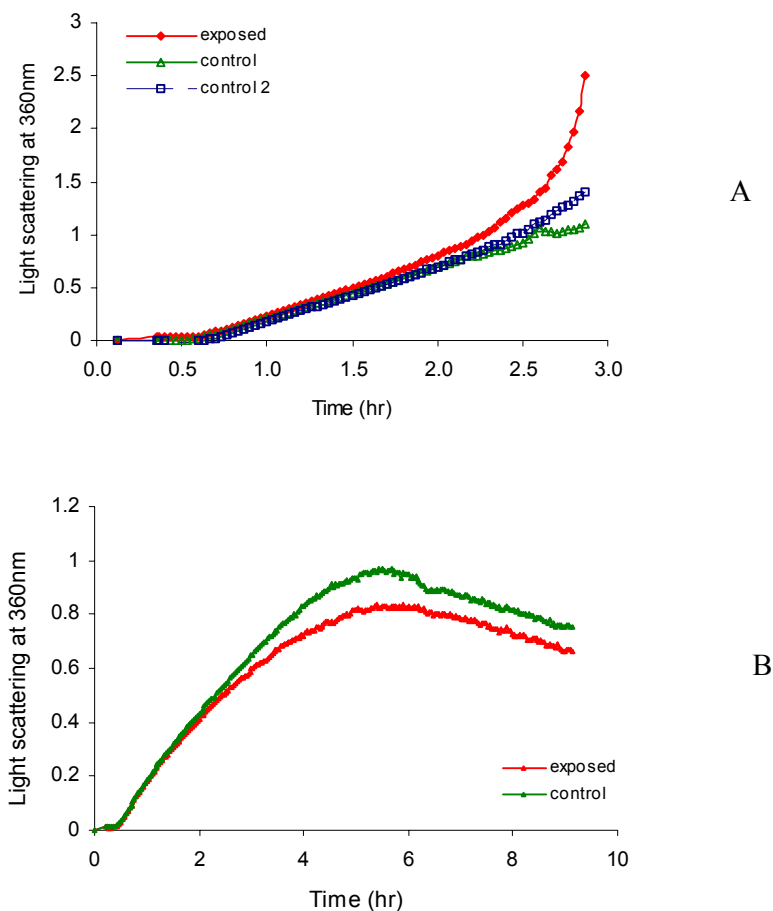


**Figure. 11.5:** Exposure of 1.0 ml of 3  $\mu\text{M}$  CS in 80 mM phosphate buffer, pH 7.5 to 10 minutes of  $5\text{kV cm}^{-1}$  DC at  $\sim 35^\circ\text{C}$  in two experiments (A and B). In one experiment (A) a second control was left in a polystyrene box for ten minutes. After exposure the samples were placed in the multi-cell holder at  $42^\circ\text{C}$ .

### 11.1.2 ALCOHOL DEHYDROGENASE (ADH)

Two 3.6  $\mu\text{M}$  samples of ADH, 1 mM 1,10 phenanthroline in 0.1 M phosphate buffer, 0.1 M NaCl, pH 7.0 were examined for differences in exposed hydrophobicity after one sample was exposed for 10 minutes to a  $10\text{ kV cm}^{-1}$  DC electric field. The temperature of the samples after exposure was  $30.1^\circ\text{C}$  and  $30.3^\circ\text{C}$  for exposed and control respectively. After titration of 50  $\mu\text{l}$ , 10mM ANS, the exposed sample exhibited greater fluorescence (68 units) compared to the

control sample (64 units) thus indicating that the exposed sample had more exposed hydrophobicity due to greater unfolding than the control sample (Figure 11.6).

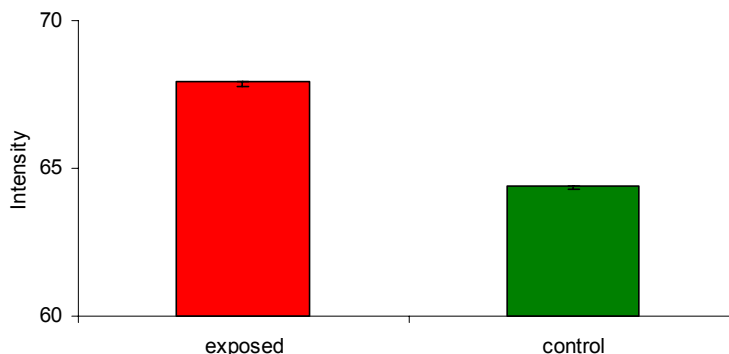


**Figure 11.6:** Binding of 50  $\mu$ l, 10 mM ANS by two samples of 3.6  $\mu$ M ADH, 1 mM 1,10 phenanthroline in 0.1 M phosphate buffer, 0.1 M NaCl, pH 7.0. One sample was exposed to 10  $\text{kV cm}^{-1}$  DC for 10 minutes at  $\sim 28^\circ\text{C}$  (measured at 13 mm from the base of the cuvette). The second sample was the control. The bar graph represents the detected intensity (average) of 479-480.8 nm.

## 11.2 APPLICATION OF A DC FIELD FOLLOWED BY MICROWAVE EXPOSURE

### 11.2.1 CITRATE SYNTHASE

In a separate experiment, CS samples were incubated in the spectrophotometer for 10 minutes at  $42^\circ\text{C}$  followed by 5 minutes incubation in the block heater and ten minute exposure to 10  $\text{kV cm}^{-1}$ . After exposure to the electric field, the exposed sample was further exposed to one pulse of microwaves (550 ml water in plastic box; pulse period 4 seconds) before both samples were returned to the multi-cell holder of the spectrophotometer. The microwave exposure was repeated four more time, at six minute intervals. The control sample stayed in the multi-cell holder. The exposed sample was compared to another CS sample that was exposed to five pulse periods under the same temperature conditions (Figure 11.7). The initial rate of precipitation was similar for all samples however, after about 0.5 hour the microwave exposed samples precipitated faster than the control. The sample that was also exposed to an electric field precipitated to a larger extent than the sample which was exposed to microwaves only.

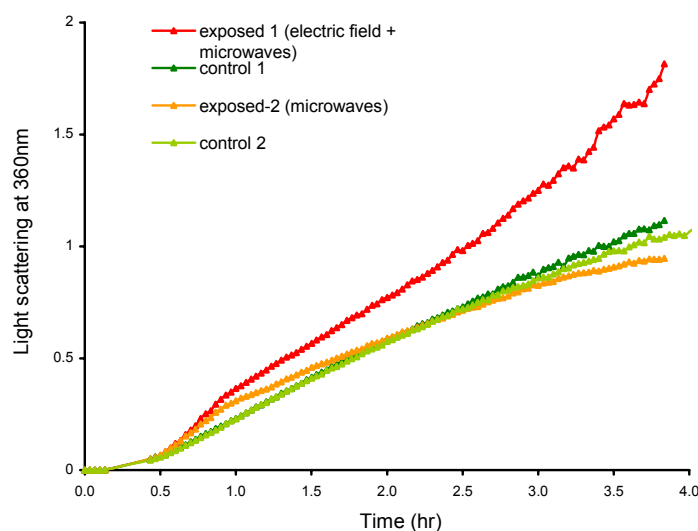


**Figure 11.7:** Comparison of two experiments on solutions of 3 $\mu$ M CS in 80mM phosphate buffer, pH 7.5 at 42°C that were exposed to either an electric field of 10kV cm<sup>-1</sup> DC (10 minutes) plus 5 pulse periods of microwaves or to 5 pulse periods of microwaves only.

### 11.3 APPLICATION OF AC ELECTRIC FIELD

#### 11.3.1 CITRATE SYNTHASE

The effect of an alternating current at 50 Hz of 4 kV cm<sup>-1</sup> to a 3  $\mu$ M CS solution was investigated for an exposure duration of ten and twenty minutes. Samples were incubated in the multi-cell holder for two minutes, the solutions were then transferred to plastic cuvettes that were wrapped with insulating tape. Two samples were placed in the heating block that was set to 43°C. The samples were incubated for 10 minutes. One sample was exposed to 4 kV cm<sup>-1</sup> for 10 minutes and the second sample was kept in the incubator as a control. The average temperature of the samples after exposure was 35.6°C. Following exposure, the solutions were transferred to quartz cuvettes and placed in the multi-cell holder of the spectrophotometer at 42°C. Light scattering measurements were taken every two minutes (Figure 11.9 A). In the second experiment (Figure 11.8 B), the protein solution, after being placed in the heating block, was immediately exposed to an AC field of 4 kV cm<sup>-1</sup> for twenty minutes. After the exposure,

the temperature of the exposed sample was 39°C (measured with an alcohol thermometer) and the control sample was 38°C.

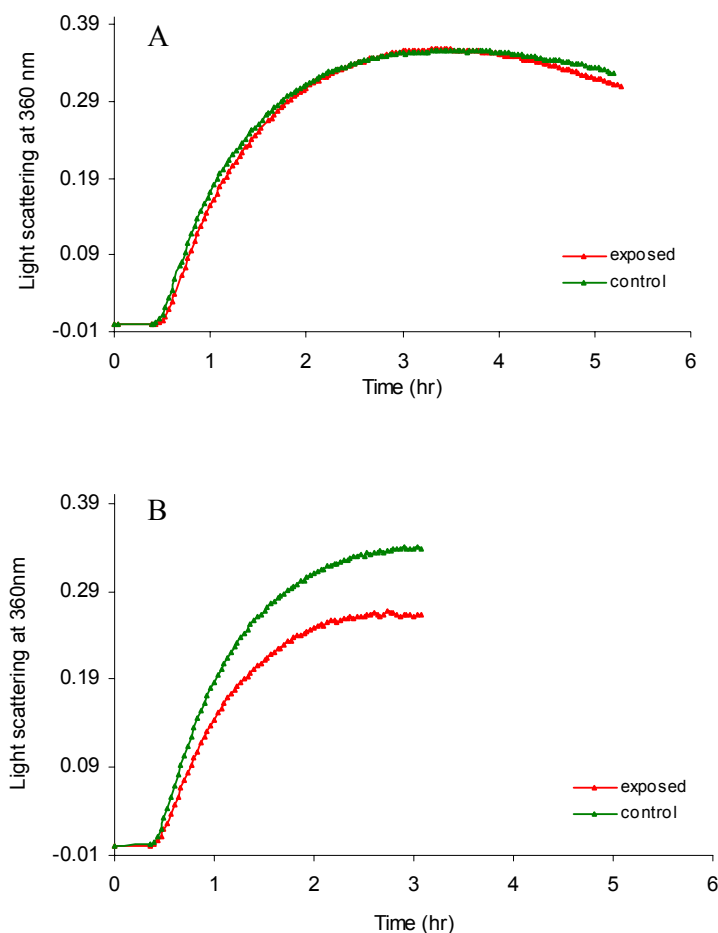


**Figure.11.8:** Exposure of 1.0 ml of 3  $\mu\text{M}$  CS in 80 mM phosphate buffer, pH 7.5 to 10 minutes (A) of  $4\text{kV cm}^{-1}$  AC at an average temperature of  $\sim 35.6^\circ\text{C}$  and 20 minutes (B) at  $\sim 39^\circ\text{C}$  (exposed) and  $\sim 38^\circ\text{C}$  (control). After exposure the samples were placed in the multi-cell holder at  $42^\circ\text{C}$ . The temperatures were measured at 17 mm from the base of the cuvette (A) and with a thermometer (B).

The ratio of the initial rate of incubation (exposed/control) for the AC electric field experiment of ten minutes duration (Figure 11.9 A) was 0.89. The precipitation profile of the exposed and control was similar. For the experiment of twenty minute duration to AC field (Figure 11.8 B), the ratio was 0.74 (exposed/control). Not only did the control precipitate at a faster rate, also the extent of precipitation was larger.

Samples in the first experiment were slightly cooler than in the second experiment which is reflected in Figures 11.8 A and B for the control samples only. The extent of the precipitation of the exposed sample in the second experiment, although a degree hotter than the control, is less than all the other samples.

#### 11.4 SUMMARY OF RESULTS

The application of a DC electric field of 5 or 10 kV cm<sup>-1</sup> to a solution of 3 μM CS did not have an effect on the initial rate of precipitation. In a few experiments, the extent of precipitation of the exposed was greatly enhanced after initial exposure (Figures 11.1, 11.5, 11.7). Hydrophobicity studies on CS after 10 minutes of electric field exposure at 32.9 and 40.5 °C showed no significant difference between exposed and control samples for CS immediately after exposure to the electric field; this could be explained in the context of the small population of CS that unfolds at that particular temperature.

A 6% difference was found in the exposed hydrophobicity of ADH samples in which one sample was exposed to 10 minutes of DC electric field. ADH is destabilised by addition of 1, 10 phenanthroline that binds to the intrinsic zinc atom in the protein. The protein, in its destabilised form responds to changes in temperature rapidly (Chapter 7). Additional experiments, e.g. light scattering experiments, are needed to verify if the exposed sample precipitates more than the control.

When a CS sample was exposed to an electric field followed by exposure to microwaves, the exposed sample that was also exposed to microwaves precipitated to a larger extent than samples that were exposed to electric field or microwaves only.

The electric field effects the net dipole of the protein so that the dipole vector moves into the direction of the field<sup>153; 225</sup>. It is postulated that when the protein starts to unfold, due to the temperature stress, the unfolded intermediates will aggregate but at the same time re-alignment with the electric field may cause the aggregates to be different in structure to the aggregates formed under control conditions. This may not be detectable in the early stages of the aggregation and precipitation process until a larger population of proteins has aggregated.

Of the two experiments (10 and 20 minutes) that explored the effect of AC fields on CS unfolding, both showed that the exposed sample precipitated slower but the extent of precipitation was much less for the sample that was exposed twice as long when compared to a control. The temperature was not considered to have contributed to the effect. Studies on ovalbumin and  $\beta$ -lactoglobulin<sup>226</sup> that were exposed to exponential decay electric pulses of 31.5 and 30.0 kV cm<sup>-1</sup> respectively, showed that exposure did not lead to modification in protein conformation. In ovalbumin, the exposure enhanced ionization of SH groups into the reactive S<sup>-</sup> form, however this effect was found to be reversible<sup>226</sup>. It was observed that electric pulses of 33-36 kV cm<sup>-1</sup> dissociated large aggregates<sup>226</sup>. This may be the reason why the light scattering was lower for exposed samples.

The results of the few experiments on CS and ADH that were exposed to electric fields would suggest that the hypothesis “that the initial rate of precipitation of target proteins exposed to an electric field of 50 Hz is significantly higher than that of a control held at the same average temperature” was not proven. However, this is only a tentative finding and the work needs to be repeated to demonstrate if the nature of the field (AC vs. DC) has an influence on the extent of precipitation compared to controls. It would be useful to measure the hydrodynamic size of particles in solution (*Z* average) at different time points after exposure.

---

## CHAPTER 12

---

### CONCLUSIONS AND FUTURE DIRECTIONS

#### *The effect of pulsed microwaves to target proteins in vitro*

In this project, a series of extra and intra cellular functional proteins were stressed by chemical or temperature means. In addition, the proteins were also exposed to pulsed microwaves or an electric field. The dual stress approach is justified as physiological processes do not occur in isolation. For example, studies have shown that the dual action of chemical cancer promoters and electromagnetic fields on cell membranes may be responsible for tumour formation<sup>227</sup>. It is therefore of fundamental importance to understand the influence of multiple stresses on protein unfolding.

The rebuilt domestic microwave oven that enabled pulses of different durations to be emitted every six minutes, proved reliable and efficient. The main difficulty in this work was to ensure that exposed and control samples were maintained at the same temperature. The application of the spectrophotometer, for incubation and light scattering measurements in tandem with the exposure source (the microwave oven and the electric field exposure unit) allowed for a robust examination of the temperature within the samples over a six minute period (*Exposure systems 2 and 3*).

It was demonstrated, using *Exposure systems 2 and 3*, that the initial rate of precipitation of stressed target proteins that were also exposed to pulsed microwaves, once every six minutes, was significantly higher than of an unexposed control held at the same average temperature. The microwave pulses caused a transient temperature jump in the temperature of the protein solution. This increase in temperature lasted in the order of a second which is the smallest time scale that could be measured. In the cases where the difference in initial rate of precipitation



was not found to be statistically significant, the result could be explained by the magnitude of the temperature relative to the unfolding temperature. Thus, only if the proteins were incubated at a temperature at which most of the protein population favoured unfolding, was a temperature excursion, caused by microwave exposure, significant. Insulin provides a good example of this case.

The effect of the microwave pulses was found to be of a thermal nature. A few experiments were undertaken at very low SAR but no differences were detected in light scattering of the solutions nor in the circular dichroism spectra. Similarly, proteins did not unfold when exposed to microwave radiation only; there was the requirement for the protein to be stressed by other means also.

Experiments exploring non-thermal effects, by utilizing the TEM cell, were not conclusive and better methods need to be developed to test the assays used in this project. The finding that the protein unfolding was enhanced when the CO<sub>2</sub> incubator was left on needs further investigation. Bohr *et al* was able to demonstrate that non-thermal microwave exposure of 5 seconds duration was enough to greatly enhance the kinetics of unfolding and folding in  $\beta$ -lactoglobulin dissolved in 4 M urea<sup>113, 114</sup>. The target proteins used in this project were dissolved in buffer to ensure a native conformation. To further understand the complexity of pulsed microwave exposure on protein conformation, studies on the effect of microwaves on the folding/unfolding kinetics of proteins utilizing different buffers and concentrations would be most useful.

#### *The average temperature and the validity of the six minute period*

The thermal unfolding pathway of a globular protein is determined by its structure and is believed to occur via a series of steps involving various intermediate states. The process can be monitored by circular dichroism and plots of the unfolding show the temperature range at which the protein seems stable and at which it rapidly or slowly unfolds, depending on the slope of the curve. It was observed that some proteins in this study were not significantly affected by a transient temperature increase when they were maintained at a certain temperature, compared to a control. However, when the incubation temperature was increased, a more rapid unfolding was

triggered in the exposed sample. This observation implies that proteins have a unique thermal unfolding pattern and when exposed to a pulse of microwaves at a critical temperature where the unfolding slope rises dramatically, even at relatively low SAR, unfolding and precipitation occurs much faster than for a control sample incubated at the same temperature. In future work, studies on the critical temperature at which a protein unfolds more rapidly should help determine thresholds for SAR.

Elemental studies on protein conformational change utilizing fluorescence, circular dichroism and electrospray mass spectrometry showed that these methods lend themselves well for future research.

The pulsed microwaves caused a transient temperature increase and the temperature of the solution fell to its baseline temperature within six minutes, prior to the next pulse exposure. Small temperature differences between the control and exposed samples were accounted for. The temperature of the protein solutions was averaged over six minutes. Thus, it could be shown that when an exposed and control sample had the same average temperature over that period, the aggregation and precipitation were still enhanced for the exposed sample for certain proteins. Plots of the initial rate of precipitation of several protein solutions that were heated at different temperatures in the same instrument showed that the initial rate of precipitation for an exposed sample held at the same average six minute temperature lay above the trendline set by the control samples. These results confirmed that the kinetics of unfolding was enhanced for the microwave exposed sample. Even though protein concentrations were quite dilute and studies with crowding agents were incomplete, it is not valid to assess the effect of a time-varying temperature exposure on the proteins studied in this work by carrying out a six-minute average as permitted in the ICNIRP guidelines <sup>62</sup>.

*sHsps were efficient in suppressing aggregation but higher concentrations were needed in the presence of pulsed microwaves*

At specific subunit molar ratios of  $\alpha$ -crystallin to stressed target proteins, aggregation and precipitation was suppressed however more  $\alpha$ -crystallin was required for the microwave

exposed samples compared to the controls. This implies that sHsps work as effective chaperones to suppress stress-induced aggregation of target proteins arising from pulsed microwave exposure.

These findings are of interest when they are extrapolated, albeit cautiously, to the physiological regime. The only way for proteins in the body to experience a short jump in temperature is through a pulse of radiation from, for example, a microwave source or a laser. A conventional heating source warms up the organism from the outside to the inside over a large area and the heat is able to dissipate throughout the body. However, a pulse of microwave energy is capable of reaching a selected area in the interior of the organism thereby transferring the energy (heat) directly to inner organs and cells. Protein turnover is a natural and a recurring process in all organisms. Therefore, it is feasible to suggest that an environmental stress such as one or several temperature jumps could interfere with the process of protein breakdown. Organs and cells are constantly attacked by outside influences such as viruses and bacteria, cigarette smoke, alcohol, environmental pollutants etc. The body's defence mechanism, the immune system, senses these "attacks" as a stress. Under stress situations the expression of molecular chaperones is increased thereby confirming that proteins are indeed affected and need protection<sup>228</sup>. Temperature jumps of only a few degrees Celsius, delivered by pulsed microwave exposure could have an effect on proteins *in vivo* especially for organs close to the epidermal tissue, such as the eyes and reproductive organs. Indeed, pulsed microwaves of 918 MHz (10-20  $\mu$ s duration at 20-40 mW/g) was found to induce cataract in rat lenses<sup>229</sup>.

It needs to be stressed that the target proteins used in the experiments were extremely dilute and are not representative of the cell environment. Studies on the effect of pulsed microwaves on proteins incubated with a crowding agent should be investigated further.

#### *The effect of low frequency electric field exposure*

More work needs to be undertaken on protein solutions exposed to an electric field before any conclusions can be drawn. The experiments did not show a difference in initial rate of

precipitation between exposed and control samples but the precipitation over time seemed to have been affected and was different for 50 Hz AC and DC fields.

### *Mechanism*

The distribution of energy to samples heated in a conventional manner like in the incubator, is through vibrational modes <sup>230</sup> that proceed in approximate thermal equilibrium. It is possible that the effect of microwaves observed in this work could be the effect of temperature rises in approximate thermal equilibrium. An additional mechanism may also occur. The electromagnetic field associated with microwaves can exert a direct action via the electric field on the sample and consequently couple with phonons or mobile species such as electrons in the molecule, driving the molecule out of approximate thermal equilibrium. The coupling could also occur via the magnetic component of the microwave field, especially materials with high susceptibility such as some ferrites <sup>230; 231</sup>. Therefore, the increase in unfolding kinetics as observed for certain proteins when exposed to pulsed microwaves could conceivably be the result of the interaction of the electromagnetic field with the protein via the aqueous medium and the layer of water molecules that surround each protein molecule <sup>1; 55</sup>. Follow-up work in this area, such as the use of different solvents, chelating agents and a selection of different metallo proteins should help identify trends. The observation that samples, incubated in a CO<sub>2</sub> environment and exposed to pulsed microwaves at relatively low SAR, unfolded faster than controls ought to be further investigated.

### *The aim of this project was achieved*

The aim of the project, *to determine the conformational effect of pulsed microwaves or an electric field on proteins that were also stressed by other means* (page 19), was achieved. Proteins that were stressed by temperature, chelation or addition of a chemical in tandem with exposure to pulsed microwaves, at specific conditions, unfolded faster than a control held at the same average temperature.

*Specific hypotheses tested*

The hypothesis that *the initial rate of precipitation of target proteins exposed to microwave pulses once every six minutes is significantly higher than that of a control held at the same average temperature, where the average is taken over a six minute period*, was accepted and is discussed in section 7.10 and table 7.8.

The hypothesis, that *the sHsp,  $\alpha$ -crystallin, prevents the aggregation and precipitation of target proteins under the above regimes*, was tested. It was accepted and is discussed in section 7.9 and table 7.8

The third hypothesis that *the initial rate of precipitation of target proteins exposed to an electric field of 50 Hz, or lower frequency, is significantly higher than that of a control held at the same average temperature* was not proven. However, this work needs to be repeated and expanded to include more proteins.

(section 11.3).

## APPENDIX 1

### BUFFERS

#### 50mM TRIS, pH 7.2 – Homogenising buffer (200ml)

TRIS acid	0.37 g
TRIS base	0.70 g
DTT (1mM)	0.035 g
NaN <sub>3</sub> (0.04%)	0.080 g

#### 50mM TRIS, pH 5 -Column buffer (2L)

TRIS acid	11.0 g
TRIS base	3.6 g
NaN <sub>3</sub>	0.4 g

### PHOSPHATE BUFFER

#### Stock solution of 50 ml 0.2M Na<sub>2</sub>HPO<sub>4</sub> (solution 1)

1.42 g. Na <sub>2</sub> HPO <sub>4</sub> in milli Q water,	49.6 ml
NaN <sub>3</sub> (5%)	0.4 ml

#### Stock solution 0.2M NaH<sub>2</sub>PO<sub>4</sub>.2H<sub>2</sub>O (solution 2)

1.56g. NaH <sub>2</sub> PO <sub>4</sub> .2H <sub>2</sub> O milli Q water,	49.6 ml
NaN <sub>3</sub> (5%)	0.4 ml

#### 0.1M phosphate buffer (50ml)

	pH 7.0	pH 7.2	pH7.5
Solution 1	15.25 ml	18 ml	21 ml
Solution 2	9.75 ml	7 ml	4 ml
Milli Q water	25 ml	25 ml	25 ml

## APPENDIX 2

### DESCRIPTION OF ELECTRONICS MICROWAVE OVEN <sup>163</sup>

The oven is a modified domestic microwave oven. The oven's normal controller was replaced with a customised BASIC Stamp microcontroller (a BS2-IC from Parallax). The customised controller turns the oven on at six minutes intervals for a preset time (set in software by constant "Default" or for a preset number of RF pulses (set by digital switches on the front panel).

The oven was initially intended to be operated in an environmental chamber, which controls the temperature and humidity of the air. To improve circulation of the air, a fan was fitted to the door.

Mounted on the front panel of the oven (to the right of the door), are a three position toggle switch that controls the operation of the oven, and a set of digital switches that set the number of RF pulses per exposure cycle (i.e. every six minutes). The three positions for the toggle switches are:

- RESET (up), which resets the controller to the start of the program and loads the settings from the digital switches into the controller. This is a momentary position and the switch should return to STOP position after it is released.
- STOP (centre) which puts the controller into idle mode.
- RUN (down), which causes the oven to turn on for a short burst every cycle. The cycle time can be changed, by reprogramming the controller. Opening the door has the same effect as switching to STOP.

A small window at the top of the front panel contains three LEDs. The green LED on the left indicates that power for the fan and the microcontroller is present. The red light indicates that RF is being detected. The yellow LED warns that at least one cycle has passed when no RF was detected; it is extinguished by resetting the controller/oven. It blinks periodically in normal operation as a result of the particular behaviour of the microcontroller. If the yellow light is flashing, it indicates that at least ten cycles (set in software by constant "MaxDuds") have

passed when the microcontroller has detected no RF and indicates a fault with the oven or bad layout inside the oven.

## OPERATION

After the door has been loaded with samples to be exposed, the number of RF pulses per cycle can be set with the digital switches and this value is loaded into the microcontroller by temporarily switching to RESET. To start exposure, the oven is switched to RUN. The controller then waits approximately ten seconds (set in software) before it starts exposure, to allow the operator the change something if need be. The same applies if the door is open, i.e. exposure will not start for about ten seconds after the door has been closed (provided the oven is switched to RUN).

If the oven is switched from RUN to STOP or the door is opened during a cycle but between RF bursts, there is no effect on the timing of the cycle provided that the door is closed and the oven switched to RUN ten seconds before the next burst starts.



### APPENDIX 3

Conversion factors for the Luxtron Fiber Optic Probes from calibration curves with thermometer temperatures, as supplied by the manufacturer:

#### *Probe 1*

$$\text{Actual temperature probe} = (\text{measurement} - 1.667)/0.99798$$

#### *Probe 2*

$$\text{Actual temperature probe} = (\text{measurement} - 1.9971)/0.98406$$

#### *Probe 3*

$$\text{Actual temperature probe} = (\text{measurement} - 2.4862)/0.98243$$

#### *Probe 4*

$$\text{Actual temperature probe} = (\text{measurement} - 2.9055)/0.97726$$

## APPENDIX 4

### BUFFER AND EXPOSURE CONDITIONS I

80mM phosphate buffer, pH 7.5; 550ml water in plastic box inside microwave;  
Duration of pulses, every six minutes, 3.2 seconds.

Measured from base of cuvette	delta T	SAR	stdev.
position 1 - 0 mm from base of cuvette	1.05	12.19	1.71
position 2 - 10 mm from base of cuvette	1.89	21.90	1.40
position 3 - 17 mm from base of cuvette	1.91	22.17	1.20
position 4 - 23 mm from base of cuvette	3.13	36.27	7.57

### BUFFER AND EXPOSURE CONDITIONS II

0.1M phosphate buffer, pH 7.0; 550ml water in plastic box inside microwave.  
Duration of pulses, every six minutes, 5 seconds.

Measured from base of cuvette	delta T	SAR	stdev.
position 1 - 0 mm from base of cuvette	2.07	24.08	3.36
position 2 - 10 mm from base of cuvette	3.12	37.18	6.10
position 3 - 17 mm from base of cuvette	3.45	40.05	3.66
position 4 - 23 mm from base of cuvette	5.23	60.68	8.11

## APPENDIX 5

### BUFFER AND EXPOSURE CONDITIONS III

0.1M phosphate buffer, 0.1M NaCl, pH 7.0; pH 7.2, 650ml water in plastic box inside microwave. Duration of pulses, every six minutes, 5 seconds.

Measured from base of cuvette	delta T	SAR	stdev.
position 1 - 0 mm from base of cuvette	1.26	14.56	2.47
position 2 - 10 mm from base of cuvette	2.14	24.67	3.90
position 3 - 17 mm from base of cuvette	2.48	28.77	1.27
position 4 - 23 mm from base of cuvette	5.38	62.50	4.23

### BUFFER AND EXPOSURE CONDITIONS IV

0.1M phosphate buffer, 0.1M NaCl, pH 7.0; 500ml water in plastic box inside microwave. Duration of pulses, every six minutes, 5 seconds.

Measured from base of cuvette	delta T	SAR	stdev.
position 1 - 0 mm from base of cuvette	2.63	30.54	1.49
position 2 - 10 mm from base of cuvette	4.33	50.27	3.94
position 3 - 17 mm from base of cuvette	4.66	54.14	3.90
position 4 - 23 mm from base of cuvette	7.35	85.33	10.71

## APPENDIX 6

### COMPARISON OF DIFFUSION CONSTANT AT 20°C AND THE DIFFUSION CONSTANT OVER DIFFERENT TEMPERATURES AS DERIVED FROM THE HYDRODYNAMIC DATA

D is  $(K_b \times \text{absolute } T)/f$  derived from the Stokes-Einstein equation:  $f = (K_b \times T)/D$

f = frictional coefficient for a compact sphere in a viscous medium

$$f = 6 \pi \eta R$$

$$\eta (\text{eta}) = \text{poise} = \text{dyne-sec/cm}^2$$

R is the hydrodynamic radius of the protein

$\eta$  water at 20deg. C is 0.01002 g/cm<sup>s</sup> - See table for buffers at different temperatures.

$$1 \text{ Pa} = 1 \text{ kg/m-s}^2$$

$$1 \text{ dyne} = 1 \text{ g}^{-1} \text{ cm/s}^2 \text{ therefore } 1 \eta = \text{g cm s} / \text{cm}^2 \text{ s}^2$$

$$\begin{aligned} K_b &= \text{Boltzmann's constant} = 1.380658 \times 10^{-23} \text{ J/K} \quad 1 \text{ J} = 1 \text{ kg m}^2/\text{s}^2 \\ &= 1.380662 \times 10^{-23} \text{ kg m}^2/\text{s}^2 - \text{K} \end{aligned}$$

#### Calculation of $\eta$ for buffers at different temperatures

Water	CRC data		37deg			43 deg		45deg		P-buffer	P-buffer	P-buffer	P-buffer	P-buffer	P-buffer
	$\eta$	$\eta$	water	water	ratio	water	ratio	water	ratio	sol.1	sol.2	sol.1	sol.2	sol.1	sol.2
°C	mPa-s	g/cm-s	25deg	37deg	i.r.t 20deg	43 deg	i.r.t 20deg	45deg	i.r.t 20deg	°C	50mM	50mM	80mM	80mM	100mM
20	1.0020	0.01002	0.009							20	<b>1.0306</b>	1.0210	1.0479	1.0339	1.0599
30	0.7977	0.00798		0.007	69.51					37	0.7164	0.7097	0.7284	0.7187	0.7367
40	0.6532	0.00653				0.006	62			42	0.6389	0.6330	0.6497	0.6410	0.6571
50	0.5470	0.00547						0.006	59.88	45	0.6171	0.6114	0.6275	0.6191	0.6347

Use highest values

Lysozyme (1:

	Translational					
	diffusion					
	constant	hydrodynamic				
	at 20deg.	radius	Using the Stokes-Einstein equation			
	in water	R	f	T	K <sub>b</sub>	D
	10 <sup>-7</sup> cm <sup>2</sup> /sec	in cm	kg/s	in K	kg m <sup>2</sup> /s <sup>2</sup> · K	10 <sup>-7</sup> cm <sup>2</sup> /sec
lysozyme (hen)	1.13E-06	1.90E-07	3.59E-11	293.15	1.38E-23	1.13E-06

										mean distance travelled = Root(D.2t)				
Using the hydropro program										Distance	Distance	Distance	Distance	Distance
CRC data					hydrodynamic					travelled	travelled	travelled	travelled	travelled
mPa-s					radius	Using the Stokes-Einstein equation				per	per	per	per	per
PDB	Tr.Diff.Coe	$\eta$	$\eta$	R	f	T	$K_b$	D		second	second	second	minute	0.5 hr
File	$10^{-7} \text{ cm}^2/\text{sec}$	$1 \text{ kg/m-s}^2$	$\text{g/cm-s}$	in cm	kg/s	in K	$\text{kg m}^2/\text{s}^2 - \text{K}$	$10^{-7} \text{ cm}^2/\text{sec}$	cm	A	mm	mm	mm	cm
6lyz	1.08E-06	1.002	0.010020	1.99E-07	3.75E-11	293.15	1.38E-23	1.08E-06	1.47E-03	1.47E+05	0.015	0.88	2.64	
buffer	37deg.		0.71638	0.007164	1.99E-07	2.68E-11	310.15	1.38E-23	1.60E-06	1.79E-03	1.79E+05	0.018	1.07	3.22
buffer	43deg		0.63893	0.006389	1.99E-07	2.39E-11	316.15	1.38E-23	1.82E-06	1.91E-03	1.91E+05	0.019	1.15	3.44
buffer	45deg		0.61712	0.006171	1.99E-07	2.31E-11	318.15	1.38E-23	1.90E-06	1.95E-03	1.95E+05	0.019	1.17	3.51
														0.00
1dpx	1.09E-06	1.002	0.010020	1.96E-07	3.70E-11	293.15	1.38E-23	1.09E-06	1.48E-03	1.48E+05	0.015	0.89	2.66	
										mean distance travelled = Root(D.2t)				
										Distance	Distance	Distance	Distance	Distance
Using variants of temperature, density and viscosity in the 6lyz file										travelled	travelled	travelled	travelled	travelled
Hydropro					Calculated					per	per	per	per	per
Tr.Diff.Coe	$\eta$	$\eta$	R	f	T	$K_b$	D			second	second	second	minute	1 hr
file	6lyz	$10^{-7} \text{ cm}^2/\text{sec}$	$1 \text{ kg/m-s}^2$	$\text{g/cm-s}$	in cm	kg/s	in K	$\text{kg m}^2/\text{s}^2 - \text{K}$	$10^{-7} \text{ cm}^2/\text{sec}$	cm	A	mm	mm	cm
3.1lys	20deg.	1.08E-06	1.002	0.01002	1.99E-07	3.75E-11	293.2	1.4E-23	1.08E-06	1.47E-03	1.47E+05	0.015	0.88	2.64
6.1lys	20deg.	1.07E-06		0.01002	2.00E-07	3.77E-11	293.2	1.4E-23	1.07E-06	1.46E-03	1.46E+05	0.015	0.88	2.64
	37deg.		0.716	0.007164	2E-07	2.68E-11	310.2	1.4E-23	1.60E-06	1.79E-03	1.79E+05	0.018	1.07	3.22
5.1lys	37deg.	1.1E-06		0.007164	2E-07	2.68E-11	310.2	1.4E-23	1.60E-06	1.79E-03	1.79E+05	0.018	1.07	3.22
7.1lys	45deg	1.92E-06		0.006171	2.02E-07	2.35E-11	318	1.4E-23	1.87E-06	1.93E-03	1.93E+05	0.019	1.16	3.48
	45deg		0.617	0.006171	2E-07	2.31E-11	318.2	1.4E-23	1.90E-06	1.95E-03	1.95E+05	0.019	1.17	3.51
8.1lys	45deg	1.95E-06	0.617	0.006171	1.99E-07	2.31E-11	318	1.4E-23	1.90E-06	1.95E-03	1.95E+05	0.019	1.17	3.51
Hydropro										Calculated	per	per	per	per
Tr.Diff.Coe	$\eta$	$\eta$	R	f	T	$K_b$	D			second	second	second	minute	1 hr
pdb.file	temp	$10^{-7} \text{ cm}^2/\text{sec}$	$1 \text{ kg/m-s}^2$	$\text{g/cm-s}$	in cm	kg/s	in K	$\text{kg m}^2/\text{s}^2 - \text{K}$	$10^{-7} \text{ cm}^2/\text{sec}$	cm	A	mm	mm	cm
1ykf -ADH	37	7.29E-07		0.007367	4.45E-07	6.18E-11	310.2	1.4E-23	6.93E-07	1.18E-03	1.18E+05	0.012	0.71	2.12
1A06 -BSA	45	8.33E-07		0.006347	4.66E-07	5.57E-11	318.2	1.4E-23	7.88E-07	1.26E-03	1.26E+05	0.013	0.75	2.26
1e78 - BSA	45	7.58E-07		0.006347	5.12E-07	6.13E-11	318.2	1.4E-23	7.17E-07	1.20E-03	1.20E+05	0.012	0.72	2.16
4b1c -catalase	42	7.75E-07		0.006571	4.98E-07	6.17E-11	315.2	1.4E-23	7.05E-07	1.19E-03	1.19E+05	0.012	0.71	2.14
4cts -citrate synthase	42	1.01E-06		0.006497	3.81E-07	4.66E-11	315.2	1.4E-23	9.33E-07	1.37E-03	1.37E+05	0.014	0.82	2.46
2ins - insulin	37	1.72E-06		0.007367	1.88E-07	2.61E-11	310.2	1.4E-23	1.64E-06	1.81E-03	1.81E+05	0.018	1.09	3.26
1ovt -ovotransferrin	45	1.04E-06		0.006347	3.72E-07	4.45E-11	318.2	1.4E-23	9.87E-07	1.40E-03	1.40E+05	0.014	0.84	2.53

## APPENDIX 7

Temperature determinations in the cell block heater of the spectrophotometer.

Four positions were measured in 1.0 ml of solution (0, 10, 17 en 23 mm from the base of the cuvette).

The data are represented graphically in figure 3.1.

Cell	0 mm	10 mm	17 mm	23 mm	Average 10 and 17 mm
<b>Software 38°C</b>					
Cell 2		$36.82 \pm 0.06$ n=3	$36.85 \pm 0.11$ n=3	$36.99 \pm 0.16$ n=3	$36.83 \pm 0.07$
Cell 3	$36.57 \pm 0.12$ n=9	$36.68 \pm 0.09$ n=9	$36.84 \pm 0.10$ n=9	$36.98 \pm 0.08$ n=9	$36.76 \pm 0.12$
Cell 4	$36.27 \pm 0.41$ n=15	$36.76 \pm 0.17$ n=12	$36.99 \pm 0.06$ n=10	$37.06 \pm 0.13$ n=25	$36.87 \pm 0.17$
Cell 5	$36.61 \pm 0.26$ n=18	$36.88 \pm 0.06$ n=16	$37.02 \pm 0.12$ n=17	$37.14 \pm 0.07$ n=23	$36.95 \pm 0.12$
Cell 6	$36.47 \pm 0.27$ n=10	$36.91 \pm 0.21$ n=9	$37.16 \pm 0.09$ n=10	$37.20 \pm 0.11$ n=14	$37.04 \pm 0.20$
<b>Software 43°C</b>					
Cell 2	$40.55 \pm 0.35$ n=10	$41.68 \pm 0.19$ n=10	$41.82 \pm 0.25$ n=10	$42.03 \pm 0.24$ n=10	$41.75 \pm 0.21$
Cell 3	$41.36 \pm 0.34$ n=18	$41.75 \pm 0.20$ n=18	$41.86 \pm 0.24$ n=18	$42.03 \pm 0.10$ n=18	$41.80 \pm 0.23$
Cell 4	$41.01 \pm 0.44$ n=11	$41.69 \pm 0.12$ n=10	$42.01 \pm 0.07$ n=10	$42.09 \pm 0.07$ n=10	$41.89 \pm 0.20$
Cell 5	$41.49 \pm 0.19$ n=11	$41.81 \pm 0.11$ n=12	$42.06 \pm 0.14$ n=11	$42.26 \pm 0.06$ n=10	$41.93 \pm 0.16$
Cell 6	$41.18 \pm 0.26$ n=10	$42.03 \pm 0.06$ n=8	$42.27 \pm 0.13$ n=7	$42.43 \pm 0.09$ n=8	$42.14 \pm 0.15$
<b>Software 46°C</b>					
Cell 3	$44.37 \pm 0.30$ n=13	$44.39 \pm 0.22$ n=16	$44.67 \pm 0.20$ n=12	$44.98 \pm 0.20$ n=12	$44.51 \pm 0.25$
Cell 4	$43.93 \pm 0.42$ n=18	$44.75 \pm 0.17$ n=22	$45.04 \pm 0.16$ n=18	$45.16 \pm 0.10$ n=18	$44.87 \pm 0.21$
Cell 5	$44.51 \pm 0.30$ n=16	$44.75 \pm 0.10$ n=17	$45.12 \pm 0.22$ n=17	$45.33 \pm 0.13$ n=17	$44.93 \pm 0.24$
Cell 6	$44.61 \pm 0.37$ n=13	$45.06 \pm 0.12$ n=13	$45.34 \pm 0.16$ n=13	$45.49 \pm 0.13$ n=13	$45.20 \pm 0.17$

## APPENDIX 8

### UNITS OF CIRCULAR DICHROISM <sup>232</sup>

The raw output of the circular dichroism (CD) spectrometer is in ellipticity. It is measured in milli degrees and is known by the symbol  $\theta$

**Molar ellipticity  $[\theta]$**  is reported with the units **deg.cm<sup>2</sup>.dmol<sup>-1</sup>**:

$$[\theta] = \theta / (10 \times C \times l)$$

where  $C$  is the molar concentration of the sample (mol/L) and  $l$  is the pathlength in cm.

**Mean residue molar ellipticity  $[\theta]_{\text{MRW}}$**  is reported with the units **deg.cm<sup>2</sup>.dmol<sup>-1</sup>**:

$$[\theta]_{\text{MRW}} = \theta / (10 \times Cn \times l)$$

where  $C$  is the molar concentration (mol/L),  $n$  is the number of residues in the protein and  $l$  is the path length in cm.

---

---

---

**REFERENCES BY NUMBER**

---

1. Creighton, T. E. (1993). *Proteins: structures and molecular properties*. 2nd edition, W.H. Freeman and Company.
2. The National Health Museum Washington DC. (2004). <http://www.accessexcellence.org>.
3. Radford, S. E. (2000). Protein folding: progress made and promises ahead. *Trends in Biochemical Sciences* 25, 611-618.
4. Mathews, C. K., van Holde, K. E. and Ahern, K. G. (2000). *Biochemistry*. 3rd edition, Benjamin Cummings, San Francisco, Calif.
5. Glickman, M. H. and Ciechanover, A. (2002). The ubiquitin-proteasome proteolytic pathway: destruction for the sake of construction. *Physiological Reviews* 82, 373-428.
6. Berke, S. J. and Paulson, H. L. (2003). Protein aggregation and the ubiquitin proteasome pathway: gaining the UPPER hand on neurodegeneration. *Current Opinion in Genetics & Development* 13, 253-61.
7. Kungl Vetenskapsakademien. The Royal Swedish Academy of Sciences. (2004). *Advanced information on the Nobel Prize in Chemistry, Ubiquitin-mediated proteolysis*, Stockholm.
8. Parsell, D. A. and Lindquist, S. (1993). The function of heat-shock proteins in stress tolerance - Degradation and reactivation of damaged proteins [Review]. *Annual Review of Genetics* 27, 437-496.
9. Braun, B. C., Glickman, M., Kraft, R., Dahlmann, B., Kloetzel, P. M., Finley, D. and Schmidt, M. (1999). The base of the proteasome regulatory particle exhibits chaperone-like activity. *Nature Cell Biology* 1, 221-226.
10. Jolly, J. and Morimoto, R. I. (2000). Role of heat shock response and molecular chaperones in oncogenesis and cell death. *Journal of National Cancer Institute* 92, 1564-1772.
11. Treweek, T. M., Morris, A. M. and Carver, J. A. (2003). Intracellular protein unfolding and aggregation: The role of small heat-shock chaperone proteins. *Australian Journal of Chemistry* 56, 357-367.
12. Morimoto, R. I. (1993). Cells in stress: transcriptional activation of heat shock genes. *Science* 259, 1409-1410.
13. Gething, M. J. and Sambrook, J. (1992). Protein folding in the cell. *Nature* 355, 33-45.
14. Clark, J. I. and Muchowski, P. J. (2000). Small heat-shock proteins and their potential role in human disease [Review]. *Current Opinion in Structural Biology* 10, 52-59.
15. Jakob, U., Gaestel, M., Engel, K. and Buchner, J. (1993). Small heat shock proteins are molecular chaperones. *Journal of Biological Chemistry* 268, 1517-1520.
16. Abgar, S., Backmann, J., Aerts, T., Vanhoudt, J. and Clauwaert, J. (2000). The structural differences between bovine lens  $\alpha$ A- and  $\alpha$ B-crystallin. *European Journal of Biochemistry* 267, 5916-5925.
17. Hartl, F. U. and Hayer-Hartl, M. (2002). Molecular chaperones in the cytosol: from nascent chain to folded protein. *Science* 295, 1852-1858.
18. Ellis, R. J. (1997). Molecular chaperones: avoiding the crowd. *Current Biology* 7, R531-533.



19. Ellis, R. J. and Hartl, F. U. (1999). Principles of protein folding in the cellular environment. *Current Opinion in Structural Biology* 9, 102-110.
20. Uversky, V. N. (2003). Protein folding revisited. A polypeptide chain at the folding-misfolding-nonfolding cross-roads: which way to go? *Cellular & Molecular Life Sciences* 60, 1852-1871.
21. Loh, S. N., Kay, M. S. and Baldwin, R. L. (1995). Structure and stability of a second molten globule intermediate in the apomyoglobin folding pathway. *Proceedings of the National Academy of Sciences of the United States of America* 92, 5446-5450.
22. Shi, Z., Woody, R. W. and Kallenbach, N. R. (2002). Is polyproline II a major backbone conformation in unfolded proteins? In *Advances in Protein Chemistry* (Richards, F. M. E., D.S.; Kuriyan, J., ed.), Vol. 62, pp. 163-240. Academic Press, San Diego, Ca.
23. Arai, M. and Kuwajima, K. (2000). Role of the molten globule state in protein folding. *Advances in Protein Chemistry* 53, 209-282.
24. Blake, M. J., Fargnoli, J., Gershon, D. and Holbrook, N. J. (1991). Concomitant decline in heat-induced hyperthermia and HSP70 mRNA expression in aged rats. *American Journal of Physiology* 260, R663-667.
25. Li, Z., Arnaud, L., Rockwell, P. and Figueiredo-Pereira, M. E. (2004). A single amino acid substitution in a proteasome subunit triggers aggregation of ubiquitinated proteins in stressed neuronal cells. *Journal of Neurochemistry* 90, 19-28.
26. Bence, N. F., Sampat, R. M. and Kopito, R. R. (2001). Impairment of the ubiquitin-proteasome system by protein aggregation. *Science* 292, 1552-1555.
27. Ben-Zvi, A. P. and Goloubinoff, P. (2001). Review: mechanisms of disaggregation and refolding of stable protein aggregates by molecular chaperones. *Journal of Structural Biology* 135, 84-93.
28. Dobson, C. M. (2001). The structural basis of protein folding and its links with human disease. *Philos. Trans. R. Soc. Lond. B. Biol. Sci.* 356, 133-145.
29. Nilsson, M. R. and Dobson, C. M. (2003). In vitro characterization of lactoferrin aggregation and amyloid formation. *Biochemistry* 42, 375-382.
30. Goers, J., Permyakov, S. E., Permyakov, E. A., Uversky, V. N. and Fink, A. L. (2002). Conformational prerequisites for alpha-lactalbumin fibrillation. *Biochemistry* 41, 12546-12551.
31. Rochet, J. C. and Lansbury, P. T. (2000). Amyloid fibrillogenesis: themes and variations [Review]. *Current Opinion in Structural Biology* 10, 60-68.
32. *Webster's New World Medical Dictionary*. (2005). 2nd edition. Wiley Publishing Inc.
33. Meehan, S., Berry, Y., Luisi, B., Dobson, C. M., Carver, J. A. and MacPhee, C. E. (2004). Amyloid fibril formation by lens crystallin proteins and its implications for cataract formation. *Journal of Biological Chemistry* 279, 3413-3419.
34. Krebs, M. R., Wilkins, D. K., Chung, E. W., Pitkeathly, M. C., Chamberlain, A. K., Zurdo, J., Robinson, C. V. and Dobson, C. M. (2000). Formation and seeding of amyloid fibrils from wild-type hen lysozyme and a peptide fragment from the beta-domain. *Journal of Molecular Biology* 300, 541-549.
35. Canet, D., Sunde, M., Last, A. M., Miranker, A., Spencer, A., Robinson, C. V. and Dobson, C. M. (1999). Mechanistic studies of the folding of human lysozyme and the origin of amyloidogenic behavior in its disease-related variants. *Biochemistry* 38, 6419-6427.
36. Dobson, C. M. (1999). Protein misfolding, evolution and disease. *Trends in Biochemical Sciences* 24, 329-332.

37. Zerovnik, E., Turk, V. and Waltho, J. P. (2002). Amyloid fibril formation by human stefin B: influence of the initial pH-induced intermediate state. *Biochemical Society Transactions* 30, 543-547.
38. Soti, C. and Csermely, P. (2002). Chaperones and aging: role in neurodegeneration and in other civilizational diseases. *Neurochemistry International* 41, 383-389.
39. Glover, J. R. and Lindquist, S. (1998). Hsp104, Hsp70, and Hsp40 - a novel chaperone system that rescues previously aggregated proteins. *Cell* 94, 73-82.
40. Carver, J. A., Nicholls, K. A., Aquilina, J. A. and Truscott, R. J. (1996). Age-related changes in bovine alpha-crystallin and high-molecular-weight protein. *Experimental Eye Research* 63, 639-647.
41. Truscott, R. J. (2000). Age-related nuclear cataract: a lens transport problem. *Ophthalmic Research* 32, 185-194.
42. Harding, J. (1991). *Cataract. Biochemistry, epidemiology and pharmacology*. 1st edition, Chapman & Hall, London.
43. Hood, B. D., Garner, B. and Truscott, R. J. (1999). Human lens coloration and aging. Evidence for crystallin modification by the major ultraviolet filter, 3-hydroxy-kynurenine O-beta-D-glucoside. *Journal of Biological Chemistry* 274, 32547-32550.
44. Tang, D., Borchman, D., Yappert, M. C. and Cenedella, R. J. (1998). Influence of cholesterol on the interaction of alpha-crystallin with phospholipids. *Experimental Eye Research* 66, 559-567.
45. Srivastava, O. P. and Srivastava, K. (1989). Human lens membrane proteinase: purification and age-related distributional changes in the water-soluble and insoluble protein fractions. *Experimental Eye Research* 48, 161-175.
46. Hanson, S. R., Hasan, A., Smith, D. L. and Smith, J. B. (2000). The major in vivo modifications of the human water-insoluble lens crystallins are disulfide bonds, deamidation, methionine oxidation and backbone cleavage. *Experimental Eye Research* 71, 195-207.
47. Harrington, V., McCall, S., Huynh, S., Srivastava, K. and Srivastava, O. P. (2004). Crystallins in water soluble-high molecular weight protein fractions and water insoluble protein fractions in aging and cataractous human lenses. *Molecular Vision* 10, 476-489.
48. Lund, A. L., Smith, J. B. and Smith, D. L. (1996). Modifications of the water-insoluble human lens alpha-crystallins. *Experimental Eye Research* 63, 661-672.
49. Kelly, J. W. (1998). The alternative conformations of amyloidogenic proteins and their multi-step assembly pathways. *Current Opinion in Structural Biology* 8, 101-106.
50. Caughey, B. and Lansbury, P. T. (2003). Protofibrils, pores, fibrils, and neurodegeneration: separating the responsible protein aggregates from the innocent bystanders. *Annual Review of Neuroscience* 26, 267-298.
51. Benson, M. D. (2001). Amyloidosis. In *Nature Encyclopedia of Life Sciences*, pp. 1-8. Nature Publishing Group, London.
52. Walsh, D. M., Hartley, D. M., Kusumoto, Y., Fezoui, Y., Condron, M. M., Lomakin, A., Benedek, G. B., Selkoe, D. J. and Teplow, D. B. (1999). Amyloid beta-protein fibrillogenesis. Structure and biological activity of protofibrillar intermediates. *Journal of Biological Chemistry* 274, 25945-25952.
53. Molecular Nano-Optics and Spins (MoNOS). University of Leiden.  
<http://www.monos.leidenuniv.nl/smo/index.html?basics/light.htm>.

54. National Aeronautics and Space Administration. (NASA). NASA explores. <http://www.nasa.gov>.
55. Tuery, J. (1992). *Microwaves: Industrial, scientific and medical applications*. Trans. Gabriel, C. (Grant, E. H., Ed.), Artech House Inc.
56. Young, E. (1979). *The new penguin dictionary of electronics*. Penguin Book, Harmondsworth.
57. (1985). *Reglement des radiocommunications. 2 vol.* Union Internationale des Telecommunications.
58. Australian Radiation Protection and Nuclear Safety Agency (ARPANSA). (2001). The controversy over electromagnetic fields and possible adverse health effects, pp. 1-6.
59. (1994). *Biological effects and safety of EMR*. Commonwealth Scientific and Industrial Research Organisation.(CSIRO).
60. National Radiological Protection Board. (2001). *ELF Electromagnetic fields and the risk of cancer: report of an advisory group on non-ionising radiation*. Doll, R.
61. Independent Expert Group on Mobile Phones. (2000). *Mobile Phones and Health* (Chaired by Sir W. Stewart, Ed.), National Radiological Protection Board, UK.
62. International Commission on Non-Ionising Radiation Protection (ICNIRP). (1998). Guidelines for limiting exposure to time-varying electric, magnetic, and electromagnetic fields (up to 300 GHz). *Health Physics* 74, 494-522.
63. Scientific Steering Committee of the European Commission. (1998). Report and opinion adopted at the meeting of the scientific steering committee of 25-26.
64. Senate Environment Communications Information Technology and the Arts references Committee. (2001). *Inquiry into Electromagnetic Radiation*, The Parliament of the Commonwealth of Australia.
65. World Health Organisation. (1997). *Low-level exposure to radiofrequency electromagnetic fields: health effects and research needs*. Bioelectromagnetics conference.
66. Rosen, A. e. and Rosen, H. D. e. (1995). *New frontiers in medical device technology*, John Wiley & Sons Inc.
67. Department of Physics University of Malta. <http://www.phys.um.edu.mt/mea.html>.
68. International Clinical Hyperthermia Society. <http://www.hyperthermia-ichs.org/>.
69. National Health and Medical Research Council. (1989). *Interim Guidelines on Limits of Exposure to 50/60 Hz electric and magnetic fields*, Canberra.
70. Energy Network Association. (2004). <http://www.emfs.info/default.asp>.
71. Milham, S. and Ossiander, E. M. (2001). Historical evidence that residential electrification caused the emergence of the childhood leukemia peak. *Medical Hypotheses* 56, 290-295.
72. Feychting, M. and Ahlbom, A. (1993). Magnetic fields and cancer in children residing near Swedish high-voltage power lines. *American Journal of Epidemiology* 138, 467-481.
73. Nave, C. R. (2000). HyperPhysics, Vol. 2004. Department of Physics and Astronomy, Georgia State University.
74. Chaplin, M. (2004). Water structure and behaviour. London South Bank University.

75. Leonard, A., Berteaud, A. J. and Bruyere, A. (1983). An evaluation of the mutagenic, carcinogenic and teratogenic potential of microwaves. *Mutation Research* 123, 31-46.
76. Jauchem, J. R. (2003). A literature review of medical side effects from radio-frequency energy in the human environment: involving cancer, tumors, and problems of the central nervous system. *Journal of Microwave Power & Electromagnetic Energy* 38, 103-123.
77. Meltz, M. L. (2003). Radiofrequency exposure and mammalian cell toxicity, genotoxicity, and transformation. *Bioelectromagnetics* Suppl 6, S196-213.
78. D'Andrea, J. A., Chou, C. K., Johnston, S. A. and Adair, E. R. (2003). Microwave effects on the nervous system. *Bioelectromagnetics* Suppl 6, S107-147.
79. Mileva, K., Georgieva, B. and Radicheva, N. (2003). About the biological effects of high and extremely high frequency electromagnetic fields. *Acta Physiologica et Pharmacologica Bulgarica* 27, 89-100.
80. Ho, M.-W., Popp, F.-A. and Warnke, U., (1994). *Bioelectrodynamics and biocommunication*. World Scientific. NJ.
81. International Commission on Non-Ionising Radiation Protection. (ICNIRP). (1994). Guidelines on Limits of Exposure to Static Magnetic Fields. *Health Physics* 66, 100-106.
82. Commonwealth of Australia. (2002). *Radiation protection standard, maximum exposure levels to radiofrequency fields - 3 KHz to 300 GHz*. Australian Radiation Protection and Nuclear Safety Agency. (ARPANSA). 2002.
83. Laurence, J. A., French, P. W., Lindner, R. A. and McKenzie, D. R. (2000). Biological effects of electromagnetic fields-mechanisms for the effects of pulsed microwave radiation on protein conformation. *Journal of Theoretical Biology* 206, 291-298.
84. Blank, M. and Soo, L. (1996). The threshold for Na,K-ATPase stimulation by electromagnetic fields. *Bioelectrochemistry and Bioenergetics* 40, 63-65.
85. Blank, M. and Soo, L. (1992). Na,K-ATPase Activity in Alternating Currents from Electric and Magnetic-Fields. *Faseb Journal* 6, A134-A134.
86. Blank, M. and Soo, L. (1997). Frequency dependence of Na,K-ATPase function in magnetic fields. *Bioelectrochemistry and Bioenergetics* 42, 231-234.
87. Blank, M., Soo, L. and Papstein, V. (1995). Effects of low-frequency magnetic-fields on Na,K-ATPase activity. *Bioelectrochemistry and Bioenergetics* 38, 267-273.
88. Blank, M. and Soo, L. (1992). Temperature-dependence of electric-field effects on Na,K-ATPase. *Bioelectrochemistry and Bioenergetics* 28, 291-299.
89. Blank, M. and Soo, L. (1989). The effects of alternating currents on Na,K-ATPase function. *Bioelectrochemistry and Bioenergetics* 22, 313-322.
90. Blank, M. and Soo, L. (1992). Threshold for inhibition of Na, K-ATPase by ELF alternating currents. *Bioelectromagnetics* 13, 329-333.
91. Blank, M. (1995). Biological effects of environmental electromagnetic fields: molecular mechanisms. *Biosystems* 35, 175-178.
92. Blank, M. and Soo, L. (1998). Enhancement of cytochrome oxidase activity in 60 Hz magnetic fields. *Bioelectrochemistry and Bioenergetics* 45, 253-259.
93. Blank, M. and Soo, L. (1998). Frequency dependence of cytochrome oxidase activity in magnetic fields. *Bioelectrochemistry and Bioenergetics* 46, 139-143.

94. Blank, M. and Soo, L. (2001). Electromagnetic acceleration of electron transfer reactions. *Journal of Cellular Biochemistry* 81, 278-283.
95. Blank, M. and Soo, L. (2001). Optimal frequencies for magnetic acceleration of cytochrome oxidase and Na,K-ATPase reactions. *Bioelectrochemistry* 53, 171-174.
96. Blank, M. and Soo, L. (2003). Electromagnetic acceleration of the Belousov-Zhabotinski reaction. *Bioelectrochemistry* 61, 93-97.
97. Wei, L. X., Goodman, R. and Henderson, A. (1990). Changes in levels of c-myc and histone H2B following exposure of cells to low-frequency sinusoidal electromagnetic fields: evidence for a window effect. *Bioelectromagnetics* 11, 269-272.
98. Blank, M., Soo, L., Lin, H., Henderson, A. S. and Goodman, R. (1992). Changes in transcription in H1-60 cells following exposure to alternating currents from electric-fields. *Bioelectrochemistry and Bioenergetics* 28, 301-309.
99. Goodman, R. and Shirleyhenderson, A. (1991). Transcription and translation in cells exposed to extremely low-frequency electromagnetic-fields. *Bioelectrochemistry and Bioenergetics* 25, 335-355.
100. Goodman, R., Wei, L. X., Xu, J. C. and Henderson, A. (1989). Exposure of human cells to low-frequency electromagnetic fields results in quantitative changes in transcripts. *Biochimica et Biophysica Acta* 1009, 216-220.
101. Goodman, R., Blank, M., Lin, H., Dai, R., Khorkova, O., Soo, L., Weisbrot, D. and Henderson, A. (1994). Increased levels of Hsp70 transcripts induced when cells are exposed to low frequency electromagnetic fields. *Bioelectrochemistry & Bioenergetics* 33, 115-120.
102. Golfert, F., Hofer, A., Thummler, M., Bauer, H. and Funk, R. H. (2001). Extremely low frequency electromagnetic fields and heat shock can increase microvesicle motility in astrocytes. *Bioelectromagnetics* 22, 71-78.
103. Junkersdorf, B., Bauer, H. and Gutzeit, H. O. (2000). Electromagnetic fields enhance the stress response at elevated temperatures in the nematode *Caenorhabditis elegans*. *Bioelectromagnetics* 21, 100-106.
104. Goodman, R. and Blank, M. (1998). Magnetic field stress induces expression of hsp70 (review). *Cell Stress. Chaperones* 3, 79-88.
105. Han, L., Lin, H. N., Head, M., Jin, M., Blank, M. and Goodman, R. (1998). Application of magnetic field-induced heat shock protein 70 for presurgical cytoprotection. *Journal of Cellular Biochemistry* 71, 577-583.
106. DiCarlo, A. L., Farrell, J. M. and Litovitz, T. A. (1998). A simple experiment to study electromagnetic field effects: protection induced by short-term exposures to 60 Hz magnetic fields. *Bioelectromagnetics* 19, 498-500.
107. de Pomerai, D., Daniells, C., David, H., Allan, J., Duce, I., Mutwakil, M., Thomas, D., Sewell, P., Tattersall, J., Jones, D. and Candido, P. (2000). Non-thermal heat-shock response to microwaves. *Nature* 405, 417-418.
108. Kwee, S., Raskmark, P. and Velizarov, S. (2001). Changes in cellular proteins due to environmental non-ionizing radiation. I. Heat-shock proteins. *Electro Magnetobiol* 20, 141-152.
109. Leszczynski, D., Joenvaara, S., Reivinen, J. and Kuokka, R. (2002). Non-thermal activation of the hsp27/p38MAPK stress pathway by mobile phone radiation in human endothelial cells: Molecular mechanism for cancer- and blood-brain barrier-related effects. *Differentiation* 70, 120-129.

110. Shallom, J. M., Di Carlo, A. L., Ko, D., Penafiel, L. M., Nakai, A. and Litovitz, T. A. (2002). Microwave exposure induces Hsp70 and confers protection against hypoxia in chick embryos. *Journal of Cellular Biochemistry* 86, 490-496.
111. La Cara, F., D'Auria, S., Scarfi, M. R., Zeni, O., Massa, R., d'Ambrosio, G., Franceschetti, G., De Rosa, M. and Rossi, M. (1999). Microwave exposure effect on a thermophilic alcohol dehydrogenase. *Protein and Peptide Letters* 6, 155-162.
112. La Cara F, Scarfi M.R., D'Auria S, Massa R, d'Ambrosio G, Franceschetti G, Rossi M and M., D. R. (1999). Different effects of microwave energy and conventional heat on the activity of a thermophilic beta-galactosidase from *Bacillus acidocaldarius*. *Bioelectromagnetics* 20, 172-176.
113. Bohr, H. and Bohr, J. (2000). Microwave-enhanced folding and denaturation of globular proteins. *Physical Review E. Statistical Physics, Plasmas, Fluids, & Related Interdisciplinary Topics* 61, 4310-4314.
114. Bohr, H. and Bohr, J. (2000). Microwave enhanced kinetics observed in ORD studies of a protein. *Bioelectromagnetics* 21, 68-72.
115. Ortner, M. J., Galvin, M. J., Chignell, C. F. and McRee, D. I. (1981). A circular dichroism study of human erythrocyte ghost proteins during exposure to 2450 MHz microwave radiation. *Cell Biophysics* 3, 335-347.
116. Ortner, M. J., Galvin, M. J. and Irwin, R. D. (1983). The effect of 2450-MHz microwave radiation during microtubular polymerization in vitro. *Radiation Research* 93, 353-363.
117. Porcelli, M., Cacciapuoti, G., Fusco, S., Massa, R., Dambrosio, G., Bertoldo, C., Derosa, M. and Zappia, V. (1997). Non-Thermal Effects of Microwaves On Proteins - Thermophilic Enzymes As Model System. *FEBS Letters* 402, 102-106.
118. de Pomerai, D. I., Smith, B., Dawe, A., North, K., Smith, T., Archer, D. B., Duce, I. R., Jones, D. and Candido, P. M. (2003). Microwave radiation can alter protein conformation without bulk heating. *Febs Letters* 543, 93-97.
119. Budi, A., Legge, S., Treutlein, H. and Yarovsky, I. (2005). (2005). *Protein Response to Electric Field Stress*. 16th Biennial Congress 2005, The Australian Institute of Physics, Australian National University, Canberra.
120. Pickard, W. F. and Moros, E. G. (2001). Energy deposition processes in biological tissue: nonthermal biohazards seem unlikely in the ultra-high frequency range. *Bioelectromagnetics* 22, 97-105.
121. Laurence, J. A., McKenzie, D. R. and Foster, K. R. (2003). Application of the heat equation to the calculation of temperature rises from pulsed microwave exposure. *Journal of Theoretical Biology* 222, 403-405.
122. Stuerger, D. A. C. and Gaillard, P. (1996). Microwave Athermal Effects in Chemistry - a Myths Autopsy .2. Orienting Effects and Thermodynamic Consequences of Electric Field. *Journal of Microwave Power & Electromagnetic Energy* 31, 101-113.
123. Saxena, A., Jacobson, J., Yamanashi, W., Scherlag, B., Lamberth, J. and Saxena, B. (2003). A hypothetical mathematical construct explaining the mechanism of biological amplification in an experimental model utilizing picoTesla (PT) electromagnetic fields. *Medical Hypotheses* 60, 821-839.
124. Blank, M. and Goodman, R. (1997). Do electromagnetic fields interact directly with DNA. *Bioelectromagnetics* 18, 111-115.
125. Blank, M. and Goodman, R. (1999). Electromagnetic fields may act directly on DNA. *Journal of Cellular Biochemistry* 75, 369-374.

126. Goodman, R. and Blank, M. (2002). Insights into electromagnetic interaction mechanisms. *Journal of Cellular Physiology* 192, 16-22.
127. Blank, M. and Goodman, R. (2000). Stimulation of the stress response by low-frequency electromagnetic fields: Possibility of direct interaction with DNA. *IEEE Transactions on Plasma Science* 28, 168-172.
128. Dodson, C. T. J. (2005). *A geometry view*. School of Mathematics, The University of Manchester. <http://www.ma.umist.ac.uk/kd/geomview/geometry.html>
129. Bohr, J., Bohr, H. G. and Brunak, S. (1996). The formation of protein structure. *Europhysics News* 27, 50-54.
130. Bohr, J. and Bohr, H. G. (1997). The implication of topology for protein structure and aggregation. *Zeitschrift für Physik D-Atoms Molecules & Clusters* 40, 186-189.
131. Bohr, H. (1997). Molecular wring resonances in chain molecules. *Bioelectromagnetics* 18, 187-189.
132. Bohr, J., Bohr, H. and Brunak, S. (1997). Protein folding and wring resonances. *Biophysical Chemistry* 63, 97-105.
133. Swiss Institute of Bioinformatics. ExpASY Proteomics Server. <http://au.expasy.org/>.
134. Research Collaboratory Structural Bioinformatics. (RCSB). Introduction to Biological Units and the PDB Archive. <http://www.rcsb.org/pdb/>.
135. Research Collaboratory Structural Bioinformatics. (RCSB). Protein Data Bank (PDB). <http://www.rcsb.org/pdb/>.
136. Buchner, M. and Sund, H. (1969). Yeast alcohol dehydrogenase: -SH groups, di-sulfide groups, quaternary structure, and reactivation by reductive cleavage of disulfide groups. *European Journal Biochemistry* 11, 73-79.
137. Bova, M. P., Yaron, O., Huang, Q. L., Ding, L. L., Haley, D. A., Stewart, P. L. and Horwitz, J. (1999). Mutation R120G in alpha B-crystallin, which is linked to a desmin-related myopathy, results in an irregular structure and defective chaperone-like function. *Proceedings of the National Academy of Sciences of the United States of America* 96, 6137-6142.
138. Carver, J. A., Aquilina, J. A., Cooper, P. G., Williams, G. A. and Truscott, R. J. W. (1994). Alpha-Crystallin - Molecular Chaperone and Protein Surfactant. *Biochim Biophys Acta Protein Struct M* 1204, 195-206.
139. Horwitz, J., Huang, Q., Ding, L. and Bova, M. P. (1998). Lens  $\alpha$ -Crystallin: Chaperone-Like Properties. *Methods in Enzymology* 290, 365-383.
140. Sharma, K. K. (1997). Functional elements in molecular chaperone alpha-crystallin: identification of binding sites in alpha B-crystallin. *Biochem. Biophys. Res. Commun.* 239, 217-222.
141. Lindner, R. A., Kapur, A., Mariani, M., Titmuss, S. J. and Carver, J. A. (1998). Structural Alterations of Alpha-Crystallin During Its Chaperone Action. *European Journal of Biochemistry* 258, 170-183.
142. Arakawa, T. and Kita, Y. (2000). Protection of bovine serum albumin from aggregation by tween 80. *Journal of Pharmaceutical Sciences* 89, 646-651.

143. Humphreys, D. T., Carver, J. A., Easterbrook-Smith, S. B. and Wilson, M. R. (1999). Clusterin has chaperone-like activity similar to that of small heat shock proteins. *Journal of Biological Chemistry* 274, 6875-6881.
144. Hook, D. W. and Harding, J. J. (1998). Protection of enzymes by alpha-crystallin acting as a molecular chaperone. *International Journal of Biological Macromolecules* 22, 295-306.
145. Poon, S., Easterbrook-Smith, S. B., Rybchyn, M. S., Carver, J. A. and Wilson, M. R. (2000). Clusterin is an ATP-independent chaperone with very broad substrate specificity that stabilizes stressed proteins in a folding-competent state. *Biochemistry* 39, 15953-15960.
146. Wang, K. Y. and Spector, A. (2000). alpha-Crystallin prevents irreversible protein denaturation and acts cooperatively with other heat-shock proteins to renature the stabilized partially denatured protein in an ATP-dependent manner. *European Journal of Biochemistry* 267, 4705-4712.
147. Haslbeck, M., Walke, S., Stromer, T., Ehrnsperger, M., White, H. E., Chen, S., Saibil, H. and Buchner, J. (1999). Hsp26: a temperature-regulated chaperone. *EMBO J* 18, 6744-6751.
148. Buchner, J., Grallert, H. and Jakob, U. (1998). Analysis of chaperone function using citrate synthase as nonnative substrate protein. *Methods in Enzymology* 290, 323-338.
149. Colorado State University., (2000). *Hypertexts for Biomedical Sciences*. Edited by Austgen, L., Bowen, R. A. & Rouge, M. <http://arbl.cvmbs.colostate.edu/hbooks>.
150. Abgar, S., Yevlampieva, N., Aerts, T., Vanhoudt, J. and Clauwaert, J. (2000). Chaperone-like activity of bovine lens alpha-crystallin in the presence of dithiothreitol-destabilized proteins: characterization of the formed complexes. *Biochem Biophys Res Commun* 276, 619-625.
151. Chrysina, E. D., Brew, K. and Acharya, K. R. (2000). Crystal Structures of Apo- and Holo-bovine alpha -Lactalbumin at 2.2-A Resolution Reveal an Effect of Calcium on Inter-lobe Interactions. *J. Biol. Chem.* 275, 37021-37029.
152. Ren, J., Stuart, D. I. and Acharya, K. R. (1993). Alpha-lactalbumin possesses a distinct zinc binding site. *Journal of Biological Chemistry* 268, 19292-19298.
153. Lindner, R. A., Treweek, T. M. and Carver, J. A. (2001). The molecular chaperone alpha-crystallin is in kinetic competition with aggregation to stabilize a monomeric molten-globule form of alpha-lactalbumin. *Biochemical Journal* 354, 79-87.
154. Lindner, R. A., Kapur, A. and Carver, J. A. (1997). The Interaction of the Molecular Chaperone, Alpha-Crystallin, With Molten Globule States of Bovine Alpha-Lactalbumin. *Journal of Biological Chemistry* 272, 27722-27729.
155. Worthington enzyme manual. (<http://www.worthington-biochem.com/CTL>)
156. Brew, K., Vanaman, T. C. and Hill, R. L. (1967). Comparison of the amino acid sequence of bovine alpha-lactalbumin and hens egg white lysozyme. *Journal of Biological Chemistry* 242, 3747-3749.
157. Abgar, S., Vanhoudt, J., Aerts, T. and Clauwaert, J. (2001). Study of the chaperoning mechanism of bovine lens alpha-crystallin, a member of the alpha-small heat shock superfamily. *Biophysical Journal* 80, 1986-1995.
158. Guagliardi, A., Cerchia, L., Bartolucci, S. and Rossi, M. (1994). The chaperonin from the archaeon *Sulfolobus solfataricus* promotes correct refolding and prevents thermal denaturation in vitro. *Protein Science* 3, 1436-1443.
159. Carver, J. A., Lindner, R. A., Lyon, C., Canet, D., Hernandez, H., Dobson, C. M. and Redfield, C. (2002). The interaction of the molecular chaperone alpha-crystallin with unfolding alpha-



- lactalbumin: a structural and kinetic spectroscopic study. *Journal of Molecular Biology* 318, 815-827.
160. Horwitz, J. (1992). Alpha-crystallin can function as a molecular chaperone. *Proceedings of the National Academy of Sciences of the United States of America* 89, 10449-10453.
161. Fasman, G. D., (1976). CRC Handbook of biochemistry and molecular biology. 3rd edition. Vol. Proteins - II. Cleveland, Ohio: CRC Press.
162. Laurence, J. A. (2003). *The Heat Shock Response Induced by Radio Frequency Radiation*. Doctor of Philosophy, University of Sydney.
163. Department of Applied and Plasma Physics, University of Sydney. (2001). *Documentation of modified microwave oven*. Denniss, P.
164. Robinson, C. V., Gross, M., Eyles, S. J., Ewbank, J. J., Mayhew, M., Hartl, F. U., Dobson, C. M. and Radford, S. E. (1994). Conformation of GroEL-bound alpha-lactalbumin probed by mass spectrometry. *Nature* 372, 646-651.
165. Orbis Technologies Ltd. <http://www.orbitech.co.uk/lux500.html>.
166. Zar, J. H. (1984). *Biostatistical analysis*. 2nd edition, Prentice-Hall International, Inc, New Jersey.
167. Garcia De La Torre, J., Huertas, M. L. and Carrasco, B. (2000). Calculation of hydrodynamic properties of globular proteins from their atomic-level structure. *Biophysical Journal* 78, 719-730.
168. Department of Physical Chemistry. University of Marcial. <http://leonardo.fcu.um.es/macromol/programs/hydropro/hydropro.htm>.
169. Marchesini, S. and King, M. W., (2003). *TCA cycle.: Biochemistry on the web*. <http://www.med.unibs.it/~marchesi/index2.html>.
170. Srere, P. A. (1966). Citrate-condensing Enzyme-Oxalacetate Binary Complex. *The Journal of Biological Chemistry* 241, 2157-2165.
171. Speed, M. A., King, J. and Wang, D. I. C. (1997). Polymerization mechanism of polypeptide chain aggregation. *Biotechnology and Bioengineering* 54, 333-343.
172. Dollinger, G., Cunico, B., Kunitani, M., Johnson, D. and Jones, R. (1992). Practical Online Determination of Biopolymer Molecular-Weights by High-Performance Liquid-Chromatography with Classical Light-Scattering Detection. *Journal of Chromatography* 592, 215-228.
173. Atkins, P. (1998). *Physical Chemistry*. 6th edition, Oxford University Press, Oxford.
174. Kurganov, B. I. (1998). Kinetics of Heat Aggregation of Proteins. *Biochemistry-Moscow* 63, 364-366.
175. Ferrone, F. (1999). Analysis of protein aggregation kinetics. *Methods in Enzymology* 309, 256-274.
176. Griko, Y. V., Freire, E. and Privalov, P. L. (1994). Energetics of the alpha-lactalbumin states: a calorimetric and statistical thermodynamic study. *Biochemistry* 33, 1889-1899.
177. Kuwajima, K. (1996). The molten globule state of alpha-lactalbumin. *FASEB Journal* 10, 102-109.
178. Burkhardt, M., Pokovic, K., Gnos, M., Schmid, T. and Kuster, N. (1996). Numerical and experimental dosimetry of Petri dish exposure setups. *Bioelectromagnetics* 17, 483-493.

179. Hermansson, A. M. (1979). Aggregation and denaturation involved in gel formation. In *Functionality and Protein Structure* (Pour-El, A., ed.), Vol. Series 92. ACS Symposium, American Chemical Society, Washington, DC.
180. Shimada, K. and Matsushita, S. (1980). Relationship between Thermocoagulation of Proteins and Amino-Acid Compositions. *Journal of Agricultural and Food Chemistry* 28, 413-417.
181. Shimada, K. and Matsushita, S. (1980). Thermal Coagulation of Egg-Albumin. *Journal of Agricultural and Food Chemistry* 28, 409-412.
182. Lampi, K. J., Kim, Y. H., Bachinger, H. P., Boswell, B. A., Lindner, R. A., Carver, J. A., Shearer, T. R., David, L. L. and Kapfer, D. M. (2002). Decreased heat stability and increased chaperone requirement of modified human betaB1-crystallins. *Molecular Vision* 8, 359-366.
183. Carver, J. A., Guerreiro, N., Nicholls, K. A. and Truscott, R. J. W. (1995). On the interaction of alpha-crystallin with unfolded proteins. *Biochimica et Biophysica Acta - Protein Structure & Molecular Enzymology* 1252, 251-260.
184. Huttman, G. and Birngruber, R. (1999). On the possibility of high-precision photothermal microeffects and the measurement of fast thermal denaturation of proteins. *Selected Topics in Quantum Electronics, IEEE Journal of* 5, 954-962.
185. Kleinschmidt, J. H. and Tamm, L. K. (1996). Folding intermediates of a beta-barrel membrane protein. Kinetic evidence for a multi-step membrane insertion mechanism. *Biochemistry* 35, 12993-13000.
186. Steel, B. C., Bilek, M. M., McKenzie, D. R. and dos Remedios, C. G. (2002). A technique for microsecond heating and cooling of a thin (submicron) biological sample. *European Biophysics Journal with Biophysics Letters* 31, 378-382.
187. Murphy, K. P. and Freire, E. (1993). Structural Energetics of Protein Stability and Folding Cooperativity. *Pure and Applied Chemistry* 65, 1939-1946.
188. Hirst, J. D. and Brooks, C. L., 3rd. (1994). Helicity, circular dichroism and molecular dynamics of proteins. *Journal of Molecular Biology* 243, 173-178.
189. Sun, T. X., Das, B. K. and Liang, J. J. N. (1997). Conformational and Functional Differences between Recombinant Human Lens Alpha-a- and Alpha-B-Crystallin. *Journal of Biological Chemistry* 272, 6220-6225.
190. Zhi, W., Srere, P. A. and Evans, C. T. (1991). Conformational stability of pig citrate synthase and some active-site mutants. *Biochemistry* 30, 9281-9286.
191. Budi, A., Legge, S., Treutlein, H. and Yarovsky, I. (2004). Effect of external stresses on protein conformation: a computer modelling study. *European Biophysics Journal with Biophysics Letters* 33, 121-129.
192. Lide, D. R. (2001 -2002). *CRC Handbook of chemistry and physics*. 82nd edition. CRC Press LLC.
193. Kelly, S. M. and Price, N. C. (1997). The Application of Circular Dichroism to Studies of Protein Folding and Unfolding [Review]. *Biochimica et Biophysica Acta - Protein Structure & Molecular Enzymology* 1338, 161-185.
194. Cantor, C. R. and Schimmel, P. R. (1980). *Biophysical Chemistry. Part II: Techniques for the study of biological structure and function*, W.H. Freeman & Co., New York.
195. Smulders, R. H. P. H., Carver, J. A., Lindner, R. A., van Boekel, M. A. M., Bloemendal, H. and de Jong, W. W. (1996). Immobilization of the C-terminal Extension of Bovine alpha A-Crystallin Reduces Chaperone-like Activity. *J. Biol. Chem.* 271, 29060-29066.

196. Prajapati, S., Bhakuni, V., Babu, K. R. and Jain, S. K. (1998). Alkaline unfolding and salt-induced folding of bovine liver catalase at high pH. *European Journal of Biochemistry* 255, 178-184.
197. West, S. M., Kelly, S. M. and Price, N. C. (1990). The unfolding and attempted refolding of citrate synthase from pig heart. *Biochimica et Biophysica Acta (BBA) - Protein Structure and Molecular Enzymology* 1037, 332-336.
198. Dolgikh, D. A., Gilmanshin, R. I., Brazhnikov, E. V., Bychkova, V. E., Semisotnov, G. V., Venyaminov, S. and Ptitsyn, O. B. (1981). Alpha-Lactalbumin: compact state with fluctuating tertiary structure? *FEBS Letters* 136, 311-315.
199. Ikeguchi, M., Sugai, S., Fujino, M., Sugawara, T. and Kuwajima, K. (1992). Contribution of the 6-120 disulfide bond of alpha-lactalbumin to the stabilities of its native and molten globule states. *Biochemistry* 31, 12695-12700.
200. Ewbank, J. J. and Creighton, T. E. (1991). The molten globule protein conformation probed by disulphide bonds. *Nature* 350, 518-520.
201. Ewbank, J. J. and Creighton, T. E. (1993). Pathway of disulfide-coupled unfolding and refolding of bovine alpha-lactalbumin. *Biochemistry* 32, 3677-3693.
202. Ewbank, J. J. and Creighton, T. E. (1993). Structural characterization of the disulfide folding intermediates of bovine alpha-lactalbumin. *Biochemistry* 32, 3694-3707.
203. Polverino de Laureto, P., Vinante, D., Scaramella, E., Frare, E. and Fontana, A. (2001). Stepwise proteolytic removal of the beta subdomain in alpha-lactalbumin. The protein remains folded and can form the molten globule in acid solution. *European Journal of Biochemistry* 268, 4324-4333.
204. Demarest, S. J., Boice, J. A., Fairman, R. and Raleigh, D. P. (1999). Defining the core structure of the alpha-lactalbumin molten globule state. *Journal of Molecular Biology* 294, 213-221.
205. Vassilenko, K. S. and Uversky, V. N. (2002). Native-like secondary structure of molten globules. *Biochimica et Biophysica Acta* 1594, 168-177.
206. Kuwajima, K., Ikeguchi, M., Sugawara, T., Hiraoka, Y. and Sugai, S. (1990). Kinetics of disulfide bond reduction in alpha-lactalbumin by dithiothreitol and molecular basis of superreactivity of the Cys6-Cys120 disulfide bond. *Biochemistry* 29, 8240-8249.
207. Horng, J. C., Demarest, S. J. and Raleigh, D. P. (2003). pH-dependent stability of the human alpha-lactalbumin molten globule state: contrasting roles of the 6 - 120 disulfide and the beta-subdomain at low and neutral pH. *Proteins* 52, 193-202.
208. Gursky, O. and Atkinson, D. (1996). Thermal unfolding of human high-density apolipoprotein A-1: implications for a lipid-free molten globular state. *Proceedings of the National Academy of Sciences of the United States of America* 93, 2991-2995.
209. Freifelder, D. (1982). *Physical Biochemistry, Applications to Biochemistry and Molecular Biology*. 2nd edition, W.H. Freeman and Company, New York.
210. Matulis, D., Baumann, C. G., Bloomfield, V. A. and Lovrien, R. E. (1999). 1-anilino-8-naphthalene sulfonate as a protein conformational tightening agent. *Biopolymers* 49, 451-458.
211. Kundu, B. and Guptasarma, P. (2002). Use of a hydrophobic dye to indirectly probe the structural organization and conformational plasticity of molecules in amorphous aggregates of carbonic anhydrase. *Biochemical & Biophysical Research Communications* 293, 572-577.
212. Fessas, D., Iametti, S., Schiraldi, A. and Bonomi, F. (2001). Thermal unfolding of monomeric and dimeric {beta}-lactoglobulins. *Eur J Biochem* 268, 5439-5448.

213. Vanhoudt, J., Abgar, S., Aerts, T. and Clauwaert, J. (2000). Native quaternary structure of bovine alpha-crystallin. *Biochemistry* 39, 4483-4492.
214. Englander, S. W., Mayne, L., Bai, Y. and Sosnick, T. R. (1997). Hydrogen exchange: The modern legacy of Linderstrom-Lang. *Protein Science* 6, 1101-1109.
215. Nemirovskiy, O., Giblin, D. E. and Gross, M. L. (1999). Electrospray ionization mass spectrometry and hydrogen/deuterium exchange for probing the interaction of calmodulin with calcium. *Journal of the American Society for Mass Spectrometry* 10, 711-718.
216. Nettleton, E. J., Tito, P., Sunde, M., Bouchard, M., Dobson, C. M. and Robinson, C. V. (2000). Characterization of the oligomeric states of insulin in self-assembly and amyloid fibril formation by mass spectrometry. *Biophysical Journal* 79, 1053-1065.
217. Miranker, A., Robinson, C. V., Radford, S. E., Aplin, R. T. and Dobson, C. M. (1993). Detection of Transient Protein-Folding Populations by Mass-Spectrometry. *Science* 262, 896-900.
218. Spilimbergo, S., Dehghani, F., Bertuccio, A. and Foster, N. R. (2003). Inactivation of bacteria and spores by pulse electric field and high pressure CO<sub>2</sub> at low temperature. *Biotechnology and Bioengineering* 82, 118-125.
219. Ishikawa, H., Shimoda, M., Yonekura, A., Mishima, K., Matsumoto, K. and Osajima, Y. (2000). Irreversible unfolding of myoglobin in an aqueous solution by supercritical carbon dioxide. *Journal of Agricultural and Food Chemistry* 48, 4535-4539.
220. Wright, W. W., Owen, C. S. and Vanderkooi, J. M. (1992). Penetration of analogues of H<sub>2</sub>O and CO<sub>2</sub> in proteins studied by room temperature phosphorescence of tryptophan. *Biochemistry* 31, 6538-6544.
221. van den Berg, B., Ellis, R. J. and Dobson, C. M. (1999). Effects of macromolecular crowding on protein folding and aggregation. *EMBO Journal* 18, 6927-6933.
222. Eggers, D. K. and Valentine, J. S. (2001). Crowding and hydration effects on protein conformation: a study with sol-gel encapsulated proteins. *Journal of Molecular Biology* 314, 911-922.
223. Minton, A. P. (1983). The effect of volume occupancy upon the thermodynamic activity of proteins: some biochemical consequences. *Molecular & Cellular Biochemistry* 55, 119-140.
224. Tsong, T. Y. and Astumian, R. D. (1988). Electroconformational coupling: how membrane-bound ATPase transduces energy from dynamic electric fields. *Annual Review of Physiology* 50, 273-290.
225. Rochu, D., Pernet, T., Renault, F., Bon, C. and Masson, P. (2001). Dual effect of high electric field in capillary electrophoresis study of the conformational stability of Bungarus fasciatus acetylcholinesterase. *Journal of Chromatography. A* 910, 347-357.
226. Barsotti, L., Dumay, E., Mu, T. H., Diaz, M. D. F. and Cheftel, J. C. (2001). Effects of high voltage electric pulses on protein-based food constituents and structures. *Trends in Food Science & Technology* 12, 136-144.
227. Adey, W. R. (1996). A Growing Scientific Consensus on the Cell and Molecular Biology Mediating. In *Biological Effects of Magnetic and Electromagnetic Fields* (Ueno, S., ed.), pp. 45-61. Plenum Press, New York.
228. Zugel, U. and Kaufmann, S. H. (1999). Role of heat shock proteins in protection from and pathogenesis of infectious diseases. *Clinical Microbiology Reviews* 12, 19-39.
229. Stewart-DeHaan, P. J., Creighton, M. O., Larsen, L. E., Jacobi, J. H., Sanwal, M., Baskerville, J. C. and Trevithick, J. R. (1985). In vitro studies of microwave-induced cataract: reciprocity

- between exposure duration and dose rate for pulsed microwaves. *Experimental Eye Research* 40, 1-13.
230. Harrison, A., Ibberson, R., Robb, G., Whittaker, G., Wilson, C. and Youngson, D. (2003). In situ neutron diffraction studies of single crystals and powders during microwave irradiation. *Faraday Discussions* 122, 363-379; discussion 381-393.
231. Cranfield, C., Wieser, H. G., Al Madan, J. and Dobson, J. (2003). Preliminary evaluation of nanoscale biogenic magnetite-based ferromagnetic transduction mechanisms for mobile phone bioeffects. *IEEE Transactions on Nanobioscience* 2, 40-43.
232. Astbury Centre for Structural Molecular Biology. (2004). Circular Dichroism Facility. University of Leeds, <http://www.astbury.leeds.ac.uk/Facil/cdpage.htm>.
233. National Institute of Environmental Health Sciences (2002). Electric and Magnetic Fields associated with the use of electric power. EMF Rapid Report No. 02-4493, National Institute of Health.

---

**REFERENCES BY NAME**


---

- Abgar, S., J. Backmann, et al. (2000). The structural differences between bovine lens  $\alpha$ A- and  $\alpha$ B-crystallin. *European Journal of Biochemistry* 267(19): 5916-5925.
- Abgar, S., J. Vanhoudt, et al. (2001). Study of the chaperoning mechanism of bovine lens alpha-crystallin, a member of the alpha-small heat shock superfamily. *Biophysical Journal* 80(4): 1986-1995.
- Abgar, S., N. Yevlampieva, et al. (2000). Chaperone-like activity of bovine lens alpha-crystallin in the presence of dithiothreitol-destabilized proteins: characterization of the formed complexes. *Biochem Biophys Res Commun* 276(2): 619-625.
- Adey, W. R. (1996). A Growing Scientific Consensus on the Cell and Molecular Biology Mediating. *Biological Effects of Magnetic and Electromagnetic Fields*. S. Ueno. New York, Plenum Press: 45-61.
- Arai, M. and K. Kuwajima (2000). Role of the molten globule state in protein folding. *Advances in Protein Chemistry* 53: 209-282.
- Arakawa, T. and Y. Kita (2000). Protection of bovine serum albumin from aggregation by tween 80. *Journal of Pharmaceutical Sciences* 89(5): 646-651.
- Astbury Centre for Structural Molecular Biology (2004). Circular Dichroism Facility. <http://www.astbury.leeds.ac.uk/Facil/cdpage.htm>, University of Leeds.
- Atkins, P. (1998). *Physical Chemistry*. Oxford, Oxford University Press.
- Australian Radiation Protection and Nuclear Safety Agency (ARPANSA). (2001). The controversy over electromagnetic fields and possible adverse health effects: 1-6.
- Australian Radiation Protection and Nuclear Safety Agency. (ARPANSA). (2002). Radiation protection standard, maximum exposure levels to radiofrequency fields - 3 KHz to 300 GHz. Canberra, Commonwealth of Australia.
- Barsotti, L., E. Dumay, et al. (2001). Effects of high voltage electric pulses on protein-based food constituents and structures. *Trends in Food Science & Technology* 12(3-4): 136-144.
- Bence, N. F., R. M. Sampat, et al. (2001). Impairment of the ubiquitin-proteasome system by protein aggregation. *Science* 292(5521): 1552-1555.
- Benson, M. D. (2001). Amyloidosis. *Nature Encyclopedia of Life Sciences*. London, Nature Publishing Group: 1-8.
- Ben-Zvi, A. P. and P. Goloubinoff (2001). Review: mechanisms of disaggregation and refolding of stable protein aggregates by molecular chaperones. *Journal of Structural Biology* 135(2): 84-93.
- Berke, S. J. and H. L. Paulson (2003). Protein aggregation and the ubiquitin proteasome pathway: gaining the UPPER hand on neurodegeneration. *Current Opinion in Genetics & Development* 13(3): 253-61.
- Blake, M. J., J. Fargnoli, et al. (1991). Concomitant decline in heat-induced hyperthermia and HSP70 mRNA expression in aged rats. *American Journal of Physiology* 260(4 Pt 2): R663-667.
- Blank, M. (1995). Biological effects of environmental electromagnetic fields: molecular mechanisms. *Biosystems* 35(2-3): 175-178.

- Blank, M. and R. Goodman (1997). Do electromagnetic fields interact directly with DNA. *Bioelectromagnetics* 18(2): 111-115.
- Blank, M. and R. Goodman (1999). Electromagnetic fields may act directly on DNA. *Journal of Cellular Biochemistry* 75(3): 369-374.
- Blank, M. and R. Goodman (2000). Stimulation of the stress response by low-frequency electromagnetic fields: Possibility of direct interaction with DNA. *IEEE Transactions on Plasma Science* 28(1): 168-172.
- Blank, M. and L. Soo (1989). The effects of alternating currents on Na,K-ATPase function. *Bioelectrochemistry and Bioenergetics* 22(3): 313-322.
- Blank, M. and L. Soo (1992). Na,K-ATPase Activity in Alternating Currents from Electric and Magnetic Fields. *Faseb Journal* 6(1): A134-A134.
- Blank, M. and L. Soo (1992). Temperature-dependence of electric-field effects on Na,K-ATPase. *Bioelectrochemistry and Bioenergetics* 28(1-2): 291-299.
- Blank, M. and L. Soo (1992). Threshold for inhibition of Na, K-ATPase by ELF alternating currents. *Bioelectromagnetics* 13(4): 329-333.
- Blank, M. and L. Soo (1996). The threshold for Na,K-ATPase stimulation by electromagnetic fields. *Bioelectrochemistry and Bioenergetics* 40(1): 63-65.
- Blank, M. and L. Soo (1997). Frequency dependence of Na,K-ATPase function in magnetic fields. *Bioelectrochemistry and Bioenergetics* 42(2): 231-234.
- Blank, M. and L. Soo (1998). Enhancement of cytochrome oxidase activity in 60 Hz magnetic fields. *Bioelectrochemistry and Bioenergetics* 45(2): 253-259.
- Blank, M. and L. Soo (1998). Frequency dependence of cytochrome oxidase activity in magnetic fields. *Bioelectrochemistry and Bioenergetics* 46(1): 139-143.
- Blank, M. and L. Soo (2001). Electromagnetic acceleration of electron transfer reactions. *Journal of Cellular Biochemistry* 81(2): 278-283.
- Blank, M. and L. Soo (2001). Optimal frequencies for magnetic acceleration of cytochrome oxidase and Na,K-ATPase reactions. *Bioelectrochemistry* 53(2): 171-174.
- Blank, M. and L. Soo (2003). Electromagnetic acceleration of the Belousov-Zhabotinski reaction. *Bioelectrochemistry* 61(1-2): 93-97.
- Blank, M., L. Soo, et al. (1992). Changes in transcription in HL-60 cells following exposure to alternating currents from electric-fields. *Bioelectrochemistry and Bioenergetics* 28(1-2): 301-309.
- Blank, M., L. Soo, et al. (1995). Effects of low-frequency magnetic-fields on Na,K-ATPase activity. *Bioelectrochemistry and Bioenergetics* 38(2): 267-273.
- Bohr, H. (1997). Molecular wring resonances in chain molecules. *Bioelectromagnetics* 18(2): 187-189.
- Bohr, H. and J. Bohr (2000). Microwave enhanced kinetics observed in ORD studies of a protein. *Bioelectromagnetics* 21(1): 68-72.
- Bohr, H. and J. Bohr (2000). Microwave-enhanced folding and denaturation of globular proteins. *Physical Review E. Statistical Physics, Plasmas, Fluids, & Related Interdisciplinary Topics* 61(4 Pt B): 4310-4314.
- Bohr, J., H. Bohr, et al. (1997). Protein folding and wring resonances. *Biophysical Chemistry* 63(2-3): 97-105.

- Bohr, J. and H. G. Bohr (1997). The implication of topology for protein structure and aggregation. *Zeitschrift fur Physik D-Atoms Molecules & Clusters* 40(1-4): 186-189.
- Bohr, J., H. G. Bohr, et al. (1996). The formation of protein structure. *Europhysics News* 27(1): 50-54.
- Bova, M. P., O. Yaron, et al. (1999). Mutation R120G in alpha B-crystallin, which is linked to a desmin-related myopathy, results in an irregular structure and defective chaperone-like function. *Proceedings of the National Academy of Sciences of the United States of America* 96(11): 6137-6142.
- Braun, B. C., M. Glickman, et al. (1999). The base of the proteasome regulatory particle exhibits chaperone-like activity. *Nature Cell Biology* 1: 221-226.
- Brew, K., T. C. Vanaman, et al. (1967). Comparison of the amino acid sequence of bovine alpha-lactalbumin and hens egg white lysozyme. *Journal of Biological Chemistry* 242(16): 3747-3749.
- Buchner, J., H. Grallert, et al. (1998). Analysis of chaperone function using citrate synthase as nonnative substrate protein. *Methods in Enzymology* 290: 323-338.
- Buchner, M. and H. Sund (1969). Yeast alcohol dehydrogenase: -SH groups, di-sulfide groups, quaternary structure, and reactivation by reductive cleavage of disulfide groups. *European Journal Biochemistry* 11: 73-79.
- Budi, A., S. Legge, et al. (2004). Effect of external stresses on protein conformation: a computer modelling study. *European Biophysics Journal with Biophysics Letters* 33(2): 121-129.
- Budi, A., S. Legge, et al. (2005). (2005). *Protein Response to Electric Field Stress*. 16th Biennial Congress 2005, The Australian Institute of Physics, Australian National University, Canberra.
- Burkhardt, M., K. Pokovic, et al. (1996). Numerical and experimental dosimetry of Petri dish exposure setups. *Bioelectromagnetics* 17(6): 483-493.
- Canet, D., M. Sunde, et al. (1999). Mechanistic studies of the folding of human lysozyme and the origin of amyloidogenic behavior in its disease-related variants. *Biochemistry* 38(20): 6419-6427.
- Cantor, C. R. and P. R. Schimmel (1980). *Biophysical Chemistry. Part II: Techniques for the study of biological structure and function*. New York, W.H. Freeman & Co.
- Carver, J. A., J. A. Aquilina, et al. (1994). Alpha-Crystallin - Molecular Chaperone and Protein Surfactant. *Biochim Biophys Acta Protein Struct M* 1204(2): 195-206.
- Carver, J. A., N. Guerreiro, et al. (1995). On the interaction of alpha-crystallin with unfolded proteins. *Biochimica et Biophysica Acta - Protein Structure & Molecular Enzymology* 1252(2): 251-260.
- Carver, J. A., R. A. Lindner, et al. (2002). The interaction of the molecular chaperone alpha-crystallin with unfolding alpha-lactalbumin: a structural and kinetic spectroscopic study. *Journal of Molecular Biology* 318(3): 815-827.
- Carver, J. A., K. A. Nicholls, et al. (1996). Age-related changes in bovine alpha-crystallin and high-molecular-weight protein. *Experimental Eye Research* 63(6): 639-647.
- Caughey, B. and P. T. Lansbury (2003). Protofibrils, pores, fibrils, and neurodegeneration: separating the responsible protein aggregates from the innocent bystanders. *Annual Review of Neuroscience* 26: 267-298.
- Chaplin, M. (2004). Water structure and behaviour, London South Bank University.



- Chrysina, E. D., K. Brew, et al. (2000). Crystal Structures of Apo- and Holo-bovine alpha -Lactalbumin at 2.2-A Resolution Reveal an Effect of Calcium on Inter-lobe Interactions. *J. Biol. Chem.* 275(47): 37021-37029.
- Clark, J. I. and P. J. Muchowski (2000). Small heat-shock proteins and their potential role in human disease [Review]. *Current Opinion in Structural Biology* 10(1): 52-59.
- Colorado State University., (2000). *Hypertexts for Biomedical Sciences*.  
<http://arbl.cvmbs.colostate.edu/hbooks>.
- Commonwealth Scientific and Industrial Research Organisation.(CSIRO). (1994). Biological effects and safety of EMR.
- Cranfield, C., H. G. Wieser, et al. (2003). Preliminary evaluation of nanoscale biogenic magnetite-based ferromagnetic transduction mechanisms for mobile phone bioeffects. *IEEE Transactions on Nanobioscience* 2(1): 40-43.
- Creighton, T. E. (1993). *Proteins: structures and molecular properties*, W.H. Freeman and Company.
- D'Andrea, J. A., C. K. Chou, et al. (2003). Microwave effects on the nervous system. *Bioelectromagnetics* Suppl 6: S107-147.
- de Pomerai, D., C. Daniells, et al. (2000). Non-thermal heat-shock response to microwaves. *Nature* 405(25 May): 417-418.
- de Pomerai, D. I., B. Smith, et al. (2003). Microwave radiation can alter protein conformation without bulk heating. *Febs Letters* 543(1-3): 93-97.
- Demarest, S. J., J. A. Boice, et al. (1999). Defining the core structure of the alpha-lactalbumin molten globule state. *Journal of Molecular Biology* 294(1): 213-221.
- Denniss, P. (2001). *Documentation of modified microwave oven*, Department of Applied and Plasma Physics, University of Sydney.
- Department of Physical Chemistry. University of Marcia.  
<http://leonardo.fc.u.br/macromol/programs/hydropro/hydropro.htm>.
- Department of Physics University of Malta. <http://www.phys.um.edu.mt/mea.html>.
- DiCarlo, A. L., J. M. Farrell, et al. (1998). A simple experiment to study electromagnetic field effects: protection induced by short-term exposures to 60 Hz magnetic fields. *Bioelectromagnetics* 19(8): 498-500.
- Dobson, C. M. (1999). Protein misfolding, evolution and disease. *Trends in Biochemical Sciences* 24(9): 329-332.
- Dobson, C. M. (2001). The structural basis of protein folding and its links with human disease. *Philos. Trans. R. Soc. Lond. B. Biol. Sci.* 356(1406): 133-145.
- Dodson, C. T. J. (2005). *A geometry view.*, School of Mathematics, The University of Manchester.  
<http://www.ma.umist.ac.uk/kd/geomview/geometry.html>
- Dolgikh, D. A., R. I. Gilmanshin, et al. (1981). Alpha-Lactalbumin: compact state with fluctuating tertiary structure? *FEBS Letters* 136(2): 311-315.
- Doll, R. (2001). ELF Electromagnetic fields and the risk of cancer: report of an advisory group on non-ionising radiation. Chilton, National Radiological Protection Board: 1-184.
- Dollinger, G., B. Cunico, et al. (1992). Practical Online Determination of Biopolymer Molecular-Weights by High-Performance Liquid-Chromatography with Classical Light-Scattering Detection. *Journal of Chromatography* 592(1-2): 215-228.

- Eggers, D. K. and J. S. Valentine (2001). Crowding and hydration effects on protein conformation: a study with sol-gel encapsulated proteins. *Journal of Molecular Biology* 314(4): 911-922.
- Ellis, R. J. (1997). Molecular chaperones: avoiding the crowd. *Current Biology* 7(9): R531-533.
- Ellis, R. J. and F. U. Hartl (1999). Principles of protein folding in the cellular environment. *Current Opinion in Structural Biology* 9(1): 102-110.
- Energy Network Association. (2004). <http://www.emfs.info/default.asp>.
- Englander, S. W., L. Mayne, et al. (1997). Hydrogen exchange: The modern legacy of Linderstrom-Lang. *Protein Science* 6(5): 1101-1109.
- Ewbank, J. J. and T. E. Creighton (1991). The molten globule protein conformation probed by disulphide bonds. *Nature* 350(6318): 518-520.
- Ewbank, J. J. and T. E. Creighton (1993). Pathway of disulfide-coupled unfolding and refolding of bovine alpha-lactalbumin. *Biochemistry* 32(14): 3677-3693.
- Ewbank, J. J. and T. E. Creighton (1993). Structural characterization of the disulfide folding intermediates of bovine alpha-lactalbumin. *Biochemistry* 32(14): 3694-3707.
- Fasman, G. D., (1976). *CRC Handbook of biochemistry and molecular biology*. 3rd edition. Cleveland, Ohio, CRC Press.
- Ferrone, F. (1999). Analysis of protein aggregation kinetics. *Methods in Enzymology* 309: 256-274.
- Fessas, D., S. Iametti, et al. (2001). Thermal unfolding of monomeric and dimeric {beta}-lactoglobulins. *Eur J Biochem* 268(20): 5439-5448.
- Feychting, M. and A. Ahlbom (1993). Magnetic fields and cancer in children residing near Swedish high-voltage power lines. *American Journal of Epidemiology* 138(7): 467-481.
- Freifelder, D. (1982). *Physical Biochemistry, Applications to Biochemistry and Molecular Biology*. W.H. Freeman and Company, New York.
- Garcia De La Torre, J., M. L. Huertas, et al. (2000). Calculation of hydrodynamic properties of globular proteins from their atomic-level structure. *Biophysical Journal* 78(2): 719-730.
- Gething, M. J. and J. Sambrook (1992). Protein folding in the cell. *Nature* 355(6355): 33-45.
- Glickman, M. H. and A. Ciechanover (2002). The ubiquitin-proteasome proteolytic pathway: destruction for the sake of construction. *Physiological Reviews* 82(2): 373-428.
- Glover, J. R. and S. Lindquist (1998). Hsp104, Hsp70, and Hsp40 - a novel chaperone system that rescues previously aggregated proteins. *Cell* 94(1): 73-82.
- Goers, J., S. E. Permyakov, et al. (2002). Conformational prerequisites for alpha-lactalbumin fibrillation. *Biochemistry* 41(41): 12546-12551.
- Golfert, F., A. Hofer, et al. (2001). Extremely low frequency electromagnetic fields and heat shock can increase microvesicle motility in astrocytes. *Bioelectromagnetics* 22(2): 71-78.
- Goodman, R. and M. Blank (1998). Magnetic field stress induces expression of hsp70 (review). *Cell Stress. Chaperones* 3(2): 79-88.
- Goodman, R. and M. Blank (2002). Insights into electromagnetic interaction mechanisms. *Journal of Cellular Physiology* 192(1): 16-22.

- Goodman, R., M. Blank, et al. (1994). Increased levels of Hsp70 transcripts induced when cells are exposed to low frequency electromagnetic fields. *Bioelectrochemistry & Bioenergetics* 33(2): 115-120.
- Goodman, R. and A. Shirleyhenderson (1991). Transcription and translation in cells exposed to extremely low-frequency electromagnetic-fields. *Bioelectrochemistry and Bioenergetics* 25(3): 335-355.
- Goodman, R., L. X. Wei, et al. (1989). Exposure of human cells to low-frequency electromagnetic fields results in quantitative changes in transcripts. *Biochimica et Biophysica Acta* 1009(3): 216-220.
- Griko, Y. V., E. Freire, et al. (1994). Energetics of the alpha-lactalbumin states: a calorimetric and statistical thermodynamic study. *Biochemistry* 33(7): 1889-1899.
- Guagliardi, A., L. Cerchia, et al. (1994). The chaperonin from the archaeon *Sulfolobus solfataricus* promotes correct refolding and prevents thermal denaturation in vitro. *Protein Science* 3(9): 1436-1443.
- Gursky, O. and D. Atkinson (1996). Thermal unfolding of human high-density apolipoprotein A-1: implications for a lipid-free molten globular state. *Proceedings of the National Academy of Sciences of the United States of America* 93(7): 2991-2995.
- Han, L., H. N. Lin, et al. (1998). Application of magnetic field-induced heat shock protein 70 for presurgical cytoprotection. *Journal of Cellular Biochemistry* 71(4): 577-583.
- Hanson, S. R., A. Hasan, et al. (2000). The major in vivo modifications of the human water-insoluble lens crystallins are disulfide bonds, deamidation, methionine oxidation and backbone cleavage. *Experimental Eye Research* 71(2): 195-207.
- Harding, J. (1991). *Cataract. Biochemistry, epidemiology and pharmacology*. London, Chapman & Hall.
- Harrington, V., S. McCall, et al. (2004). Crystallins in water soluble-high molecular weight protein fractions and water insoluble protein fractions in aging and cataractous human lenses. *Molecular Vision* 10: 476-489.
- Harrison, A., R. Ibberson, et al. (2003). In situ neutron diffraction studies of single crystals and powders during microwave irradiation. *Faraday Discussions* 122: 363-379; discussion 381-393.
- Hartl, F. U. and M. Hayer-Hartl (2002). Molecular chaperones in the cytosol: from nascent chain to folded protein. *Science* 295(5561): 1852-1858.
- Haslbeck, M., S. Walke, et al. (1999). Hsp26: a temperature-regulated chaperone. *EMBO J* 18(23): 6744-6751.
- Hermansson, A. M. (1979). Aggregation and denaturation involved in gel formation. *Functionality and Protein Structure*. A. Pour-El. Washington, DC., ACS Symposium, American Chemical Society. Series 92.
- Hirst, J. D. and C. L. Brooks, 3rd (1994). Helicity, circular dichroism and molecular dynamics of proteins. *Journal of Molecular Biology* 243(2): 173-178.
- Ho, M.-W., F.-A. Popp, et al., (1994). *Bioelectrodynamics and biocommunication*. World Scientific, NJ.
- Hood, B. D., B. Garner, et al. (1999). Human lens coloration and aging. Evidence for crystallin modification by the major ultraviolet filter, 3-hydroxy-kynurenine O-beta-D-glucoside. *Journal of Biological Chemistry* 274(46): 32547-32550.
- Hook, D. W. and J. J. Harding (1998). Protection of enzymes by alpha-crystallin acting as a molecular chaperone. *International Journal of Biological Macromolecules* 22(3-4): 295-306.

- Horng, J. C., S. J. Demarest, et al. (2003). pH-dependent stability of the human alpha-lactalbumin molten globule state: contrasting roles of the 6 - 120 disulfide and the beta-subdomain at low and neutral pH. *Proteins* 52(2): 193-202.
- Horwitz, J. (1992). Alpha-crystallin can function as a molecular chaperone. *Proceedings of the National Academy of Sciences of the United States of America* 89(21): 10449-10453.
- Horwitz, J., Q. Huang, et al. (1998). Lens  $\alpha$ -Crystallin: Chaperone-Like Properties. *Methods in Enzymology* 290: 365-383.
- Humphreys, D. T., J. A. Carver, et al. (1999). Clusterin has chaperone-like activity similar to that of small heat shock proteins. *Journal of Biological Chemistry* 274(11): 6875-6881.
- Huttmann, G. and R. Birngruber (1999). On the possibility of high-precision photothermal microeffects and the measurement of fast thermal denaturation of proteins. *Selected Topics in Quantum Electronics, IEEE Journal of* 5(4): 954-962.
- Ikeguchi, M., S. Sugai, et al. (1992). Contribution of the 6-120 disulfide bond of alpha-lactalbumin to the stabilities of its native and molten globule states. *Biochemistry* 31(50): 12695-12700.
- Independent Expert Group on Mobile Phones (2000). *Mobile Phones and Health*. UK, National Radiological Protection Board.
- International Clinical Hyperthermia Society. <http://www.hyperthermia-ichs.org/>.
- International Commission on Non-Ionising Radiation Protection (ICNIRP). (1998). Guidelines for limiting exposure to time-varying electric, magnetic, and electromagnetic fields (up to 300 GHz). *Health Physics* 74(4): 494-522.
- International Commission on Non-Ionising Radiation Protection. (ICNIRP). (1994). Guidelines on Limits of Exposure to Static Magnetic Fields. *Health Physics* 66(1): 100-106.
- Ishikawa, H., M. Shimoda, et al. (2000). Irreversible unfolding of myoglobin in an aqueous solution by supercritical carbon dioxide. *Journal of Agricultural and Food Chemistry* 48(10): 4535-4539.
- Jakob, U., M. Gaestel, et al. (1993). Small heat shock proteins are molecular chaperones. *Journal of Biological Chemistry* 268(3): 1517-1520.
- Jauchem, J. R. (2003). A literature review of medical side effects from radio-frequency energy in the human environment: involving cancer, tumors, and problems of the central nervous system. *Journal of Microwave Power & Electromagnetic Energy* 38(2): 103-123.
- Jolly, J. and R. I. Morimoto (2000). Role of heat shock response and molecular chaperones in oncogenesis and cell death. *Journal of National Cancer Institute* 92(19): 1564-1772.
- Junkersdorf, B., H. Bauer, et al. (2000). Electromagnetic fields enhance the stress response at elevated temperatures in the nematode *Caenorhabditis elegans*. *Bioelectromagnetics* 21(2): 100-106.
- Kelly, J. W. (1998). The alternative conformations of amyloidogenic proteins and their multi-step assembly pathways. *Current Opinion in Structural Biology* 8(1): 101-106.
- Kelly, S. M. and N. C. Price (1997). The Application of Circular Dichroism to Studies of Protein Folding and Unfolding [Review]. *Biochimica et Biophysica Acta - Protein Structure & Molecular Enzymology* 1338(2): 161-185.
- Kleinschmidt, J. H. and L. K. Tamm (1996). Folding intermediates of a beta-barrel membrane protein. Kinetic evidence for a multi-step membrane insertion mechanism. *Biochemistry* 35(40): 12993-13000.

- Krebs, M. R., D. K. Wilkins, et al. (2000). Formation and seeding of amyloid fibrils from wild-type hen lysozyme and a peptide fragment from the beta-domain. *Journal of Molecular Biology* 300(3): 541-549.
- Kundu, B. and P. Guptasarma (2002). Use of a hydrophobic dye to indirectly probe the structural organization and conformational plasticity of molecules in amorphous aggregates of carbonic anhydrase. *Biochemical & Biophysical Research Communications* 293(1): 572-577.
- Kungl Vetenskapsakademien. The Royal Swedish Academy of Sciences (2004). *Advanced information on the Nobel Prize in Chemistry, Ubiquitin-mediated proteolysis*. Stockholm.
- Kurganov, B. I. (1998). Kinetics of Heat Aggregation of Proteins. *Biochemistry-Moscow* 63(3): 364-366.
- Kuwajima, K. (1996). The molten globule state of alpha-lactalbumin. *FASEB Journal* 10(1): 102-109.
- Kuwajima, K., M. Ikeguchi, et al. (1990). Kinetics of disulfide bond reduction in alpha-lactalbumin by dithiothreitol and molecular basis of superreactivity of the Cys6-Cys120 disulfide bond. *Biochemistry* 29(36): 8240-8249.
- Kwee, S., P. Raskmark, et al. (2001). Changes in cellular proteins due to environmental non-ionizing radiation. I. Heat-shock proteins. *Electro Magnetobiol* 20(2): 141-152.
- La Cara F, Scarfi M.R., et al. (1999). Different effects of microwave energy and conventional heat on the activity of a thermophilic beta-galactosidase from *Bacillus acidocaldarius*. *Bioelectromagnetics* 20(3): 172-176.
- La Cara, F., S. D'Auria, et al. (1999). Microwave exposure effect on a thermophilic alcohol dehydrogenase. *Protein and Peptide Letters* 6(3): 155-162.
- Lampi, K. J., Y. H. Kim, et al. (2002). Decreased heat stability and increased chaperone requirement of modified human betaB1-crystallins. *Molecular Vision* 8: 359-366.
- Laurence, J. A. (2003). *The Heat Shock Response Induced by Radio Frequency Radiation*. Department of Applied and Plasma Physics. Sydney, University of Sydney.
- Laurence, J. A., P. W. French, et al. (2000). Biological effects of electromagnetic fields-mechanisms for the effects of pulsed microwave radiation on protein conformation. *Journal of Theoretical Biology* 206(2): 291-298.
- Laurence, J. A., D. R. McKenzie, et al. (2003). Application of the heat equation to the calculation of temperature rises from pulsed microwave exposure. *Journal of Theoretical Biology* 222(3): 403-405.
- Leonard, A., A. J. Berteaud, et al. (1983). An evaluation of the mutagenic, carcinogenic and teratogenic potential of microwaves. *Mutation Research* 123(1): 31-46.
- Leszczynski, D., S. Joenvaara, et al. (2002). Non-thermal activation of the hsp27/p38MAPK stress pathway by mobile phone radiation in human endothelial cells: Molecular mechanism for cancer- and blood-brain barrier-related effects. *Differentiation* 70(2-3): 120-129.
- Li, Z., L. Arnaud, et al. (2004). A single amino acid substitution in a proteasome subunit triggers aggregation of ubiquitinated proteins in stressed neuronal cells. *Journal of Neurochemistry* 90(1): 19-28.
- Lide, D. R., (2001 -2002). *CRC Handbook of chemistry and physics*. 82nd edition, CRC Press LLC.
- Lindner, R. A., A. Kapur, et al. (1997). The Interaction of the Molecular Chaperone, Alpha-Crystallin, With Molten Globule States of Bovine Alpha-Lactalbumin. *Journal of Biological Chemistry* 272(44): 27722-27729.

- Lindner, R. A., A. Kapur, et al. (1998). Structural Alterations of Alpha-Crystallin During Its Chaperone Action. *European Journal of Biochemistry* 258(1): 170-183.
- Lindner, R. A., T. M. Treweek, et al. (2001). The molecular chaperone alpha-crystallin is in kinetic competition with aggregation to stabilize a monomeric molten-globule form of alpha-lactalbumin. *Biochemical Journal* 354(Pt 1): 79-87.
- Loh, S. N., M. S. Kay, et al. (1995). Structure and stability of a second molten globule intermediate in the apomyoglobin folding pathway. *Proceedings of the National Academy of Sciences of the United States of America* 92(12): 5446-5450.
- Lund, A. L., J. B. Smith, et al. (1996). Modifications of the water-insoluble human lens alpha-crystallins. *Experimental Eye Research* 63(6): 661-672.
- Marchesini, S. and M. W. King, (2003). *TCA cycle.*, Biochemistry on the web. <http://www.med.unibs.it/~marchesi/index2.html>.
- Mathews, C. K., K. E. van Holde, et al. (2000). *Biochemistry*, Benjamin Cummings, San Francisco, Calif.
- Matulis, D., C. G. Baumann, et al. (1999). 1-anilino-8-naphthalene sulfonate as a protein conformational tightening agent. *Biopolymers* 49(6): 451-458.
- Meehan, S., Y. Berry, et al. (2004). Amyloid fibril formation by lens crystallin proteins and its implications for cataract formation. *Journal of Biological Chemistry* 279(5): 3413-3419.
- Meltz, M. L. (2003). Radiofrequency exposure and mammalian cell toxicity, genotoxicity, and transformation. *Bioelectromagnetics* Suppl 6: S196-213.
- Mileva, K., B. Georgieva, et al. (2003). About the biological effects of high and extremely high frequency electromagnetic fields. *Acta Physiologica et Pharmacologica Bulgarica* 27(2-3): 89-100.
- Milham, S. and E. M. Osslander (2001). Historical evidence that residential electrification caused the emergence of the childhood leukemia peak. *Medical Hypotheses* 56(3): 290-295.
- Minton, A. P. (1983). The effect of volume occupancy upon the thermodynamic activity of proteins: some biochemical consequences. *Molecular & Cellular Biochemistry* 55(2): 119-140.
- Miranker, A., C. V. Robinson, et al. (1993). Detection of Transient Protein-Folding Populations by Mass-Spectrometry. *Science* 262(5135): 896-900.
- Molecular Nano-Optics and Spins (MoNOS). University of Leiden., <http://www.monos.leidenuniv.nl/smo/index.html?basics/light.htm>.
- Morimoto, R. I. (1993). Cells in stress: transcriptional activation of heat shock genes. *Science* 259(5100): 1409-1410.
- Murphy, K. P. and E. Freire (1993). Structural Energetics of Protein Stability and Folding Cooperativity. *Pure and Applied Chemistry* 65(9): 1939-1946.
- National Aeronautics and Space Administration. (NASA). NASA explores, <http://www.nasa.gov>.
- National Health and Medical Research Council (1989). *Interim Guidelines on Limits of Exposure to 50/60 Hz electric and magnetic fields*, Canberra.
- National Institute of Environmental Health Sciences (2002). Electric and Magnetic Fields associated with the use of electric power. EMF Rapid Report No. 02-4493, National Institute of Health.
- Nave, C. R. (2000). *HyperPhysics*. Department of Physics and Astronomy, Georgia State University.

- Nemirovskiy, O., D. E. Giblin, et al. (1999). Electrospray ionization mass spectrometry and hydrogen/deuterium exchange for probing the interaction of calmodulin with calcium. *Journal of the American Society for Mass Spectrometry* 10(8): 711-718.
- Nettleton, E. J., P. Tito, et al. (2000). Characterization of the oligomeric states of insulin in self-assembly and amyloid fibril formation by mass spectrometry. *Biophysical Journal* 79(2): 1053-1065.
- Nilsson, M. R. and C. M. Dobson (2003). In vitro characterization of lactoferrin aggregation and amyloid formation. *Biochemistry* 42(2): 375-382.
- Orbis Technologies Ltd. <http://www.orbitech.co.uk/lux500.html>.
- Ortner, M. J., M. J. Galvin, et al. (1981). A circular dichroism study of human erythrocyte ghost proteins during exposure to 2450 MHz microwave radiation. *Cell Biophysics* 3(4): 335-347.
- Ortner, M. J., M. J. Galvin, et al. (1983). The effect of 2450-MHz microwave radiation during microtubular polymerization in vitro. *Radiation Research* 93(2): 353-363.
- Parsell, D. A. and S. Lindquist (1993). The function of heat-shock proteins in stress tolerance - Degradation and reactivation of damaged proteins [Review]. *Annual Review of Genetics* 27: 437-496.
- Pickard, W. F. and E. G. Moros (2001). Energy deposition processes in biological tissue: nonthermal biohazards seem unlikely in the ultra-high frequency range. *Bioelectromagnetics* 22(2): 97-105.
- Polverino de Laureto, P., D. Vinante, et al. (2001). Stepwise proteolytic removal of the beta subdomain in alpha-lactalbumin. The protein remains folded and can form the molten globule in acid solution. *European Journal of Biochemistry* 268(15): 4324-4333.
- Poon, S., S. B. Easterbrook-Smith, et al. (2000). Clusterin is an ATP-independent chaperone with very broad substrate specificity that stabilizes stressed proteins in a folding-competent state. *Biochemistry* 39(51): 15953-15960.
- Porcelli, M., G. Cacciapuoti, et al. (1997). Non-Thermal Effects of Microwaves On Proteins - Thermophilic Enzymes As Model System. *FEBS Letters* 402(2-3): 102-106.
- Prajapati, S., V. Bhakuni, et al. (1998). Alkaline unfolding and salt-induced folding of bovine liver catalase at high pH. *European Journal of Biochemistry* 255(1): 178-184.
- Radford, S. E. (2000). Protein folding: progress made and promises ahead. *Trends in Biochemical Sciences* 25(12): 611-618.
- Ren, J., D. I. Stuart, et al. (1993). Alpha-lactalbumin possesses a distinct zinc binding site. *Journal of Biological Chemistry* 268(26): 19292-19298.
- Research Collaboratory Structural Bioinformatics. (RCSB). Introduction to Biological Units and the PDB Archive. <http://www.rcsb.org/pdb/>.
- Research Collaboratory Structural Bioinformatics. (RCSB). Protein Data Bank (PDB). <http://www.rcsb.org/pdb/>.
- Robinson, C. V., M. Gross, et al. (1994). Conformation of GroEL-bound alpha-lactalbumin probed by mass spectrometry. *Nature* 372(6507): 646-651.
- Rochet, J. C. and P. T. Lansbury (2000). Amyloid fibrillogenesis: themes and variations [Review]. *Current Opinion in Structural Biology* 10(1): 60-68.
- Rochu, D., T. Pernet, et al. (2001). Dual effect of high electric field in capillary electrophoresis study of the conformational stability of Bungarus fasciatus acetylcholinesterase. *Journal of Chromatography. A* 910(2): 347-357.

- Rosen, A. e. and H. D. e. Rosen (1995). *New frontiers in medical device technology*, John Wiley & Sons Inc.
- Saxena, A., J. Jacobson, et al. (2003). A hypothetical mathematical construct explaining the mechanism of biological amplification in an experimental model utilizing picoTesla (PT) electromagnetic fields. *Medical Hypotheses* 60(6): 821-839.
- Scientific Steering Committee of the European Commission. (1998). Report and opinion adopted at the meeting of the scientific steering committee of 25-26.
- Senate Environment Communications Information Technology and the Arts references Committee (2001). *Inquiry into Electromagnetic Radiation*, The Parliament of the Commonwealth of Australia.
- Shallom, J. M., A. L. Di Carlo, et al. (2002). Microwave exposure induces Hsp70 and confers protection against hypoxia in chick embryos. *Journal of Cellular Biochemistry* 86(3): 490-496.
- Sharma, K. K. (1997). Functional elements in molecular chaperone alpha-crystallin: identification of binding sites in alpha B-crystallin. *Biochem. Biophys. Res. Commun.* 239(1): 217-222.
- Shi, Z., R. W. Woody, et al. (2002). Is polyproline II a major backbone conformation in unfolded proteins ? *Advances in Protein Chemistry*. F. M. E. Richards, D.S.; Kuriyan, J. San Diego, Ca., Academic Press. 62: 163-240.
- Shimada, K. and S. Matsushita (1980). Relationship between Thermocoagulation of Proteins and Amino-Acid Compositions. *Journal of Agricultural and Food Chemistry* 28(2): 413-417.
- Shimada, K. and S. Matsushita (1980). Thermal Coagulation of Egg-Albumin. *Journal of Agricultural and Food Chemistry* 28(2): 409-412.
- Smulders, R. H. P. H., J. A. Carver, et al. (1996). Immobilization of the C-terminal Extension of Bovine alpha A-Crystallin Reduces Chaperone-like Activity. *J. Biol. Chem.* 271(46): 29060-29066.
- Soti, C. and P. Csermely (2002). Chaperones and aging: role in neurodegeneration and in other civilizational diseases. *Neurochemistry International* 41(6): 383-389.
- Speed, M. A., J. King, et al. (1997). Polymerization mechanism of polypeptide chain aggregation. *Biotechnology and Bioengineering* 54(4): 333-343.
- Spilimbergo, S., F. Dehghani, et al. (2003). Inactivation of bacteria and spores by pulse electric field and high pressure CO<sub>2</sub> at low temperature. *Biotechnology and Bioengineering* 82(1): 118-125.
- Srere, P. A. (1966). Citrate-condensing Enzyme-Oxalacetate Binary Complex. *The Journal of Biological Chemistry* 241(9): 2157-2165.
- Srivastava, O. P. and K. Srivastava (1989). Human lens membrane proteinase: purification and age-related distributional changes in the water-soluble and insoluble protein fractions. *Experimental Eye Research* 48(2): 161-175.
- Steel, B. C., M. M. Bilek, et al. (2002). A technique for microsecond heating and cooling of a thin (submicron) biological sample. *European Biophysics Journal with Biophysics Letters* 31(5): 378-382.
- Stewart-DeHaan, P. J., M. O. Creighton, et al. (1985). In vitro studies of microwave-induced cataract: reciprocity between exposure duration and dose rate for pulsed microwaves. *Experimental Eye Research* 40(1): 1-13.
- Stuerga, D. A. C. and P. Gaillard (1996). Microwave Athermal Effects in Chemistry - a Myths Autopsy .2. Orienting Effects and Thermodynamic Consequences of Electric Field. *Journal of Microwave Power & Electromagnetic Energy* 31(2): 101-113.



- Sun, T. X., B. K. Das, et al. (1997). Conformational and Functional Differences between Recombinant Human Lens Alpha-a- and Alpha-B-Crystallin. *Journal of Biological Chemistry* 272(10): 6220-6225.
- Swiss Institute of Bioinformatics. ExPASy Proteomics Server. <http://au.expasy.org/>.
- Tang, D., D. Borchman, et al. (1998). Influence of cholesterol on the interaction of alpha-crystallin with phospholipids. *Experimental Eye Research* 66(5): 559-567.
- The National Health Museum Washington DC (2004). <http://www.accessexcellence.org>.
- Thuery, J. (1992). *Microwaves: Industrial, scientific and medical applications*, Artech House Inc.
- Treweek, T. M., A. M. Morris, et al. (2003). Intracellular protein unfolding and aggregation: The role of small heat-shock chaperone proteins. *Australian Journal of Chemistry* 56(5): 357-367.
- Truscott, R. J. (2000). Age-related nuclear cataract: a lens transport problem. *Ophthalmic Research* 32(5): 185-194.
- Tsong, T. Y. and R. D. Astumian (1988). Electroconformational coupling: how membrane-bound ATPase transduces energy from dynamic electric fields. *Annual Review of Physiology* 50: 273-290.
- Union Internationale des Telecommunications. (1985). Reglement des radiocommunications. 2 vol. Geneve.
- Uversky, V. N. (2003). Protein folding revisited. A polypeptide chain at the folding-misfolding-nonfolding cross-roads: which way to go? *Cellular & Molecular Life Sciences* 60(9): 1852-1871.
- van den Berg, B., R. J. Ellis, et al. (1999). Effects of macromolecular crowding on protein folding and aggregation. *EMBO Journal* 18(24): 6927-6933.
- Vanhoudt, J., S. Abgar, et al. (2000). Native quaternary structure of bovine alpha-crystallin. *Biochemistry* 39(15): 4483-4492.
- Vassilenko, K. S. and V. N. Uversky (2002). Native-like secondary structure of molten globules. *Biochimica et Biophysica Acta* 1594(1): 168-177.
- Walsh, D. M., D. M. Hartley, et al. (1999). Amyloid beta-protein fibrillogenesis. Structure and biological activity of protofibrillar intermediates. *Journal of Biological Chemistry* 274(36): 25945-25952.
- Wang, K. Y. and A. Spector (2000). alpha-Crystallin prevents irreversible protein denaturation and acts cooperatively with other heat-shock proteins to renature the stabilized partially denatured protein in an ATP-dependent manner. *European Journal of Biochemistry* 267(15): 4705-4712.
- Webster's New World Medical Dictionary*. (2005). Wiley Publishing Inc.
- Wei, L. X., R. Goodman, et al. (1990). Changes in levels of c-myc and histone H2B following exposure of cells to low-frequency sinusoidal electromagnetic fields: evidence for a window effect. *Bioelectromagnetics* 11(4): 269-272.
- West, S. M., S. M. Kelly, et al. (1990). The unfolding and attempted refolding of citrate synthase from pig heart. *Biochimica et Biophysica Acta (BBA) - Protein Structure and Molecular Enzymology* 1037(3): 332-336.
- World Health Organisation. (1997). *Low-level exposure to radiofrequency electromagnetic fields: health effects and research needs*. Bioelectromagnetics conference.
- Worthington enzyme manual. (<http://www.worthington-biochem.com/CTL>).

- Wright, W. W., C. S. Owen, et al. (1992). Penetration of analogues of H<sub>2</sub>O and CO<sub>2</sub> in proteins studied by room temperature phosphorescence of tryptophan. *Biochemistry* 31(28): 6538-6544.
- Young, E. (1979). *The new penguin dictionary of electronics*. Penguin Book, Harmondsworth.
- Zar, J. H. (1984). *Biostatistical analysis*. Prentice-Hall International, Inc, New Jersey.
- Zerovnik, E., V. Turk, et al. (2002). Amyloid fibril formation by human stefin B: influence of the initial pH-induced intermediate state. *Biochemical Society Transactions* 30(4): 543-547.
- Zhi, W., P. A. Srere, et al. (1991). Conformational stability of pig citrate synthase and some active-site mutants. *Biochemistry* 30(38): 9281-9286.
- Zugel, U. and S. H. Kaufmann (1999). Role of heat shock proteins in protection from and pathogenesis of infectious diseases. *Clinical Microbiology Reviews* 12(1): 19-39.